UNIVERSIDADE DE SÃO PAULO
Escola de Engenharia de São Carlos

Future perspectives of extreme events and water availability in Brazilian catchments

André Simões Ballarin
Orientador: Prof. Tit. Edson Cezar Wendland

EESC · USP

UNIVERSIDADE DE SÃO PAULO
ESCOLA DE ENGENHARIA DE SÃO CARLOS

ANDRÉ SIMÕES BALLARIN

Future perspectives of extreme events and water availability in Brazilian catchments

Versão Corrigida
São Carlos
2024

ANDRÉ SIMÕES BALLARIN

Future perspectives of extreme events and water availability in Brazilian catchments

Tese apresentada à Escola de Engenharia de São Carlos da Universidade de São Paulo, para obtenção do título de Doutor em Ciências - Programa de Pós-Graduação em Engenharia Hidráulica e Saneamento.

Área de concentração: Hidráulica e Saneamento

Supervisor: Edson Cezar Wendland

São Carlos
2024

Ficha catalográfica elaborada pela Biblioteca Prof. Dr. Sérgio Rodrigues Fontes da EESC/USP com os dados inseridos pelo(a) autor(a).

Simões Ballarin, André
S171f Future perspectives of extreme events and water availability in Brazilian catchments / André Simões Ballarin; orientador Edson Cezar Wendland. São Carlos, 2024.

Tese (Doutorado) - Programa de Pós-Graduação em Engenharia Hidráulica e Saneamento e Área de Concentração em Hidráulica e Saneamento -- Escola de Engenharia de São Carlos da Universidade de São Paulo, 2024.

1. Extreme events. 2. global warming. 3. heavy rainfall. 4. droughts. 5. water security. I. Título.

Eduardo Graziosi Silva - CRB - 8/8907

FOLHA DE JULGAMENTO

Candidato: Engenheiro **ANDRÉ SIMÕES BALLARIN**.

Título da tese: "Perspectivas futuras de eventos extremos e disponibilidade hídrica em bacias hidrográficas brasileiras"".

Data da defesa: 12/04/2024.

Comissão Julgadora	**Resultado**
Prof. Titular Edson Cezar Wendland (Orientador) (Escola de Engenharia de São Carlos/EESC-USP)	Aprovado
Prof. Dr. Eduardo Mario Mendiondo (Escola de Engenharia de São Carlos/EESC-USP)	Aprovado
Prof. Dr. Dirceu Silveira Reis Júnior (Universidade de Brasília/UnB)	Aprovado
Profa. Dra. Noemi Vergopolan da Rocha (Princeton University / Rice University)	Aprovado
Prof. Dr. Celso Augusto Guimarães Santos (Universidade Federal da Paraíba/UFPB)	Aprovado

Coordenador do Programa de Pós-Graduação em Engenharia Hidráulica e Saneamento:
Prof. Assoc. **Juliano Jose Corbi**

Presidente da Comissão de Pós-Graduação:
Prof. Titular **Carlos De Marqui Junior**

ACKNOWLEDGEMENTS

I dedicate this thesis to my beloved wife Mariana and to my family, Luisa, Adriano, Raquel, and Caio. Thank you very much for the unwavering support and unconditional love, and for always being present in my life. You mean everything to me! Thank you for the teachings, experiences, for believing in me, and for showing me how to live and envision a fairer world alongside you. You are a huge part of who I am today, and I am grateful for that.

I extend my heartfelt gratitude to my advisor, Prof. Edson Cezar Wendland, for his invaluable guidance, patience, and support. I also express my sincere appreciation to Prof. Simon Papalexiou, and for my unofficial mentors, Profs. Antônio Meira Neto, Jamil Anache, and Paulo Tarso, for their insightful guidance, friendship, and encouragement throughout the doctoral process that were instrumental in shaping my research journey and academic pursuits.

To my lifelong friends. Your friendship have made this academic journey all the more meaningful and enjoyable. A special thanks to all my friends from the Laboratório de Hidráulica Computacional (LHC) and the friends from the University of Calgary, for the unforgettable moments shared.

I am deeply grateful to the São Carlos School of Engineering at the University of São Paulo (EESC/USP) for providing the institutional support and resources necessary for the completion of this thesis. I extend my appreciation to the Hydraulics and Sanitation program, particularly to Rose and Sá, for their assistance and support throughout this endeavor.

Finally, I acknowledge the financial support received from the Coordenação de Aperfeiçoamento de Pessoal de Nível Superior – Brasil (CAPES) – Grant Finance Code 001 and FAPESP (Grants: 2020/08140-0 and 2022/06017-1). Their support has been essential in facilitating the execution of this research project.

ABSTRACT

BALLARIN, A, S. **Future perspectives of extreme events and water availability in Brazilian catchments.** 2024. Tese – Doutorado – Escola de Engenharia de São Carlos, Universidade de São Paulo, São Carlos, 2024.

Global warming is projected to alter the frequency and magnitude of extreme events, posing major challenges to water resources worldwide. Understanding how these changes are projected to occur is paramount to tackle water scarcity-related experiences by guiding policymakers on developing local-to-regional adaptation plans. The present thesis has as its primary goal to investigate the projected impacts of climate change on extreme events and water availability in Brazilian catchments. To this end, we first present, in *Chapter 2*, the CLIMBra dataset, which comprises bias-corrected CMIP6 historical and future simulations for different climate variables for the Brazilian territory. These projections provide valuable insights into future climate scenarios and are the cornerstone for the development of the present thesis. By using the developed dataset, we further assessed how rainfall events of different magnitudes are projected to change across Brazilian catchments in *Chapter 3*. Our results indicated a widespread intensification of extreme rainfall events throughout the country, mainly dictated by changes in frequency, rather than intensity. Such projected changes in rainfall events, added to an expected increase in atmospheric water demand, are also expected to affect meteorological droughts across the Brazilian territory. As we show in *Chapter 4*, most of the evaluated Brazilian catchments are expected to experience longer, more intense, and frequent droughts in the future, with high CMIP6-model agreement. Beyond assessing projected changes of future drought events, we discussed in this chapter droughts' occurrence under both land use and water demand perspectives and propose a new framework to better understand their link with changes in long- and short-term conditions of precipitation and potential evapotranspiration. Finally, in *Chapter 5*, we propose a Budyko-based framework for assessing future water availability and security scenarios across Brazilian catchments, considering both climatic and anthropogenic factors. The study revealed that most catchments are expected to exhibit a worse water security condition by the end of the century, driven primarily by enhanced human water use. We believe the present thesis contributes to advancing the current understanding of climate variability and its impacts on hydrological processes and water resources management in Brazil. By providing insights into future climate change scenarios of extreme rainfall events, meteorological drought, and water availability, this research might be valuable to inform decision-making processes aimed at enhancing Brazilian water resilience in the face of global warming.

Keywords: Extreme events; global warming; heavy rainfall; droughts; water security.

RESUMO

BALLARIN, A, S. **Perspectivas futuras de eventos extremos e disponibilidade hídrica em bacias hidrográficas brasileiras.** 2024. Tese – Doutorado – Escola de Engenharia de São Carlos, Universidade de São Paulo, São Carlos, 2024.

O aquecimento global tem o potencial de modificar a frequência e intensidade dos eventos extremos, trazendo desafios significativos para os recursos hídricos globais. Uma melhor compreensão sobre como essas mudanças ocorrerão é fundamental para lidar com os desafios ligados à escassez hídrica, devido ao seu potencial de auxiliar na formulação de políticas de adaptação e mitigação das mudanças climáticas em diferentes escalas espaciais. Esta tese tem como objetivo principal examinar os potenciais impactos das mudanças climáticas nos eventos extremos e na disponibilidade hídrica das bacias hidrográficas brasileiras. Para isso, introduzimos, no Capítulo 2, a base de dados CLIMBra, que disponibiliza simulações históricas e futuras com correção de viés de modelos climáticos do CMIP6. Essas projeções oferecem informações cruciais sobre os potenciais impactos do aquecimento global no clima brasileiro e constituem a base para o desenvolvimento desta tese. Em sequência, utilizando esse conjunto de dados, avaliou-se no Capítulo 3, como os eventos de precipitação de diferentes magnitudes irão alterar no futuro. Os resultados indicaram que, em geral, eventos extremos de precipitação serão mais frequentes e intensos em todo o país no final do século, sendo que as mudanças esperadas na frequência superam às esperadas na magnitude. Essas mudanças, combinadas com o aumento esperado na demanda hídrica atmosférica, expressa em termos do potencial de evapotranspiração, também devem afetar as secas meteorológicas em todo o território brasileiro, conforme discutido no Capítulo 4. A maioria das bacias hidrográficas brasileiras avaliadas deve experienciar secas mais longas, intensas e frequentes no futuro. Além de avaliar as mudanças previstas nos eventos de seca futuros, foi discutido, no Capítulo 4, a ocorrência de secas sob as perspectivas do uso da terra e da demanda hídrica, propondo um novo quadro para entender melhor sua relação com as mudanças nas condições de precipitação e evapotranspiração potencial, tanto a curto quanto a longo prazo. Por fim, no Capítulo 5, avaliou-se, através de uma metodologia baseada na hipótese de Budyko, cenários futuros de disponibilidade e segurança hídrica no país, considerando tanto fatores climáticos quanto antropogênicos. O estudo revelou que a maioria das bacias hidrográficas deve apresentar uma condição de segurança hídrica pior no final do século, impulsionada principalmente pelo aumento da demanda hídrica. Acredita-se que a presente tese contribui para o avanço da compreensão atual da variabilidade climática e seus impactos nos processos hidrológicos e na gestão dos recursos hídricos no Brasil. Ao fornecer informações sobre cenários futuros de mudança climática de eventos extremos de precipitação, secas meteorológicas e disponibilidade hídrica, esta pesquisa representa uma contribuição valiosa para os processos de tomada de decisão associados aos recursos hídricos do país diante do aquecimento global.

Palavras-chave: Eventos extremos; aquecimento global; chuvas intensas; secas; segurança hídrica.

FIGURES LIST

Chapter 1

Chapter 2

Chapter 3

Chapter 4

Chapter 5

TABLE LIST

Chapter 2

Chapter 5

CONTENTS

CHAPTER 1

General Introduction

1.1 CONTEXTUALIZATION

Over the past few decades, there has been a notable increase in the scientific community's interest in studying extreme weather events (Diffenbaugh *et al.*, 2017). This heightened interest stems from the multifaceted impacts these events have on society, with significant implications for both human and natural systems (McBean; Rodgers, 2010). For instance, extreme rainfall often trigger flood events, resulting in countless human casualties and billions of dollars in infrastructure damage every year (Basso *et al.*, 2023; Bertola *et al.*, 2023). Drought events, on the water-deficit side, also inflict severe consequences on society, affecting different societal sectors, such as agricultural and food production, ecological system functioning, and economic activities (Chiang; Mazdiyasni; AghaKouchak, 2021; Dai, 2013; Trenberth *et al.*, 2014).

Despite high spatial variability of changes across the globe, both observations and model-based simulations suggest that extreme events have been more intense and severe in the last decades (Fischer; Knutti, 2016; Milly *et al.*, 2008). There is a wide scientific consensus that anthropogenic actions, along with other natural factors, have been contributing to changes in the hydrological cycle, which in turn lead to these increases in the magnitude and frequency of extreme weather events (Dai, 2013; Fischer; Knutti, 2015; Fischer; Sippel; Knutti, 2021; IPCC, 2022; Min *et al.*, 2011; Westra; Alexander; Zwiers, 2013). In fact, several studies have already identified positive trends in the frequency and/or magnitude of extremes across the globe (Vicente-Serrano *et al.*, 2022; Westra; Alexander; Zwiers, 2013), underscoring the need for efforts towards a better comprehension of global warming impacts on climate dynamics and potential driving mechanisms of extreme events.

In Brazil, various studies have sought to address this issue, recognizing the intensification of extreme weather events in the country, such as intense rainfall and historical droughts. In terms of heavy rainfall, Haylock *et al.* (2006) and Skansi *et al.*, (2013) observed positive trends in extreme precipitation events across the Brazilian territory. Similar results were found by Marengo *et al.*, (2020), Silva Dias *et al.*, (2013), and Zilli *et al.* (2017) for the Southeast region of the country. Cortez *et al.*, (2022) using future climate model simulations and a non-stationary approach, identified an intensification of extreme precipitation events over more than 90% of the national territory. Ballarin, Anache, and Wendland (2022)

observed a pattern of intensification in extreme precipitation events in the state of São Paulo, with more significant results for events with return periods of up to 10 years. Medeiros, Oliveira and Avila-Diaz, (2022), using future climate models-based simulations suggested that extreme events are expected to be more frequent and severe in the future. Regarding drought events, different studies reported an increase in the occurrence of such events in the national territory over the last few decades (Ballarin *et al.*, 2021; Coelho *et al.*, 2016; Filho *et al.*, 2020; Marengo *et al.*, 2008; Marengo; Torres; Alves, 2017; Nobre *et al.*, 2016).

Such intensification in the occurrence and magnitude of extreme events is accompanied by a greater likelihood of disasters, with numerous impacts in various systems (Getirana; Libonati; Cataldi, 2021; Libonati *et al.*, 2022; Travassos *et al.*, 2021). According to the IPCC (2022), the intensified climate is already impacting agricultural production, human health and ecosystem functioning in Brazil. For instance, the number of natural disaster occurrences more than doubled in 2000s compared to the 1990s, with more than 80% of these occurrences related to extreme droughts or intense rainfall events (CEPED/UFSC, 2013). In the global context, disaster events attributed to natural hazards affected approximately 100 million people and caused nearly 190 billion dollars of economic losses only in 2020 (Jones; Guha-Sapir; Tubeuf, 2022), and are expected to almost double in the future (Kreibich *et al.*, 2022).

Besides the impact on extreme events, climate change are also projected to affect water security in the country, reducing in more than 40% the water availability in some regions (ANA, 2024). These climate change effects on water resources, coupled with the growing water demand to support an ever-increasing population and agricultural expansion can pose a significant threat to the national water resources, despite the country's privileged position with respect to water resources (Gesualdo *et al.*, 2021). Therefore, given its potential impacts on both natural and social systems, it is paramount to enhance our understanding of global warming and its impacts on extreme events and water availability, seeking to improve mitigation and adaptation plans, risk and water resources management, and infrastructure design (Abdelmoaty; Papalexiou, 2023; Alam *et al.*, 2018).

The characterization of extreme weather events is usually grounded in the statistical frequency analysis (Nguyen; Nguyen, 2019). According to this approach, observed climate data are fitted to one or more probability distributions, which are used to associate events of

a certain magnitude with a frequency of occurrence, usually referred to as a return period (Ballarin *et al.*, 2022; Nguyen *et al.*, 2017). Thus, characteristic/design values and risk probabilities can be defined for the design of hydraulic systems. Despite being a well-established practice, the characterization of extreme events via statistical frequency analysis has a high degree of uncertainty (Salinas *et al.*, 2014a, 2014b). There are various modeling techniques, varying in the way historical series are obtained, the probability distribution models used, and the techniques for estimating their parameters (Gaume, 2018; Nerantzaki; Papalexiou, 2022; Okoli *et al.*, 2019), without a consensus on the most appropriate procedure.

This methodological variability results in a high degree of uncertainty, potentially leading to severe under- or overestimations of extreme events due to a misrepresentation of the variable of interest (Papalexiou; Koutsoyiannis, 2013). Furthermore, this methodology assumes that historical data are representative of the future behavior, enabling the inference of future properties from the observed, historical data (Lins; Cohn, 2011). Hence, it implicitly assumes that no significant changes will occur in the properties of the observed variables (i.e., stationarity; Ragno *et al.*, 2018) . However, in the current context of global warming and associated heightened extreme events (Asadieh; Krakauer, 2015), the representativeness of past events is under scrutiny (Ballarin *et al.*, 2022; Merz; Blöschl, 2008; Montanari; Koutsoyiannis, 2014).

To address this issue and take into account the potential impacts of global warming in the characterization process, several studies have been considering temporal variations in climate variables through the use of nonstationary models (Abdelmoaty; Papalexiou, 2023; Cheng *et al.*, 2014; Cheng; Aghakouchak, 2014; Kwon; Lall, 2016; Ragno *et al.*, 2018, 2019; Salas; Obeysekera, 2014; Salas; Obeysekera; Vogel, 2018). Nevertheless, despite addressing potential changes in climate variables, these models still rely on observed data to infer the behavior of possible future trends. Therefore, they are highly influenced by the availability and quality of the observed data and their statistical properties. Besides, nonstationary models require a deep understanding of the causal relationships between the climate variables involved in the phenomenon under study (Serinaldi; Kilsby, 2015). When these relationships are not precisely understood, the use of nonstationary models only adds more sources of uncertainty to the analysis (Koutsoyiannis; Montanari, 2015). Due to these

limitations, the use of these models has been widely questioned (and criticized) in recent studies, as they can result in unrealistic values and misrepresent the statistical properties of the natural phenomenon of interest (Cohn; Lins, 2005; Koutsoyiannis; Montanari, 2015; Luke *et al.*, 2017; Montanari; Koutsoyiannis, 2014; Serinaldi; Kilsby, 2015).

An alternative to solely relying on historical data to infer statistical properties of future events is the use of Earth System Models (ESMs, also called GCMs; Fischer; Sippel; Knutti, 2021; Hosseinzadehtalaei; Tabari; Willems, 2018; Li *et al.*, 2023; Schardong; Simonovic, 2019; So *et al.*, 2017; Zhang *et al.*, 2023). Such models are capable to consider the interplay between various components of the Earth System, including the atmosphere, oceans, land surface, cryosphere, and biosphere; being widely used to study the Earth's climate and its response to external forcings to project future climate under different socio-economic development conditions (Eyring *et al.*, 2016; O'Neill *et al.*, 2016; Tebaldi *et al.*, 2021). Despite their valuable contribution in advancing our understanding of the Earth climate system, ESMs/GCMs usually exhibit (i) low spatial and temporal resolution, which hampers their use for certain practical purposes, such as for the design and management of hydraulic systems in small catchments (Srivastav; Schardong; Simonovic, 2014); and (ii) systematic errors, failing to represent the different statistical properties of observed events (Abdelmoaty *et al.*, 2021; Papalexiou *et al.*, 2021).

Given these limitations, the use of ESMs/GCMs often requires further post-processing and bias-correction techniques to improve their spatiotemporal resolution and enhance models' performance in characterizing local observed events, respectively (Bürger *et al.*, 2013; So *et al.*, 2017; Werner; Cannon, 2016; Xu *et al.*, 2021). These techniques, usually called downscaling, can be classified in two categories: dynamic and statistical. In the former, boundary conditions derived from ESMs/GCMs are used to run fine-resolution, regional climate models (RCMs) that consider local features and dynamics, such as topography and its impact on atmospheric circulations, to improve simulations' resolution and representativeness (Chou *et al.*, 2014b, 2014a). The statistical downscaling, in contrast, relies on applying statistical transfer functions or mapping schemes to the ESMs/GCMs simulations to resemble locally observed data (Cannon; Sobie; Murdock, 2015). Given to its relatively lower computational efforts and higher performance in representing observed variables, the statistical downscaling is usually preferred over the dynamical one (Zhang *et al.*, 2020).

Nevertheless, their use are still not widespread across the country, with only few studies adopting bias-correction/downscaling techniques for climate-change impact assessments (Ferreira *et al.*, 2023). In general, previous studies focused on specific regions of the country and/or relied on previous versions of the climate models of the Coupled Model Intercomparison Project (CMIP).

In view of the aforementioned, namely (a) the heightened occurrence and consequent impacts of extreme events in the country over the past few decades; (b) the variability of methodologies employed to address the potential effects of global warming on the water cycle and weather extremes; and (c) the lack of countrywide climate-change impacts assessment using the climate simulations from the sixth phase of the Intergovernmental Panel on Climate Change (GCMs), it becomes imperative to develop new researches aiming to enhance our understanding of the potential consequences of global warming in Brazil. These studies are pivotal to guide climate change mitigation and adaptation policies and help-decision makers to improve water resources management. For example, an enhanced understanding of how different rainfall events (i.e, light, moderate, or heavy) are projected to change spatially in the future is a crucial information for an effective allocation of public resources, prioritizing the development of hydraulic infrastructure where heavy rainfall events are expected to increase or reservoirs systems where total rainfall is expected to decrease. Such information is also fundamental for developing risk management, insurance-based practices to mitigate potential financial losses due to the effects of climate change on the water cycle (Gesualdo *et al.*, 2024).

1.2 Problem Statement and Objectives

The present thesis has the following research questions: *(a) How are extreme events and water availability projected to change in the future across Brazilian catchments, and (b) how will these changes impact both Brazilian natural and social systems?* As far as we know, no study has investigated these aspects yet using bias-corrected, CMIP6 simulations from a catchment-scale, countrywide perspective. Given the myriad of aspects that can be explored when dealing with future climate-change based simulations and their impacts on climate dynamics and water cycle, here we bounded the ultimate purpose of this research to

assessing projected changes in future water availability, heavy rainfall, and meteorological droughts, along with their potential impacts. To this end, we delineated the following specific objectives:

i. Consolidate a national climate-change dataset, encompassing both raw and bias-corrected CMIP6 historical and future simulations, in both gridded and catchment scales, seeking to advance climate change impact assessments in the country;
ii. Assess the performance of raw and bias-corrected CMIP6 simulations in representing observed historical data;
iii. Explore projected changes in the frequency and intensity of future rainfall events of different magnitudes across Brazilian catchments, assessing the role of this properties on driving future changes;
iv. Investigate how meteorological droughts are projected to change in different CMIP6-based future scenarios and their potential impacts across Brazilian catchments, exploring the potential meteorological drivers of future droughts;
v. Explore expected changes in future water security of Brazilian catchments, contrasting the effects of climate change and human behavior (i.e., water demand) in dictating these changes;

1.3 Thesis Outline

In *Chapter 2*, we described the methodology designed to develop the CLIMBra – Climate Change Dataset for Brazil. The dataset encompasses raw and bias-corrected CMIP6 simulations for both historical and future periods. *Chapter 2* serves as the cornerstone of the entire thesis, as no national, bias-corrected CMIP6 dataset was available during the thesis development. Some global-scale datasets have emerged since then (e.g., Gebrechorkos *et al.*, 2023; Thrasher *et al.*, 2022), but they do not encompass all the variables required to conduct the analysis proposed in the following chapters and do not use national, station-based observations in the bias-correcting procedure, relying on satellite and/or reanalysis data. The findings of *Chapter 2* were published in the *Scientific Data* (Ballarin *et al.*, 2023b), and are freely available at: https://doi.org/10.1038/s41597-023-01956-z.

In *Chapter 3*, we assessed projected changes in the frequency and magnitude of different rainfall events (e.g, light, moderate, and heavy), and further discussed the role of these two properties (intensity and frequency) in driving future rainfall events. This aspect is usually neglected in climate-based impact assessments - which commonly focus solely in intensity to assess future rainfall changes - but is fundamental for guiding water resources management practices (Markonis *et al.*, 2019). The results found in *Chapter 3* were published in the international journal *Earth's Future* (Ballarin *et al.*, 2024b), and are freely available at: https://doi.org/10.1029/2023EF004053.

In *Chapter 4*, we explored how meteorological droughts are projected to changes according to future CMIP6-based scenarios across Brazilian catchments. We further assessed such changes in view of both land-cover and water-demand perspectives, discussing how changes in meteorological droughts can affect forest, pasture and croplands and water security, respectively. Finally, we explored the relationship between projected changes in meteorological drought characteristics and meteorological properties, shedding light on the link between atmospheric demand and supply (potential evapotranspiration and precipitation) and drought events. The results of *Chapter 4* were published in the *Environmental Research Letters* (Ballarin *et al.*, 2024a) and are freely available at: https://doi.org/10.1088/1748-9326/ad3e18.

In *Chapter 5,* we investigated future water security scenarios in the national territory. Employing a Budyko-based, water-balance framework future water-demand projections of the Manual of Consumptive Water Use in Brazil (ANA, 2019), we assessed future projections of water availability and security in the country, and discussed the drawbacks of some traditional assumptions (e.g., open vs closed water balance and neglecting CO_2 effects on plants water use) in assessing water availability. The results of *Chapter 5* were published in *Water Resources Research* (Ballarin *et al.*, 2023a), and are available at: https://doi.org/10.1029/2023WR034914.

The general conclusion of the thesis is drawn in *Chapter 6*, where we discussed and summarized the main conclusions of each previous chapter, highlighting some limitations and recommendations of potential future research opportunities. In Figure 1.1, we display a flowchart with the core steps of this research, linking each Chapter with the specific

objectives. Namely, In *Chapter 2, 3, 4,* and *5* we addressed the specific objective i, iii, iv, and v, respectively, whereas the specific objective ii was tackled in all Chapters.

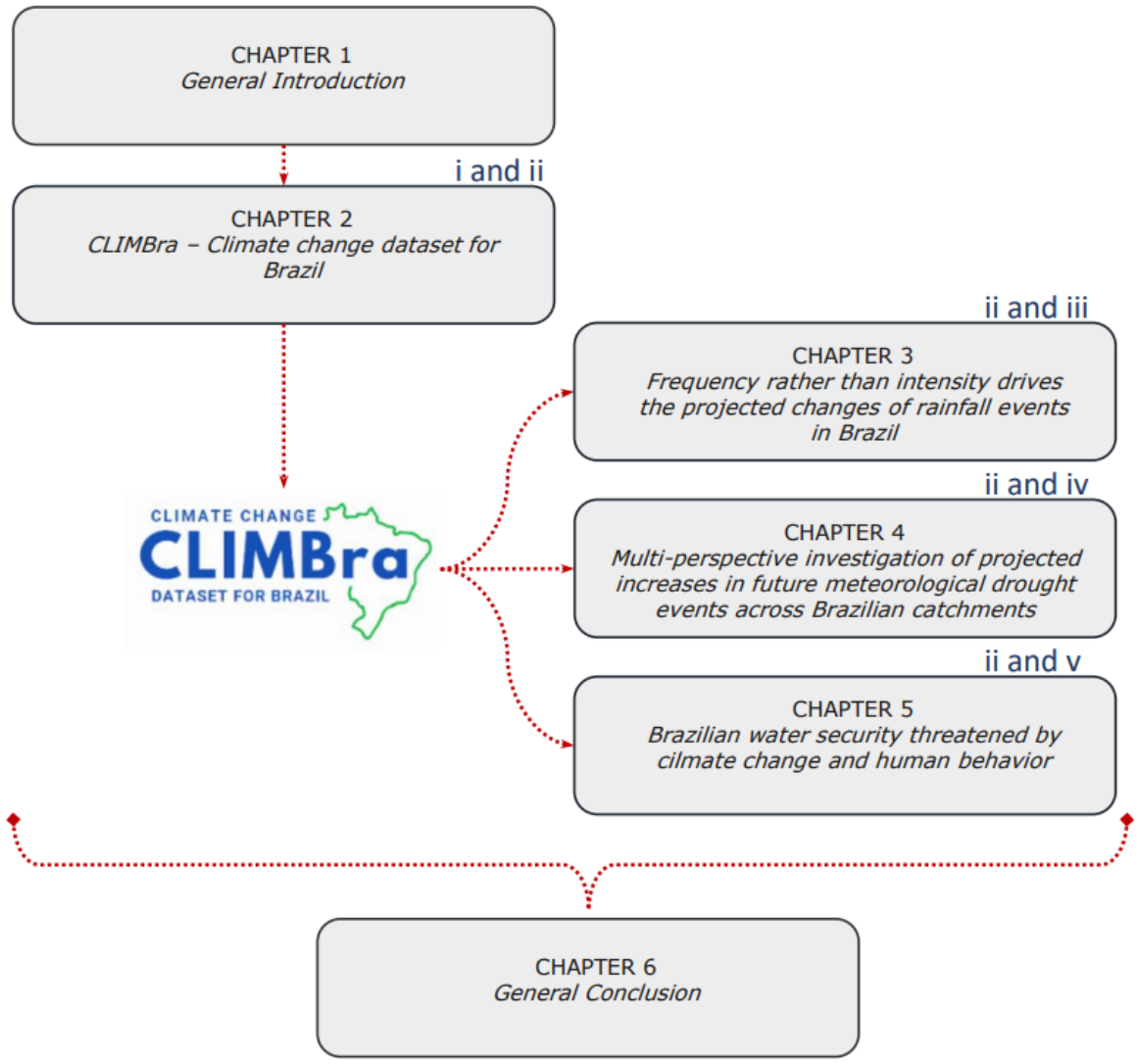

Figure 1.1. Schematic diagram depicting the outline of the thesis structure liking each thesis' chapters with the specific objectives (in dark blue, on the top-right corner.

1.4 REFERENCES

ABDELMOATY, H. M. *et al.* Biases Beyond the Mean in CMIP6 Extreme Precipitation: A Global Investigation. **Earth's Future**, [*s. l.*], v. 9, n. 10, p. 1–17, 2021.

ABDELMOATY, H. M.; PAPALEXIOU, S. M. Changes of Extreme Precipitation in CMIP6 Projections: should We use Stationary or Nonstationary Models?. **Journal of Climate**, [*s. l.*], n. January, p. 1–40, 2023.

ALAM, M. A. *et al.* Best-fit probability distributions and return periods for maximum monthly rainfall in Bangladesh. **Climate**, [*s. l.*], v. 6, n. 1, 2018.

ANA. **Impacto da Mundança Climática nos Recursos Hídricos do Brasil**. Brasilia, Brazil: [*s. n.*], 2024.

ANA. **Manual of Consumptive Water Use in Brazil**. Brasilia, Brazil: [*s. n.*], 2019.

ASADIEH, B.; KRAKAUER, N. Y. Global trends in extreme precipitation: Climate models versus observations. **Hydrology and Earth System Sciences**, [*s. l.*], v. 19, n. 2, p. 877–891, 2015.

BALLARIN, A. S. *et al.* A copula-based drought assessment framework considering global simulation models. **Journal of Hydrology: Regional Studies**, [*s. l.*], v. 38, n. October, p. 0–3, 2021.

BALLARIN, A. S. *et al.* Brazilian Water Security Threatened by Climate Change and Human Behavior. **Water Resources Research**, [*s. l.*], v. 59, p. e2023WR034914, 2023a.

BALLARIN, A. S. *et al.* CLIMBra - Climate Change Dataset for Brazil. **Scientific Data**, [*s. l.*], p. 1–31, 2023b.

BALLARIN, A. S. *et al.* Combined predictive and descriptive tests for extreme rainfall probability distribution selection. **Hydrological Sciences Journal**, [*s. l.*], n. May, 2022.

BALLARIN, A. S. *et al.* Drought intensification in Brazilian catchments: implications for water and land management. **Environmental Research Letters**, [*s. l.*], n.5, v. 19, p. 054030, 2024a.

BALLARIN, A. S. *et al.* Frequency Rather Than Intensity Drives Projected Changes of Rainfall Events in Brazil. **Earth's Future**, [*s. l.*], v. 12, n. 1, p. e2023EF004053, 2024b.

BALLARIN, A. S.; ANACHE, J. A. A.; WENDLAND, E. Trends and abrupt changes in extreme rainfall events and their influence on design quantiles: a case study in São Paulo, Brazil. **Theoretical and Applied Climatology**, [*s. l.*], v. 149, n. 3–4, p. 1753–1767, 2022.

BASSO, S. *et al.* Extreme flooding controlled by stream network organization and flow regime. **Nature Geoscience**, [*s. l.*], v. 16, n. 4, p. 339–343, 2023.

BERTOLA, M. *et al.* Megafloods in Europe can be anticipated from observations in hydrologically similar catchments. **Nature Geoscience**, [*s. l.*], v. 16, n. 11, p. 982–988, 2023.

BÜRGER, G. *et al.* Downscaling extremes: An intercomparison of multiple methods for future climate. **Journal of Climate**, [*s. l.*], v. 26, n. 10, p. 3429–3449, 2013.

CANNON, A. J.; SOBIE, S. R.; MURDOCK, T. Q. Bias correction of GCM precipitation by quantile mapping: How well do methods preserve changes in quantiles and extremes?. **Journal of Climate**, [*s. l.*], v. 28, n. 17, p. 6938–6959, 2015.

CEPED/UFSC. **Atlas brasileiro de desastres naturais 1991 a 2012: volume Brasil**. Florianópolis: Universidade Federal de Santa Catarina, 2013.

CHENG, L. *et al.* Non-stationary extreme value analysis in a changing climate. **Climatic Change**, [*s. l.*], v. 127, n. 2, p. 353–369, 2014.

CHENG, L.; AGHAKOUCHAK, A. Nonstationary precipitation intensity-duration-frequency curves for infrastructure design in a changing climate. **Scientific Reports**, [*s. l.*], v. 4, p. 1–6, 2014.

CHIANG, F.; MAZDIYASNI, O.; AGHAKOUCHAK, A. Evidence of anthropogenic impacts on global drought frequency, duration, and intensity. **Nature Communications**, [*s. l.*], v. 12, n. 1, p. 1–10, 2021.

CHOU, S. C. *et al.* Assessment of Climate Change over South America under RCP 4.5 and 8.5 Downscaling Scenarios. **American Journal of Climate Change**, [*s. l.*], v. 03, n. 05, p. 512–527, 2014a.

CHOU, S. C. *et al.* Evaluation of the Eta Simulations Nested in Three Global Climate Models. **American Journal of Climate Change**, [*s. l.*], v. 03, n. 05, p. 438–454, 2014b.

COELHO, C. A. S. *et al.* The 2014 southeast Brazil austral summer drought: regional scale mechanisms and teleconnections. **Climate Dynamics**, [*s. l.*], v. 46, n. 11–12, p. 3737–3752, 2016.

COHN, T. A.; LINS, H. F. Nature's style: Naturally trendy. **Geophysical Research Letters**, [*s. l.*], v. 32, n. 23, p. 1–5, 2005.

CORTEZ, B. N. *et al.* Nonstationary extreme precipitation in Brazil. **Hydrological Sciences Journal**, [*s. l.*], v. 67, n. 9, p. 1372–1383, 2022.

DAI, A. Increasing drought under global warming in observations and models. **Nature Climate Change**, [*s. l.*], v. 3, n. 1, p. 52–58, 2013.

DIFFENBAUGH, N. S. *et al.* Quantifying the influence of global warming on unprecedented extreme climate events. **Proceedings of the National Academy of Sciences of the United States of America**, [*s. l.*], v. 114, n. 19, p. 4881–4886, 2017.

EYRING, V. *et al.* Overview of the Coupled Model Intercomparison Project Phase 6 (CMIP6) experimental design and organization. **Geoscientific Model Development**, [*s. l.*], v. 9, n. 5, p. 1937–1958, 2016.

FERREIRA, G. W. de S. *et al.* Assessment of Precipitation and Hydrological Droughts in South America through Statistically Downscaled CMIP6 Projections. **Climate**, [*s. l.*], 2023.

FILHO, J. D. P. *et al.* Copula-Based Multivariate Frequency Analysis of the 2012–2018 Drought in Northeast Brazil. **Water 2020, Vol. 12, Page 834**, [*s. l.*], v. 12, n. 3, p. 834, 2020.

FISCHER, E. M.; KNUTTI, R. Anthropogenic contribution to global occurrence of heavy-precipitation and high-temperature extremes. **Nature Climate Change**, [*s. l.*], v. 5, n. 6, p. 560–564, 2015.

FISCHER, E. M.; KNUTTI, R. Observed heavy precipitation increase confirms theory and early models. **Nature Climate Change**, [*s. l.*], v. 6, n. 11, p. 986–991, 2016.

FISCHER, E. M.; SIPPEL, S.; KNUTTI, R. Increasing probability of record-shattering climate extremes. **Nature Climate Change**, [*s. l.*], v. 11, n. 8, p. 689–695, 2021.

GAUME, E. Flood frequency analysis: The Bayesian choice. **Wiley Interdisciplinary Reviews: Water**, [*s. l.*], v. 5, n. 4, p. e1290, 2018.

GEBRECHORKOS, S. *et al.* A high-resolution daily global dataset of statistically downscaled CMIP6 models for climate impact analyses. **Scientific Data**, [*s. l.*], v. 10, n. 1, p. 1–15, 2023.

GESUALDO, G. C. *et al.* Index-based insurance to mitigate current and future extreme events financial losses for water utilities. **International Journal of Disaster Risk Reduction**, [*s. l.*], v. 100, p. 104218, 2024.

GESUALDO, G. C. *et al.* Unveiling water security in Brazil: current challenges and future perspectives. **Hydrological Sciences Journal**, [*s. l.*], v. 66, n. 5, p. 759–768, 2021.

GETIRANA, A.; LIBONATI, R.; CATALDI, M. Brazil is in water crisis — it needs a drought plan. **Nature**, [*s. l.*], v. 600, n. 7888, p. 218–220, 2021.

HAYLOCK, M. R. *et al.* Trends in total and extreme South American rainfall in 1960-2000 and links with sea surface temperature. **Journal of Climate**, [*s. l.*], v. 19, n. 8, p. 1490–1512, 2006.

HOSSEINZADEHTALAEI, P.; TABARI, H.; WILLEMS, P. Precipitation intensity–duration–frequency curves for central Belgium with an ensemble of EURO-CORDEX simulations,

and associated uncertainties. **Atmospheric Research**, [*s. l.*], v. 200, n. September 2016, p. 1–12, 2018.

IPCC. **Climate Change 2022: Impacts, Adaptation, and Vulnerability.** Cambridge, UK and New York, NY, USA,: Cambridge University Press, 2022.

JONES, R. L.; GUHA-SAPIR, D.; TUBEUF, S. Human and economic impacts of natural disasters: can we trust the global data?. **Scientific Data**, [*s. l.*], v. 9, n. 1, p. 572, 2022.

KOUTSOYIANNIS, D.; MONTANARI, A. Negligent killing og scientific concepts: the stationarity case. **Hydrological Sciences Journal**, [*s. l.*], v. 60, n. 7–8, p. 1174–1183, 2015.

KREIBICH, H. *et al.* The challenge of unprecedented floods and droughts in risk management. **Nature**, [*s. l.*], v. 608, n. 7921, p. 80–86, 2022.

KWON, H.-H.; LALL, U. A copula-based nonstationary frequency analysis for the 2012–2015 drought in California. **Water Resources Research**, [*s. l.*], v. 52, p. 5662–5675, 2016.

LI, B. *et al.* Future Global Population Exposure to Record-Breaking Climate Extremes. **Earth's Future**, [*s. l.*], v. 11, p. e2023EF003786, 2023.

LIBONATI, R. *et al.* Drought–heatwave nexus in Brazil and related impacts on health and fires: A comprehensive review. **Annals of the New York Academy of Sciences**, [*s. l.*], v. 1517, n. 1, p. 44–62, 2022.

LINS, H. F.; COHN, T. A. Stationarity: Wanted dead or alive?. **Journal of the American Water Resources Association**, [*s. l.*], v. 47, n. 3, p. 475–480, 2011.

LUKE, A. *et al.* Predicting nonstationary flood frequencies: Evidence supports an updated stationarity thesis in the United States. **Water Resources Research**, [*s. l.*], v. 53, p. 5469–5494, 2017.

MARENGO, J. A. *et al.* The drought of Amazonia in 2005. **Journal of Climate**, [*s. l.*], v. 21, n. 3, p. 495–516, 2008.

MARENGO, J. A. *et al.* Trends in extreme rainfall and hydrogeometeorological disasters in the Metropolitan Area of São Paulo: a review. **Annals of the New York Academy of Sciences**, [*s. l.*], p. 1–16, 2020.

MARENGO, J. A.; TORRES, R. R.; ALVES, L. M. Drought in Northeast Brazil—past, present, and future. **Theoretical and Applied Climatology**, [*s. l.*], v. 129, n. 3–4, p. 1189–1200, 2017.

MARKONIS, Y. *et al.* Assessment of Water Cycle Intensification Over Land using a Multisource Global Gridded Precipitation DataSet. **Journal of Geophysical Research: Atmospheres**, [*s. l.*], v. 124, n. 21, p. 11175–11187, 2019.

MCBEAN, G.; RODGERS, C. Climate hazards and disasters: The need for capacity building. **Wiley Interdisciplinary Reviews: Climate Change**, [*s. l.*], v. 1, n. 6, p. 871–884, 2010.

MEDEIROS, F. j.; OLIVEIRA, C. P.; AVILA-DIAZ, A. Evaluation of extreme precipitation climate indices and their projected changes for Brazil: From CMIP3 to CMIP6. **Weather and Climate Extremes**, [*s. l.*], v. 38, n. July, p. 100511, 2022.

MERZ, R.; BLÖSCHL, G. Flood frequency hydrology: 1. Temporal, spatial, and causal expansion of information. **Water Resources Research**, [*s. l.*], v. 44, n. 8, p. 1–17, 2008.

MILLY, P. C. D. *et al.* Stationarity is dead: Whither water management?. **Science**, [*s. l.*], v. 319, n. 5863, p. 573–574, 2008.

MIN, S. K. *et al.* Human contribution to more-intense precipitation extremes. **Nature**, [*s. l.*], v. 470, n. 7334, p. 378–381, 2011.

MONTANARI, A.; KOUTSOYIANNIS, D. Modeling and mitigating natural hazards: Stationarity is immortal!. **Water Resources Research**, [*s. l.*], n. 50, p. 9748–9756, 2014.

NERANTZAKI, S. D.; PAPALEXIOU, S. M. Assessing extremes in hydroclimatology: A review on probabilistic methods. **Journal of Hydrology**, [*s. l.*], v. 605, n. December 2021, p. 127302, 2022.

NGUYEN, T. H. *et al.* A systematic approach to selecting the best probability models for annual maximum rainfalls – A case study using data in Ontario (Canada). **Journal of Hydrology**, [*s. l.*], v. 553, p. 49–58, 2017.

NGUYEN, T. H.; NGUYEN, V. T. V. Decision-Support Tool for Constructing Robust Rainfall IDF Relations in Consideration of Model Uncertainty. **Journal of Hydrologic Engineering**, [*s. l.*], v. 24, n. 7, p. 1–10, 2019.

NOBRE, C. A. *et al.* Some Characteristics and Impacts of the Drought and Water Crisis in Southeastern Brazil during 2014 and 2015. **Journal of Water Resource and Protection**, [*s. l.*], v. 8, n. 2, p. 252–262, 2016.

OKOLI, K. *et al.* Design flood estimation: Exploring the potentials and limitations of two alternative approaches. **Water (Switzerland)**, [*s. l.*], v. 11, n. 4, 2019.

O'NEILL, B. C. *et al.* The Scenario Model Intercomparison Project (ScenarioMIP) for CMIP6. **Geoscientific Model Development**, [*s. l.*], v. 9, n. 9, p. 3461–3482, 2016.

PAPALEXIOU, S. M. *et al.* Probabilistic Evaluation of Drought in CMIP6 Simulations. **Earth's Future**, [*s. l.*], v. 9, n. 10, p. 1–18, 2021.

PAPALEXIOU, S. M.; KOUTSOYIANNIS, D. Battle of extreme value distributions: A global survey on extreme daily rainfall. **Water Resources Research**, [*s. l.*], v. 49, n. 1, p. 187–201, 2013.

RAGNO, E. *et al.* A generalized framework for process-informed nonstationary extreme value analysis. **Advances in Water Resources**, [*s. l.*], v. 130, p. 270–282, 2019.

RAGNO, E. *et al.* Quantifying Changes in Future Intensity-Duration-Frequency Curves Using Multimodel Ensemble Simulations. **Water Resources Research**, [*s. l.*], v. 54, n. 3, p. 1751–1764, 2018.

SALAS, J. D.; OBEYSEKERA, J. Revisiting the concepts of return period and risk for nonstationary hydrologic extreme events. **Journal of Hydrologic Engineering**, [*s. l.*], v. 19, n. 3, p. 554–568, 2014.

SALAS, J. D.; OBEYSEKERA, J.; VOGEL, R. M. Techniques for assessing water infrastructure for nonstationary extreme events: a review. **Hydrological Sciences Journal**, [*s. l.*], v. 63, n. 3, p. 325–352, 2018.

SALINAS, J. L. *et al.* Regional parent flood frequency distributions in Europe - Part 1: Is the GEV model suitable as a pan-European parent?. **Hydrology and Earth System Sciences**, [*s. l.*], v. 18, n. 11, p. 4381–4389, 2014a.

SALINAS, J. L. *et al.* Regional parent flood frequency distributions in Europe - Part 2: Climate and scale controls. **Hydrology and Earth System Sciences**, [*s. l.*], v. 18, n. 11, p. 4391–4401, 2014b.

SCHARDONG, A.; P. SIMONOVIC, S. Application of Regional Climate Models for Updating Intensity-duration-frequency Curves under Climate Change. **International Journal of Environment and Climate Change**, [*s. l.*], v. 9, n. 5, p. 311–330, 2019.

SERINALDI, F.; KILSBY, C. G. Stationarity is undead: Uncertainty dominates the distribution of extremes. **Advances in Water Resources**, [*s. l.*], v. 77, p. 17–36, 2015.

SILVA DIAS, M. A. F. *et al.* Changes in extreme daily rainfall for São Paulo, Brazil. **Climatic Change**, [*s. l.*], v. 116, n. 3–4, p. 705–722, 2013.

SKANSI, M. de los M. *et al.* Warming and wetting signals emerging from analysis of changes in climate extreme indices over South America. **Global and Planetary Change**, [*s. l.*], v. 100, p. 295–307, 2013.

SO, B. J. *et al.* Stochastic extreme downscaling model for an assessment of changes in rainfall intensity-duration-frequency curves over South Korea using multiple regional climate models. **Journal of Hydrology**, [*s. l.*], v. 553, p. 321–337, 2017.

SRIVASTAV, R. K.; SCHARDONG, A.; SIMONOVIC, S. P. Equidistance Quantile Matching Method for Updating IDFCurves under Climate Change. **Water Resources Management**, [*s. l.*], v. 28, n. 9, p. 2539–2562, 2014.

TEBALDI, C. *et al.* Climate model projections from the Scenario Model Intercomparison Project (ScenarioMIP) of CMIP6. **Earth System Dynamics**, [*s. l.*], v. 12, p. 253–293, 2021.

THRASHER, B. *et al.* NASA Global Daily Downscaled Projections, CMIP6. **Scientific Data**, [*s. l.*], p. 1–6, 2022.

TRAVASSOS, L. *et al.* Why do extreme events still kill in the São Paulo Macro Metropolis Region? Chronicle of a death foretold in the global south. **International Journal of Urban Sustainable Development**, [*s. l.*], v. 13, n. 1, p. 1–16, 2021.

TRENBERTH, K. E. *et al.* Global warming and changes in drought. **Nature Climate Change**, [*s. l.*], v. 4, n. 1, p. 17–22, 2014.

VICENTE-SERRANO, S. M. *et al.* Global drought trends and future projections. **Philosophical Transactions of the Royal Society A: Mathematical, Physical and Engineering Sciences**, [*s. l.*], v. 380, n. 2238, 2022.

WERNER, A. T.; CANNON, A. J. Hydrologic extremes - An intercomparison of multiple gridded statistical downscaling methods. **Hydrology and Earth System Sciences**, [*s. l.*], v. 20, n. 4, p. 1483–1508, 2016.

WESTRA, S.; ALEXANDER, L. V.; ZWIERS, F. W. Global increasing trends in annual maximum daily precipitation. **Journal of Climate**, [*s. l.*], v. 26, n. 11, p. 3904–3918, 2013.

XU, Z. *et al.* Bias-corrected CMIP6 global dataset for dynamical downscaling of the historical and future climate (1979–2100). **Scientific Data**, [*s. l.*], v. 8, n. 1, p. 1–11, 2021.

ZHANG, L. *et al.* Comparison of Statistical and Dynamic Downscaling Techniques in Generating High-Resolution Temperatures in China from CMIP5 GCMs. **Journal of Applied Meteorology and Climatology**, [*s. l.*], v. 59, n. 2, p. 207–235, 2020.

ZHANG, Y. *et al.* Future global streamflow declines are probably more severe than previously estimated. **Nature Water**, [*s. l.*], 2023.

ZILLI, M. T. *et al.* A comprehensive analysis of trends in extreme precipitation over southeastern coast of Brazil. **International Journal of Climatology**, [*s. l.*], v. 37, n. 5, p. 2269–2279, 2017.

CHAPTER 2

CLIMBra – Climate change dataset for Brazil

ABSTRACT

General Circulation and Earth System Models are the most advanced tools for investigating climate responses to future scenarios of greenhouse gas emissions, playing the role of projecting the climate throughout the century. Nevertheless, climate projections are model-dependent and may show systematic biases, requiring a bias correction for any further application. Here, we provide a dataset based on an ensemble of 19 bias-corrected CMIP6 climate models projections for the Brazilian territory based on the SSP2-4.5 and SSP5-8.5 scenarios. We used the Quantile Delta Mapping approach to bias-correct daily time-series of precipitation, maximum and minimum temperature, solar net radiation, near-surface wind speed, and relative humidity. The bias-corrected dataset is available for both historical (1980-2013) and future (2015-2100) simulations at a 0.25° × 0.25° spatial resolution. Besides the gridded product, we provide area-averaged projections for 735 catchments included in the Catchments Attributes for Brazil (CABra) dataset. The dataset provides important variables commonly used in environmental and hydroclimatological studies, paving the way for the development of high-quality research on climate change impacts in Brazil.

2.1 INTRODUCTION

General Circulation and Earth System Models (GCMs/ESMs) play an important role in simulating the physics and dynamics of the Earth system, as well as in assessing and understanding projected changes in the global climate (Ukkola *et al.*, 2018; Werner; Cannon, 2016). The employment of climate models along with observed meteorological data is key to inform policy and decision-making based on hydroclimatic modelling (Mishra; Bhatia; Tiwari, 2020; Moustakis *et al.*, 2021; Ombadi *et al.*, 2018; Tang; Clark; Papalexiou, 2022). Nevertheless, to provide a large volume of climatic data at a global scale, GCMs/ESMs often present (i) coarse spatial resolution (100-300 km), hampering the development of reliable and detailed studies at finer scales (Gao *et al.,* 2022); and (ii) systematic biases, leading to misrepresentation of different statistical properties of observed climate variables (Abdelmoaty *et al.,* 2021; Papalexiou *et al.,* 2021). Apart from these two limitations, these climate models have intrinsic uncertainties that undermine studies on climate change impacts (Xu *et al.,* 2021). In this context, statistical and dynamical downscaling approaches are used to bridge the inherent gap between projected and observed data by improving the spatial resolution of GCMs products to a finer scale. Dynamical downscaling is based on the integration of Regional Climate Models (RCMs) — which are able to capture local features and dynamics to better represent the climate of a specific and limited area — with the initial and lateral boundary conditions derived from GCMs (Chou *et al.,* 2014; Lyra *et al.,* 2018). Despite the improvement in GCMs resolution and the incorporation of local scale-effects into their projections, RCMs may still contain systematic biases that are propagated through the future simulations. These remaining biases, derived from the GCMs used or incorporated during the dynamical downscaling procedure due to limited understanding of the processes, may lead to the need of further corrections of the dynamically downscaled product (Ballarin *et al.,* 2021; Kotlarski *et al.,* 2014; Xu; Yang, 2012) at a large computational effort (Simonovic *et al.,* 2016). On the other hand, the statistical downscaling is based on statistical transfer functions that adjust the probability distribution function of projections to resemble observed data at local/regional sites (Gudmundsson *et al.,* 2012). The statistical framework is able to correct systematic biases found in the original projections of both RCMs - generally referred to as “hybrid downscaling” (Bedia *et al.,* 2020; Turco *et al.,* 2011) - and GCMs using simple modelling structures that require less computational effort (Cannon; Sobie; Murdock,

2015; Mandal; Srivastav; Simonovic, 2016). Given these advantages, the statistical approach is generally preferred over the dynamical for climate-based studies (Gutmann *et al.,* 2014; Mishra; Bhatia; Tiwari, 2020).

Despite the importance of a dataset with historical and future data for meteorological and hydrological studies, to our knowledge there is no dataset of bias-corrected climate change data available for the Brazilian territory based on the recently released Sixth Assessment Report (AR6) of the Coupled Model Intercomparison Project phase 6 (CMIP6). Brazil is a continental country with diverse hydroclimatic conditions, and climate-related hazards have become more frequent, widespread, and interconnected (Dalagnol *et al.,* 2022; Feng *et al.,* 2021; Filho *et al.,* 2020; Marengo; Torres; Alves, 2017; Nobre *et al.,* 2016, 2013). Thereby, here we developed the Climate Change Dataset for Brazil - CLIMBra, a bias-corrected dataset comprising six important meteorological variables used in hydro-climatic and economic studies related to climate change: precipitation (pr), maximum (tasmax) and minimum temperature (tasmin), net shortwave surface radiation (rss), near-surface wind speed (sfcWind) and relative humidity (hur). Besides the bias-corrected gridded daily data at a spatial resolution of 0.25°, we provide an area-averaged, point-based scale data for 735 catchments of the Catchments Attribute for Brazil (CABra) large-sample dataset (Almagro *et al.,* 2021). The developed dataset consists of bias-corrected historical (1980-2013) and future (2015-2100) simulations of 19 GCMs/ESMs, forced by the CMIP6 SSP2-4.5 and SSP5-8.5 scenarios.

2.2 METHODS

2.2.1 DATASETS

To generate the bias-corrected product, we used observed data covering the historical period (1980 - 2013) and simulated data covering both historical and future (2015 - 2100) periods. As observed data, we adopted the meteorological dataset developed by Xavier *et al.* (2016), which includes gridded daily series with 0.25° × 0.25° spatial resolution for the six meteorological variables evaluated in this study. This dataset uses data from 3,625 ground-based rain gauges and 735 weather stations provided by the National Institute of Meteorology (INMET), National Water and Sanitation Agency (ANA), and the Water and Electric Power Department of São Paulo (DAEE/SP) as input to produce interpolations. Six

different interpolation techniques were evaluated: arithmetic averaging, thin plate spline, natural neighbor, inverse distance weighting, angular distance weighting, and ordinary point kriging. In general, the dataset shows a good performance in describing the weather station observations and is widely applied in hydrological and climatological studies in Brazil (Cortez *et al.,* 2022; David *et al.,* 2022), and as the ground truth to GCMs/RCMs projections assessment and impact studies (Almagro *et al.,* 2017, 2020).

For historical and future projections, we used daily data from 19 CMIP6 GCMs\ESMs (Table 2. 1). The models were selected based on the following criteria: (1) availability of daily data for the evaluated climate variables under the r1i1p1f1 variant, and (2) nominal spatial resolution up to 250 km. For relative humidity (hur), wind speed (sfcWind), and net solar radiation (rss), only 10 GCMs were available at the stipulated conditions. For future projected changes, we considered two Shared Socioeconomic Pathways: the middle of the road (SSP2-4.5) and the fossil-fueled development (SSP5-8.5). The latter scenario represents the high end of future pathways with enough emissions to achieve a radiative forcing of 8.5 W.m-2 by 2100, whilst SSP2-4.5 represents the medium part of the range of future pathways. The two scenarios are an update of the previous Representative Concentration Pathways (RCPs) from the CMIP5(O'Neill *et al.,* 2016; Tebaldi *et al.,* 2021). The SSPs include mitigation and adaptation efforts based on economic and social changes, such as societal-economic development(Song *et al.,* 2021). There are two underlying reasons behind considering these scenarios: (1) since they represent the intermediate (SSP2-4.5) and extreme (SSP5-8.5) future climate change conditions, they are able to represent a wide range of expected changes in global climate dynamics, encompassing other scenarios, such as the SSP3-7.0, which were not available for all evaluated CMIP6 GCMs/ESMs at the time of the pre and post-processing tasks; (2) they are the most used future scenarios in Brazilian climate change studies(Almagro *et al.,* 2017, 2020; Dereczynski *et al.,* 2020; Lyra *et al.,* 2018). The main climatological institute of the country, the National Institute for Space Research (INPE), provides RCM-simulated future data for the country considering the two forcing-equivalent CMIP5 RCPs scenarios (RCP4.5 and RCP8.5; Chou *et al.,* 2014). Therefore, the use of these scenarios here may enable future CMIP5-CMIP6 comparison studies.

Table 2. 1. CMIP6-GCMs\ESMs used in our dataset

Model	Country/Region	Resolution
MRI-ESM2*	Japan	1.12° × 1.12°
EC-EARTH3*	Europe	0.7° × 0.7°
CMCC-ESM2*	Europe	0.9° × 1.25°
INM-CM4-8*	Russia	1.5° × 2.0°
NorESM2-MM*	Norway	0.9° × 1.25°
MPI-ESM1.2-HR*	Germany	0.9° × 0.9°
INM-CM5*	Russia	1.5° × 2.0°
ACCESS-ESM1-5*	Australia	1.87° × 1.25°
TaiESM1	Taiwan	1.9° × 1.25°
NESM3	China	1.9° × 1.9°
KIOST-ESM	South Korea	1.87° × 1.87°
K-ACE	South Korea	1.87° × 1.25°
GFDL-CM4	USA	1.0° × 1.25°
GFDL-ESM4	USA	1.0° × 1.25°
ACCESS-CM2	Australia	1.87° × 1.25°
HadGEM3-GC31-LL	UK	1.87° × 1.25°
IPSL-CM6A*	France	2.5° × 1.3°
UKESM1.0	UK	1.87° × 1.25°
MIROC6*	Japan	1.4° × 1.4°

2.2.2 PRE AND POST-PROCESSING

Given the coarse and different spatial resolutions of the CMIP6 GCMs/ESMs, we performed a bilinear interpolation following previous studies (Mishra; Bhatia; Tiwari, 2020; Mukherjee *et al.,* 2018; Tang; Clark; Papalexiou, 2022; Xu *et al.,* 2021) to regrid all models to a common 0.25° spatial grid. Moreover, to obtain a multi-model ensemble seeking to encompass different representations and uncertainties of all evaluated models, the GCMs outputs need

to be in the same spatial grid resolution (Clark *et al.,* 2016; Gleckler; Taylor; Doutriaux, 2008). It is worth mention that regridding may severely impact the statistical properties of meteorological variables, especially those linked to extreme events (Rajulapati *et al.,* 2021). Hence, such limitations should be considered in future studies using our dataset.

Besides the coarse spatial resolution exhibited by GCM/ESMs, they also show an inherent inability to simulate the present-day climate conditions leading to systematic errors that are propagated for future simulations (Christensen *et al.*, 2008). Thus, climate products often require bias correction. Here, we used the Quantile Delta Mapping (QDM) approach (Cannon; Sobie; Murdock, 2015) since it explicitly preserves relative or absolute changes in quantiles between historical and future simulations (Tang; Clark; Papalexiou, 2021). This method is based on two widely used correction procedures: the quantile delta change and the detrend quantile mapping (Bürger *et al.,* 2013; Sone *et al.,* 2022). According to Cannon *et al.* (2015), the QDM can be performed in three steps. First, all the individual future projected quantiles are detrended. Then, the detrended quantiles are bias-corrected using the quantile mapping technique. Lastly, the projected changes are then superimposed on the bias-corrected outputs. Let denote o and p as observed and projected data, and h and f as historical and future periods, respectively. The definition of the non-exceedance probability of observed ($x_{h,o}$) and projected historical ($x_{h,p}$) data, and future data ($x_{f,p}$) are accounted as:

$$p_{f,p}(t) = F\left(x_{f,p}(t)\right) \tag{2.1}$$

$$p_{h,p}(t) = F\left(x_{h,p}(t)\right) \tag{2.2}$$

$$p_{h,o}(t) = F\left(x_{h,o}(t)\right) \tag{2.3}$$

where p and F respectively denote the non-exceedance probability associated with a specific value at time t and the empirical cumulative distribution function (ECDF). We adopted the non-parametric probability distributions as they showed better performance over the parametric ones when downscaling both RCMs and GCMs\ESMs outputs (Gudmundsson *et*

al., 2012). Also, it is easier to apply it to different meteorological variables, despite their different underlying distributions (Mishra; Bhatia; Tiwari, 2020). Then, we computed a change factor (Equations 2.4 and 2.5), which associates the historical simulation output with that of the future period:

$$\Delta^M(t) = \frac{F_{f,p}^{-1}\left(p_{f,p}(t)\right)}{F_{h,p}^{-1}\left(p_{f,p}(t)\right)} = \frac{x_{f,p}(t)}{F_{h,p}^{-1}\left(p_{f,p}(t)\right)} \quad (2.4)$$

$$\Delta^A(t) = F_{f,p}^{-1}\left(p_{f,p}(t)\right) - F_{h,p}^{-1}\left(p_{f,p}(t)\right) = x_{f,p}(t) - F_{h,p}^{-1}\left(p_{f,p}(t)\right) \quad (2.5)$$

where F^{-1} indicates the inverse ECDF; and $\Delta^M(t)$ and $\Delta^A(t)$ are respectively the multiplicative and the additive change factor between simulated quantiles of the historical and future periods. The former is suitable for precipitation variables preserving relative changes between quantiles, whereas the latter preserves absolute changes in projected quantiles, suitable for temperature-derived variables (Cannon; Sobie; Murdock, 2015; Tang; Clark; Papalexiou, 2021). For precipitation, a frequency adaptation suggested by Themeßl *et al.* (2012) was also applied to account for a methodological problem that arises when the frequency of modelled dry days is greater than the frequency of observed dry days, resulting in a systematic wet bias. Moreover, we used a wet-day threshold of 1 mm/day following previous studies (Gudmundsson *et al.,* 2012; Mishra; Bhatia; Tiwari, 2020; Piani; Haerter; Coppola, 2010) to minimize drizzle effects.

The bias-corrected projected data are computed according to Equations 2.6 and 2.7, following the (i) quantile-mapping technique, which statistically transforms the distribution of the projected data to resemble the distribution of the observed data; and (ii) the change factor approach, which superimposes relative (or absolute) changes between historical and future projected values:

$$\hat{x}_{f,p}(t) = \Delta^M(t) \,.\, F_{h,o}^{-1}\left(p_{f,p}(t)\right) \quad (2.6)$$

$$\hat{x}_{f,p}(t) = \Delta^A(t) + F_{h,o}^{-1}\left(p_{f,p}(t)\right) \quad (2.7)$$

We considered the entire observed period (1980-2013) to correct the future projections (2015-2100) with the QDM algorithm. Both pre and post-processing tasks, depicted in Figure 1, were carried out using the *downscaleR* package, which is an R-based framework developed to address the needs of different climate impact studies within the Climate4R project (Bedia *et al.,* 2020; Iturbide *et al.,* 2019). Despite the wide range of applications of QDM in climate change impact assessments, we must point out the main limitations and uncertainties related to its usage. In general, the QDM (1) shows high sensitivity to the historical reference data used for calibration and (2) may be affected by the downscaling process due to a resolution mismatch between the model simulations and observations (Casanueva *et al.,* 2020). To reduce this uncertainty, high-quality reference data are required. Therefore, we used a high-resolution meteorological gridded dataset (Xavier; King; Scanlon, 2016) that comprises the largest number of ground-based observations in Brazil. We also highlight our effort to mitigate the introduction of more uncertainty and overcome some methodological limitations for the development of a reliable product for climate change assessment in this country. Nevertheless, it is known that the use of bias-correction methods is controversial (Switanek *et al.,* 2017) as they are not able to retain spatial and intervariable dependencies (White; Toumi, 2013). Lastly, bias-corrections methods may produce physically unrealistic values and also hide some fundamental models' deficiencies (Casanueva *et al.,* 2020; Switanek *et al.,* 2017).

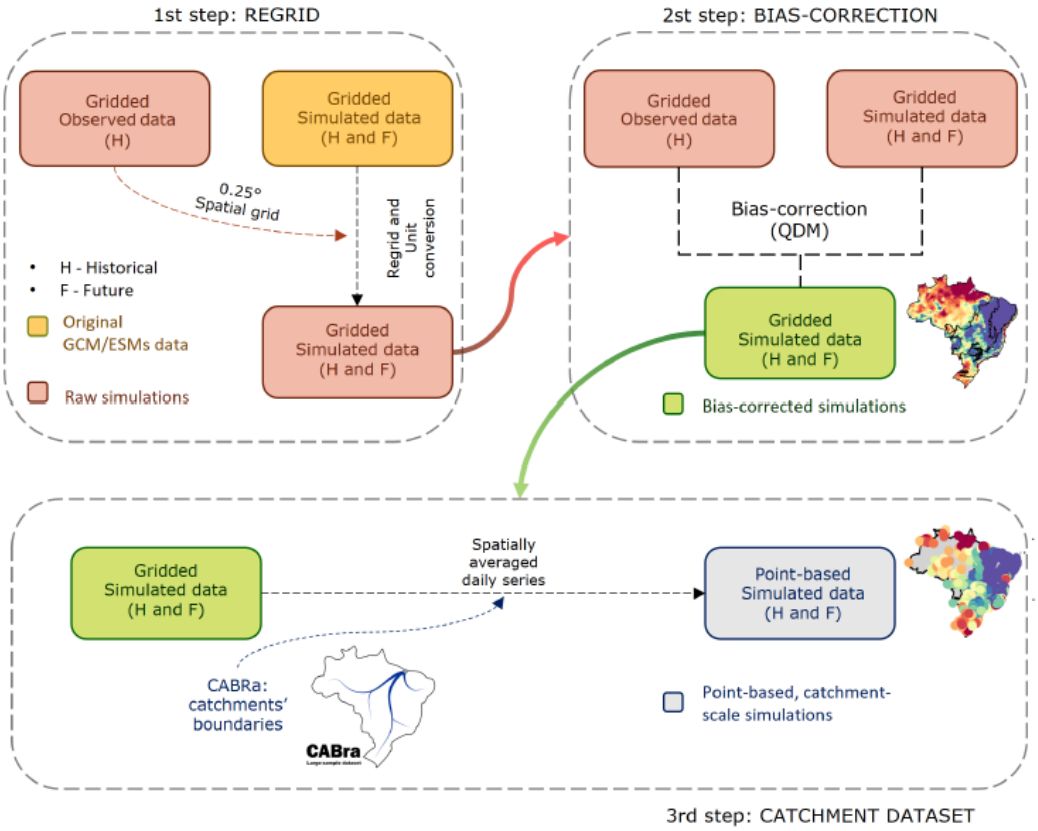

Figure 2.1. Flowchart representing the core steps used to generate the CLIMBra's products. Step 1 and 2 represent the regrid and bias-correction tasks, respectively. Step 3 represents the framework required to rescaled the gridded dataset to the CABra's catchments.

2.2.3 CATCHMENT-SCALE DATASET

The development of a regional gridded meteorological dataset aims at advancing hydro-climate studies in Brazil. Nevertheless, working with gridded climate variables is not a trivial task, often requiring high computation effort. Therefore, we also developed a catchment-scale version of the dataset in order to assist climate-change impact studies/applications (Figure 2.1) for both scientific and technical fields. To this end, we rescaled our gridded dataset to match the catchments in the CABra large-sample dataset (Almagro *et al.,* 2021). CABra includes a set of more than 100 observed climate, hydrological, and physiographic attributes for 735 Brazilian catchments (Figure 2.2).

For each CABra's catchment, we generated a gridded meteorological daily series comprising its extension. In sequence, we spatially averaged the grid-cell time series within the catchment boundaries. This process was conducted for each variable and climate change

scenario. Given the continental extensions of Brazil, the country shows a large range of catchment areas. Thus, for some catchments, the daily time series were obtained using only one grid and, for others, averaging more than 50 grids. Moreover, our gridded dataset only comprises the Brazilian territory, and hence the average daily time-series only accounted for the catchments' area within the country boundaries. To compute the spatial averaged daily time series, we weighted the grids according to their latitude, as, for regular grids, the grid cell's area changes as you move towards the poles. It is also worth noting that the averaged time-series may hinder extreme events in large catchments since extreme high or low events recorded in a specific grid may be smoothed by non-extreme events recorded in neighboring grids when taking the average.

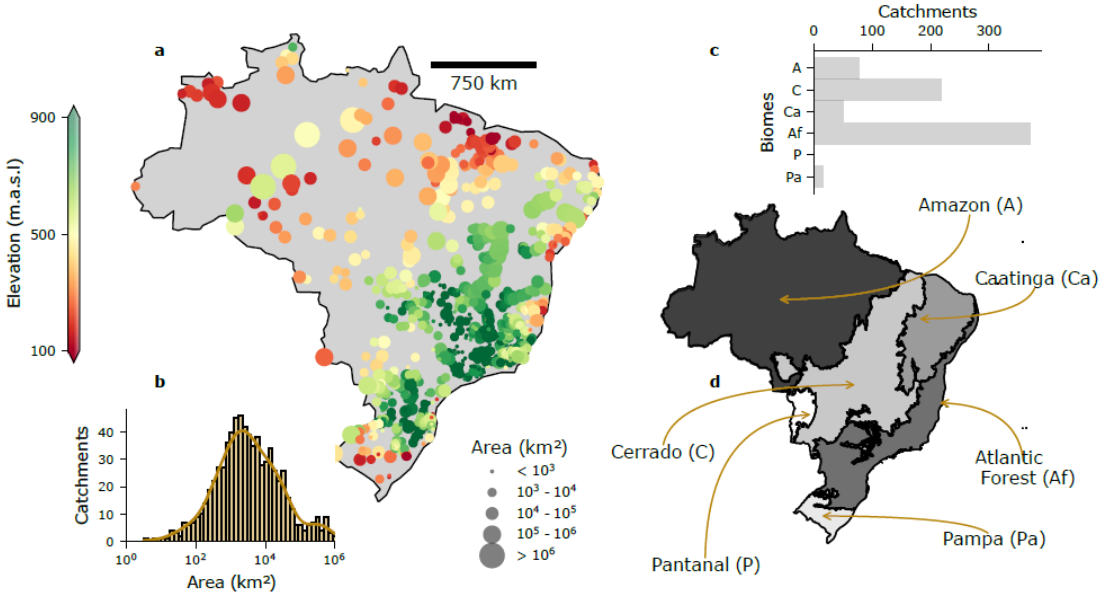

Figure 2.2. (a) Streamflow gauge coordinates of CABra's catchments, colored according to their mean elevation and sized by their area. (b) Histogram of catchments' area. (c) Distribution of catchments per Brazilian biome. (d) Six main Brazilian biomes.

2.2.4 SUMMARY OF DATA RECORDS

The present study describes a gridded dataset (0.25° × 0.25°) and a spatially averaged dataset at a catchment-scale. The first includes raw and bias-corrected gridded (netCDF) daily time-series (pr, tasmax, tasmin, rss*, sfcWind*, and hur*) of 19 (10*) CMIP6 GCMs/ESMs (Table 2. **1**) for both the historical (1980-2013) and future (2015-2100) periods. For the future period, two CMIP6 SSP-scenarios were considered: SSP2-4.5 and

SSP5-8.5. The second part of the dataset consists of a point-based (.csv) daily time-series derived from the aforementioned bias-corrected gridded dataset for 735 Brazilian catchments in the CABra dataset(Almagro *et al.,* 2021). The time-series from this dataset were also generated considering the two SSP scenarios simulated by the 19 (10) CMIP6 GCMs\ESMs. Both datasets are freely available (CC0 license) at Ballarin *et al.* (2022).

2.2.5 Code Availability

Pre- and post-processing tasks were carried out using the R-packages of the *Climate4R* project, extensively described in Bedia *et al.* (2020) and Iturbide *et al.* (2019). This framework was developed to address the needs of different climate-impact studies and includes a roll of R-packages to access, pre- and post-process, and visualize climate data. All the packages and documentation, including tutorials and example-notebooks, are available through the following Github link: https://github.com/SantanderMetGroup/climate4R.

2.3 Results

2.3.1 Bias-correction performance - Mean and Extreme values

To get a preliminary overview of the bias-correction performance in describing the observed data, we computed the relative bias between the estimated and observed long-term means for the historical period (Figure 2.3). We used absolute bias for the variables tasmax and tasmin since the denominator approaches zero in many catchments, resulting in very high relative bias values. For both raw and bias corrected datasets, we estimated the long-term mean for each individual model and then computed the multi-model ensemble. We repeated this process for all validation analyses of the study. The bias correction significantly improved the performance of the historical simulations in describing observed long-term mean values for all the meteorological variables by reducing the bias to approximately zero.

We found the largest bias for sfcWind and hur when analyzing the ensemble data prior to bias correction. For sfcWind, overestimations of more than 30% were observed throughout the country. The same was noted in hur, but with the opposite signal. In general, the raw simulations were unable to capture long-term mean maximum and minimum temperatures. Similar to the findings of Mishra *et al.* (2020), the raw multi-model ensemble exhibited an overall cold bias (-1.70 °C) for tasmax and a warm bias (0.87 °C) for tasmin. Regarding the long-term mean precipitation, we observed an overall wet relative bias over

the country (11.74%), except in the Amazon and Pampa biomes (northern and southern of Brazil, respectively) where we noted a relative dry bias. In general, the CMIP6 models exhibited good performance in estimating the long-term mean rss, showing a smaller mean bias (-4.34%) compared with the deviations found for the other variables.

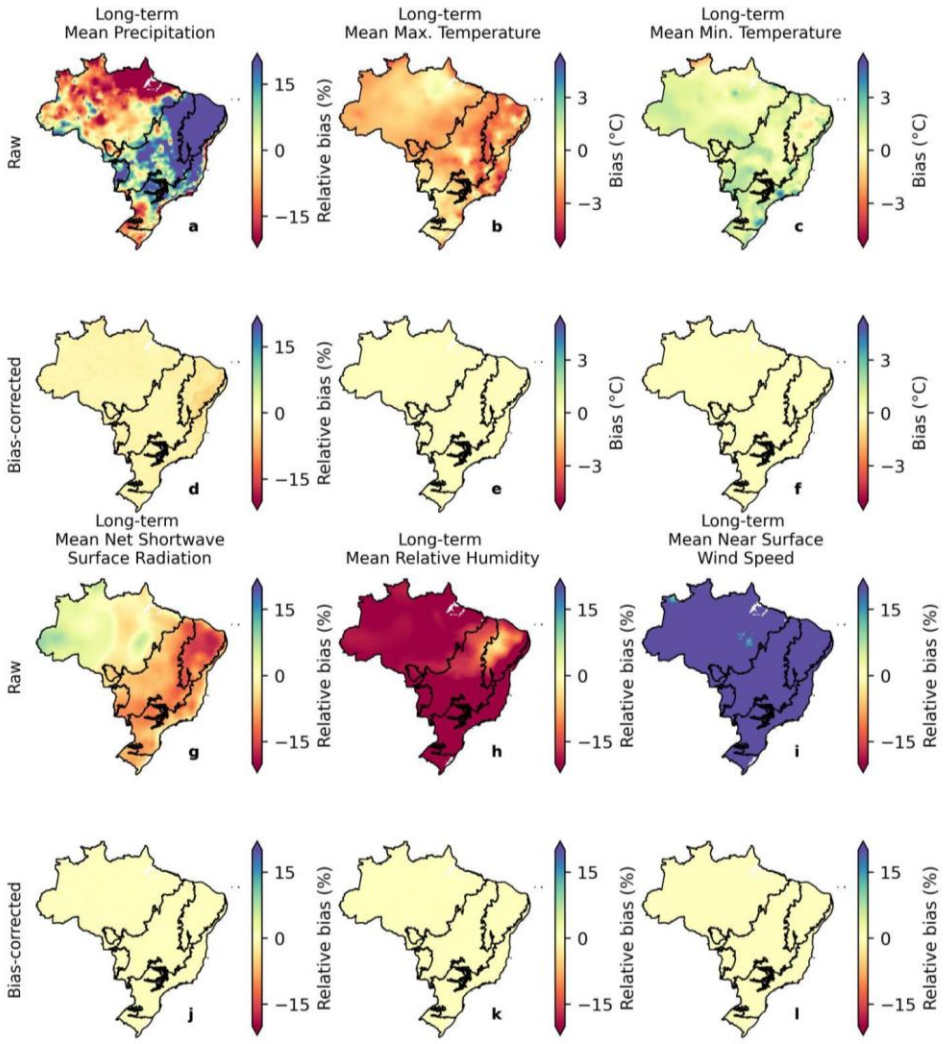

Figure 2.3. Biases in long-term mean precipitation, maximum and minimum temperature, net shortwave surface radiation, relative humidity, and near surface wind speed considering the gridded dataset in both raw and bias-corrected conditions. The limits of Brazilian biomes are indicated in black borderlines.

In the remainder of this section, we discuss the dataset's performance considering our catchment-scale product, which is the main product of this study, since it provides ready-for-

use meteorological time-series required for most hydrological studies and climate change impacts simulation. Nevertheless, similar conclusions can be drawn for the gridded dataset, which was the basis for the development of the catchment-scale product. To explore the models' performance beyond the characterization of mean values, we also computed the bias in the variables' long-term extreme properties: 90th (and/or 10th) percentiles and maximum (and/or minimum) records (Figure 2.4 and Figure 2.5). It is worth mentioning that the spatial distribution of the bias in the long-term mean for the gridded (Figure 2.3) and catchment-scale datasets is alike (the first column in Figure 2.4 and Figure 2.5, plots a, d, and g), corroborating their equivalence in terms of performance. That is, although we spatially averaged the gridded dataset, the catchment-scale product is able to maintain the spatial distribution of relative bias.

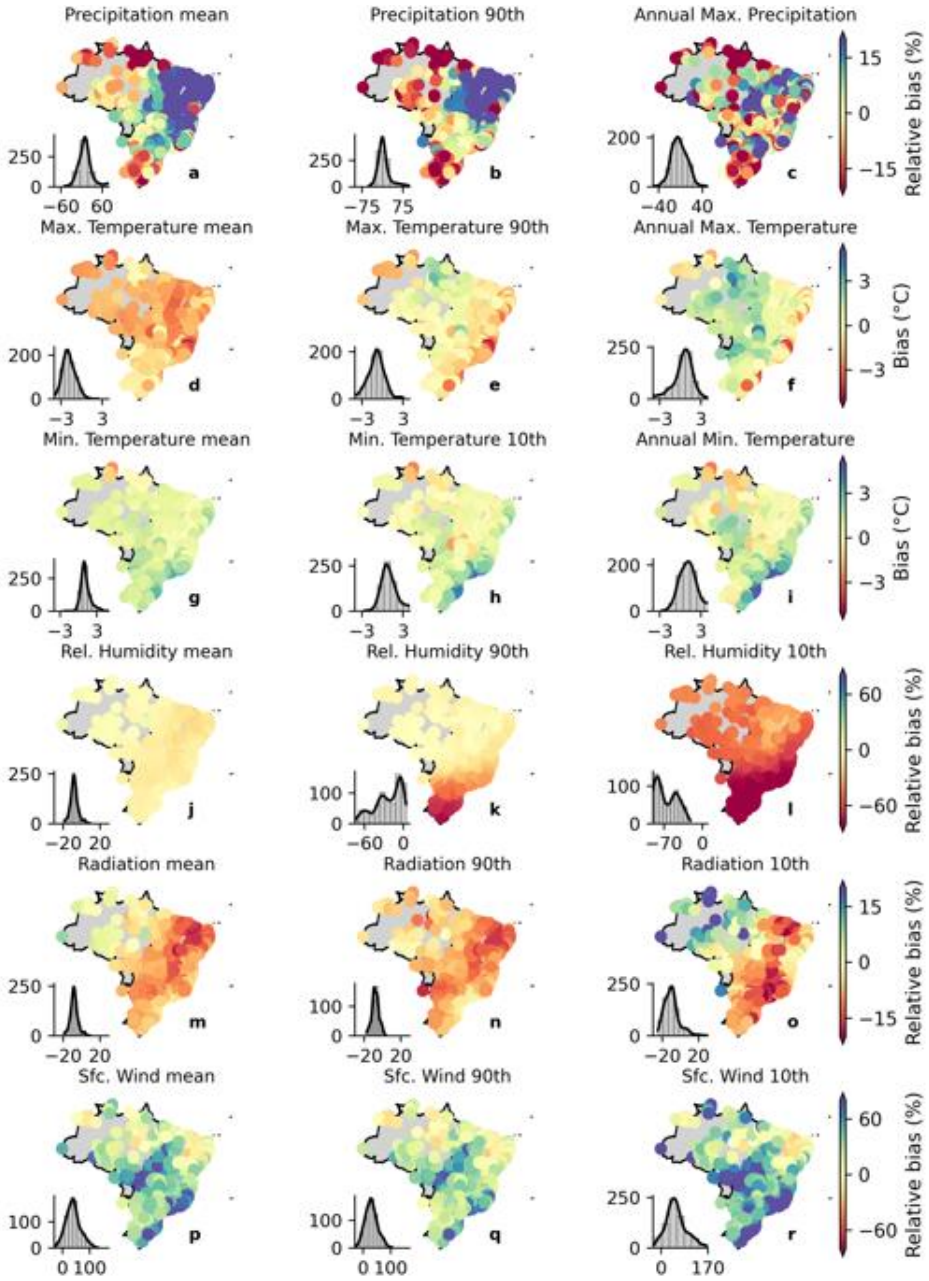

Figure 2.4. Biases in the long-term mean and extreme values of precipitation, maximum and minimum temperature, net shortwave surface radiation, relative humidity, and near surface wind speed (catchment-scale dataset) for the raw simulations. Histograms in each of the panels indicate the frequency of occurrence of bias.

In general, the CMIP6 models exhibited poor performance in simulating extreme values. The raw multi-model ensemble showed an overall warm bias (overestimation) for the long-term 10th percentile of tasmin and a cold bias (underestimation) for the long term 90th percentile

of tasmax. For the long-term maximum tasmax and minimum tasmin, we found an overall warm bias with a more heterogeneous spatial distribution than those observed in the long-term extreme percentiles. Interestingly, tasmax and tasmin showed a contrasting spatial distribution of bias respectively for the maximum and minimum values. This highlights that the raw output of the CMIP6 models fails to capture both extreme values and the temperature's amplitude.

Raw simulations of precipitation (pr) presented an absolute relative bias of up to 60% and 40% for the long-term 90th percentile and maximum values, respectively (Figure 2.4), corroborating with the findings of Pereima *et al.* (2022). Like tasmax and tasmin, the spatial distribution of the precipitation's relative biases in the long-term extreme percentile was alike to those found for the long-term mean: dry biases in the Amazon and Pampa biomes and an overall wet bias in the rest of the country. The long-term maximum precipitation did not show a clear spatial pattern. As observed in the mean long-term, the climate models were not able to characterize the extreme values of hur and sfcWind. For the former, underestimations of more than 20% and 50% were respectively found for the 90th and 10th percentiles. For the latter, the errors were even more significant, with relative biases of around 80% and 100% for the 90th and 10th percentiles, respectively. Again, the simulations of rss exhibited the best performance with relative biases of nearly 10% of magnitude and a tendency to slightly underestimate the observations.

The bias correction procedure significantly improved the estimations (Figure 2.5), successfully removing most of the bias in both long-term mean and extreme values for almost all variables, except for the long-term maximum precipitation, where the improvement was not so perceptible. After the correction, the bias reduced to nearly 0% in all catchments (see histograms in Figure 2.5). This is true even for hur and sfcWind, which were significantly misrepresented by the raw GCMs/ESMs. These results indicate that the QDM was able to overcome one of the main limitations of commonly used bias-correction methods: correcting systematic errors in different quantiles of the probability distributions of raw simulations, such as biases present in the mean and in the tail of the GCMs probability distribution (White; Toumi, 2013).

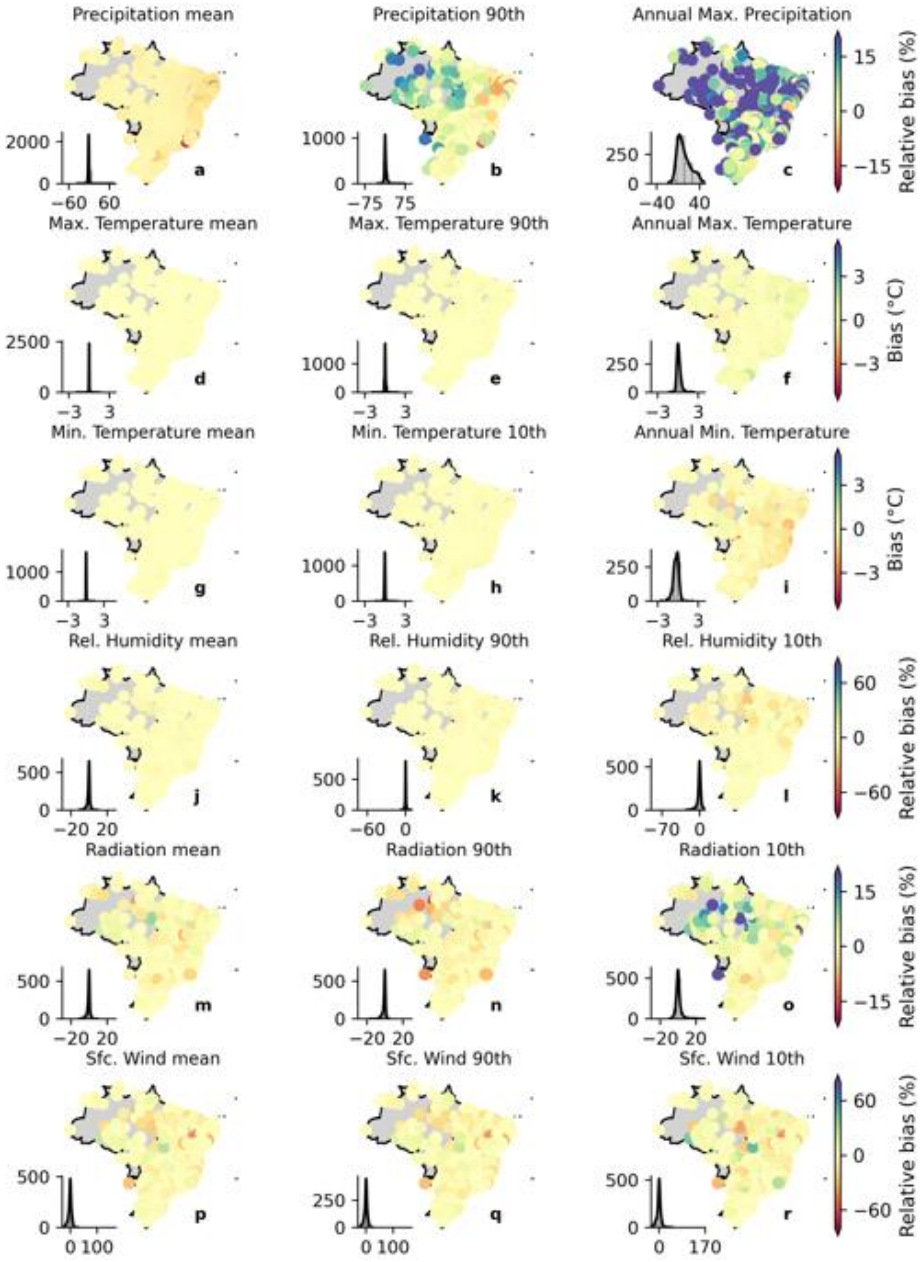

Figure 2.5. Biases in the long-term mean and extreme values of precipitation, maximum and minimum temperature, net shortwave surface radiation, relative humidity, and near surface wind speed (catchment-scale dataset) for the bias-corrected simulations. Histograms in each of the panels indicate the frequency of occurrence of bias.

2.3.2 BIAS-CORRECTION PERFORMANCE - SEASONALITY

We assessed the intra-annual variability of pr, tasmax, and tasmin in each Brazilian biome (Figure 2.6 and Figure 2.7 for raw and bias-corrected datasets, respectively). The intra-annual performance of the other variables is available in the Appendix A (Figures S2.1 and S2.2) since these variables are not available in all 19 CMIP6 climate models. This investigation seeks to confirm if the simulations are able to reproduce the intra-annual cycle of the evaluated variables, an important aspect to assess especially for hydrological modelling purposes. Overall, both the raw and bias products exhibited good performance in reproducing the seasonal cycle of pr, tasmax, and tasmin. The confidence intervals, defined by the minimum and maximum values found in the 19 GCMs\ESMs, encompassed the observed pattern of the three variables in all biomes.

The smallest uncertainties, indicated by the confidence intervals, were found for tasmin followed by pr and tasmax. The models showed excellent performance in reproducing the intra-annual variability of tasmin, with a narrowed confidence interval and an ensemble mean close to the observations. Despite the large hydroclimatic variability in the country, we noted a clear seasonal pattern in pr. Both the raw and bias-corrected datasets exhibited a larger uncertainty in the characterization of the rainy season (October to March), as indicated by wider confidence intervals and a large difference between the ensemble mean and observations. Similar results were also found by Almazroui *et al.* (2021) when evaluating the performance of CMIP6 models in characterizing mean properties of rainfall and temperature in South America. In fact, more extreme rainfall events, which were significantly misrepresented by the models (Figure 2.4), are more likely to be experienced in the rainy season. In contrast, in the dry period, the ensemble mean approaches the observation showing also narrower confidence intervals. The exception here is the Pampa, where we did not find a clear pattern in both rainy and dry seasons since they are not well-defined in this biome (Almagro *et al.,* 2017). An opposite situation was found for tasmax: larger confidence intervals in the dry period when the highest temperature amplitude and, consequently, climatic variability occur in Brazil (Landau *et al.,* 2009). In all biomes, raw models showed a slight underestimation of tasmax.

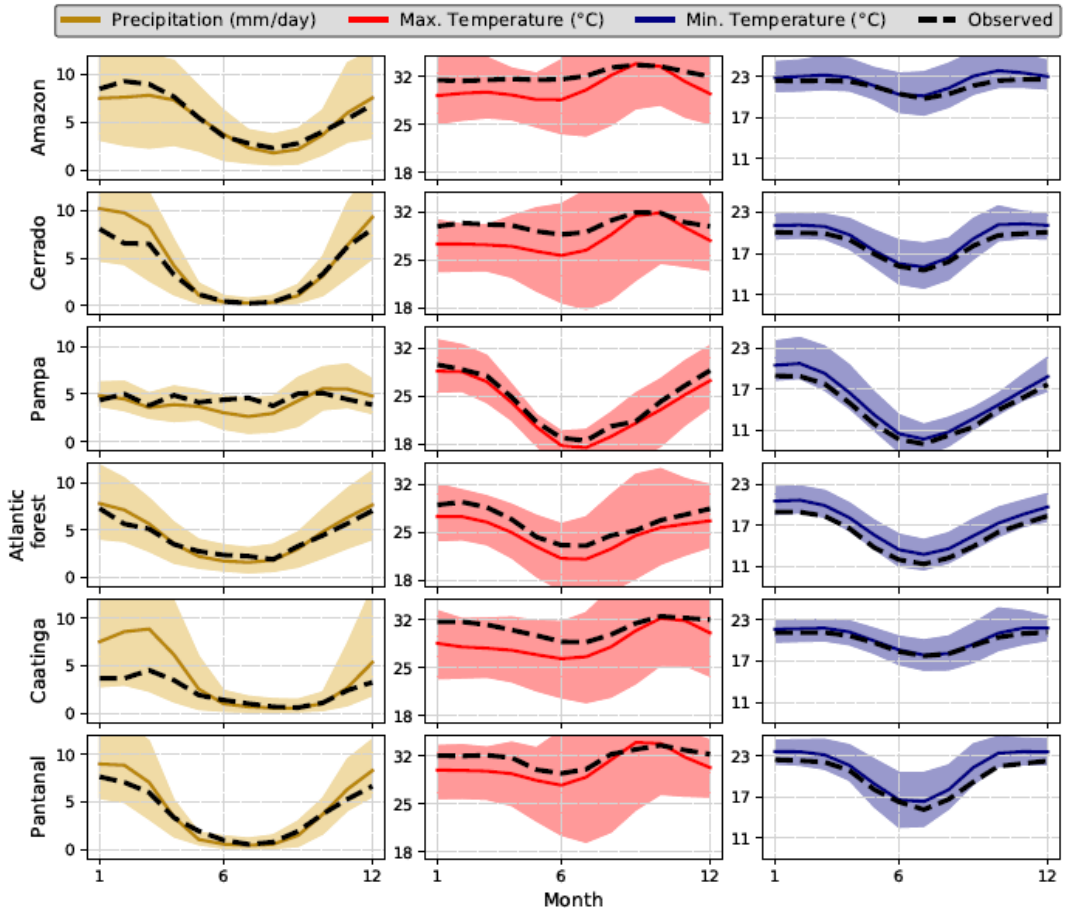

Figure 2.6. Long-term (1980-2013) monthly mean of precipitation and maximum and minimum temperature in each Brazilian biome. Highlighted lines represent the intra-annual cycle simulated by the raw multi-model ensemble. Dashed lines indicate the observed mean intra-annual cycle. Confidence intervals represent the maximum and minimum values simulated by the raw 19 CMIP6 GCMs/ESMs.

The bias-corrected simulations exhibited, again, excellent performance in characterizing the observed data (Figure 2.7). They were able to significantly reduce the average biases approaching the observed and simulated monthly cycles, in addition to reducing the uncertainties expressed by narrower confidence intervals. Despite this, the limitations present in the raw simulations remained, albeit with a less clear pattern: greater uncertainties in the simulation of pr and tasmax in the rainy and dry seasons, respectively. Similar conclusion can be drawn for rss, hur, and sfcWind (Figures S2.1 and S2.2). Although not as significantly as observed for the tasmax, tasmin and pr, the bias correction improved the performance of the raw simulations in describing the monthly cycles of these variables,

which showed smaller uncertainties and better accuracy. This can be explained by the fact that the GCMs/ESMs showed a lower performance in the characterization of the seasonality of these three variables, especially sfcWind and hur.

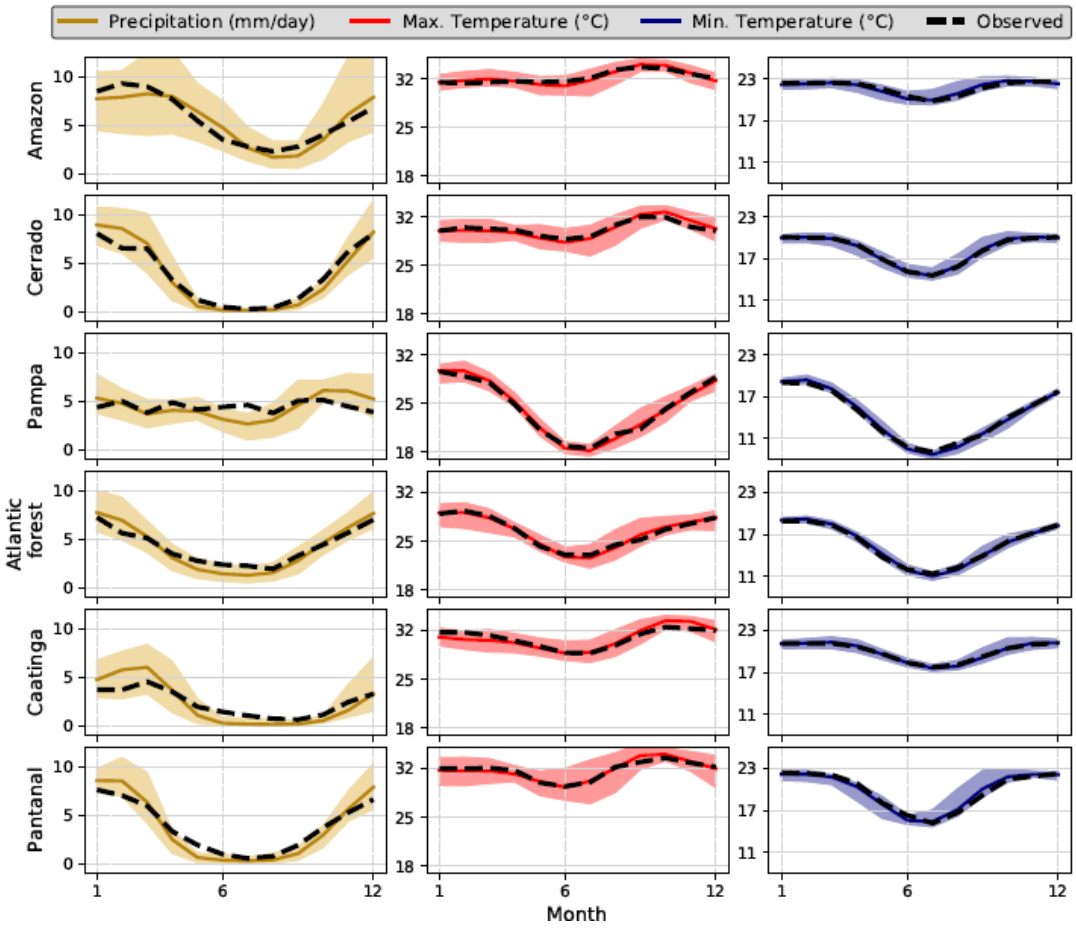

Figure 2.7. Long-term (1980-2013) monthly mean of precipitation and maximum and minimum temperature in each Brazilian biome. Highlighted lines represent the intra-annual cycle simulated by the bias-corrected multi-model ensemble. Dashed lines indicate the observed mean intra-annual cycle. Confidence intervals represent the maximum and minimum values simulated by the bias-corrected 19 CMIP6 GCMs/ESMs.

2.3.3 PROJECTED CHANGES - MEAN AND EXTREME VALUES

To analyze projected changes simulated by the bias-corrected CMIP6 models, we computed relative changes between the historical (1980-2013) and distant future (2070-2100) periods considering the long-term mean and extremes properties for both SSP2-4.5 and SSP5-8.5 scenarios (Figure 2.8 and Figure 2.9, respectively). For tasmax and tasmin, we computed

absolute changes (°C) to avoid extremely high values of relative changes due to denominator values close to zero. Projected changes simulated by the raw models are shown in the Appendix A (Figures S2.3 and S2.4). It is worth noting that the projected changes were similar for both raw and corrected simulations (Figures 2.8 and S2.3 for SSP2-4.5 and Figures 2.9 and S2.4 for SSP5-8.5), indicating that the QDM method was capable to overcome another limitation of commonly used bias correction methods: it did not deteriorate trends and/or relative changes projected by the models, which may hamper the fully understanding of climate change effects (Hagemann et al., 2011; Maurer; Pierce, 2014).

As expected, the changes simulated by the SSP5-8.5 scenario exhibited greater magnitude than those by the SSP2-4.5. Among the six evaluated variables, tasmax, tasmin, pr, and sfcWind presented significant changes ($> 10\%$) between historical and future simulations in most parts of the Brazilian territory considering both scenarios. For hur and rss, the projected changes showed a smaller magnitude ($<10\%$). Long-term mean precipitation and the 90th percentile exhibited similar spatial patterns of change over the country. A reduction in projected long-term mean pr was observed in the Amazon, Caatinga, and part of the Cerrado biomes. This expected reduction also corroborates the findings of Du et al. (2022). In the Pampa and Atlantic Forest biomes, a slight increase is expected. Similar conclusions can be drawn for the 90th percentile of precipitation. This pattern of change is more evident considering the SSP5-8.5 scenario (Figure 2.9). Regarding the long-term maximum pr, a significant increase was observed ($> 10\%$ for the SSP2-4.5 scenario and $> 20\%$ for the SSP5-8.5 scenario) throughout the country, even in the biomes where a reduction in mean precipitation was projected (Figure 2.8 and Figure 2.9).

In general, an increase in both tasmax and tasmin was observed in the two scenarios in Brazil. The projected increase in the long-term maximum temperature is slightly higher in the Amazon, Pantanal, and part of the Cerrado biomes than in the others. Furthermore, the positive magnitude of change in extreme values is larger than that projected for the long-term mean values. That is, both scenarios projected changes with greater magnitude in the extreme characteristics of tasmax (maximum and the 90th percentile) than in its mean values. This is also valid for tasmin, but with a lower difference between magnitudes of change.

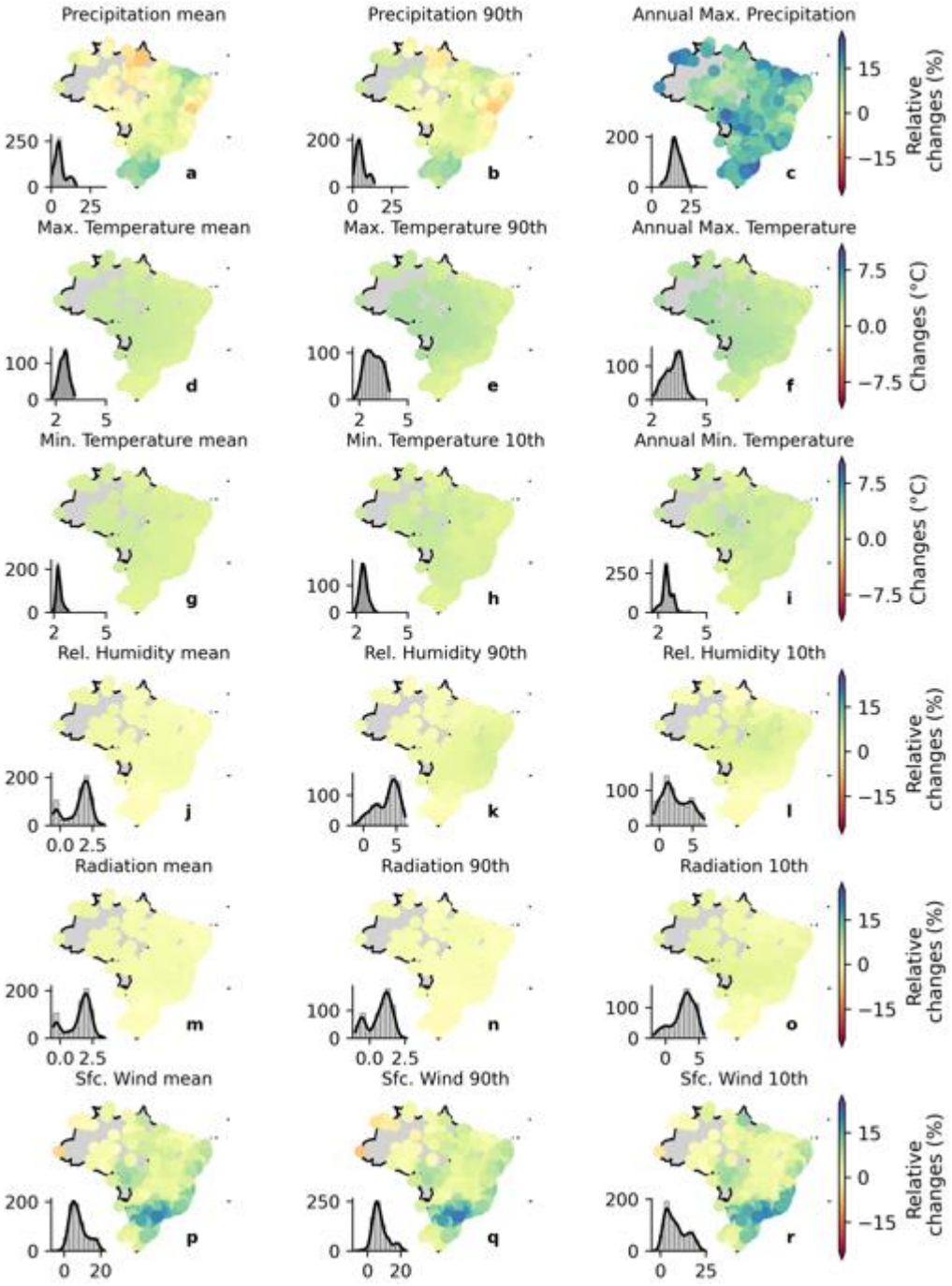

Figure 2.8. Relative changes in the long-term mean and extreme values of precipitation, maximum and minimum temperature, net shortwave solar radiation, relative humidity, and near surface wind speed between the historical (1980-2013) and distant future (2070-2100; SSP2-4.5) periods (bias-corrected catchment-scale dataset). Histograms in each panel indicate the frequency of occurrence of relative changes.

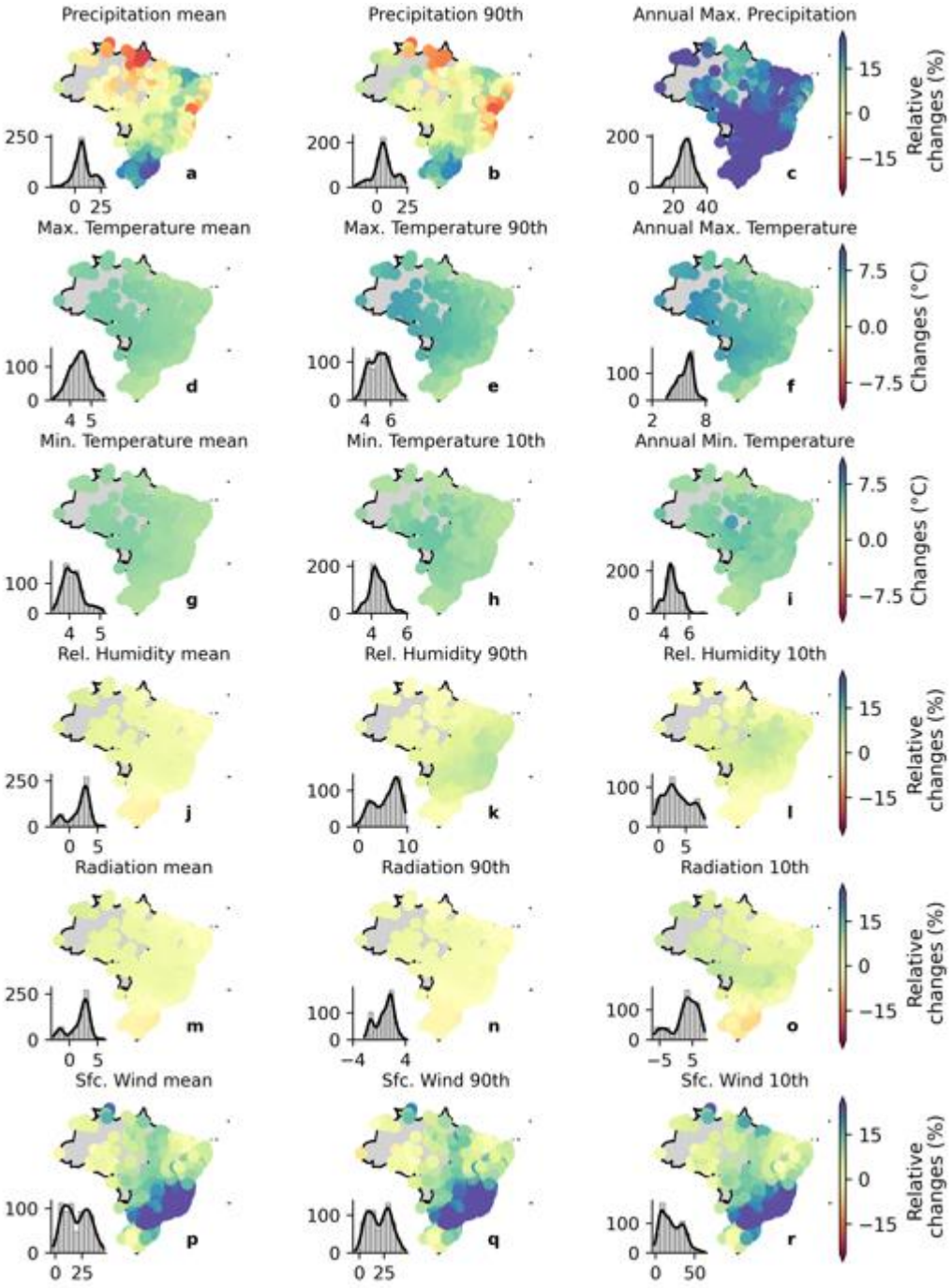

Figure 2.9. Relative changes in the long-term mean and extreme values of precipitation, maximum and minimum temperature, net shortwave solar radiation, relative humidity, and near surface wind speed between the historical period (1980-2013) and the distant future (2070-2100; SSP5-8.5) (bias-corrected catchment-scale dataset). Histograms in each of the panels indicate the frequency of occurrence of relative changes.

The projected changes in rss and hur showed smaller magnitude when compared with the other variables. For the former, an average increase in the long-term mean of about 2% and 4% is projected in the SSP2-4.5 and SSP5-8.5, respectively. Unlike pr, tasmax, and tasmin, there is no clear difference between the expected changes in mean and extreme values of rss, except the 10th percentile in the SSP5-8.5 scenario showing a negative variation in the Pampa biome and in part of the Atlantic Forest biome and a positive variation in the central region of the country. The hur variable also showed a similar pattern of projected changes in the long-term mean and extreme values across the country, indicating a slight increase of $< 2.5\%$ in the SSP2-4.5. For the SSP5-8.5 scenario, we noted slightly larger changes ($< 5\%$) in both the mean and extreme values. Interestingly, the 10th and 90th percentiles showed an opposite spatial distribution in the SSP5-8.5 scenario, in which we found larger increases in the 90th percentile and smaller increases in the 10th percentile of hur. Lastly, large increases in the sfcWind of 15% in SSP2-4.5 and 25% in SSP5-8.5 are expected especially in the Pampa (South region) and Atlantic Forest biomes (Southeast region). In the other regions, smaller increases were noted. It was also not possible to distinguish different spatial patterns between the changes in mean and extreme events.

2.3.4 PROJECTED CHANGES – SEASONALITY

Significant changes in intra-annual cycles are also expected (Figure 2. 10). For better visualization, we only detailed the relative changes (multi-model ensemble) expected in the monthly averages of pr, tasmax, and tasmin. The results for the other three variables are provided in the Appendix A (Figure S2.5). We considered the bias-corrected simulations of the historical (1980-2013) and 'distant' future (SSP5-8.5; 2070-2100) to compute the relative changes. However, very similar changes were observed for the simulations without bias correction.

Changes in projected precipitation' seasonal cycles varied among the biomes (Figure 2. **10**). For the Atlantic Forest and Cerrado, a shift in seasonality is projected, indicated by a large increase in precipitation in the first months of the dry period (April to July) and a reduction in the last months (August and September). For the Amazon, Caatinga, and Pantanal biomes, an overall decrease in precipitation is expected, but with the maintenance of seasonal cycles. Finally, a general increase in precipitation is projected in the Pampas

biome, however, with a heterogeneous distribution throughout the year: larger variations were observed at the beginning of both dry (April to June) and rainy seasons (October to December). We also found positive relative changes for tasmin and tasmax. For the former, a more significant increase is projected between May and September in all biomes, especially in the Pampas, Pantanal and Atlantic Forest biomes where the increase was more significant (up to 35%). The projected increase in tasmax is expected to be more uniform throughout the year than those projected for tasmin, being concentrated in the second half of the year, except for the Caatinga and Amazon biomes, which presented a similar rate of increase throughout the year for both tasmin and tasmax.

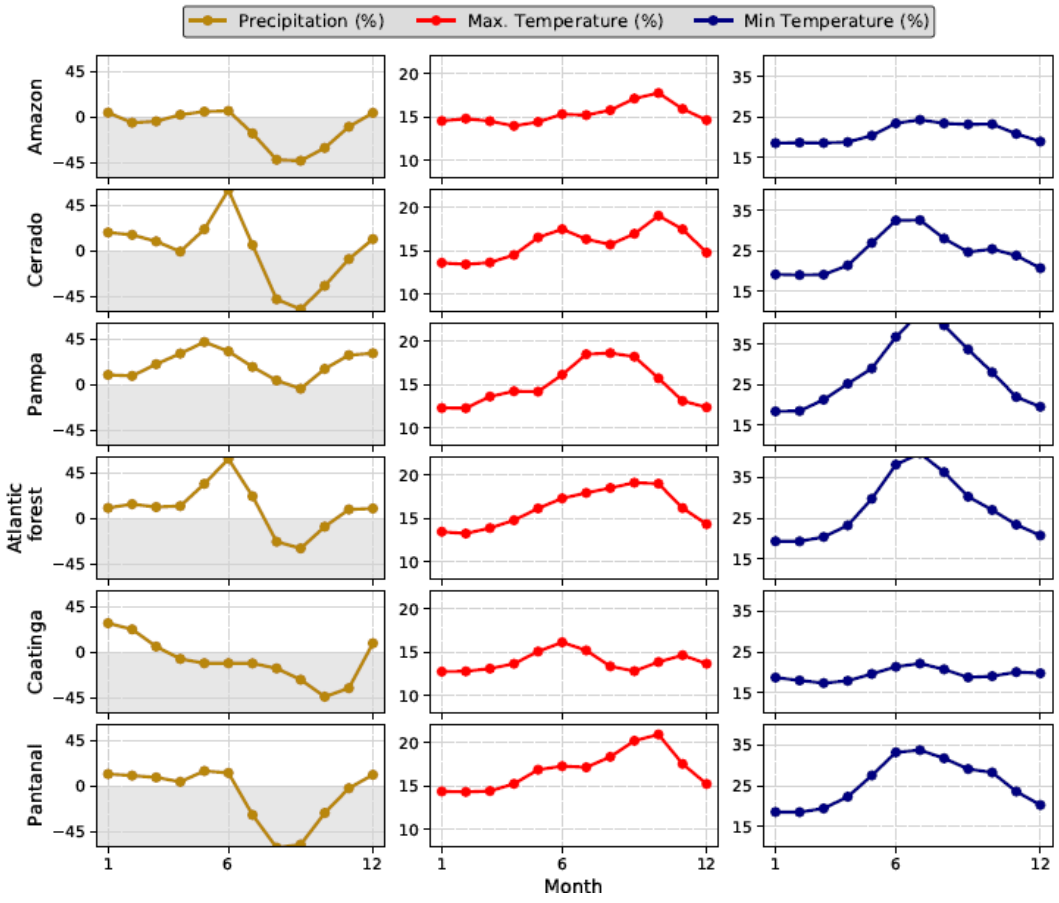

Figure 2. 10. Relative changes in the long-term mean intra-annual cycles of precipitation and maximum and minimum temperatures between the historical (1980-2013) and distant future (2070-2100, SSP5-8.5) periods. Highlighted lines represent the changes in the intra-annual cycle simulated by the bias-corrected multi-model ensemble.

2.4 Final Remarks

Here, we described the CLIMBra - Climate Change Dataset for Brazil, that provides raw and bias-corrected daily time series of six meteorological variables at both gridded and catchment scales using simulations of up to 19 CMIP6 GCM/ESMs. The simulations were provided for both historical (1980-2013) and future periods (2015-2100) forced by two different emission scenarios: SSP2-4.5 and SSP5-8.5. CLIMBra products may be useful for different hydroclimatic purposes such as hydrological modeling and climate change impact assessment. Moreover, CLIMBra may also be of interest to users not only in the hydrometeorological field but also in others such as agriculture, public health, and ecology. The high-resolution of the gridded data (0.25° × 0.25°) is key to developing regional assessments, providing information to decision and policy-making not only in Brazil but also in South America given the Brazil's continental proportion and its role in global climate dynamics.

Our main product, the catchment-scale dataset, is provided as comma-separated values format (.csv), which is easier to handle and download in comparison with netCDF files. Both the gridded and catchment-scale datasets are freely available at the Science Data Bank (https://doi.org/10.57760/sciencedb.02316). Despite the importance of the developed product, it is important to highlight some of its limitations. (1) Data users should be aware of significant bias when using our raw database due to its weak performance in representing observations, depending on its application. Thus, a performance analysis should be conducted to investigate whether the raw historical data are able to simulate observations. (2) Even exhibiting a better performance than the raw simulations (mainly in reproducing seasonal variability and extreme properties of the evaluated variables), the bias-corrected products may present inherent uncertainties, physically unrealistic values, and hide some fundamental deficiencies presented by the climate models. Finally, (3) data users should consider that the area-averaging process used to develop the catchment-scale dataset may hinder or smooth extreme events and misrepresent transboundary catchments.

2.5 REFERENCES

ABDELMOATY, H. M. *et al.* Biases Beyond the Mean in CMIP6 Extreme Precipitation: A Global Investigation. **Earth's Future**, [*s. l.*], v. 9, n. 10, p. e2021EF002196, 2021.

ALMAGRO, A. *et al.* CABra: A novel large-sample dataset for Brazilian catchments. **Hydrology and Earth System Sciences**, [*s. l.*], v. 25, n. 6, p. 3105–3135, 2021.

ALMAGRO, A. *et al.* Performance evaluation of Eta/HadGEM2-ES and Eta/MIROC5 precipitation simulations over Brazil. **Atmospheric Research**, [*s. l.*], v. 244, p. 105053, 2020.

ALMAGRO, A. *et al.* Projected climate change impacts in rainfall erosivity over Brazil. **Scientific Reports 2017 7:1**, [*s. l.*], v. 7, n. 1, p. 1–12, 2017.

ALMAZROUI, M. *et al.* Assessment of CMIP6 Performance and Projected Temperature and Precipitation Changes Over South America. **Earth Systems and Environment 2021 5:2**, [*s. l.*], v. 5, n. 2, p. 155–183, 2021.

BALLARIN, A. S. *et al.* A copula-based drought assessment framework considering global simulation models. **Journal of Hydrology: Regional Studies**, [*s. l.*], v. 38, p. 100970, 2021.

BALLARIN, A. S. *et al.* CLIMBra - Climate Change Dataset for Brazil. **Science Data Bank**, [*s. l.*], 2022.

BEDIA, J. *et al.* Statistical downscaling with the downscaleR package (v3.1.0): Contribution to the VALUE intercomparison experiment. **Geoscientific Model Development**, [*s. l.*], v. 13, n. 3, p. 1711–1735, 2020.

BÜRGER, G. *et al.* Downscaling Extremes: An Intercomparison of Multiple Methods for Future Climate. **Journal of Climate**, [*s. l.*], v. 26, n. 10, p. 3429–3449, 2013.

CANNON, A. J.; SOBIE, S. R.; MURDOCK, T. Q. Bias Correction of GCM Precipitation by Quantile Mapping: How Well Do Methods Preserve Changes in Quantiles and Extremes?. **Journal of Climate**, [*s. l.*], v. 28, n. 17, p. 6938–6959, 2015.

CAO, J. *et al.* The NUIST Earth System Model (NESM) version 3: Description and preliminary evaluation. **Geoscientific Model Development**, [*s. l.*], v. 11, n. 7, p. 2975–2993, 2018.

CASANUEVA, A. *et al.* Testing bias adjustment methods for regional climate change applications under observational uncertainty and resolution mismatch. **Atmospheric Science Letters**, [*s. l.*], v. 21, n. 7, p. e978, 2020.

CHOU, S. C. *et al.* Evaluation of the Eta Simulations Nested in Three Global Climate Models. **American Journal of Climate Change**, [*s. l.*], v. 3, n. 5, p. 438–454, 2014.

CHRISTENSEN, J. H. *et al.* On the need for bias correction of regional climate change projections of temperature and precipitation. **Geophysical Research Letters**, [*s. l.*], v. 35, n. 20, 2008.

CLARK, M. P. *et al.* Characterizing Uncertainty of the Hydrologic Impacts of Climate Change. **Current Climate Change Reports**, [*s. l.*], v. 2, n. 2, p. 55–64, 2016.

CORTEZ, B. N. *et al.* Nonstationary extreme precipitation in Brazil. **Hydrological Sciences Journal**, [*s. l.*], v. 67, n. 9, p. 1372–1383, 2022.

DALAGNOL, R. *et al.* Extreme rainfall and its impacts in the Brazilian Minas Gerais state in January 2020: Can we blame climate change?. **Climate Resilience and Sustainability**, [*s. l.*], v. 1, n. 1, p. e15, 2022.

DAVID, P. C. *et al.* Correspondence Between Model Structures and Hydrological Signatures: A Large-Sample Case Study Using 508 Brazilian Catchments. **Water Resources Research**, [*s. l.*], v. 58, n. 3, p. e2021WR030619, 2022.

DERECZYNSKI, C. *et al.* Downscaling of climate extremes over South America – Part I: Model evaluation in the reference climate. **Weather and Climate Extremes**, [*s. l.*], v. 29, p. 100273, 2020.

DU, Y. *et al.* Comprehensive assessment of CMIP5 and CMIP6 models in simulating and projecting precipitation over the global land. **International Journal of Climatology**, [*s. l.*], 2022.

FENG, X. *et al.* How deregulation, drought and increasing fire impact Amazonian biodiversity. **Nature 2021 597:7877**, [*s. l.*], v. 597, n. 7877, p. 516–521, 2021.

FILHO, J. D. P. *et al.* Copula-Based Multivariate Frequency Analysis of the 2012–2018 Drought in Northeast Brazil. **Water 2020, Vol. 12, Page 834**, [*s. l.*], v. 12, n. 3, p. 834, 2020.

GAO, S. *et al.* WRF ensemble dynamical downscaling of precipitation over China using different cumulus convective schemes. **AtmRe**, [*s. l.*], v. 271, p. 106116, 2022.

GLECKLER, P. J.; TAYLOR, K. E.; DOUTRIAUX, C. Performance metrics for climate models. **Journal of Geophysical Research: Atmospheres**, [*s. l.*], v. 113, n. D6, p. 6104, 2008.

GUDMUNDSSON, L. *et al.* Technical Note: Downscaling RCM precipitation to the station scale using statistical transformations – A comparison of methods. **Hydrology and Earth System Sciences**, [*s. l.*], v. 16, n. 9, p. 3383–3390, 2012.

GUTMANN, E. *et al.* An intercomparison of statistical downscaling methods used for water resource assessments in the United States. **Water Resources Research**, [*s. l.*], v. 50, n. 9, p. 7167–7186, 2014.

HAGEMANN, S. *et al.* Impact of a Statistical Bias Correction on the Projected Hydrological Changes Obtained from Three GCMs and Two Hydrology Models. **Journal of Hydrometeorology**, [*s. l.*], v. 12, n. 4, p. 556–578, 2011.

ITURBIDE, M. *et al.* The R-based climate4R open framework for reproducible climate data access and post-processing. **Environmental Modelling & Software**, [*s. l.*], v. 111, p. 42–54, 2019.

KOTLARSKI, S. *et al.* Regional climate modeling on European scales: A joint standard evaluation of the EURO-CORDEX RCM ensemble. **Geoscientific Model Development**, [*s. l.*], v. 7, n. 4, p. 1297–1333, 2014.

LANDAU, E. C. *et al.* Geoespacialização da Amplitude Térmica no Brasil. *In*: , 2009, Canela. **III Simpósio Internacional de Climatologia**. Canela: [*s. n.*], 2009.

LAW, R. M. *et al.* The carbon cycle in the Australian Community Climate and Earth System Simulator (ACCESS-ESM1) - Part 1: Model description and pre-industrial simulation. **Geoscientific Model Development**, [*s. l.*], v. 10, n. 7, p. 2567–2590, 2017.

LYRA, A. *et al.* Climate change projections over three metropolitan regions in Southeast Brazil using the non-hydrostatic Eta regional climate model at 5-km resolution. **Theoretical and Applied Climatology**, [*s. l.*], v. 132, n. 1–2, p. 663–682, 2018.

MANDAL, S.; SRIVASTAV, R. K.; SIMONOVIC, S. P. Use of beta regression for statistical downscaling of precipitation in the Campbell River basin, British Columbia, Canada. **Journal of Hydrology**, [*s. l.*], v. 538, p. 49–62, 2016.

MARENGO, J. A.; TORRES, R. R.; ALVES, L. M. Drought in Northeast Brazil—past, present, and future. **Theoretical and Applied Climatology**, [*s. l.*], v. 129, n. 3–4, p. 1189–1200, 2017.

MAURER, E. P.; PIERCE, D. W. Bias correction can modify climate model simulated precipitation changes without adverse effect on the ensemble mean. **Hydrology and Earth System Sciences**, [*s. l.*], v. 18, n. 3, p. 915–925, 2014.

MISHRA, V.; BHATIA, U.; TIWARI, A. D. Bias-corrected climate projections for South Asia from Coupled Model Intercomparison Project-6. **Scientific Data 2020 7:1**, [*s. l.*], v. 7, n. 1, p. 1–13, 2020.

MOUSTAKIS, Y. *et al.* Seasonality, Intensity, and Duration of Rainfall Extremes Change in a Warmer Climate. **Earth's Future**, [*s. l.*], v. 9, n. 3, p. e2020EF001824, 2021.

MUKHERJEE, S. *et al.* Increase in extreme precipitation events under anthropogenic warming in India. **Weather and Climate Extremes**, [*s. l.*], v. 20, p. 45–53, 2018.

NOBRE, P. *et al.* Climate Simulation and Change in the Brazilian Climate Model. **Journal of Climate**, [*s. l.*], v. 26, n. 17, p. 6716–6732, 2013.

NOBRE, C. A. *et al.* Some Characteristics and Impacts of the Drought and Water Crisis in Southeastern Brazil during 2014 and 2015. **Journal of Water Resource and Protection**, [*s. l.*], v. 8, n. 2, p. 252–262, 2016.

OMBADI, M. *et al.* Developing Intensity-Duration-Frequency (IDF) Curves From Satellite-Based Precipitation: Methodology and Evaluation. **Water Resources Research**, [*s. l.*], v. 54, n. 10, p. 7752–7766, 2018.

O'NEILL, B. C. *et al.* The Scenario Model Intercomparison Project (ScenarioMIP) for CMIP6. **Geoscientific Model Development**, [*s. l.*], v. 9, n. 9, p. 3461–3482, 2016.

PAPALEXIOU, S. M. *et al.* Probabilistic Evaluation of Drought in CMIP6 Simulations. **Earth's Future**, [*s. l.*], v. 9, n. 10, p. e2021EF002150, 2021.

PEREIMA, M. F. R. *et al.* A systematic analysis of climate model precipitation in southern Brazil. **International Journal of Climatology**, [*s. l.*], v. 42, n. 8, p. 4240–4257, 2022.

PIANI, C.; HAERTER, J. O.; COPPOLA, E. Statistical bias correction for daily precipitation in regional climate models over Europe. **Theoretical and Applied Climatology**, [*s. l.*], v. 99, n. 1–2, p. 187–192, 2010.

RAJULAPATI, C. R. *et al.* The Perils of Regridding: Examples Using a Global Precipitation Dataset. **Journal of Applied Meteorology and Climatology**, [*s. l.*], v. 60, n. 11, p. 1561–1573, 2021.

SIMONOVIC, S. P. *et al.* A web-based tool for the development of Intensity Duration Frequency curves under changing climate. **Environmental Modelling & Software**, [*s. l.*], v. 81, p. 136–153, 2016.

SONE, J. S. *et al.* Water Security in an Uncertain Future: Contrasting Realities from an Availability-Demand Perspective. **Water Resources Management**, [*s. l.*], v. 36, n. 8, p. 2571–2587, 2022.

SONG, Y. H. *et al.* Advances in CMIP6 INM-CM5 over CMIP5 INM-CM4 for precipitation simulation in South Korea. **Atmospheric Research**, [*s. l.*], v. 247, p. 105261, 2021.

SWITANEK, B. M. *et al.* Scaled distribution mapping: A bias correction method that preserves raw climate model projected changes. **Hydrology and Earth System Sciences**, [*s. l.*], v. 21, n. 6, p. 2649–2666, 2017.

TANG, G.; CLARK, M. P.; PAPALEXIOU, S. M. EM-Earth: The Ensemble Meteorological Dataset for Planet Earth. **Bulletin of the American Meteorological Society**, [*s. l.*], v. 103, n. 4, p. E996–E1018, 2022.

TANG, G.; CLARK, M. P.; PAPALEXIOU, S. M. SC-Earth: A Station-Based Serially Complete Earth Dataset from 1950 to 2019. **Journal of Climate**, [*s. l.*], v. 34, n. 16, p. 6493–6511, 2021.

TEBALDI, C. *et al.* Climate model projections from the Scenario Model Intercomparison Project (ScenarioMIP) of CMIP6. **Earth System Dynamics**, [*s. l.*], v. 12, n. 1, p. 253–293, 2021.

THEMESSL, M. J.; GOBIET, A.; HEINRICH, G. Empirical-statistical downscaling and error correction of regional climate models and its impact on the climate change signal. **Climatic Change**, [*s. l.*], v. 112, n. 2, p. 449–468, 2012.

TURCO, M. *et al.* Testing MOS precipitation downscaling for ENSEMBLES regional climate models over Spain. **Journal of Geophysical Research: Atmospheres**, [*s. l.*], v. 116, n. D18, p. 18109, 2011.

UKKOLA, A. M. *et al.* Evaluating CMIP5 Model Agreement for Multiple Drought Metrics. **Journal of Hydrometeorology**, [*s. l.*], v. 19, n. 6, p. 969–988, 2018.

WANG, Y. C. *et al.* Performance of the Taiwan Earth System Model in Simulating Climate Variability Compared With Observations and CMIP6 Model Simulations. **Journal of Advances in Modeling Earth Systems**, [*s. l.*], v. 13, n. 7, p. e2020MS002353, 2021.

WERNER, A. T.; CANNON, A. J. Hydrologic extremes - An intercomparison of multiple gridded statistical downscaling methods. **Hydrology and Earth System Sciences**, [*s. l.*], v. 20, n. 4, p. 1483–1508, 2016.

WHITE, R. H.; TOUMI, R. The limitations of bias correcting regional climate model inputs. **Geophysical Research Letters**, [*s. l.*], v. 40, n. 12, p. 2907–2912, 2013.

XAVIER, A. C.; KING, C. W.; SCANLON, B. R. Daily gridded meteorological variables in Brazil (1980–2013). **International Journal of Climatology**, [*s. l.*], v. 36, n. 6, p. 2644–2659, 2016.

XU, Z. *et al.* Bias-corrected CMIP6 global dataset for dynamical downscaling of the historical and future climate (1979–2100). **Scientific Data 2021 8:1**, [*s. l.*], v. 8, n. 1, p. 1–11, 2021.

XU, Z.; YANG, Z. L. An Improved Dynamical Downscaling Method with GCM Bias Corrections and Its Validation with 30 Years of Climate Simulations. **Journal of Climate**, [*s. l.*], v. 25, n. 18, p. 6271–6286, 2012.

ZIEHN, T. *et al.* The Australian Earth System Model: ACCESS-ESM1.5. **Journal of Southern Hemisphere Earth Systems Science**, [*s. l.*], v. 70, n. 1, p. 193–214, 2020.

CHAPTER 3

Frequency rather than intensity drives the projected changes of rainfall events in Brazil

ABSTRACT

Extreme rainfall events are expected to intensify with global warming, posing significant challenges to both human and natural environments. Despite the importance of such assessments, they are unevenly widespread across the globe. Here, using bias corrected climate simulations of the latest phase of the Coupled Model Intercomparison Project (CMIP6), we provide a comprehensive assessment on how different rainfall events are expected to change across Brazil. Specifically, (1) we explored the projected changes in both intensity and frequency of rainfall events belonging to right-tail of the rainfall distribution using a non-parametric approach, and (2) quantified how rainfall events associate with different return periods are expected to intensify, using a parametric approach. We found that extreme rainfall events will become more frequent and intense by the end of the century, with averaged projected changes for rainfall exceeding the historical rainfall quantile q_0.99 of nearly 100% and 10% on frequency and intensity, respectively. Non-extreme rainfall events, in contrast, are expected to be less frequent, aligning with the compensation hypothesis. For instance, Brazilian 100-year rainfall are anticipated to intensify, on average, 17% and 31% under the moderate and the highest CMIP6 emission scenarios, respectively. Finally, our findings suggest that frequency, rather than intensity, dictates the projected changes of rainfall. We believe that the evidence gathered here will certainly contribute to not only an improved understanding of Brazilian rainfall events but also to a better comprehension of the different rainfall properties, their interplay and how the different ways of assessing them may affect climate studies.

3.1 INTRODUCTION

Extreme precipitation events underlie many of the most significant challenges society faces (Kirchmeier-Young; Zhang, 2020). Their negative impacts on both natural and human environments are responsible for billions of dollars in economic damages and immeasurable human losses (Doocy *et al.*, 2013; McBean; Rodgers, 2010; Nissen; Ulbrich, 2017). Consequently, the understanding of extreme rainfall has gained considerable attention in recent decades, being recognized as one of the scientific Great Challenges by the World Climate Research Programme (Diffenbaugh *et al.*, 2017; Sillmann *et al.*, 2017). Despite significant advancements in characterizing such events, there remain unresolved questions that underscore the need for an enhanced understanding of their characteristics to improve water resources management (Gründemann *et al.*, 2023). Such efforts become even more critical in the context of global warming (Fan *et al.*, 2021), as it is expected to significantly affect the intensity and frequency of extreme events (Chagas; Chaffe; Blöschl, 2022; Myhre *et al.*, 2019).

Numerous recent studies have been dedicated to assessing changes in observed extreme rainfall events (Alexander, 2016; Markonis *et al.*, 2019; Myhre *et al.*, 2019; Papalexiou; Montanari, 2019; Robinson *et al.*, 2021). Despite their importance for an improved comprehension of extreme events, there are still some shortcomings that impose a great challenge for hydrological practices in an uncertain future (Diffenbaugh *et al.*, 2017). First, many local observations span only the past few decades, not being able to capture precipitation's long-term variability and changes (Peterson *et al.*, 2013). Consequently, in some cases, observations may not be representative of the underlying events, substantially affecting the characterization of extreme events (Ballarin; Anache; Wendland, 2022; Marani; Zanetti, 2015). Furthermore, global warming is expected to alter global water cycle dynamics, potentially affecting the likelihood and magnitude of both extreme and non-extreme rainfall events (Min *et al.*, 2011; Sharifinejad; Hassanzadeh; Zaerpour, 2022). These changes on rainfall dynamics challenge an accurate projection based solely on observational analysis, as their future statistical properties might no longer be the same (Miniussi; Marani, 2020; Swain *et al.*, 2016).

In view of these limitations, several recent studies are relying on climate model projections to identify changes in extreme events (Abdelmoaty; Papalexiou, 2023;

Gründemann *et al.*, 2022; John *et al.*, 2022; Lima; Kwon; Kim, 2018). Despite the coarse resolution and inherent uncertainties exhibited by them, studies have already confirmed their robust agreement with observed data and theory (Abdelmoaty *et al.*, 2021; Asadieh; Krakauer, 2015; Fischer; Knutti, 2016; Mishra; Bhatia; Tiwari, 2020). For instance, multiple studies have been employing CMIP6-based projections to assess projected changes in the statistical properties of rainfall events worldwide, such as in India (Chaubey; Mall, 2023), China (Yu; Zhai; Li, 2023), East Africa (Gebrechorkos *et al.*, 2023), and United Kingdom (Cotterill *et al.*, 2021). This confirms the utility of climate projections for identifying and quantifying future changes in extreme rainfall events (Moustakis *et al.*, 2021; Ragno *et al.*, 2018; Ukkola *et al.*, 2018).

Nevertheless, even with the fundamental importance attached to such an assessment in shaping local-to-global water-related policies, studies on extreme rainfall are not universally prevalent across the globe. For instance, in Brazil - a country that has faced several widespread extreme climate-related hazards in the last decades (Ávila *et al.*, 2016; Cunha *et al.*, 2018; Lucas *et al.*, 2021; Marengo *et al.*, 2023; Regoto *et al.*, 2021; Santos; Lucio; Santos e Silva, 2016; Zilli *et al.*, 2017) - future extreme events have not been extensively investigated through the use of climate model projections. The existing studies (1) have focused on individual regions of the country (Gesualdo *et al.*, 2021); (2) relied on previous versions of CMIP simulations; and/or (3) focused on evaluating changes only in the intensity of extreme rainfall events, since this information is commonly required for infrastructure design (Myhre *et al.*, 2019; Sarkar; Maity, 2022). In general, previous studies did not assess how the rainfall distribution is expected to change in both intensity and frequency. Such assessment is, however, fundamental to shaping water resources management practices and to improving our understanding of the climate in the context of global warming (Harp; Horton, 2023).

Here, we address this gap by assessing how global warming is expected to affect both extreme and non-extreme rainfall events in Brazil using bias-corrected CMIP6 future projections. Instead of evaluating projected changes focusing solely in the intensity of rainfall events, here we assessed the expected changes in both their frequency and intensity (Mukherjee *et al.*, 2018; Myhre *et al.*, 2019). Finally, we examined how extremely rare rainfall events, commonly required for infrastructure design, are anticipated to change. Precisely, we aimed to address the following research questions: Will Brazilian extreme rainfall events be

more frequent and/or intense in the future? How will these changes manifest spatially across the country's domain? Will extreme events of varying magnitudes change similarly? We believe our study is significant not only for drawing a picture of future rainfall events in Brazil, but also for enhancing our comprehension of the interplay between rainfall intensity and frequency and their roles in climate change impact studies.

3.2 METHODS

3.2.1 DATA

We used here the CLIMBra - Climate Change Dataset for Brazil (Ballarin *et al.*, 2023), which provides bias-corrected rainfall time series for both historical (1980-2010) and future (2015-2100) periods under two distinct CMIP6 Shared Socioeconomic Pathways (SSP): SSP2-4.5 and SSP5-8.5. The dataset encompasses daily simulations of 19 CMIP6-climate models (Table 2. **1**) at a catchment scale (spatially-averaged, point-based time series) for 735 Brazilian catchments included in the CABRa dataset (Almagro *et al.*, 2021). The daily simulations were bias-corrected following the Quantile Delta Method (Cannon; Sobie; Murdock, 2015). For more details about the framework used to develop CLIMBra and its performance in representing observed climate variables, the readers are referred to Chapter 2.

3.2.2 CHANGES IN EXTREME RAINFALL EVENTS

Changes in rainfall properties can be assessed by evaluating the empirical distribution of the data or fitting a parametric distribution to the observations (Beranová; Kyselý; Hanel, 2018; John *et al.*, 2022; Papalexiou; Koutsoyiannis, 2016). While the latter approach enables the assessment of changes in non-observed events (Moustakis *et al.*, 2021), it requires a priori assumption regarding the statistical model used to describe the observed data (Marani; Ignaccolo, 2015). This fact, combined with the inherent uncertainties of the parameter estimation procedure (Nerantzaki; Papalexiou, 2022), may hinder an accurate assessment of the changes in rainfall properties. The non-parametric approach, on the other hand, allows the computation of changes in pre-established thresholds without requiring specific knowledge about the underlying distribution. Nevertheless, it cannot be used to assess changes in non-observed events present in the extrapolation range (Volpi, 2019). In view of these considerations, we opted here to use both non-parametric and parametric approaches.

The former will be employed to assess how different extreme and non-extreme rainfall events are expected to change, while the latter will be used to assess changes in extreme events present in the extrapolation range.

3.2.2.1 Non-parametric approach – assessing changes in the distribution of rainfall events

For the non-parametric assessment, we proposed an alternative framework based on the studies of Markonis *et al.* (2019) and Myhre *et al.* (2019). It consists in evaluating changes in the frequency and intensity of rainfall events exceeding varying q_i quantile-thresholds (where, $i = 0.5, 0.7, 0.9, 0.95, 0.99,$ and 0.999) of the right-tail of the distribution of wet days (> 1 mm). To account for the potential effects of overlapping rainfall events defined by the quantile-thresholds approach, we also repeated the analysis considering the rainfall events that falls within varying $q_{[i,i+1]}$ quantile-intervals (Figure 3.1). For instance, the first interval of the thresholds approach encompasses all events exceeding the historical rainfall quantile $q_{0.5}$, whereas the first interval of the intervals approach encompasses all rainfall events lying between the historical quantiles $q_{0.5}$ and $q_{0.7}$. The last interval in both the thresholds and intervals approaches is the same and includes all events that exceeds the historical rainfall quantiles $q_{0.999}$. In the thresholds approach, extreme rainfall events, such those exceeding $q_{0.999}$, are included (and consequently influences the relative changes) in all considered intervals. In the intervals approach, in contrast, rainfall events are stratified in different intervals, allowing for a more detailed understanding of how different rainfall events are expected to change.

For both approaches, we assessed future changes in the frequency of rainfall events by computing relative changes (Δ) in the number of events that falls within the historical q-interval, defined either by the quantile-thresholds or quantile-intervals approaches. Here, we considered relative changes as the percentage difference between historical and future periods (Gründemann *et al.*, 2022). To assess future changes in the intensity of rainfall events, we computed the future changes in the average of the rainfall events lying within the historical q-interval. Finally, to assess the relative contribution of changes in intensity and frequency to the total changes, we computed the relative changes in the total amount of rainfall events within the historical q-interval. We conducted these analyses considering a long-term temporal perspective. To account for climate models' uncertainties and variability,

we performed these analyses for each of the 19 CLIMBra's CMIP6 climate models individually, and subsequently computed multi-model ensemble statistics (mean and median).

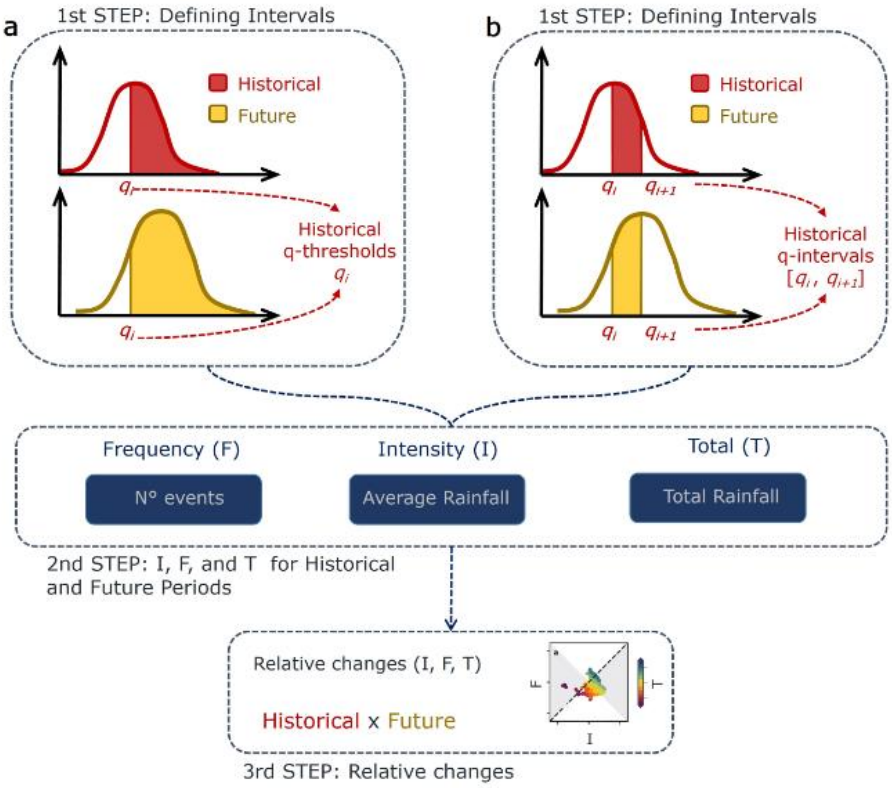

Figure 3.1. Flowchart depicting the core steps of the non-parametric approach, developed to compute relative changes in the frequency, intensity, and total rainfall between historical and future periods using the (a) quantile-thresholds and (b) quantile-intervals approaches.

3.2.2.2 Parametric approach – assessing changes in extreme rainfall events present in the extrapolation range

The non-parametric approach provides a general overview of expected changes in rainfall distribution. Nevertheless, it does not allow us to assess extremely rare rainfall events, such as those occurring once in 100 years, due to the inability of observed data to support extrapolation estimates (Volpi et al., 2019). Thus, we also employed here a parametric approach, in which we fit a statistical model to rainfall series and compute expected changes on extreme rainfall events belonging to the extrapolation range.

The most popular method for assessing extreme rainfall events relies on the extreme value theory (EVT). This approach posits that extreme events, defined as the maximum event occurring in a predefined temporal block (commonly 1 year), converge asymptotically to one of three different distribution classes (Gumbel, Frechét, and Reversed Weibull) summarized by the Generalized Extreme Value distribution (GEV). This theory assumes that (1) the events occurring in each block are independent and identically distributed and (2) the number of occurrences in each block tends to infinite (Marra *et al.*, 2019; Zorzetto; Botter; Marani, 2016). Nevertheless, these conditions are rarely met. The parent distribution of daily rainfall events is typically unknown, and the number of events in a block is not nearly sufficient to assure the asymptotic assumption (Papalexiou; Koutsoyiannis, 2013). Additionally, the EVT framework neglects a substantial proportion of observations since it uses only one observation per block (De Michele; Avanzi, 2018; Volpi *et al.*, 2019). The same limitations extend to the peak-over-threshold approach and the Pareto distribution (Zorzetto; Botter; Marani, 2016).

As an alternative to the recently questioned EVT (De Michele, 2019; Veneziano; Langousis; Lepore, 2009), some studies are turning to non-extreme distributions (Papalexiou, 2018; Zaghloul *et al.*, 2020) or proposing alternative distributions that relaxes the asymptotic assumptions, assuming a known parent distribution $F(x)$ of ordinary rainfall events (Miniussi; Marani, 2020). Here, based on the recent finds of Papalexiou (2022) and on physical reasoning (Wilson; Toumi, 2005), we assumed (and further verified) that the tail of the distribution of rainfall events is stretched-exponential or follows a Weibull distribution tail (Equation 3.1). This assumption enable us to employ the Metastatistical Extreme Value (MEV) distribution (Equation 3.2) for assessing extreme events within the extrapolation range (Marani; Ignaccolo, 2015; Marra *et al.*, 2018).

$$F_W(x) = 1 - \exp\left(-\frac{x}{\beta}\right)^{\gamma} \tag{3.1}$$

$$F_{\mathrm{MEV}}(x) = \frac{1}{T}\sum_{j=1}^{T}\left[1 - \exp\left(-\frac{x}{\beta_j}\right)^{\gamma_j}\right]^{n_j} \tag{3.2}$$

where β is a scale parameter, γ a shape parameter, n is the number of wet days within the year j, and T is the number of available years in the time series. Instead of the traditional MEV, we adopted here a simplified version of it (SMEV, Equation 3.3). In SMEV, we disregard interannual variations and compute β and γ considering all precipitation values above the quantile-based threshold for all years, while considering the average yearly number of rainfall events present in the tail, $\bar{n}$ (Schellander; Lieb; Hell, 2019). We estimated Weibull parameters using the probability weighted moment method, as it attributes a greater weight to the tail and is not very sensitive to outliers and low samples (Greenwood; Landwehr; Matalas, 1979).

$$F_{\mathrm{MEV}}(x) = \frac{1}{T}\sum_{j=1}^{T}\left[1 - \exp\left(-\frac{x}{\beta}\right)^{\gamma}\right]^{\bar{n}} \tag{3.3}$$

To validate the assumption that the parent distribution of daily rainfall can be approximated by the Weibull distribution and to determine the portion of the daily rainfall distribution that defines the tail, we conducted a Monte Carlo tail-test originally developed by Marra et al. (2022). The tail-test proceed as follows: first, we estimate Weibull parameters β and γ corresponding to daily rainfall events exceeding a specific quantile-threshold θ. In this step, we explicitly censored all the annual maxima to ensure an independent assessment of the model's performance in describing observed rainfall extremes. Using the estimated parameters, we generate 1000 synthetic rainfall daily series with the same number of rainfall events present in the tail of the observed rainfall daily series. Finally, we extracted the corresponding annual maxima series from the synthetic series and tested if the observed annual maxima series are likely sample from them.

If more than $p = 5\%$ of the observed maxima lie outside the $1 - p = 95\%$ confidence interval defined by the synthetic annual maxima series, we rejected the hypothesis that rainfall events exceeding the threshold θ follow a Weibull tail. Otherwise, we assume that the left-censored θ rainfall events can be described by a Weibull distribution. We run this test for varying left-censoring θ ($q_{0.10}$ to $q_{0.95}$, with increments of 0.05) and selected the smallest θ for which the test is not rejected to define the tail of the parent distribution. If the test was rejected for all evaluated θ, it means that the Weibull distribution cannot serve as the parent

distribution. We run the tail-test for all 735 catchments' daily historical rainfall series present in the CLIMBra dataset, considering the 19 CMIP6 climate models historical simulations. It is important to highlight that in the tail test, we assume wet days to be independent when fitting the Weibull distribution, as daily rainfall typically exhibit low values of lag-1 autocorrelation (Papalexiou, 2022). Nevertheless, following previous studies (Marra; Amponsah; Papalexiou, 2023; Zorzetto; Botter; Marani, 2016), we conducted Monte Carlo simulations to confirm that these serial correlations do not affect the fitting and our general conclusions: First we generate 10,000 random synthetic series with Weibull shape and scale parameters, of 0.9 and 10, respectively; and sample size ranging between 1500 and 2000 wet days. These parameters and sample size represent, on average, the values obtained in the tail test for our dataset. Then we fit, for each of these synthetic series, the Weibull distribution to assess the fitted shape and scale parameters. In sequence, we repeated this process, but introducing, in this second case, a lag-1 autocorrelation of 0.3, which is close to the observed AC-1 for our dataset. The fitted shape and scale parameters obtained for the first and second case are alike. For instance, for the first case, we obtained a mean (standard deviation) shape and scale parameters of 0.9 (0.02) and 10 (0.33). For the second case, the shape and scale parameters were 0.9 (0.02) and 9.99 (0.51).

Once the suitability of the Weibull distribution to represent Brazilian catchments' rainfall events was confirmed (see Figure 3.5), we fit the SMEV distribution for the future simulations driven by the SSP2-4.5 and SSP5-8.5 scenarios. For catchments where the Weibull distribution was not rejected, we used the portion of rainfall events defined in the tail-test to fit the SMEV. For the others, we adopted $q_{0.95}$ to define the tail, following Marra et al. (2023). We used the fitted SMEV to compute the projected changes in rainfall quantiles associated with varying return periods T (5, 10, 50, 100, 200, and 500 years) between historical and future simulations. Alternatively, we fit the SMEV distribution using all wet rainfall events and obtained similar results in terms of projected relative changes (not showed here).

3.3 Results

The interplay between the expected changes in intensity and frequency of rainfall events vary significantly across the evaluated quantile-thresholds intervals (Figure 3.2). Here we focus on the projected changes computed for the SSP5-8.5 future scenario, although similar results were obtained for SSP2-4.5 (see Appendix B, Figure S3.1). In general, for all quantile-

thresholds intervals, the intensity of rainfall events is projected to increase similarly. This intensification, however, does not always translate into an increase in the total rainfall due to the divergent expected changes in rainfall frequency. For example, approximately 80% (multi-model ensemble median) of the catchments are projected to exhibit an increase in rainfall for the events exceeding $q_{0.50}$. Yet, nearly 100% of the catchments are expecting heightened rainfall intensity. This somewhat counterintuitive pattern can be explained by the fact that approximately 54% of the catchments are projected to experience a reduction in the frequency of rainfall events at this specific threshold (Figure 3.2a). That is, even with an enhanced intensity, some catchments may experience a reduction in total rainfall exceeding $q_{0.50}$ due to a reduction in rainfall frequency. However, as we progress through the evaluated quantile-thresholds, we observe a gradual increase in the expected changes in rainfall frequency. When combined with the intensification of rainfall events, this leads to overall positive projected changes for the total rainfall. For instance, for events exceeding $q_{0.99}$ and $q_{0.999}$, almost all catchments showed an increase in both frequency and intensity (Figure 3.2e, f), culminating in a rise in the total rainfall.

Furthermore, it becomes evident that projected rainfall frequency changes surpass intensity changes as we progress through the evaluated intervals (Figure 3.2g). For the lower quantile-thresholds intervals (Figure 3.2a, b), the magnitudes of expected changes are quite similar. For $q_{0.50}$, we found mean changes of approximately -3% and 12% for requency and intensity, respectively. For $q_{0.70}$, the changes in frequency and intensity are approximately 6% and 11%, respectively. In these cases, CMIP6 models generally project slightly larger increases in intensity when compared to frequency for Brazilian catchments (Figure 3.2g). A contrasting scenario, however, emerges for the larger quantiles, where CMIP6 models project notably greater changes in frequency than in intensity. For instance, for the rainfall events exceeding $q_{0.99}$, the mean absolute expected changes are approximately 10% and 100% for intensity and frequency, respectively (Figure 3.2e). This implies that the projected increase in the extreme rainfall is mainly driven by an increase in rainfall frequency, rather than intensity, such as observed in previous studies (Myhre *et al.*, 2019; Sarkar; Maity, 2022).

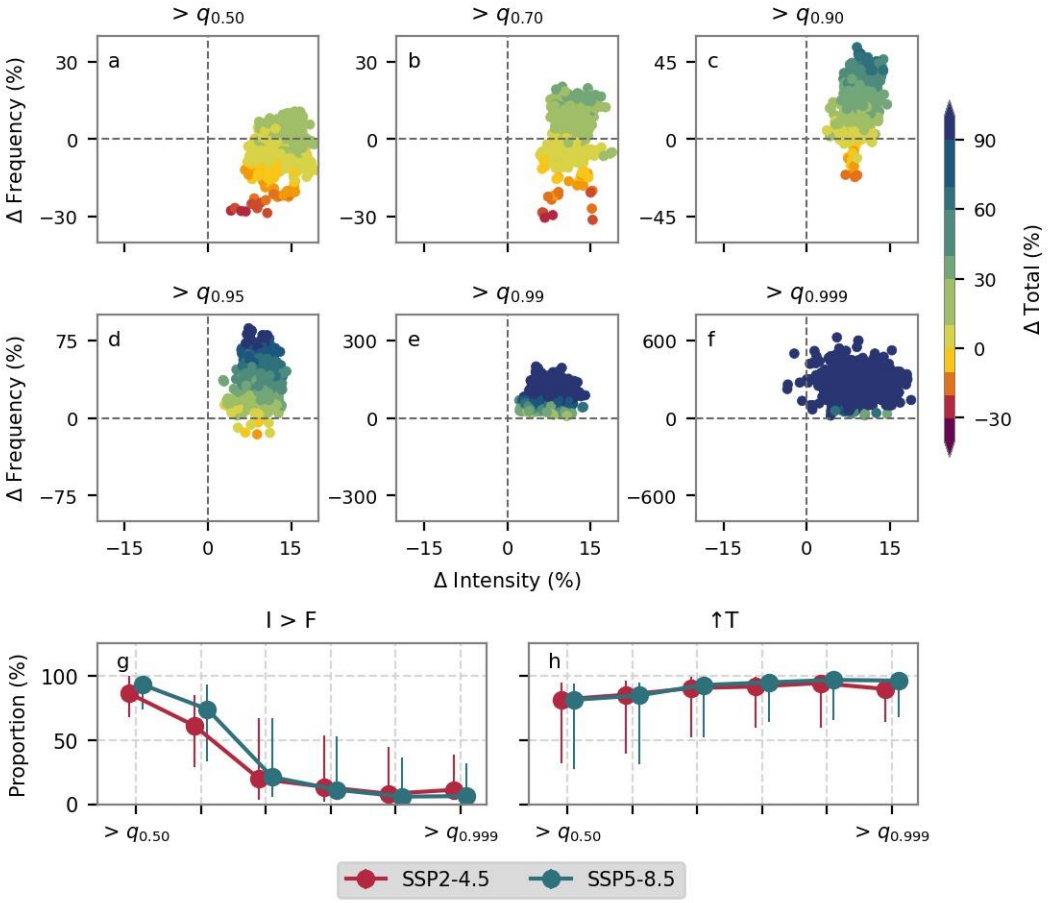

Figure 3.2. a-f, Relative changes (CMIP6 multi-model ensemble median) between historical (1980-2010) and distant future (2070-2100; SSP5-8.5) periods in frequency, intensity and total rainfall for different quantile-thresholds obtained for the 735 catchments. Changes in frequency, intensity and total rainfall were computed for CMIP6 GCMs individually and we display the CMIP6 multi-model ensemble median of these changes.(a) $> q_{0.50}$, (b), $> q_{0.70}$, (c) $> q_{0.90}$, (d) $> q_{0.95}$, (e) $> q_{0.99}$, and (f) $> q_{0.999}$. Black, dashed lines divide the quadrants(g) Proportion of catchments where the relative change in intensity was larger than the relative changes in frequency for each quantile-thresholds intervals considering both SSP2-4.5 and SSP5-8.5 scenarios. (h) Proportions of catchments with positive relative changes in total rainfall for each quantile-thresholds intervals considering both SSP2-4.5 and SSP5-8.5 scenarios. The central points (bars) indicate the median (95% confidence intervals) proportion obtained using the 19 CMIP6 climate models.

Despite the importance of such assessment, the overlapping rainfall intervals within the quantile-thresholds approach may affect it. That is, extreme high rainfall events, such as those exceeding $q_{0.999}$, influences the relative changes computed for all evaluated quantile-thresholds. To mitigate this undesired effect and gain a better understanding of projected changes, we conducted an alternative analysis using the quantile-intervals framework (Appendix B, Figure S3.2). The results of both approaches are summarized in Figure 3.3.

Unlike what we observed in the quantile-thresholds approach, there is no dominant pattern of intensification. For the lower quantile-intervals (such as the interval $q_{0.50}$ - $q_{0.70}$), we see a similar count of catchments showing increasing/decreasing intensity (Figure 3.3a). As we progress across the intervals, this proportion gradually raises, suggesting that most of Brazilian catchments are prone to have more intense extreme rainfall events. These contrasting results between approaches were also found for frequency. For the lower quantile-intervals, we found that most catchments exhibited negative changes, whereas, for the lower quantile-thresholds, only half of the catchments exhibited negative changes (Figure 3.3b). For the higher quantiles, in contrast, both approaches converge, indicating that Brazil will likely experience extreme rainfall events more frequently. In general, total rainfall of events present in the lower quantile-intervals are projected to decrease (Figure 3.3d), while the total rainfall of events present in the higher quantile-intervals are projected to increase. The increase in total rainfall was also indicated by the quantile-thresholds approach since the overlapping effects fade over across the evaluated quantiles.

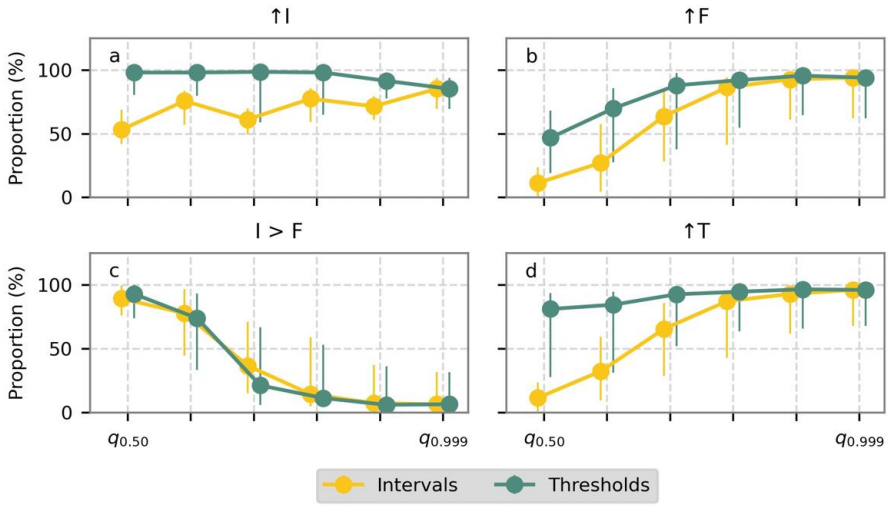

Figure 3.3. a-d, Relative changes (CMIP6 multi-model ensemble median) between historical (1980-2010) and distant future (2070-2100; SSP5-8.5) periods in frequency, intensity and total rainfall for both quantile-thresholds and quantile-intervals approaches. Changes in frequency, intensity and total rainfall were computed for CMIP6 GCMs individually and we display the CMIP6 multi-model ensemble median of these changes. (a) Proportions of catchments with positive relative changes in rainfall intensity. (b) Proportions of catchments with positive relative changes in rainfall frequency. (c) Proportion of catchments where the relative change in intensity was larger than the relative changes in frequency. (d) Proportions of catchments with positive relative changes in total rainfall. The central points (bars) indicate the median (95% confidence intervals) proportion obtained using the 19 CMIP6 climate models.

We displayed on Figure 3.4 the spatial distribution of projected changes using the quantile-intervals approach. The corresponding figures with catchments classified according to their increasing/decreasing condition considering both quantile-intervals and quantile-thresholds approach can be found in the Supporting Information (Figures S3.3 and S3.4). We did not depict projected changes of the higher rainfall quantiles as they exhibited an almost uniform pattern of increasing intensity and frequency for both approaches. In general, the entire country will experience a reduction in moderate rainfall events, primarily driven by a decrease in rainfall frequency, and an increase in extreme rainfall events (Figure S3.3). The Amazon is the biome that will experience the most substantial reduction in non-extreme rainfall events (-23%, on average), and the Pampa, the lowest one (-3%, Figure 3.4a). The others evaluated biomes - Caatinga, Cerrado, and Atlantic forest - exhibited a more diverse spatial pattern, but all of them will experience an overall reduction in moderate rainfall events (Figure 3.4a, b) accompanied by an increase in the other evaluated quantiles. It is interesting to note that, with exception of the Amazon and Pampas biomes, which exhibited a more homogenous and evident decreasing/increasing pattern, these features cannot be observed for the quantile-thresholds approach, given the overlapping-effect (Figures S3.4). Overall, such combination of decrease (increase) in moderate (extreme) rainfall events are expected to alter the shape of the distribution of rainfall events (Pendergrass; Knutti, 2018). Heavy rainfall will likely exhibit a larger contribution to the accumulated, total rainfall in the future period than the contribution observed in the historical period (Figures S3.5). For instance, according to the SSP5-8.5 distant future simulations, the ratio between total rainfall events surpassing the future $q_{0.99}$ quantile and total accumulated 30-year rainfall may increase up to 15% in comparison with the historical period (1980-2010).

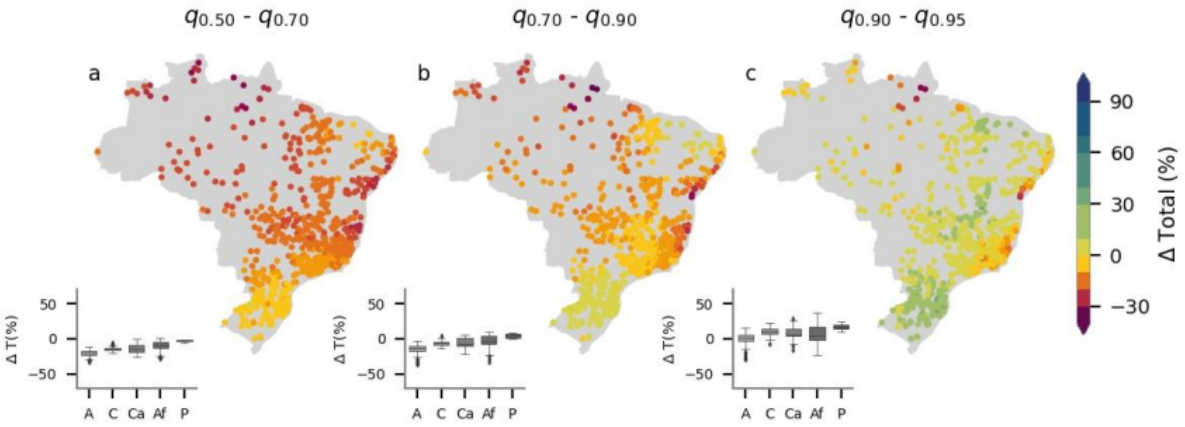

Figure 3.4. a-c, Spatial distribution of the relative changes (CMIP6 multi-model ensemble median) between historical (1980-2010) and distant future (2070-2100; SSP5-8.5) periods in total rainfall for different quantile-intervals. (a) $q_{0.50}$ - $q_{0.70}$, (b) $q_{0.70}$ - $q_{0.90}$, (c) $q_{0.90}$ - $q_{0.95}$. Changes in frequency, intensity and total rainfall were computed for CMIP6 GCMs individually, and we display the CMIP6 multi-model ensemble median of these changes. Changes per Brazilian biome are displayed in traditional boxplots (A: Amazon, C: Cerrado, Ca: Caatinga, Af: Atlantic Forest, and P: Pampa).

To assess how rainfall events within the extrapolation range are expected to alter, we used here the parametric SMEV distribution, assuming that daily rainfall tails of Brazilian catchments follow the Weibull distribution. The outcomes of the tail-test confirmed our hypothesis: the tail of Brazilian catchments' rainfall can indeed be represented by the Weibull distribution (Figure 3.5a). On average across the 19 CMIP6 historical simulations, the assumption of having historical annual maximum daily rainfall emerging from Weibull tails could not be rejected in nearly 98% of the catchments. The catchments in which the assumption was rejected are mainly situated in the Amazon biome. In these cases, extreme precipitation could have a different type of tail, such as heavier than the stretched-exponential Weibull tail, or the Weibull tail could be consist in smaller fractions of the data (Marra; Levizzani; Cattani, 2022). For almost 60% of the evaluated catchments the left-censoring threshold - defined as the smallest θ in which the null hypothesis of the tail test is not rejected - fell above $q_{0.75}$, which is in line with the proportion found by Marra et al. (2023). For the remaining 40%, only the most extreme rainfall events can be employed to represent the tail.

We also assessed the yearly number of wet-days present in the tail defined by the specific threshold (Figure 3.5b). On average, nearly 90 daily rainfall data points are available, per

year, for the estimation of the Weibull parameters. This large sample ensures a robust fit with reduced uncertainties when compared with the GEV-block maxima approach (Volpi *et al.*, 2019), commonly employed in the country (Ballarin *et al.*, 2022). It is also interesting to note the clear spatial pattern of available data points in the tail: for the Amazon and Pampa biomes more data are available for the Weibull fitting (138 and 102 wet-days per year, on average, respectively). For the Caatinga biome, a lower amount of data is available (nearly 50 wet-days per year). This is consistent with the wet and dry rainfall regimes of these biomes. The Cerrado and Atlantic Forest biomes, in contrast, did not exhibit a clear spatial pattern given their heterogeneous distribution throughout Brazil, encompassing different climate regions with varying rainfall distributions (Ballarin et al. 2023a).

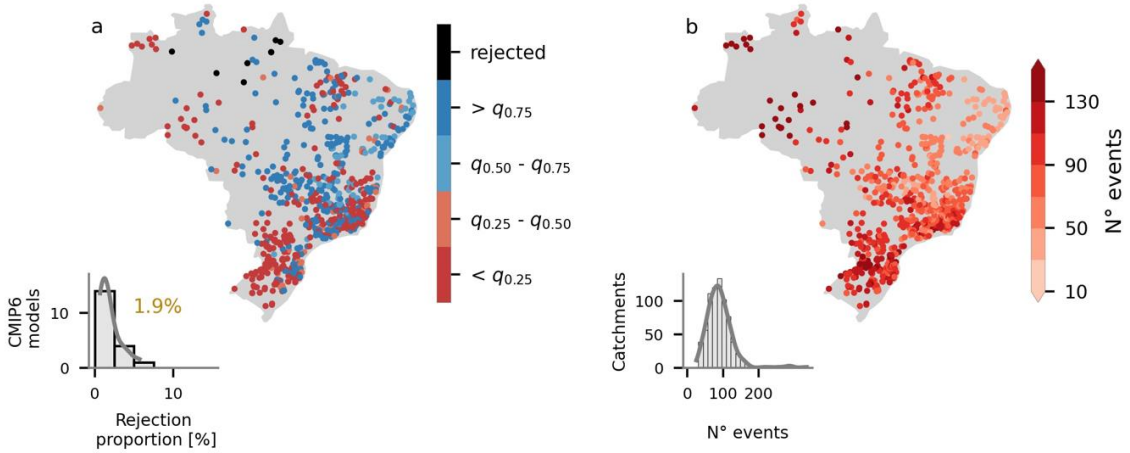

Figure 3.5. Suitability of the Weibull distribution to represent Brazilian catchments' rainfall in the historical (1980-2010) period. a, left censoring threshold θ (quantile-based) used to define the Weibull tails, as the smallest θ in which the test is not rejected. Catchments were the assumption of the Weibull tail was rejected are colored in black. The histogram exhibits the rejection proportion obtained for the 19-CMIP6 climate models simulations. Average rejection proportion is displayed in yellow. b, Average yearly number of wet-days in the tail as defined by the left-censoring threshold.

After confirming the suitability of the Weibull distribution, we used the SMEV distribution to assess how extreme events associated with different return periods might change. In general, we found that they are expected to increase throughout the country (Figure 3.6). The average changes (and also its spatial variability) are expected to be more pronounced for the rarest extreme events (Figure 3.6d-f), suggesting a future trend towards heavier-tailed rainfall. The magnitude of the differences between relative changes obtained for different return periods

are in agreement with the findings of Gründemann *et al.*, (2022), which also assessed projected changes in rainfall extremes using a MEV-based approach.

As observed in the non-parametric approach, the Pampa and part of the Cerrado biomes will experience the most significant intensification in extreme rainfall, particularly for the rarest events (Figure 3.6c). The Amazon biome, on the other hand, will exhibit the lowest increase. Actually, for a few Amazon catchments, the projected changes will be quite similar across the evaluated return periods. As expected, relative changes are notably lower in the immediate future (2010-2040) than in the distant future (2070-2100; Figure 3.6d). Interestingly, we found almost no difference between the changes projected in the immediate future under SSP2-4.5 and SSP5-8.5 scenarios. However, for the distant future, the differences are significantly greater, with the higher emission scenario SSP5-8.5 projecting greater changes. For instance, the 100-year rainfall event is expected to increase 17% and 31%, on average, in the SSP2-4.5 and SSP5-8.5 distant future, respectively. Finally, we found a relatively low variability among CMIP6 projections, indicating a strong model agreement. That is, all evaluated models projected enhanced extreme rainfall, with low between-model standard deviation (Figure S3.6).

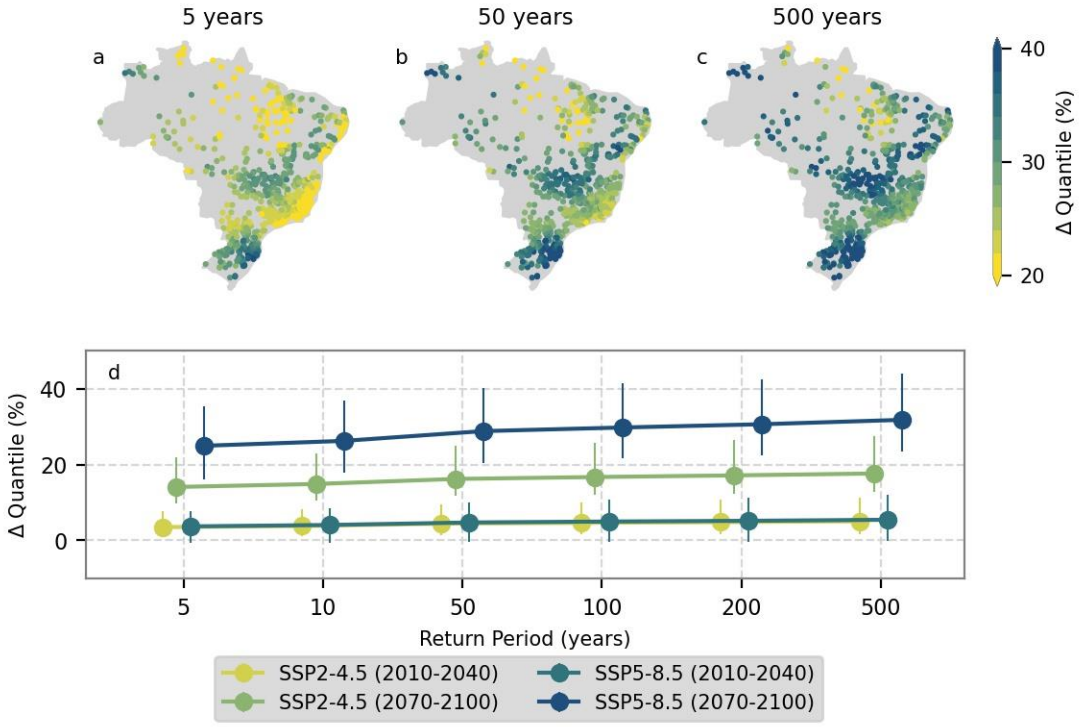

Figure 3.6. a-c, Spatial distribution of the relative changes (CMIP6 multi-model ensemble median) between historical (1980-2010) and distant future (2070-2100; SSP5-8.5) periods in the SMEV-rainfall quantiles associated to different return periods: (a) 5 years, (b) 50 years, (c) 500 years. Changes in frequency, intensity and total rainfall were computed for CMIP6 GCMs individually, and we display the CMIP6 multi-model ensemble median of these changes. (d) Summary of projected changes in future extreme rainfall events for the immediate (2010-2040) and distant (2070-2100) future under the SSP2-4.5 and SSP5-8.5 scenarios. The central points (bars) indicate the median (95% confidence intervals) projected changes obtained for the 735 Brazilian catchments considering the multi-model ensemble mean.

For simplicity, we adopted here the same Weibull tail defined for the historical period to estimate projected changes in future extreme rainfall events (Figure 3.6). Nevertheless, future rainfall can be made up by different climate processes, and therefore, might be better represented by alternative left-censoring thresholds θ (or even by other heavier/lighter tail distributions). Hence, we repeated the tail-test for the SSP5-8.5 distant future (2070-2100) simulations (Figure S3.7). The results reaffirmed the suitability of the Weibull distribution to represent future Brazilian rainfall events. The mean proportion of rejections slightly increased (from 1.9 to 3.9%) and there was a slight shift in the spatial distribution of the left-censoring threshold. Even so, the Weibull distribution was not rejected in 96% (on average) of the catchments. We employed these updated θ-values to fit the SMEV-distribution and to calculate changes between historical and future extreme rainfall quantiles (such as did in Figure 3.6). This approach helped us to assess how the use of historical (or future) left censoring thresholds affects our results (Figure 3.7). For the lower evaluated return periods, both historical and future θ-tails yielded high similar relative changes. As we progress across the return periods, the difference between the relative changes (both in terms of mean and variability) marginally increased, with future θ-tails projecting slightly heavier tails. Even so, the projected changes are of the same order of magnitude.

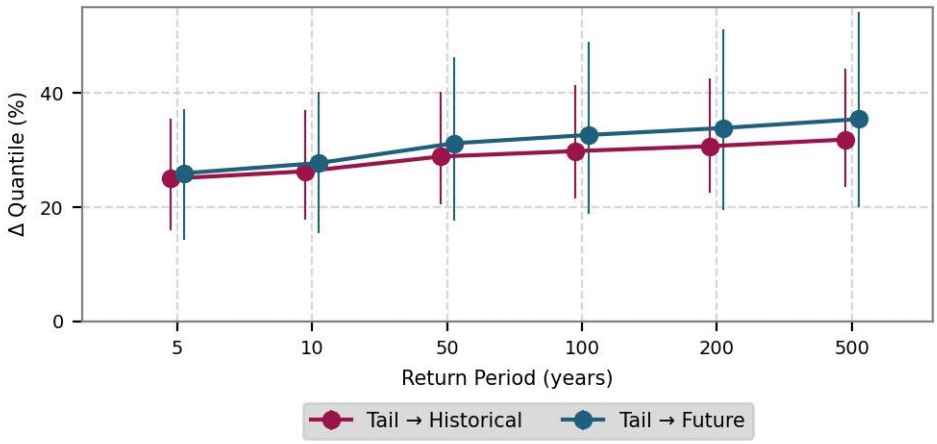

Figure 3.7. Projected changes in SMEV-rainfall quantiles computed using Weibull tails defined in the historical (1980-2010) and future (2070-2100; SSP5-8.5) periods. Changes in frequency, intensity and total rainfall were computed for CMIP6 GCMs individually, and we CMIP6 display the multi-model ensemble median of these changes. The central points (bars) indicate the median (95% confidence intervals) standard deviation of the projected changes obtained for the 735 Brazilian catchments.

3.4 DISCUSSION

Here we first examined how rainfall events are expected to change in Brazil in terms of both frequency and intensity, using two different - and complementary – non-parametric frameworks. From this two-sided perspective, three important aspects emerged. First, changes in frequency, rather than intensity, appears to dictate the projected changes of future rainfall (Myhre *et al.*, 2019; Nissen; Ulbrich, 2017; Sarkar; Maity, 2022). We observed an intensification of future rainfall events even with a reduction in rainfall intensity given an enhanced rainfall frequency. This finding underscores the importance of incorporating frequency on climate assessments (Pendergrass; Hartmann, 2014). Furthermore, it takes on even greater significance in view of the relative frequency changes observed in this study, which greatly surpassed the magnitude of changes reported in previous studies that only assessed rainfall intensity (Westra; Alexander; Zwiers, 2013).

Second, the varying pattern of changes across different rainfall quantiles (Figure 3.2 and Figure 3.3) demonstrates the advantages of assessing different parts of the rainfall distribution, rather than exclusively focusing on extreme events. Heavy and light/moderate rainfall events have different driving mechanisms and, consequently, respond differently to climate changes (Allan; Soden, 2008). Nevertheless, the majority of previous studies have primarily focused on extreme rainfall events, given their relevance for water infrastructure designing (Markonis *et al.*, 2019). Our findings indicates that in Brazil, moderate rainfall events ($< q_{0.70}$) are expected to reduce while heavy ones are expected to enhance, with both of them governed by changes in the frequency (Figure 3.3). These change patterns align with the compensation hypothesis, which states that increases in heavy rainfall events would be compensated by a reduction in light/moderate rainfall (Allen; Ingram, 2002; Fischer; Knutti, 2016; Hennessy; Gregory; Mitchell, 1997; Moustakis *et al.*, 2021). Nevertheless, it is noteworthy that this hypothesis has been formulated in the basis of climate model simulations, which in its majority reported enhanced heavy combined with reduced light/moderate rainfall. However, the underlying mechanisms of how rainfall events are predicted to change remain unclear, and the observed compensation mechanism might be an outcome of the application of climate model simulations. For instance, Markonis *et al.* (2019), when assessing changes in the rainfall distribution using a global dataset reported results

that go against the compensation mechanism, underscoring the need for future research focused on this topic.

Third, our findings highlight the importance of considering the complementary quantile-thresholds and intervals approaches to gain a deeper understanding of the expected changes in future rainfall events (Figure 3.3). While the former provides us with a general overview of the expected changes in precipitation events, the latter allows us to assess how different precipitation events are likely to change (Allan; Soden, 2008). For example, it was only possible to identify the compensation hypothesis after evaluating the quantile-intervals approach. This suggests that the light/moderate rainfall intensification pattern observed for the threshold approach is actually a consequence of the overlapping-effect. This finding is particularly important considering that many climate change impact studies relies on the quantile-thresholds reasoning, which is embedded in the indices developed by the Extreme Team on Climate Change Detection and Indices (ETCCDI; Zhang *et al.* 2011). Notably, the exclusive use of these indices to assess changes in rainfall characteristics has already faced criticism (Schär *et al.*, 2016). We showed here that indeed the overlapping effect of threshold-based approaches can lead to misleading conclusions, and therefore should be accounted for in future studies.

We further validated the intensification pattern of extreme rainfall events through a parametric approach, using a SMEV-based analysis. There is a clear pattern suggesting that the expected increase of extreme events is proportional to its rareness (Figure 3.6). Moreover, projected changes are in the same order of magnitude of changes reported in previous studies (Abdelmoaty; Papalexiou, 2023; Crévolin; Hassanzadeh; Bourdeau-Goulet, 2023; Gründemann *et al.*, 2022). For instance, for the higher emission scenario, a 100-year rainfall event is expected to increase nearly 31% in Brazil, in comparison with the averaged globally value of 32.5% obtained by Gründermann et al. (2022). Furthermore, the changes are expected to escalate over time and with varying emission scenarios. Across all return periods, changes between historical and future rainfall events will (1) be nearly 50% larger for the SSP5-8.5 scenario than for the SSP2-4.5, in the distant future; and (2) more than 100% larger in the distant future than in the immediate future, for the same scenarios.

Even though both non-parametric and parametric approaches suggested that extreme events are expected to increase, we should emphasize some aspects, as they may affect our

results. As one can note in Figure 3.7, altering the way in which we fit the parametric distribution affected our findings (albeit to a small extent in our case). This indicates that different conclusions can arise by varying, for example, the parameter estimation or the probability distribution. For instance, for a distant future, SSP5.8-5, 100-year return period, the GEV distribution projected averaged changes of 45% (not showed here) in comparison with the 33% obtained using the SMEV approach. As already mentioned, the SMEV uses way larger sample sizes in the fitting procedure, besides relaxing the asymptotic assumption, which may explain these differences. Even so, both GEV and SMEV projected positive changes for all scenarios and futures periods, reinforcing the validity of our findings.

Another factor that influences our results is the uncertainty present in climate models projections, which are known to exhibit a lower accuracy in representing extreme high and low rainfall events (Londoño Arteaga; Lima, 2021; Mishra *et al.*, 2014; Sherwood *et al.*, 2010; Trenberth; Zhang; Gehne, 2017). To reduce these undesirable effects, we used here a bias-corrected dataset that includes a variety of climate models projections to encompass different climate representations (Li *et al.*, 2017). Nevertheless, even presenting a better performance to represent observed values, the bias-corrected dataset may contain inherent uncertainties and physically unrealistic values (Casanueva *et al.*, 2020). Finally, it is important to note that we assessed projected changes from a catchment-perspective. We emphasize that using averaged daily series may hinder extreme events, especially in large basins, since extreme high events of a specific grid may be smoothed by non-extreme events recorded in neighboring grids (Ballarin et al., 2023a).

3.5 CONCLUSION

We assessed how future Brazilian rainfall events are projected to change. Rather than focusing solely on extreme events, we propose an alternative framework to assess how rainfall events of varying magnitudes are projected to change in both intensity and frequency. Our findings suggested that changes in Brazilian future rainfall are asymmetric: light/moderate rainfall are expected to reduce, while extreme rainfall are expected to increase. For instance, on average, a 100-year rainfall event is expected to increase nearly 31% across Brazil for the SSP5-8.5 CMIP6 scenario at the end of the century. This uneven change pattern aligns with the compensation hypothesis. Moreover, we showed that changes in frequency, rather than intensity, rules the projected changes of rainfall events. Namely, rainfall events exceeding the historical rainfall quantile $q_{0.99}$ are projected to increase nearly 10% and 100% in intensity and frequency, respectively. Finally, we showed that using a threshold-based approach to assess future rainfall changes can result in misleading conclusions. We believe that the evidence gathered here will certainly contribute to not only a better understanding of future rainfall events in Brazil but also to an enhanced comprehension of the different rainfall properties and their interplay. Future research towards this topic - such as investigating how rainfall properties are expected to change seasonally and how these changes are linked to temperature - should shed more light to the compensation hypothesis and to the controlling mechanisms of the changes in rainfall intensity and frequency.

3.6 REFERENCES

ABDELMOATY, H. M. *et al.* Biases Beyond the Mean in CMIP6 Extreme Precipitation: A Global Investigation. **Earth's Future**, [*s. l.*], v. 9, n. 10, p. 1–17, 2021.

ABDELMOATY, H. M.; PAPALEXIOU, S. M. Changes of Extreme Precipitation in CMIP6 Projections: should We use Stationary or Nonstationary Models?. **Journal of Climate**, [*s. l.*], n. January, p. 1–40, 2023.

ALEXANDER, L. V. Global observed long-term changes in temperature and precipitation extremes: A review of progress and limitations in IPCC assessments and beyond. **Weather and Climate Extremes**, [*s. l.*], v. 11, p. 4–16, 2016.

ALLAN, R. P.; SODEN, B. J. Atmospheric warming and the amplification of precipitation extremes. **Science**, [*s. l.*], v. 321, n. 5895, p. 1481–1484, 2008.

ALLEN, M. R.; INGRAM, W. J. Constraints on future changes in climate and the hydrologic cycle. **Nature**, [*s. l.*], v. 419, n. 6903, 2002.

ALMAGRO, A. *et al.* CABra: a novel large-sample dataset for Brazilian catchments. **Hydrology and Earth System Sciences**, [*s. l.*], p. 1–40, 2021.

ASADIEH, B.; KRAKAUER, N. Y. Global trends in extreme precipitation: Climate models versus observations. **Hydrology and Earth System Sciences**, [*s. l.*], v. 19, n. 2, p. 877–891, 2015.

ÁVILA, A. *et al.* Recent precipitation trends, flash floods and landslides in southern Brazil. **Environmental Research Letters**, [*s. l.*], v. 11, n. 11, 2016.

BALLARIN, A. S. *et al.* CLIMBra - Climate Change Dataset for Brazil. **Scientific Data**, [*s. l.*], p. 1–31, 2023.

BALLARIN, A. S. *et al.* Combined predictive and descriptive tests for extreme rainfall probability distribution selection. **Hydrological Sciences Journal**, [*s. l.*], n. May, 2022.

BALLARIN, A. S.; ANACHE, J. A. A.; WENDLAND, E. Trends and abrupt changes in extreme rainfall events and their influence on design quantiles: a case study in São Paulo, Brazil. **Theoretical and Applied Climatology**, [*s. l.*], v. 149, n. 3–4, p. 1753–1767, 2022.

BERANOVÁ, R.; KYSELÝ, J.; HANEL, M. Characteristics of sub-daily precipitation extremes in observed data and regional climate model simulations. **Theoretical and Applied Climatology**, [*s. l.*], v. 132, n. 1–2, p. 515–527, 2018.

CANNON, A. J.; SOBIE, S. R.; MURDOCK, T. Q. Bias correction of GCM precipitation by quantile mapping: How well do methods preserve changes in quantiles and extremes?. **Journal of Climate**, [*s. l.*], v. 28, n. 17, p. 6938–6959, 2015.

CASANUEVA, A. *et al.* Testing bias adjustment methods for regional climate change applications under observational uncertainty and resolution mismatch. **Atmospheric Science Letters**, [*s. l.*], v. 21, n. 7, p. 1–12, 2020.

CHAGAS, V. B. P.; CHAFFE, P. L. B.; BLÖSCHL, G. Climate and land management accelerate the Brazilian water cycle. **Nature Communications**, [*s. l.*], n. 13:5136, 2022.

CHAUBEY, P. K.; MALL, R. K. Intensification of Extreme Rainfall in Indian River Basin: Using Bias Corrected CMIP6 Climate Data. **Earth's Future**, [*s. l.*], v. 11, n. 9, p. 1–19, 2023.

COTTERILL, D. *et al.* Increase in the frequency of extreme daily precipitation in the United Kingdom in autumn. **Weather and Climate Extremes**, [*s. l.*], v. 33, p. 100340, 2021.

CRÉVOLIN, V.; HASSANZADEH, E.; BOURDEAU-GOULET, S. C. Updating the intensity-duration-frequency curves in major Canadian cities under changing climate using CMIP5 and CMIP6 model projections. **Sustainable Cities and Society**, [*s. l.*], v. 92, n. September 2022, 2023.

CUNHA, A. P. M. A. *et al.* Changes in the spatial–temporal patterns of droughts in the Brazilian Northeast. **Atmospheric Science Letters**, [*s. l.*], v. 19, n. 10, p. 1–8, 2018.

DE MICHELE, C. Advances in Deriving the Exact Distribution of Maximum Annual Precipitation. **Water**, [*s. l.*], v. 11, n. 2322, 2019.

DE MICHELE, C.; AVANZI, F. Superstatistical distribution of daily precipitation extremes: A worldwide assessment. **Scientific Reports**, [*s. l.*], v. 8, n. 1, p. 1–11, 2018.

DIFFENBAUGH, N. S. *et al.* Quantifying the influence of global warming on unprecedented extreme climate events. **Proceedings of the National Academy of Sciences of the United States of America**, [*s. l.*], v. 114, n. 19, p. 4881–4886, 2017.

DOOCY, S. *et al.* The Human Impact of Earthquakes: A Historical Review of Events 1980-2009 and Systematic Literature Review. **PLoS Currents**, [*s. l.*], n. APR 2013, p. 1–27, 2013.

FAN, X. *et al.* Future Climate Change Hotspots Under Different 21st Century Warming Scenarios. **Earth's Future**, [*s. l.*], v. 9, n. 6, 2021.

FISCHER, E. M.; KNUTTI, R. Observed heavy precipitation increase confirms theory and early models. **Nature Climate Change**, [*s. l.*], v. 6, n. 11, p. 986–991, 2016.

GEBRECHORKOS, S. H. *et al.* Future Changes in Climate and Hydroclimate Extremes in East Africa. **Earth's Future**, [*s. l.*], v. 11, n. 2, p. 1–21, 2023.

GESUALDO, G. C. *et al.* Unveiling water security in Brazil: current challenges and future perspectives. **Hydrological Sciences Journal**, [*s. l.*], v. 66, n. 5, p. 759–768, 2021.

GREENWOOD, J. A.; LANDWEHR, J. M.; MATALAS, N. C. Probability Weighted Moments: Definition and relation to parameters of several distributions expressable in inverse form. **Water Resources Research**, [*s. l.*], v. 15, n. 5, p. 1049–1054, 1979.

GRÜNDEMANN, G. J. *et al.* Extreme precipitation return levels for multiple durations on a global scale. **Journal of Hydrology**, [*s. l.*], v. 621, n. July 2022, p. 129558, 2023.

GRÜNDEMANN, G. J. *et al.* Rarest rainfall events will see the greatest relative increase in magnitude under future climate change. **Communications Earth & Environment**, [*s. l.*], n. 3:235, 2022.

HARP, R. D.; HORTON, D. E. Observed Changes in Interannual Precipitation Variability in the United States. **Geophysical Research Letters**, [*s. l.*], v. 50, n. 19, p. 1–9, 2023.

HENNESSY, K. J.; GREGORY, J. M.; MITCHELL, J. F. B. Changes in daily precipitation under enhanced greenhouse conditions. **Climate Dynamics**, [*s. l.*], v. 13, n. 9, p. 667–680, 1997.

JOHN, A. *et al.* Quantifying CMIP6 model uncertainties in extreme precipitation projections. **Weather and Climate Extremes**, [*s. l.*], v. 36, n. October 2021, p. 100435, 2022.

KIRCHMEIER-YOUNG, M. C.; ZHANG, X. Human influence has intensified extreme precipitation in North America. **Proceedings of the National Academy of Sciences of the United States of America**, [*s. l.*], v. 117, n. 24, p. 13308–13313, 2020.

LI, W. *et al.* A review on statistical postprocessing methods for hydrometeorological ensemble forecasting. **Wiley Interdisciplinary Reviews: Water**, [*s. l.*], v. 4, n. 6, 2017.

LIMA, C. H. R.; KWON, H. H.; KIM, Y. T. A local-regional scaling-invariant Bayesian GEV model for estimating rainfall IDF curves in a future climate. **Journal of Hydrology**, [*s. l.*], v. 566, n. September, p. 73–88, 2018.

LONDOÑO ARTEAGA, V.; LIMA, C. H. R. Analysis of CMIP5 simulations of key climate indices associated with the South America monsoon system. **International Journal of Climatology**, [*s. l.*], v. 41, n. 1, p. 404–422, 2021.

LUCAS, E. W. M. *et al.* Trends in climate extreme indices assessed in the Xingu river basin - Brazilian Amazon. **Weather and Climate Extremes**, [*s. l.*], v. 31, n. January, p. 100306, 2021.

MARANI, M.; IGNACCOLO, M. A metastatistical approach to rainfall extremes. **Advances in Water Resources**, [*s. l.*], v. 79, p. 121–126, 2015.

MARANI, M.; ZANETTI, S. Long-term oscillations in rainfall extremes in a 268 year daily time series. **Water Resources Research**, [*s. l.*], v. 21, p. 639–647, 2015.

MARENGO, J. A. *et al.* Heavy rainfall associated with floods in southeastern Brazil in November–December 2021. **Natural Hazards**, [*s. l.*], v. 116, n. 3, p. 3617–3644, 2023.

MARKONIS, Y. *et al.* Assessment of Water Cycle Intensification Over Land using a Multisource Global Gridded Precipitation DataSet. **Journal of Geophysical Research: Atmospheres**, [*s. l.*], v. 124, n. 21, p. 11175–11187, 2019.

MARRA, F. *et al.* A simplified MEV formulation to model extremes emerging from multiple nonstationary underlying processes. **Advances in Water Resources**, [*s. l.*], v. 127, n. April, p. 280–290, 2019.

MARRA, F. *et al.* Metastatistical Extreme Value analysis of hourly rainfall from short records: Estimation of high quantiles and impact of measurement errors. **Advances in Water Resources**, [*s. l.*], v. 117, n. March, p. 27–39, 2018.

MARRA, F.; AMPONSAH, W.; PAPALEXIOU, S. M. Non-asymptotic Weibull tails explain the statistics of extreme daily precipitation. **Advances in Water Resources**, [*s. l.*], v. 173, n. January, p. 104388, 2023.

MARRA, F.; LEVIZZANI, V.; CATTANI, E. Changes in extreme daily precipitation over Africa: Insights from a non-asymptotic statistical approach. **Journal of Hydrology X**, [*s. l.*], v. 16, n. July, p. 100130, 2022.

MCBEAN, G.; RODGERS, C. Climate hazards and disasters: The need for capacity building. **Wiley Interdisciplinary Reviews: Climate Change**, [*s. l.*], v. 1, n. 6, p. 871–884, 2010.

MIN, S. K. *et al.* Human contribution to more-intense precipitation extremes. **Nature**, [*s. l.*], v. 470, n. 7334, p. 378–381, 2011.

MINIUSSI, A.; MARANI, M. Estimation of Daily Rainfall Extremes Through the Metastatistical Extreme Value Distribution: Uncertainty Minimization and Implications for Trend Detection. **Water Resources Research**, [*s. l.*], v. 56, n. 7, p. 1–18, 2020.

MISHRA, V. *et al.* Reliability of regional and global climate models to simulate precipitation extremes over India. **Journal of Geophysical Research: Atmospheres**, [*s. l.*], v. 119, p. 9301–9323, 2014.

MISHRA, V.; BHATIA, U.; TIWARI, A. D. Bias-corrected climate projections for South Asia from Coupled Model Intercomparison Project-6. **Scientific Data**, [*s. l.*], v. 7, n. 1, p. 1–13, 2020.

MOUSTAKIS, Y. *et al.* Seasonality, Intensity, and Duration of Rainfall Extremes Change in a Warmer Climate. **Earth's Future**, [*s. l.*], v. 9, 2021.

MUKHERJEE, S. *et al.* Increase in extreme precipitation events under anthropogenic warming in India. **Weather and Climate Extremes**, [*s. l.*], v. 20, n. July 2017, p. 45–53, 2018.

MYHRE, G. *et al.* Frequency of extreme precipitation increases extensively with event rareness under global warming. **Scientific Reports**, [*s. l.*], v. 9, n. 1, p. 1–10, 2019.

NERANTZAKI, S. D.; PAPALEXIOU, S. M. Assessing extremes in hydroclimatology: A review on probabilistic methods. **Journal of Hydrology**, [*s. l.*], v. 605, n. December 2021, p. 127302, 2022.

NISSEN, K. M.; ULBRICH, U. Increasing frequencies and changing characteristics of heavy precipitation events threatening infrastructure in Europe under climate change. **Natural Hazards and Earth System Sciences**, [*s. l.*], v. 17, n. 7, p. 1177–1190, 2017.

PAPALEXIOU, S. M. Rainfall Generation Revisited: Introducing CoSMoS-2s and Advancing Copula-Based Intermittent Time Series Modeling. **Water Resources Research**, [*s. l.*], v. 58, n. 6, p. 1–33, 2022.

PAPALEXIOU, S. M. Unified theory for stochastic modelling of hydroclimatic processes: Preserving marginal distributions, correlation structures, and intermittency. **Advances in Water Resources**, [*s. l.*], v. 115, p. 234–252, 2018.

PAPALEXIOU, S. M.; KOUTSOYIANNIS, D. A global survey on the seasonal variation of the marginal distribution of daily precipitation. **Advances in Water Resources**, [*s. l.*], v. 94, p. 131–145, 2016.

PAPALEXIOU, S. M.; KOUTSOYIANNIS, D. Battle of extreme value distributions: A global survey on extreme daily rainfall. **Water Resources Research**, [*s. l.*], v. 49, n. 1, p. 187–201, 2013.

PAPALEXIOU, S. M.; MONTANARI, A. Global and Regional Increase of Precipitation Extremes Under Global Warming. **Water Resources Research**, [*s. l.*], v. 55, n. 6, p. 4901–4914, 2019.

PENDERGRASS, A. G.; HARTMANN, D. L. Changes in the distribution of rain frequency and intensity in response to global warming. **Journal of Climate**, [*s. l.*], v. 27, n. 22, p. 8372–8383, 2014.

PENDERGRASS, A. G.; KNUTTI, R. The Uneven Nature of Daily Precipitation and Its Change. **Geophysical Research Letters**, [*s. l.*], v. 45, n. 21, p. 11,980-11,988, 2018.

PETERSON, T. C. *et al.* Monitoring and understanding changes in heat waves, cold waves, floods, and droughts in the United States: State of knowledge. **Bulletin of the American Meteorological Society**, [*s. l.*], v. 94, n. 6, p. 821–834, 2013.

RAGNO, E. *et al.* Quantifying Changes in Future Intensity-Duration-Frequency Curves Using Multimodel Ensemble Simulations. **Water Resources Research**, [*s. l.*], v. 54, n. 3, p. 1751–1764, 2018.

REGOTO, P. *et al.* Observed changes in air temperature and precipitation extremes over Brazil. **International Journal of Climatology**, [*s. l.*], v. 41, n. 11, p. 5125–5142, 2021.

ROBINSON, A. *et al.* Increasing heat and rainfall extremes now far outside the historical climate. **npj Climate and Atmospheric Science**, [*s. l.*], v. 4, n. 1, p. 3–6, 2021.

SANTOS, E. B.; LUCIO, P. S.; SANTOS E SILVA, C. M. Estimating return periods for daily precipitation extreme events over the Brazilian Amazon. **Theoretical and Applied Climatology**, [*s. l.*], v. 126, n. 3–4, p. 585–595, 2016.

SARKAR, S.; MAITY, R. Future Characteristics of Extreme Precipitation Indicate the Dominance of Frequency Over Intensity: A Multi-Model Assessment From CMIP6 Across India. **Journal of Geophysical Research: Atmospheres**, [*s. l.*], v. 127, n. 16, p. 1–22, 2022.

SCHÄR, C. *et al.* Percentile indices for assessing changes in heavy precipitation events. **Climatic Change**, [*s. l.*], v. 137, n. 1–2, p. 201–216, 2016.

SCHELLANDER, H.; LIEB, A.; HELL, T. Error Structure of Metastatistical and Generalized Extreme Value Distributions for Modeling Extreme Rainfall in Austria. **Earth and Space Science**, [*s. l.*], v. 6, n. 9, p. 1616–1632, 2019.

SHARIFINEJAD, A.; HASSANZADEH, E.; ZAERPOUR, M. Assessing water system vulnerabilities under changing climate conditions using different representations of a hydrological system. **Hydrological Sciences Journal**, [*s. l.*], v. 67, n. 2, p. 287–303, 2022.

SHERWOOD, S. C. *et al.* Tropospheric water vapor, convection, and climate. **Reviews of Geophysics**, [*s. l.*], v. 48, n. 2, p. 1–29, 2010.

SILLMANN, J. *et al.* Understanding, modeling and predicting weather and climate extremes: Challenges and opportunities. **Weather and Climate Extremes**, [*s. l.*], v. 18, n. October, p. 65–74, 2017.

SWAIN, D. L. *et al.* Trends in atmospheric patterns conducive to seasonal precipitation and temperature extremes in California. **Science Advances**, [*s. l.*], v. 2, n. 4, p. 1–14, 2016.

TRENBERTH, K. E.; ZHANG, Y.; GEHNE, M. Intermittency in precipitation: Duration, frequency, intensity, and amounts using hourly data. **Journal of Hydrometeorology**, [*s. l.*], v. 18, n. 5, p. 1393–1412, 2017.

UKKOLA, A. M. *et al.* Evaluating CMIP5 model agreement for multiple drought metrics. **Journal of Hydrometeorology**, [*s. l.*], v. 19, n. 6, p. 969–988, 2018.

VENEZIANO, D.; LANGOUSIS, A.; LEPORE, C. New asymptotic and preasymptotic results on rainfall maxima from multifractal theory. **Water Resources Research**, [*s. l.*], v. 45, n. 11, p. 1–12, 2009.

VOLPI, E. On return period and probability of failure in hydrology. **WIREs Water**, [*s. l.*], v. 6:e1340, 2019.

VOLPI, E. *et al.* Save hydrological observations! Return period estimation without data decimation. **Journal of Hydrology**, [*s. l.*], v. 571, n. February, p. 782–792, 2019.

WESTRA, S.; ALEXANDER, L. V.; ZWIERS, F. W. Global increasing trends in annual maximum daily precipitation. **Journal of Climate**, [*s. l.*], v. 26, n. 11, p. 3904–3918, 2013.

WILSON, P. S.; TOUMI, R. A fundamental probability distribution for heavy rainfall. **Geophysical Research Letters**, [*s. l.*], v. 32, n. 14, p. 1–4, 2005.

YU, R.; ZHAI, P. M.; LI, W. Future Extreme Precipitation in Summer Will Become More Widespread in China Depending on Level of Warming. **Earth's Future**, [*s. l.*], v. 11, n. 11, p. 1–10, 2023.

ZAGHLOUL, M. *et al.* Revisiting flood peak distributions: A pan-Canadian investigation. **Advances in Water Resources**, [*s. l.*], v. 145, n. August, p. 103720, 2020.

ZHANG, X. *et al.* Indices for monitoring changes in extremes based on daily temperature and precipitation data. **Wiley Interdisciplinary Reviews: Climate Change**, [*s. l.*], v. 2, n. 6, p. 851–870, 2011.

ZILLI, M. T. *et al.* A comprehensive analysis of trends in extreme precipitation over southeastern coast of Brazil. **International Journal of Climatology**, [*s. l.*], v. 37, n. 5, p. 2269–2279, 2017.

ZORZETTO, E.; BOTTER, G.; MARANI, M. On the emergence of rainfall extremes from ordinary events. **Geophysical Research Letters**, [*s. l.*], v. 43, p. 8076–8082, 2016.

CHAPTER 4

Drought intensification in Brazilian catchments: implications for water demand and land cover

ABSTRACT

Droughts exert widespread impacts on both natural and social systems, and there is accumulating evidence that this situation may worsen in the context of global warming. Despite the importance of assessing changes in droughts to understand their potential future impacts on society, studies are unevenly distributed worldwide. In this study, utilizing CMIP6 bias-corrected simulations and a standard precipitation-evaporation index (SPEI) approach, we quantified expected changes in future drought properties across 735 Brazilian catchments under SSP2-4.5 and SSP5-8.5 scenarios. Beyond evaluating the statistical properties of future drought events, we assessed their occurrence under land use and water demand perspectives and propose a new framework to better understand their link with changes in long- and short-term conditions of precipitation (P) and potential evapotranspiration (PET). Our results indicate that, overall, drought events are projected to become more frequent and severe in the future, with high CMIP6 model agreement. Despite magnitude differences, droughts are expected to intensify in both evaluated scenarios. According to the SSP5-8.5 scenario, at least half of Brazilian cropland and pasture areas will experience an increase of over 30% in drought properties by the end of the century. Furthermore, among the 85% of catchments expected to experience more severe droughts, nearly 90% are also projected to exhibit increased water demand, which likely exacerbates future water scarcity. The investigation of the relationship between droughts changes and climate variables suggests that increasing atmosphere evaporative demand - expressed in terms of PET - and rainfall variability exert great influence on future droughts. For instance, over 50% of evaluated Brazilian catchments are expected to experience an intensification of drought properties even with increases in long-term average precipitation (P_{mean}). This study is essential (a) to improve Brazilian water resiliency by helping achieve the objectives of the National Water Security Plan and (b) to deepen our understanding of droughts in an uncertain future.

4.1 INTRODUCTION

Among climate-related hazards, droughts emerge as the most challenging for natural and social systems (De Luca; Donat, 2023), as they might disrupt a myriad of facets, including food production, power generation, and water resources (Cardenas Belleza; Bierkens; van Vliet, 2023; Vicente-Serrano *et al.*, 2022). Hence, understanding and predicting drought properties are essential to address their potential impacts on society and develop mitigation strategies, especially in the context of global warming, which is expected to alter the frequency and magnitude of drought events worldwide (Adeyeri *et al.*, 2023; Araujo *et al.*, 2022; Cook *et al.*, 2020).

Despite the importance of such assessments, studies of droughts are unevenly distributed globally, hindering a detailed characterization of droughts for informing local-to-regional policy decisions. This gap is particularly pronounced in Brazil, a country with paramount importance in global food security and climate regulation (Nepstad *et al.*, 2008; Pereira *et al.*, 2012). While Brazil faces rising concerns about drought events (Getirana; Libonati; Cataldi, 2021), there is a lack of studies assessing projected changes of drought from a countrywide perspective (Ferreira *et al.*, 2023). The country is already suffering from several water deficits (Lucas *et al.*, 2021; Marengo *et al.*, 2008, 2022; Nobre *et al.*, 2016; Otto *et al.*, 2015), and this condition might get even worse (Ballarin *et al.*, 2021; Sone *et al.*, 2022; Wang *et al.*, 2021). For instance, global warming is expected to exacerbate drought events in the Amazon region, likely increasing fire activity, tree mortality, and carbon emissions (Duffy *et al.*, 2015). This situation might not only affect Brazil, but the world, given the role of the Amazon forest in regulating Earth's climate and biodiversity (Feng *et al.*, 2021; O'Connor *et al.*, 2021). Therefore, understanding the impact of global warming on future droughts in Brazil is crucial for climate stakeholders.

Here, we try to bridge this gap by assessing how Brazil's meteorological drought events are expected to change. Beyond evaluating future drought properties and signal of changes - which is commonly done in the vast majority of drought-based studies (Araujo *et al.*, 2022; Zhao; Dai, 2022) - we investigate the link between drought properties and meteorological conditions, discussing the potential consequences of droughts intensification across Brazilian catchments using both a land cover and water use viewpoints. To this end, we evaluate the link between changes in P and PET properties and drought changes, employing

two different temporal perspectives: long-term (i.e., identification of change signals with climate change) and short-term (i.e., event-based impacts of drought events). This dual approach is fundamental for gaining insights into the differences between long-term and intra-annual climatological characteristics, shedding light on climate variability and its connection with drought events. Our study aims to answer the following questions: How are drought events projected to change across Brazilian catchments and what are their potential implications? How are the expected changes of drought events linked with changes in meteorological conditions? How do changes in long-term climatological conditions differ from those in drought-triggering periods? This work not only provides a general overview of expected changes in drought events in Brazil, which may help to achieve the main goals of the National Water Security Plan (PNSH; ANA, 2019b) but also contributes to an enhanced understanding of drought and their spatio-temporal characteristics.

4.2 METHODS

4.2.1 DATA

Daily climatological time series were retrieved from the CLIMBra dataset (Ballarin *et al.* 2023b). It provides raw and bias-corrected historical and future simulations of six meteorological variables for 10 climate models forced by two CMIP6 scenarios: SSP2-4.5 and SSP5-8.5. The dataset employed the delta quantile method (Cannon; Sobie; Murdock, 2015) to bias correct CMIP6-simulated daily series, which were further spatially averaged to a catchment-scale to encompass the 735 catchments present in the CABra dataset (Almagro *et al.*, 2021). PET values were computed using the formulation proposed by Yang *et al.* (2019), which modifies the Penman-Monteith equation to account for the effects of increased CO_2 concentrations on plants' water use (see Chapter 5 for details). This effect reduces vegetation water losses and diminishes dry biases in future PET estimations (Ballarin *et al.*, 2023a; Greve *et al.*, 2019; Milly; Dunne, 2016; Yang *et al.*, 2020). Land use data were retrieved from the Land Use Harmonization (LUH v2) project (Hurtt *et al.*, 2020). LUH v2 provides annual data on land use states and transitions for historical (1850-2014) and future (2015-2100). The dataset were used as input for multiple CMIP6 experiments, including the ScenarioMIP (O'Neill *et al.*, 2016) to generate future CMIP6 scenarios. The dataset comprises different land use states with a 0.25° spatial resolution, which we grouped into two different classes

(crops/pasture, and forest) to assess their susceptibility to future droughts in Brazilian's catchments. To further assess drought events from a water demand perspective, we extracted water consumption data from the ANA database (ANA, 2019a). The dataset provides historical and future projections (until the middle of the century) of water consumption for different water uses in a micro-catchment scale for Brazil. Water consumption information was further aggregated to a catchment-scale to correspond to the CABra's dataset used in the present study (see Chapter 5 for a detailed explanation).

4.2.2 DROUGHT'S IDENTIFICATION AND CHARACTERIZATION

We employed a non-parametric framework proposed by Ukkola *et al.* (2020) to identify and quantify meteorological droughts. The framework relies on the reasoning of popular standard indices - such as the Standard Precipitation and Evaporation Index (SPEI) - but does not involve assumptions about data distribution. It proceeded as follows: first, precipitation minus potentiation evapotranspiration ($P - PET$) series were transformed into a 6-month accumulation running series. Although other temporal scales can be used, we focused on 6-month accumulations since they are more suitable for characterizing meteorological drought events (Papalexiou *et al.*, 2021). Then, for each month of the historical period (1980-2010), we computed the 15-percentile threshold of 6-month accumulations. Finally, we used these thresholds to identify drought events, defined by periods when monthly 6-month accumulations fell below these thresholds. The 15-percentile corresponds approximately to the SPEI of -1, which is usually adopted in drought studies (McKee; Doesken; Kleist, 1993; Ukkola *et al.*, 2020). We also identified drought events through the traditional SPEI framework (Vicente-Serrano et al 2010) and obtained close drought events to reinforce the findings. Noteworthy, since this study aims to assess projected changes in drought events, the 15-percentile thresholds computed for the historical period were used to identify drought properties for both historical and future periods.

Using the definitions proposed by Ukkola *et al.* (2020), we computed (a) drought duration as the period between the start and end of a drought event; (b) drought intensity as the mean difference between the 15-percentile and the 6-month accumulations during a drought event, expressed by a monthly deficit, (c) drought severity as the cumulative difference between the 15-percentile and the 6-month accumulations during a drought event,

and (d) drought frequency as the number of drought events during the evaluated period. Here, we considered a 31-year, long-term perspective. Hence, drought's properties were reported on a 31-year average. To assess how drought events are expected to change, we computed the relative changes in long-term drought properties between distant future (2070-2100) and historical (1980-2010) periods. The results for the intermediate (2040-2070) and near (2040-2070) futures can be found in Appendix C.

4.2.3 Exploring changes in drought events and their link with long- and short-term changes of P and PET

To further explore future drought properties and their relationship with changes in meteorological conditions, we assessed how projected changes in P and PET are connected to changes in drought's properties. Namely, we examined the relationship between projected changes in drought properties and the following meteorological properties: number of wet days (N_w; $P > 1$ mm), (b) average precipitation of wet days (P_{mean}), (c) average potential evapotranspiration (PET_{mean}), and (d) the number of days when P surpasses PET (N_{wb}). We employed these four properties to account for both intensity and frequency of P and PET. We used two different temporal perspectives: long- and short-term (event-based). For the former, meteorological properties were reported as 31-year average values. For the latter, only drought event periods were considered to compute the meteorological averaged properties (See Text S4 in Appendix C for a detailed description). Such assessment is fundamental for better comprehending meteorological conditions in drought-triggering periods and how they differ from long-term climate characteristics (Vicente-Serrano *et al.*, 2022).

4.3 Results

4.3.1 Future intensification of meteorological drought properties

Drought events are generally expected to be more common, severe, and longer in Brazil (Figure 4.1). As anticipated, changes in the CMIP6 pessimistic scenario, SSP5-8.5, are larger and exhibit greater variability across Brazilian catchments than those observed for the moderate scenario, SSP2-4.5. On average, for the long-term period, all catchments are expected to experience an intensification of droughts' intensity. The largest increases are projected in the North and on the coastal side of Brazil, where Amazon and Atlantic Forest

biomes are located. This pattern, however, does not hold for droughts' duration and frequency. Some catchments, mainly located in the southern and northeastern parts of Brazil, are projected to experience less frequent and shorter drought events, which can be explained by the coupled effect of lower atmospheric demand and higher precipitation projected in the future for these regions (Almazroui *et al.*, 2021; Ballarin *et al.,* 2023a; Ballarin *et al.*, 2024; Reboita *et al.*, 2022). It is important to note that the projected changes in drought properties exhibit a high model agreement. In approximately 80% of the catchments, at least seven CMIP6 models (out of ten) agreed on the change signal.

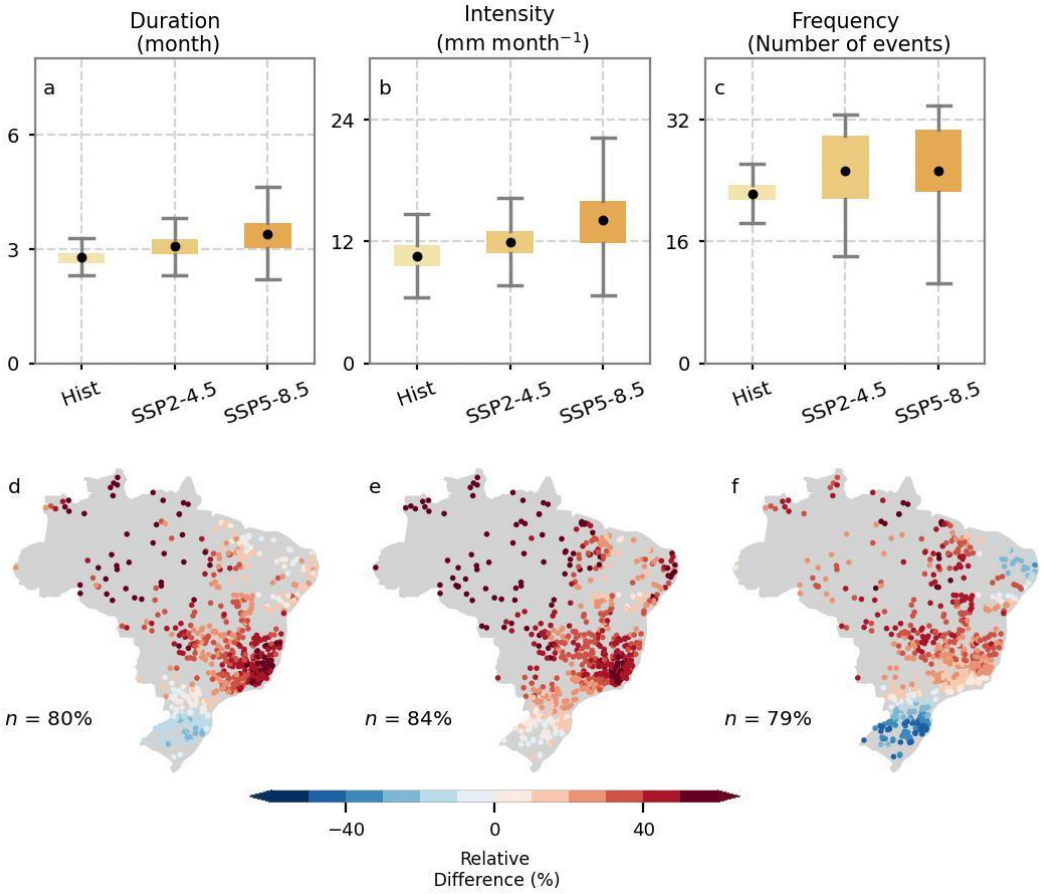

Figure 4.1. Projected changes in 30-year, long-term averaged drought's (a, d) duration, (b, e) intensity, and (c, f) frequency between historical (Hist; 1980-2010) and distant future (SSP2-4.5 and SSP5-8.5; 2070-2100) periods in Brazil. Boxplots represent the CMIP6 multi-model ensemble median observed for the 735 Brazilian catchments. The spatial distribution of changes (d-f) was computed considering the historical and SSP5-8.5 distant future. *n* in the bottom-left corner of each map indicates the percentage of catchments with at least 70% of CMIP6 model agreement (signal of change). Projected changes in drought properties for Brazil are statistically significant according to the Mann-Whitney U test and Monte Carlo resampling techniques (p-value < 0.05).

Besides the increase in long-term, averaged droughts' properties, CMIP6 future simulations also indicate that drought properties (duration and intensity) are expected to show increased variability and reduced skewness, expressed in terms of the L-variation and L-skewness (Figure S4.2, Appendix C; see Abdelmoaty *et al.* (2021) for a detailed description). We opted for the use of L-moments as they represent an advancement over traditional moments in characterizing the statistical properties of samples, such as variation, skewness and kurtosis, showing reduced sensitivity to variations in sample size and outliers (Hosking, 1990; Sankarasubramanian; Srinivasan, 1999). This increase in variability, combined with changes in the other evaluated statistical moments, affects the projected changes in rarer drought events. For instance, if we focus only on the five events with the largest values for each drought property occurring in the 31-year period (historical and future), we observe projected changes greater than those obtained considering all drought events (Figure S4.3). Such aspects, often overlooked on drought assessments, can profoundly impact water resources management practices in the country (Reyniers *et al.*, 2023).

To further explore future droughts and their potential implications for Brazilian catchments, we assessed their projected changes from both land cover and water demand perspectives (Figure 4. 2). In terms of land cover, in the end of the century for SSP5-8.5, most of Brazilian forest, pasture, and crop areas will experience enhanced drought properties (Figure 4. **2**a-f). At least half of the Brazilian cropland/pasture areas will experience an average increase of 30%, 37% and 29% in droughts' duration, intensity, and frequency, respectively. For forests, the changes are even greater, with changes on droughts intensity and duration projected to exceed more than 50% in half of catchments' forested areas. Similarly to what we observed for droughts changes, CMIP6-models exhibited a relatively high model agreement towards drought intensification in most part of Brazilian`s forests and crops.

Moving to a water-demand perspective (Figure 4. 2g, h), one can note that, according to SSP5-8.5, most catchments with anticipated increases in drought severity are also projected to exhibit augmented water consumption (Figure 4. 2g). By the middle of the century, from the almost 87% of the catchments with expected increase in drought severity, nearly 85% are also expected to present augmented water consumption in the future, mainly dictated by irrigation (Ballarin *et al.*, 2023a). The South region of the country is expected to exhibit the

best water security condition, with some catchments presenting reduced drought severity and water demand. The Central region of the country, known for intense agriculture activity, in contrast, is projected to experience the greater coupled water demand-drought impacts, which will likely affect Brazilian agricultural production, specifically coffee, soybean, and sugarcane croplands (Koh *et al.*, 2020). As highlighted by Multsch *et al.* (2020), part of this region is already experiencing a concerning condition in terms of water scarcity given the higher water use for irrigation, that may even aggravate due to agricultural expansion plans. These circumstances, however, are not restricted to this Central region: approximately 70% of crops catchments (crop cover $> 50\%$) are expected to show increased irrigation-based demand and more severe droughts in the middle of the century (Figure 4. 2h).

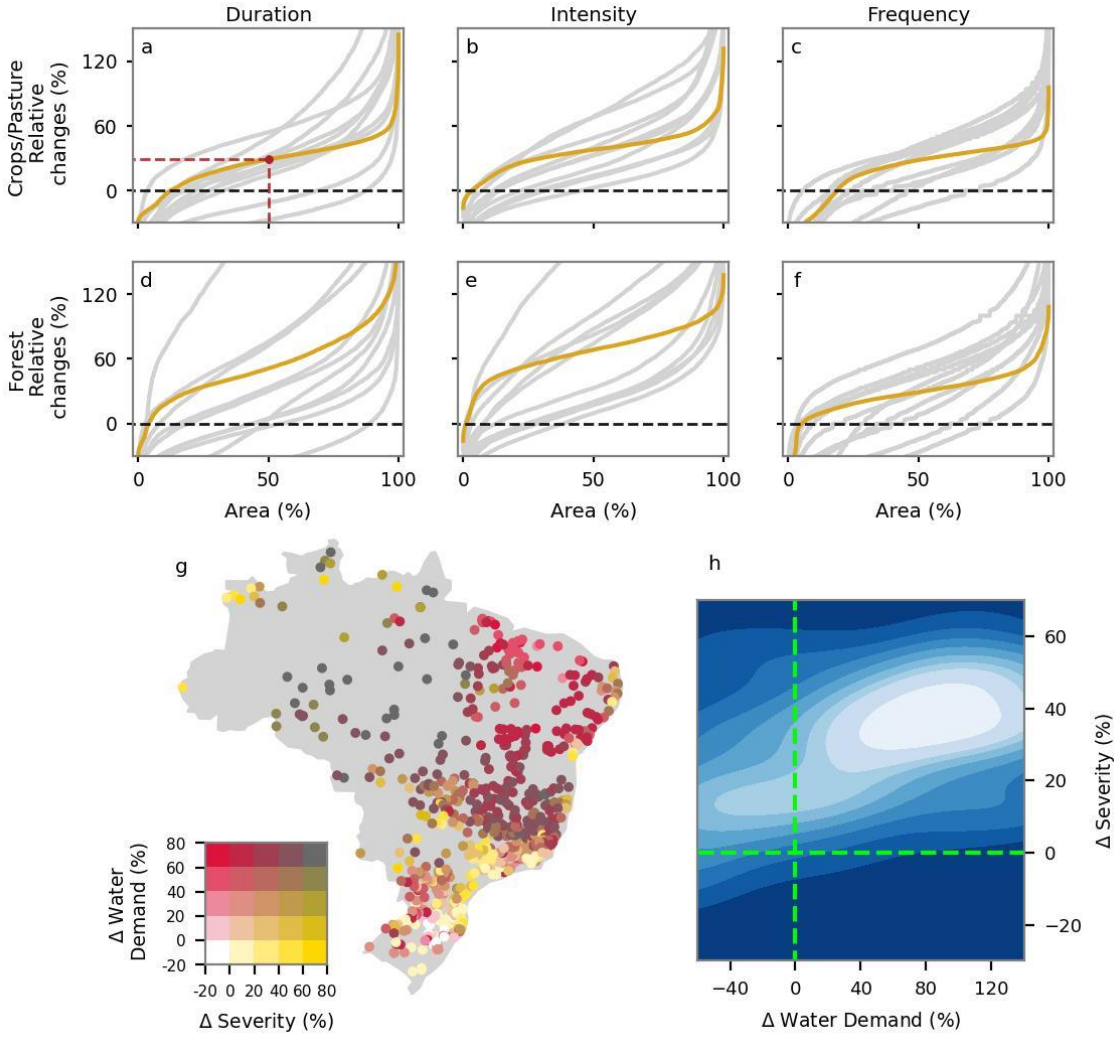

Figure 4. 2. Projected changes (%) in 30-year, long-term averaged drought's (a, d) duration, (b, e) intensity, and (c, f) frequency between historical (Hist; 1980-2010) and distant future (SSP5-8.5; 2070-2100) periods as a function of the relative area (%) of two different land uses classes: Forest and Pasture and Crops.CMIP6 multi-model ensemble median is displayed in yellow. Individual models' projections are displayed in light gray. Panels a-c can be interpreted as the proportion of crops/pasture (x-axis) projected to experience a particular relative change on drought's properties (y-axis). As an example, in panel a, red, dashed lines indicate that 50% of the crops/pasture area are projected to experience 30% of increase in drought's duration. The results for the gridded dataset were used for panels a-f. The same holds for panels d-f for forest cover. (g) Spatial distribution of relative changes in long-term, averaged drought's severity (SSP5-8.5) and total water demand for the intermediate future (2040-2070). (h) Bivariate histogram of projected relative changes in droughts severity (SSP5-8.5) and irrigation-water demand for crops catchments (crop cover > 50%) in the intermediate future (2040-2070). Green, dashed lines divide the panel into regions of negative/positive changes.

4.3.2 Future changes in droughts and their link with P and PET in Brazilian catchments

To have a better understanding of future drought events in the country, we explored their relationship with the projected changes of climate properties in both long-term and drought-triggering periods (Figure 4.3). We focused our attention on droughts' severity, which encompasses both droughts' duration and intensity, but similar conclusions can be inferred for the other properties (Figures S4.4 and S4.5). As expected, for both long- and short-term perspectives, changes in frequency and intensity of climatological properties are correlated to changes in drought properties, since enhanced PET and P-deficits can trigger and/or aggravate drought events (Mukherjee; Mishra; Trenberth, 2018). Based on the correlations obtained for both temporal perspectives, in general, catchments with larger positive changes in PET_{mean} are projected to experience drought events with larger duration, intensity and frequency. For the other climate properties, the opposite is valid: catchments with reduced P_{mean}, N_w, and N_{wb} will experience intensified droughts.

According to the long-term perspective, more than 70% of the catchments are projected to show enhanced PET_{mean}, whereas only 23% show a decreased P_{mean} (Figure 4.3g). More pronounced increases in PET_{mean} are expected to happen in the Northwestern and Central parts of Brazil, where Amazon and Cerrado are located. For P_{mean}, larger increases are projected for the southern region (see Figure S4.6 for the spatial distribution of changes). At first glance, this might indicate that droughts intensification is highly linked with enhanced PET_{mean}, but not necessarily with decreased P_{mean}, since more than 50% of the catchments are projected to undergo an increase in drought properties even with an increase in P_{mean}. For instance, one can note that the very similar spatial patterns of future increased PET_{mean} and drought properties do not match the spatial distribution of future P_{mean} decreases (Figure 4.1 and S4.6). However, looking at changes in frequency aspects (N_w and N_{wb}), it is possible to note that they also have an important role on droughts changes. More than 70% of the catchments that are expected to experience more severe droughts will also undergo a reduction in N_w and N_{wb}. Moreover, all catchments with projected decrease in drought severity (10% of the catchments) are expected to present larger N_w and N_{wb} (Figure 4.3c, d), which suggests a strong link between changes in P and PET frequency and changes in droughts properties.

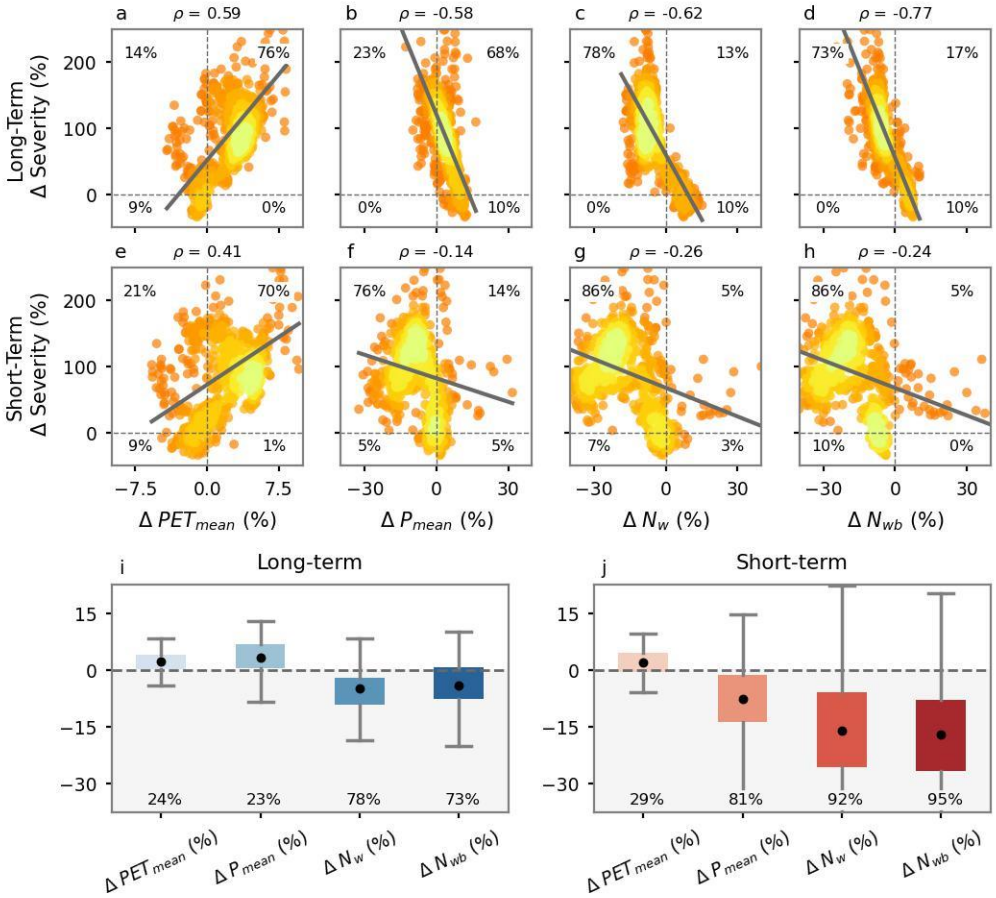

Figure 4.3. Relationship between projected changes (SSP5-8.5; distant future) in drought severity and long- (first row, a-d) and short-term (second row, e-g) meteorological properties (PET_{mean}, P_{mean}, N_w, and N_{wb}; from left to right) for the Brazilian catchments. Pearson's correlation between projected changes is displayed on each subplot's top. Only significant correlations (p-value < 0.05) were considered. Black, dashed lines divide the quadrants. The regression line is displayed in dark grey. The percentage of catchments (points) in each quadrant is indicated on the corners. For all plots, light colour regions indicate high density. Boxplots in the bottom of the figure summarize the projected relative changes in meteorological properties (PET_{mean}, P_{mean}, N_w, and N_{wb}) for the long- and short-term (i and j, respectively) across the Brazilian catchments. The percentage below each boxplot indicate the proportion of catchments with projected negative changes. A black, dashed line represents the region with no changes.

In the short-term perspective, we found a similar pattern for PET_{mean}, N_w, and N_{wb}: catchments with projected increases in drought severity are projected to show, in general, increases in PET and decreases in N_w and N_{wb} (see Figure S4.7 for spatial distribution). For instance, from the 90% of the catchments with expected enhanced drought severity, nearly

80% and 95% of them are expected to show enhanced PET and decreased N_w and N_{wb}, respectively, confirming the role of evapotranspiration and climate frequency on the changes of droughts properties in a warmer world (Otkin *et al.*, 2018; Vicente-Serrano *et al.*, 2014; Wang; Sun, 2023b). Interestingly, a different situation was found for P_{mean}. According to this event-based perspective, P_{mean} is expected to decrease in more than 80% of the catchments during drought-triggering periods (Figure 4.3i), which contrasts with the results found for the long-term perspective. That is, even showing enhanced P in the future, some catchments in Brazil are projected to show more severe droughts due to changes in intra-annual variability of P towards less frequent, and more extreme and concentrated events (Ballarin *et al.*, 2024).

4.4 Discussion and Final Remarks

Although there is an extensive literature about projected changes in future drought properties according to CMIP6 models outputs (Ukkola *et al.*, 2020; Wang *et al.*, 2021; Wang; Sun, 2023b, 2023a; Xu *et al.*, 2023), little is known about how droughts are expected to change and impact Brazilian catchments and what are the link between changes in droughts and meteorological conditions. This aspect is paramount to assisting decision-makers in developing mitigation strategies and improved water resources management practices. This study addresses this gap by assessing projected changes in Brazilian droughts and meteorological conditions and their potential impacts on Brazilian catchments from both land use and water demand viewpoints.

CMIP6 models suggest robust and generally severe conditions of long-term mean drought properties in Brazil. Such patterns were also observed by Ferreira *et al.* (2023) when assessing rainfall patterns in the country. Although certain catchments may experience decreased droughts' duration and frequency, which aligns with the future wetter conditions reported for some Brazilian regions by previous studies (Medeiros; Oliveira; Avila-Diaz, 2022; Reboita *et al.*, 2022), the overall trend for the country indicates a general increase in all droughts properties. Beyond the long-term mean, changes in the variability and extremes of droughts are also projected (Figure S4.2 and S4.3), which will likely pose even greater consequences to the country in the future (Getirana; Libonati; Cataldi, 2021; Gutiérrez *et al.*, 2014; Satoh *et al.*, 2022). This challenging scenario may not affect only Brazil but global proportions as well, given the country's role in global food security and agricultural

production (Maluf *et al.*, 2022; Pereira *et al.*, 2012; Strassburg *et al.*, 2014). As highlighted, most Brazilian's forests, pasture, and croplands areas are projected to experience worse drought events. This, added, to the expected increases in water consumption throughout the Brazilian territory, will certainly affect water security and food production in the country. For instance, the greater water demand-drought impact is expected to happen in the Central region of the country (Figure 4.2g), known for the high agricultural activity. As highlighted by Koh *et al* (2020) and Silva *et al* (2023), climate impacts are already reducing coffee and soybean yields in the region, and are expected to be aggravated by water use increases due to agriculture expansion. Such findings are pivotal to inform Brazilian water resources and food agriculture practices, mainly for the Cerrado ecoregion, which is expected to experience the larger intensification of droughts due to both climate and water uses changes (Multsch *et al.*, 2020).

The assessment of the relationship between changes in drought properties and meteorological conditions highlighted two aspects. From the long-term perspective approach, we observed that droughts' intensification is mainly linked to an increase in PET_{mean} and a reduction of N_w and N_{wb}, confirming that changes in the atmospheric demand and rainfall frequency affect drought characteristics (Araujo *et al.*, 2022; Greve *et al.*, 2019; Trenberth *et al.*, 2014). For example, more than 50% of the catchments are expected to experience an increase in drought properties even with enhanced P_{mean}. Nevertheless, if we turn our attention to the event-based approach, we note that even these catchments with an expected greater long-term P_{mean} are projected to show reduced P_{mean} before and during drought events, reinforcing the role of rainfall variability and timing in controlling drought events (Ukkola *et al.*, 2020). Indeed, as underscored by Ballarin *et al* (2024), the country is expected to experience less, but more concentrated and extreme rainfall events. The Southern/Southeastern of Brazil presents an interesting case for such findings. From a long-term perspective, both P_{mean} and N_w are expected to increase, while PET_{mean} shows small changes, which would suggest a wetter condition in the region (see Figures S4.6 and S4.7). Nevertheless, according to the short-term perspective, the region will experience a slight reduction in N_w and P_{mean} which likely explains the expected increase in drought severity. Hence, according to this dual approach, the intensification of drought properties in Brazil can generally be linked to both an intensification of PET and P-variability, which trigger or

aggravate drought events even in places with a projected averaged wetter condition. That is, changes in future droughts in the country are not linked only with the amount of water, but also with its timing. Such information can be pivotal for water resources planning in the country seeking to improve water security and achieve the objectives of the National Water Security Plan (ANA, 2019b).

Despite the high model agreement towards drought intensification, it should be stressed that some aspects might introduce uncertainties and affect our findings. It is known that 'offline' PET formulations may not faithfully represent physical or biological processes and consequently affect drought characterization (Milly; Dunne, 2016; Swann *et al.*, 2016; Wang; Sun, 2023b; Yang *et al.*, 2019). To avoid possible misrepresentations, we used the formulation proposed by Yang et al. (2019) which considers CO_2 effects on plants and reduces potential drying biases. Nevertheless, we also computed projected drought changes across Brazil using the reference crop Peanman-Monteith formulation and obtained a slightly higher (although similar) intensification of drought properties (Figure S4.8).

Another factor influencing our findings is the inherent uncertainties associated with climate model outputs and pre- and post-processing tasks related to bias adjustment and spatial downscaling. For instance, reggriding climate simulations may affect the statistical properties of time series, especially those related to extreme events (Rajulapati *et al.*, 2021). Furthermore, although usually required for improving the applicability of climate simulations (Ansari *et al.*, 2023; Johnson; Sharma, 2015), bias correction outputs may show physically unrealistic values and hide climate model deficiencies (Casanueva *et al.*, 2020). In this context, we repeated our analysis using the raw simulations present in the CLIMBra dataset. The results suggest a worse scenario in terms of changes in droughts' duration and intensity and a similar condition in terms of droughts' frequency (Figure S4.9). In comparison to the bias-corrected outputs, raw simulations project, in general, (1) lower P_{mean}, (2) higher PET_{mean}, and (3) higher N_w, which is probably causing the differences in projected droughts' properties (Figure S4.10). Nevertheless, despite the divergences in the magnitude of changes, both outputs agree with the overall intensification of drought properties in the future. We also repeated the analysis considering different wet thresholds (0.1 and 1 mm) and obtained quite similar findings (Figure S4.11 and S4.12).

Finally, we highlight that the results reported here are related to the pessimistic CMIP6 scenario (SSP5-8.5) for the distant future (2070-2100). Alternative pathways with lower projected changes for drought properties were found when considering the immediate (2010-2040) and intermediate (2040-2070) future (Figure S4.13 and S4.14). As expected, almost no changes are projected for the former, whereas changes with lower magnitude are projected for the latter, which highlights the role of climate policies on reducing potential impacts on water resources. We found a lower model agreement for both future periods compared to the distant future. Nevertheless, on average, both point towards intensifying drought properties, except for drought frequency in the immediate future.

Further studies on this topic are needed to improve water resources management in Brazil. For instance, understanding how rainfall events of different magnitudes contribute to drought conditions and how these projected changes in droughts might impact food production and crop yields certainly contributes to an enhanced comprehension of drought impacts in an uncertain future. Furthermore, it is noteworthy to mention that while we focused here on changes in future drought conditions and their connection with local climate dynamics, Brazil is not an isolated system, and, as such, complementary research exploring future drought changes in terms of climate indices (e.g., ENSO) can certainly contribute to an improved understanding of droughts dynamics (Kay *et al.*, 2022). Even so, we believe that the evidence gathered here is insightful for water-related practices in the country and that the proposed approach to assess drought relationship to climate change under different temporal perspective can serve as a valuable method for understanding drought characteristics and patterns in Brazil.

4.5 REFERENCES

ABDELMOATY, H. M. *et al.* Biases Beyond the Mean in CMIP6 Extreme Precipitation: A Global Investigation. **Earth's Future**, [*s. l.*], v. 9, n. 10, p. 1–17, 2021.

ADEYERI, O. E. *et al.* Multivariate Drought Monitoring, Propagation, and Projection Using Bias-Corrected General Circulation Models. **Earth's Future**, [*s. l.*], v. 11, n. 4, p. 1–16, 2023.

ALMAGRO, A. *et al.* CABra: a novel large-sample dataset for Brazilian catchments. **Hydrology and Earth System Sciences**, [*s. l.*], p. 1–40, 2021.

ALMAZROUI, M. *et al.* Assessment of CMIP6 Performance and Projected Temperature and Precipitation Changes Over South America. **Earth Systems and Environment**, [*s. l.*], v. 5, n. 2, p. 155–183, 2021.

ANA. **Manual of Consumptive Water Use in Brazil**. Brasilia, Brazil: [*s. n.*], 2019a.

ANA. **Plano Nacional de Segurança Hídrica**. Brasilia, Brazil: ANA - National Water Agency, 2019b.

ANSARI, R. *et al.* Evaluation of bias correction methods for a multivariate drought index: case study of the Upper Jhelum Basin. **Geoscientific Model Development**, [*s. l.*], v. 16, n. 7, p. 2055–2076, 2023.

ARAUJO, D. S. A. *et al.* Today's 100 year droughts in Australia may become the norm by the end of the century. **Environmental Research Letters**, [*s. l.*], n. 17, 2022.

BALLARIN, A. S. *et al.* A copula-based drought assessment framework considering global simulation models. **Journal of Hydrology: Regional Studies**, [*s. l.*], v. 38, n. October, p. 0–3, 2021.

BALLARIN, A. S. *et al.* Brazilian Water Security Threatened by Climate Change and Human Behavior. **Water Resources Research**, [*s. l.*], v. 59, p. e2023WR034914, 2023.

BALLARIN, A. S. *et al.* CLIMBra - Climate Change Dataset for Brazil. **Scientific Data**, [*s. l.*], p. 1–31, 2023.

BALLARIN, A. S. *et al.* Frequency Rather Than Intensity Drives Projected Changes of Rainfall Events in Brazil. **Earth's Future**, [*s. l.*], v. 12, n. 1, p. e2023EF004053, 2024.

CANNON, A. J.; SOBIE, S. R.; MURDOCK, T. Q. Bias correction of GCM precipitation by quantile mapping: How well do methods preserve changes in quantiles and extremes?. **Journal of Climate**, [*s. l.*], v. 28, n. 17, p. 6938–6959, 2015.

CARDENAS BELLEZA, G. A.; BIERKENS, M. F. P.; VAN VLIET, M. Sectoral water use responses to droughts and heatwaves: analyses from local to global scales for 1990-2019. **Environmental Research Letters**, [*s. l.*], 2023.

CASANUEVA, A. *et al.* Testing bias adjustment methods for regional climate change applications under observational uncertainty and resolution mismatch. **Atmospheric Science Letters**, [*s. l.*], v. 21, n. 7, p. 1–12, 2020.

COOK, B. I. *et al.* Twenty-First Century Drought Projections in the CMIP6 Forcing Scenarios. **Earth's Future**, [*s. l.*], v. 8, p. e2019EF001461, 2020.

DE LUCA, P.; DONAT, M. G. Projected Changes in Hot, Dry and Compound Hot-Dry Extremes over Global Land Regions. **Geophysical Research Letters**, [*s. l.*], 2023. Disponível em: https://eartharxiv.org/repository/view/5511/.

DUFFY, P. B. *et al.* Projections of future meteorological drought and wet periods in the Amazon. **Proceedings of the National Academy of Sciences of the United States of America**, [*s. l.*], v. 112, n. 43, p. 13172–13177, 2015.

FENG, X. *et al.* How deregulation, drought and increasing fire impact Amazonian biodiversity. **Nature**, [*s. l.*], v. 597, n. 7877, p. 516–521, 2021.

FERREIRA, G. W. de S. *et al.* Assessment of Precipitation and Hydrological Droughts in South America through Statistically Downscaled CMIP6 Projections. **Climate**, [*s. l.*], 2023.

GETIRANA, A.; LIBONATI, R.; CATALDI, M. Brazil is in water crisis — it needs a drought plan. **Nature**, [*s. l.*], v. 600, n. 7888, p. 218–220, 2021.

GREVE, P. *et al.* The aridity Index under global warming. **Environmental Research Letters**, [*s. l.*], v. 14, p. 124006, 2019.

GUTIÉRREZ, A. P. A. *et al.* Drought preparedness in Brazil. **Weather and Climate Extremes**, [*s. l.*], v. 3, p. 95–106, 2014.

HOSKING, J. R. M. L-Moments: Analysis and Estimation of Distributions Using Linear Combination of Order Statistics. **Journal of the Royal Statistical Society**, [*s. l.*], v. 52, n. 1, p. 105–124, 1990.

HURTT, G. C. *et al.* Harmonization of global land use change and management for the period 850 – 2100 (LUH2) for CMIP6. **Geoscientific Model Development**, [*s. l.*], p. 5425–5464, 2020.

JOHNSON, F.; SHARMA, A. **What are the impacts of bias correction on future drought projections?** [*S. l.: s. n.*], 2015-. ISSN 00221694.v. 525

KAY, G. *et al.* Assessing the chance of unprecedented dry conditions over North Brazil during El Niño events. **Environmental Research Letters**, [*s. l.*], v. 17, n. 6, p. 064016, 2022.

KOH, I. *et al.* Climate risks to Brazilian coffee production. **Environmental Research Letters**, [*s. l.*], v. 15, n. 10, p. 104015, 2020.

LUCAS, M. C. *et al.* Significant baseflow reduction in the sao francisco river basin. **Water (Switzerland)**, [*s. l.*], v. 13, n. 1, p. 1–17, 2021.

MALUF, R. S. *et al.* Sustainability, justice and equity in food systems: Ideas and proposals in dispute in Brazil. **Environmental Innovation and Societal Transitions**, [*s. l.*], v. 45, n. October, p. 183–199, 2022.

MARENGO, J. A. *et al.* Drought in Northeast Brazil: A review of agricultural and policy adaptation options for food security. **Climate Resilience and Sustainability**, [*s. l.*], v. 1, n. 1, p. 1–20, 2022.

MARENGO, J. A. *et al.* The drought of Amazonia in 2005. **Journal of Climate**, [*s. l.*], v. 21, n. 3, p. 495–516, 2008.

MCKEE, T. B.; DOESKEN, N. J.; KLEIST, J. The relationship of drought frequency and duration to time scales. **American Metereological Society**, [*s. l.*], n. Boston, p. 179–184, 1993.

MEDEIROS, F. j.; OLIVEIRA, C. P.; AVILA-DIAZ, A. Evaluation of extreme precipitation climate indices and their projected changes for Brazil: From CMIP3 to CMIP6. **Weather and Climate Extremes**, [*s. l.*], v. 38, n. July, p. 100511, 2022.

MILLY, P. C. D.; DUNNE, K. A. Potential evapotranspiration and continental drying. **Nature Climate Change**, [*s. l.*], v. 6, n. 10, p. 946–949, 2016.

MUKHERJEE, S.; MISHRA, A.; TRENBERTH, K. E. Climate Change and Drought: a Perspective on Drought Indices. **Current Climate Change Reports**, [*s. l.*], v. 4, n. 2, p. 145–163, 2018.

MULTSCH, S. *et al.* Assessment of potential implications of agricultural irrigation policy on surface water scarcity in Brazil. **Hydrology and Earth System Sciences**, [*s. l.*], v. 24, n. 1, p. 307–324, 2020.

NEPSTAD, D. C. *et al.* Interactions among Amazon land use, forests and climate: Prospects for a near-term forest tipping point. **Philosophical Transactions of the Royal Society B: Biological Sciences**, [*s. l.*], v. 363, n. 1498, p. 1737–1746, 2008.

NOBRE, C. A. *et al.* Some Characteristics and Impacts of the Drought and Water Crisis in Southeastern Brazil during 2014 and 2015. **Journal of Water Resource and Protection**, [*s. l.*], v. 08, n. 02, p. 252–262, 2016.

O'CONNOR, J. C. *et al.* Atmospheric moisture contribution to the growing season in the Amazon arc of deforestation. **Environmental Research Letters**, [*s. l.*], v. 16, n. 8, 2021.

O'NEILL, B. C. *et al.* The Scenario Model Intercomparison Project (ScenarioMIP) for CMIP6. **Geoscientific Model Development**, [*s. l.*], v. 9, n. 9, p. 3461–3482, 2016.

OTKIN, J. A. *et al.* Flash droughts: A review and assessment of the challenges imposed by rapid-onset droughts in the United States. **Bulletin of the American Meteorological Society**, [*s. l.*], v. 99, n. 5, p. 911–919, 2018.

OTTO, F. E. L. *et al.* Factors other than climate change: main drivers of 2014/2015 water shortage in southeast Brazil. **Bulletin of the American Meteorological Society**, [*s. l.*], v. 96, n. 12, p. 35–40, 2015.

PAPALEXIOU, S. M. *et al.* Probabilistic Evaluation of Drought in CMIP6 Simulations. **Earth's Future**, [*s. l.*], v. 9, n. 10, p. 1–18, 2021.

PEREIRA, P. A. A. *et al.* The development of Brazilian agriculture and future challenges. **Agriculture & Food Security**, [*s. l.*], v. 1, n. April, p. 1–12, 2012.

RAJULAPATI, C. R. *et al.* The Perils of Regridding: Examples using a Global Precipitation Dataset. **Journal of Applied Meteorology and Climatology**, [*s. l.*], n. October, 2021.

REBOITA, M. S. *et al.* South America climate change revealed through climate indices projected by GCMs and Eta-RCM ensembles. **Climate Dynamics**, [*s. l.*], v. 58, n. 1–2, p. 459–485, 2022.

REYNIERS, N. *et al.* Projected changes in droughts and extreme droughts in Great Britain strongly influenced by the choice of drought index. **Hydrology and Earth System Sciences**, [*s. l.*], p. 1151–1171, 2023.

SANKARASUBRAMANIAN, A.; SRINIVASAN, K. Investigation and comparison of sampling properties of L-moments and conventional moments. **Journal of Hydrology**, [*s. l.*], v. 218, n. 1–2, p. 13–34, 1999.

SATOH, Y. *et al.* The timing of unprecedented hydrological drought under climate change. **Nature Communications**, [*s. l.*], v. 13, n. 1, 2022.

SILVA, D. S. *et al.* Temperature effect on Brazilian soybean yields, and farmers' responses. **International Journal of Agricultural Sustainability**, [*s. l.*], v. 21, n. 1, p. 2173370, 2023.

SONE, J. S. *et al.* Water Security in an Uncertain Future: Contrasting Realities from an Availability-Demand Perspective. **Water Resources Management**, [*s. l.*], 2022. Disponível em: https://link.springer.com/10.1007/s11269-022-03160-x.

STRASSBURG, B. B. N. *et al.* When enough should be enough: Improving the use of current agricultural lands could meet production demands and spare natural habitats in Brazil. **Global Environmental Change**, [*s. l.*], v. 28, n. 1, p. 84–97, 2014.

SWANN, A. L. S. *et al.* Plant responses to increasing CO2 reduce estimates of climate impacts on drought severity. **Proceedings of the National Academy of Sciences of the United States of America**, [*s. l.*], v. 113, n. 36, p. 10019–10024, 2016.

TRENBERTH, K. E. *et al.* Global warming and changes in drought. **Nature Climate Change**, [*s. l.*], v. 4, n. 1, p. 17–22, 2014.

UKKOLA, A. M. *et al.* Robust Future Changes in Meteorological Drought in CMIP6 Projections Despite Uncertainty in Precipitation. **Geophysical Research Letters**, [*s. l.*], p. 1–9, 2020.

VICENTE-SERRANO, S. M. *et al.* Evidence of increasing drought severity caused by temperature rise in southern Europe. **Environmental Research Letters**, [*s. l.*], v. 9, n. 4, 2014.

VICENTE-SERRANO, S. M. *et al.* Global drought trends and future projections. **Philosophical Transactions of the Royal Society A: Mathematical, Physical and Engineering Sciences**, [*s. l.*], v. 380, n. 2238, 2022.

WANG, T. *et al.* Global data assessment and analysis of drought characteristics based on CMIP6. **Journal of Hydrology**, [*s. l.*], v. 596, n. December 2020, 2021.

WANG, T.; SUN, F. Integrated drought vulnerability and risk assessment for future scenarios: An indicator based analysis. **Science of the Total Environment**, [*s. l.*], v. 900, n. June, p. 165591, 2023a.

WANG, T.; SUN, F. Socioeconomic exposure to drought under climate warming and globalization: The importance of vegetation-CO2 feedback. **International Journal of Climatology**, [*s. l.*], n. June, p. 5778–5796, 2023b.

XAVIER, A. C.; KING, C. W.; SCANLON, B. R. Daily gridded meteorological variables in Brazil (1980–2013). **International Journal of Climatology**, [*s. l.*], v. 36, n. 6, p. 2644–2659, 2016.

XU, F. *et al.* Projections of Global Drought and Their Climate Drivers Using CMIP6 Global Climate Models. **Water (Switzerland)**, [*s. l.*], v. 15, n. 12, 2023.

YANG, Y. *et al.* Comparing Palmer Drought Severity Index drought assessments using the traditional offline approach with direct climate model outputs. **Hydrology and Earth System Sciences**, [*s. l.*], v. 24, n. 6, p. 2921–2930, 2020.

YANG, Y. *et al.* Hydrologic implications of vegetation response to elevated CO2 in climate projections. **Nature Climate Change**, [*s. l.*], v. 9, n. 1, p. 44–48, 2019.

ZHAO, T.; DAI, A. CMIP6 Model-Projected Hydroclimatic and Drought Changes and Their Causes in the Twenty-First Century. **Journal of Climate**, [*s. l.*], v. 35, p. 897–921, 2022.

CHAPTER 5

Brazilian water security threatened by climate change and human behavior

ABSTRACT

Water scarcity is a growing concern globally, with climate change and increasing population exacerbating the issue. Here, we introduce a new framework for assessing water availability in 708 Brazilian catchments that considers the effect of CO_2 concentrations on potential evapotranspiration, uses CMIP6 bias-corrected climate change simulations, and presumes an open water balance assumption, while considering the human-aspect by incorporating water demand projections. We note an average reduction of water security in 81% of the analyzed catchments by 2100. Among these catchments, 37% presented a reduction of future water availability, while 63% undergo a worse scenario due to an increase in human water use, which highlights the role of the human aspect in water security assessment. Our study shows important aspects for both advancing future water availability studies and for drawing a picture of the impacts of changes in climate and water use on Brazilian future water security that may be useful for water resources management practices and advancing hydrologic studies.

5.1 INTRODUCTION

Continental water availability is of paramount importance for ecological and human well-being (Greve; Seneviratne, 2015; Milly; Dunne; Vecchia, 2005). Many of the global impacts on agriculture, ecosystem services, human health, and economic activities are related to changes in water fluxes (D'Odorico et al., 2020; Roderick et al., 2014). Global climate change is expected to alter the water cycle dynamics (Haddeland et al., 2014) and the frequency and magnitude of extreme events (Aghakouchak et al., 2020), which will likely increase water availability-related issues (Rockström et al., 2009; Zhou et al., 2022). Along with climate change, water resources are also threatened by the growing water demand required to support an ever-increasing population (Hanasaki et al., 2013a, 2013b; Liu et al., 2017). The compound effect of climate change and rising water demand is likely to exacerbate water scarcity around the globe (He et al., 2021), negatively impacting terrestrial ecosystems and potentially hindering progress towards the United Nations Sustainable Development Goals 6: Clean Water and Sanitation, which aims to ensure "clean and accessible water for all" (van Vliet et al., 2021; Vanham et al., 2018).

This challenging scenario is also seen in Brazil, even though the country contains nearly 15% of the world's renewable water resources (Getirana; Libonati; Cataldi, 2021). Given its continental dimensions and highly heterogeneous hydroclimatic conditions, Brazil faces water scarcity due to its highly uneven distribution of water resources and intensification of water uses (Gesualdo *et al.*, 2021). Additionally, Brazil is strongly dependent on hydroelectricity: approximately 60% of power generation comes from this sector (Hunt.; Stilpen; de Freitas, 2018). Notwithstanding, the country is expected to expand its irrigated areas, which may aggravate water stress (Multsch *et al.*, 2020). This concerning situation will not only affect Brazil but may take on global proportions. Brazil plays a key role in global food security, being one of the largest agricultural producers (Pereira *et al.*, 2012) and having areas classified as a global biodiversity hotspot (Myers *et al.*, 2000). Therefore, understanding the present and future context of Brazilian water availability is urgently needed to ensure the nexus of water-food-energy-ecosystems services and a sustainable future for an increasing global population (McDonald *et al.*, 2014).

At long-term temporal scales, water availability, also known as runoff (Q), may be quantified as the difference between precipitation (P) and evapotranspiration (E) (Jawitz;

Klammler; Reaver, 2022). Hence, a precise understanding of P-partitioning into E and Q is fundamental to tackle water availability-related issues, since changes in the spatiotemporal dynamics of these water balance components may likely affect future water security (Konapala *et al.,* 2020). A simple but effective way to assess the long-term water balance components is using the Budyko framework (Budyko, 1974; Guo et al., 2019; Renner; Bernhofer, 2012; Roderick; Farquhar, 2011; Roderick; Greve; Farquhar, 2015). Budyko's hypothesis assumes the partitioning of P into E and Q as a functional balance between water supply (P) and demand (PET), expressed in terms of the aridity index ($\phi = PET/P$). However, in a context characterized by changes in climate dynamics and anthropogenic activities, this approach may show some limitations.

First, the Budyko hypothesis neglects inter-catchment water exchanges by assuming a closed water balance (CWB; Ballarin *et al.*, 2022; Gordon *et al.*, 2022). Nevertheless, it has been shown that these hydrological fluxes cannot be neglected and may account for a major part of the hydrological fluxes within a catchment (Fan, 2019; Le Moine *et al.*, 2007; Safeeq *et al.*, 2021; Schaller; Fan, 2009). Second, climate models usually exhibit systematic errors that impair the reproduction of observed water availability, requiring further bias corrections for a reliable assessment of future water security (Christensen *et al.*, 2008). Third, climate change studies are often conducted using 'offline' PET, which implies that it is computed using models that rely on other commonly used climate variables, such as Penman-Monteith-based models (Milly; Dunne, 2016). These approaches, however, do not account for the vegetation response to elevated CO_2 concentrations in future scenarios, which reduces plants' water losses by an increase in their surface resistance, affecting, consequently, PET values (Milly; Dunne, 2016). Finally, water availability is usually assessed from a unique climate perspective, disregarding the human aspect related to the expected increasing water demand caused by economic and population growth, since this kind of information is often difficult to obtain or predict. Nevertheless this simplification hinders accurate depiction of future water security (Greve *et al.*, 2018), as water consumption is expected to significantly increase in the next decades (He *et al.*, 2021). For instance, according to the Brazilian National Water and Sanitation Agency (ANA) projections, most of the Brazilian catchments are expected to experience an increase of over 50% in total water consumption in the next decades (Fig. S5.1 and S5.2).

In this study, we comprehensively assess the impacts of both climate change and water demand in future Brazilian's water security conditions from an integrated climate-human perspective, considering future changes in both climate dynamics - using climate projections from 10 bias-corrected CMIP6-climate models - and water consumption – using water demand projections from the ANA. In our proposed framework we assume an open water balance (OWB) through the catchment's effective area (Liu *et al.*, 2020) and account for CO_2 concentration effects on the water balance partitioning (Yang *et al.*, 2019). We first quantified climate change-based effects in Brazilian's water availability using Budyko-based functional forms for more than 700 catchments with diverse climate conditions and then discussed the potential impacts of these two assumptions on water balance partitioning. To draw Brazilian future water stress scenarios, we included the human-based perspective by using the ANA's future projections of water consumption. This work provides a systematic framework to depict an overview of Brazil's water scarcity in future scenarios of changing climate and water uses that can potentially be used by decision-makers when dealing with water-related issues. Furthermore, the comparison of multiple approaches for depicting future water security scenarios aims to advance hydrologic studies and water resources management practices.

5.2 Material and Methods

5.2.1 Observed data and Climate model projections

We used daily climatological time series from the CLIMBra dataset (Ballarin *et al.*, 2023), which provides spatially-averaged observed data, and raw and bias-corrected projections of 10 CMIP6 climate models for the 735 Brazilian catchments included in the CABra dataset (Almagro *et al.*, 2021). We removed from our analysis 27 catchments that exhibited a mismatch between observed long-term term P and E ($P < E$) or an aridity index greater than 3, as these catchments are not well represented by Budyko-based functional forms used to assess future water availability (Ballarin *et al.*, 2022). The CMIP6, catchment-scale daily series available in the CLIMBra dataset encompass both historical (1980-2010) and future (2015-2100) periods under two different CMIP6-Shared Socioeconomic Pathways (SSP2-4.5

and SSP5-8.5), which represents the moderate and high end emissions scenarios proposed by the ScenarioMIP CMIP6 project (O'Neill *et al.*, 2016; Tebaldi *et al.*, 2021).

5.2.2 Computing Potential Evapotranspiration (PET)

We used the Penman-Monteith (PM) framework to compute PET, as it can be considered as representative of the ensemble mean of different PET formulations (Lemaitre-Basset *et al.*, 2022); explicitly considers both radiative and aerodynamic components in its formulation (Milly; Dunne, 2016); and is the most widely used method to compute PET in climate impact studies (Dai, 2013; Huang *et al.*, 2016; Oudin; Michel; Anctil, 2005; Roderick; Greve; Farquhar, 2015; Yang *et al.*, 2019). Basically, this equation requires daily series of maximum and minimum temperature, net solar radiation, surface wind speed, and relative humidity, which are all available in the CLIMBra's dataset. There are two commonly used variants of the original PM equation: the open water Penman model, designed for water surfaces assuming a null surface resistance (r_s); and the reference crop Penman-Monteith (PM-RC) formulation for an idealized reference crop in the current climate, setting r_s to a constant value of 70 s.m^{-1} (Equation 5.1). Nevertheless, these offline formulations do not account for the influence of increasing CO_2 concentrations on plant water use, which may significantly reduce their water losses and, consequently, future PET (Milly; Dunne, 2017; Swann *et al.*, 2016). In light of this, we adopted a modified version of the PM-RC formulation that takes into account the effects of CO_2 on plants' water use by making the surface resistance (r_s) as a function of CO_2 (Yang *et al.*, 2019; Equation 5.2).

$$PET = \frac{0.408.s.(R_n - G) + \gamma.\left(\frac{900}{T+273}\right).u.D}{s + \gamma.(1 + 0.34.u)} \quad (5.1)$$

$$PET = \frac{0.408.s.(R_n - G) + \gamma.\left(\frac{900}{T+273}\right).u.D}{s + \gamma.\{1 + u.[0.34 + 2.4 \times 10^{-4}(CO_2 - 300)]\}} \quad (5.2)$$

where s is the gradient of the saturation pressure (Pa.K^{-1}), R_n is the net radiation flux (MJ.m^{-2}.day^{-1}), G is the sensible heat flux into the soil (MJ.m^{-2}.day^{-1}), γ is the psychrometric constant (Pa.K^{-1}), T is the mean air temperature (°C), u is the near-surface (2 m) wind speed (m.s^{-1}),

D is the difference between saturated and actual vapour pressure (Pa), and the term $2.4 \times 10^{-4}(CO_2 - 300)$ accounts for the effects of CO_2 concentrations on plant water use.

For a detailed description of PET formulations, see Yang et al. 2019). It is worth emphasizing that rather than adopt a homogeneous evolution of CO_2 concentration, we considered here its non-uniform spatial and temporal distribution by using the dataset of Cheng *et al.* (2022; see Fig S5.3). For this task, we first spatially averaged monthly future CO_2 concentrations for each CABra's catchment and then computed their mean yearly PET values.

5.2.3 COMPUTING WATER AVAILABILITY (Q)

Historical and future water availability were estimated using the functional forms originally proposed by Meira Neto et al. (2020; Equation 5.3 to 5.5), which describes water availability as a function of ϕ. The mathematical reasoning of this formulation is based on the theoretical framework presented by L'vovich and Budyko (Budyko, 1974). The former describes the water balance as a two-stage process: First, precipitation P is partitioned in wetting catchment W, which represents the water stored in the catchment, and direct runoff (Q_D), the quick component of streamflow to precipitation. In a second stage, W is then evaporated (E) or transformed in baseflow (Q_B), which is the slow response of the catchment to a rainfall event. The latter assumes the partition of P into E and Q - which is the simple sum of the streamflow components Q_B and Q_D - as a function of ϕ, suggesting the balance between atmosphere's water demand and supply as the main controlling mechanism of long-term water balance partitioning. With simple algebraic manipulations of Budyko and L'vovich formulations and applying their limit conditions, Meira Neto et al. (Meira Neto *et al.*, 2020) proposed the following equations:

$$f_D(\phi) = \exp\left(-\phi^a + \ln\left[\left\{\frac{Q_D}{P}\right\}_{\max}\right]^{\frac{1}{b}}\right)^b \quad (5.3)$$

$$f_B(\phi) = \exp\left(-\phi^c + \ln\left[1 - \left\{\frac{Q_D}{P}\right\}_{\max}\right]^{\frac{1}{d}}\right)^d \quad (5.4)$$

$$f_Q(\phi) = f_B(\phi) + f_D(\phi) \tag{5.5}$$

where $f_B(\phi)$, $f_D(\phi)$, and $f_Q(\phi)$ are the functional forms describing Q_B/P, Q_D/P and Q/P as a function of ϕ; a, b, c, and d are shape parameters, and the terms of the form $ln[*]$ are shift coefficients to satisfy the limiting conditions proposed by Budyko (Budyko, 1974). That is, when aridity approaches to infinity, Q/P, and, consequently, Q_B/P and Q_D/P, will tend to 0 ($\phi \to \infty$; $f_D, f_B \to 0$). On the other hand, when aridity reaches 0, Q/P and, consequently, the sum of Q_B/P and Q_D/P will be 1. Here, following Meira Neto et al. (2020), we assumed that maximum values of Q_B/P and Q_D/P occur at this limiting condition ($\phi \to 0$; $f_D \to [Q_D/P]_{max}$; $f_B \to [Q_B/P]_{max} = 1 - [Q_D/P]_{max}$).

These functional forms, however, were formulated under the assumption of a closed water balance, which may not be valid as, in many cases, catchments cannot be considered as closed hydraulic entities (Fan, 2019; Roderick *et al.*, 2014). Hence, we adopted in this study the framework proposed by Ballarin et al. (2022), which links the Budyko-based functional forms (Equations 5.3 to 5.5) to the effective area (A_{eff}) approach, proposed by Liu et al. (2020), to account for inter-catchment groundwater exchanges under an open-water balance assumption. Basically, this framework uses an effective area (A_{eff}, Equation 5.6), rather than the topographic one (A_{topo}), as the basic spatial unit to compute catchments' hydrological fluxes. The reasoning behind the A_{eff} concept is that catchments water availability Q is not only influenced by only catchments' water recharge ($P - E$) but also by other external fluxes, such as neighboring catchments water exchanges, which are not limited by the catchment's topographic boundaries. According to this reasoning, if the catchments show no influence of these external fluxes, A_{eff} is equal to A_{topo}. If the catchment is losing water, $Q < P - E$, and $A_{eff} < A_{topo}$. Finally, if the catchments is gaining water, $Q > P - E$, and $A_{eff} > A_{topo}$.

$$\frac{A_{eff}}{A_{topo}} = \frac{Q}{P - E} \tag{5.6}$$

The functional forms' calibrated parameters for both close (CWB) and open (OWB) water balance assumptions are displayed in Table 5.1. Details about the calibration-validation

procedure, which was conducted using observed catchments' daily streamflow timeseries available in the CABra's dataset, can be found in Ballarin et al. (2022). Since we are interested in disentangle climate change's impacts on water availability, we assumed here that catchments will follow their Budyko-based trajectories in the future. Nevertheless, it is important to underscore that catchments may not follow their expected trajectories in the future since the water balance partitioning is also affected by other factors than climate, such as land cover and water uses, that are not taking into account here (Destouni; Jaramillo; Prieto, 2013; Jaramillo *et al.*, 2018, 2022).

To ensure the robustness of our analysis in view of the inherent variability and uncertainty of climate models' projections (Tebaldi; Knutti, 2007), we based our results in both multi-model ensemble mean and standard deviation (hereinafter, *std*). Hence, we computed water availability for each of the 10 CMIP6-climate models separately, using the functional forms and ϕ derived from the climate models forcing outputs, and, subsequently, we calculated the multi-model ensemble mean and standard deviation in order to display and discuss our results.

Table 5. 1. Functional forms calibrated parameters for both closed (CWB) and open (OWB) water balance assumptions.

Parameters	CWB	OWB
a	1.10	0.71
b	1.23	1.30
c	1.20	0.75
d	0.74	0.80
$\left\{\frac{Q_D}{P}\right\}_{max}$	0.38	0.38

5.2.4 COMPUTING WATER SCARCITY

We assessed Brazilian future water security using the widely used approach that computes water scarcity as the ratio between water demand and water availability Q (Liu *et al.*, 2017; Rodrigues; Gupta; Mendiondo, 2014; van Vliet *et al.*, 2021). The total water demand was extracted from the ANA database (Equation 5.8). The demand was divided into six categories: households, industry, mining, cooling water for thermal power plants, livestock, and

irrigation. The data for households were subdivided into urban and rural areas based on population counts and estimates. The data for the industry was based on the number of employees in each industrial category by Brazilian city. The data for mining was based on mineral production by type or group of substance. The data for cooling water for thermal power plants were based on effective power generation data. The data for livestock were based on agricultural censuses. The data for irrigation were mapped from satellite images and characterized using national agricultural censuses. More information and data can be found in the ANA's Manual of Consumptive Water Use in Brazil (ANA, 2019). The collected data were initially aggregated by micro-catchments. Then, these micro-catchments were aggregated in the 708 catchments analyzed in this work according to their geographic locations. The relative difference between the projected data for 2040 and the data from 2020 is displayed in Fig. S5.1. A linear regression analysis was then conducted to estimate data for the distant future (2070–2100).

$$Scarcity = Q/Dem_{TOTAL} \tag{5.7}$$

$$Dem_{TOTAL} = \sum_{j=1}^{6} Dem_j, \tag{5.8}$$

where $j = 1, \dots, 6$ represent the six different water uses in ANA's Manual of Consumptive Water Use in Brazil: Urban and rural households, industry, mining, cooling water for thermal power plants, livestock, and irrigation.

5.3 Results and Discussion

5.3.1 The effects of considering an open water balance (OWB), CO_2 concentration, and bias-corrected climate models outputs on the estimation of future water availability

To examine the effects of considering catchments as open hydrologic entities, we compared the performance of Budyko-based functional forms in reproducing observed long-term water availability assuming both an OWB and a CWB. Our results indicate that this assumption affects water balance components as catchments may import (or export) a major part of their water budgets. In Brazil, this seems to be the rule rather than the exception (Schwamback *et al.*, 2022). Approximately 30% of the evaluated catchments exhibit a deviation of more than 30% in their water balance closure, which means that these catchments are losing (or gaining) a substantial part of their water (Figure 5.1a). This finding undermines the close water balance assumption, and, consequently, traditional Budyko-based formulations that rely on this simplification. Indeed, assuming an OWB by means of the effective area framework (Ballarin *et al.*, 2022; Liu *et al.*, 2020) significantly improved the performance of the functional forms to explain between-catchment streamflow variability (Figure 5.1c, d), which suggests inter-catchment groundwater flow as an important control mechanism of long-term water balance partitioning. A similar result was found when we compared the use of raw and bias-corrected climate models outputs: The latter significantly improved the performance of the functional forms to explain between-catchment streamflow variability (Figure 5.1e, f), given that raw climate simulations often fail to accurately reproduce climate observations. It is worth highlighting that even using bias-corrected simulations and assuming an OWB, the functional forms was not able to represent the water availability of a few catchments, exhibiting deviations of more than 300 $mm.year^{-1}$ in some cases (4 catchments). Nevertheless, we don't believe that these deviations affect our overall results. For instance, more than 90% of the catchments exhibited relative bias $< 30\%$ between observed and estimated water availability (see Fig. S5.4 and S5.5 for more details).

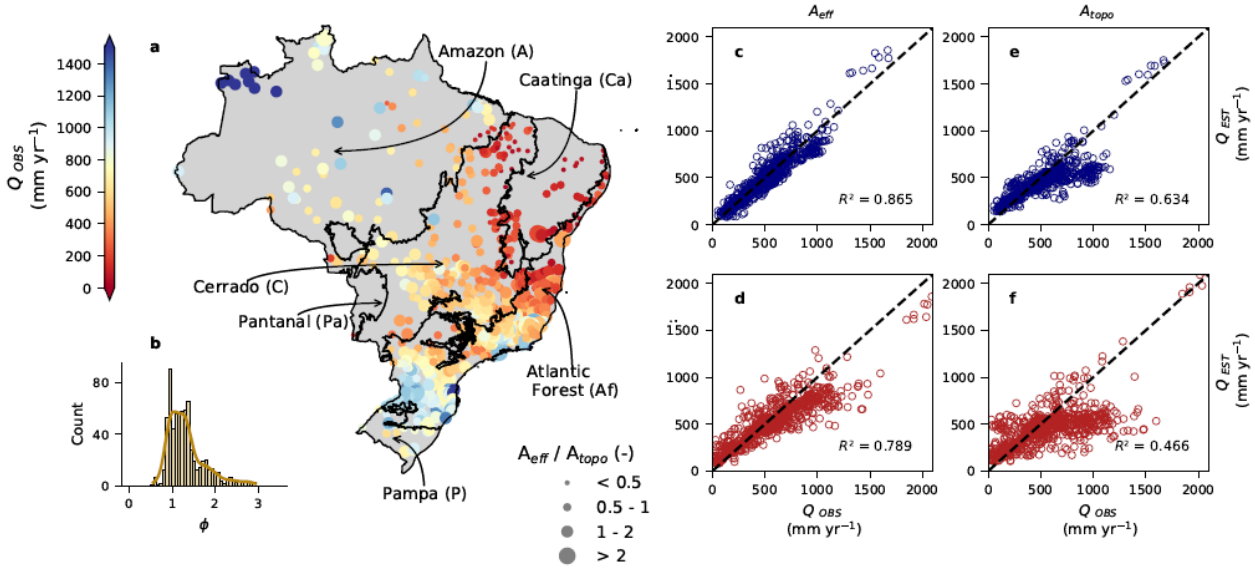

Figure 5.1. Current water availability in Brazil. a, Long-term observed water availability (Q_{OBS}) of the 708 evaluated catchments, sized by their A_{eff}/A_{topo} ratio. Solid black lines indicate the limits of the 6 main Brazilian biomes (A: Amazon, C: Cerrado, Ca: Caatinga, Af: Atlantic Forest, Pa: Pantanal, and P: Pampa).b, Histogram of catchments' aridity index (ϕ). c, d, Performance of the A_{eff}-corrected (open water balance assumption) functional forms to estimate observed water availability using bias-corrected and raw CMIP6-multimodel ensemble, respectively. e, f, Same as c and d, but using the no-correction (closed water balance assumption) functional forms.

To understand the influence of CO_2 concentration on future water availability characterization, we compared the future *PET* estimations using the traditional Penman-Monteith (PM) approach with those made by the modified Penman-Monteith (PM-CO_2) approach, proposed by Yang et al. (2019). Similar to previous studies (Lemaitre-Basset; Oudin; Thirel, 2022; Milly; Dunne, 2016; Yang *et al.*, 2019), we found overestimations of up to 200 mm.year^{-1} in future multi-model ensemble mean *PET* computed ignoring the effects of CO_2 concentrations (Fig S5.6). These differences may lead to misleading results of water availability assessment, especially when dealing with Budyko-based formulations that strongly depend on *PET* values to water balance partitioning (Guo *et al.*, 2019). If CO_2 effects are not considered, we obtain a different picture of future water availability in Brazil (Figure 5.2). Offline *PET* computations that do not account for the effects of CO_2 concentration tend to overestimate the terrestrial drying due to an overestimation of *PET* (Milly; Dunne, 2017), not being able to reproduce the hydrologic information of fully coupled climate models and misrepresenting their future projections (Milly; Dunne, 2016; Yang *et al.*, 2019). In our case,

almost 51% (21% *std*) of the evaluated catchments exhibit a reduction in water availability, against 33% (20% *std*) when using the PM-CO_2 approach (Figure 5.2c, d). Actually, unlike the PM-CO_2 framework, which project both increases and decreases of PET values, the traditional PM equation projected a rise in future PET values for all evaluated catchments (Figure 5.2).

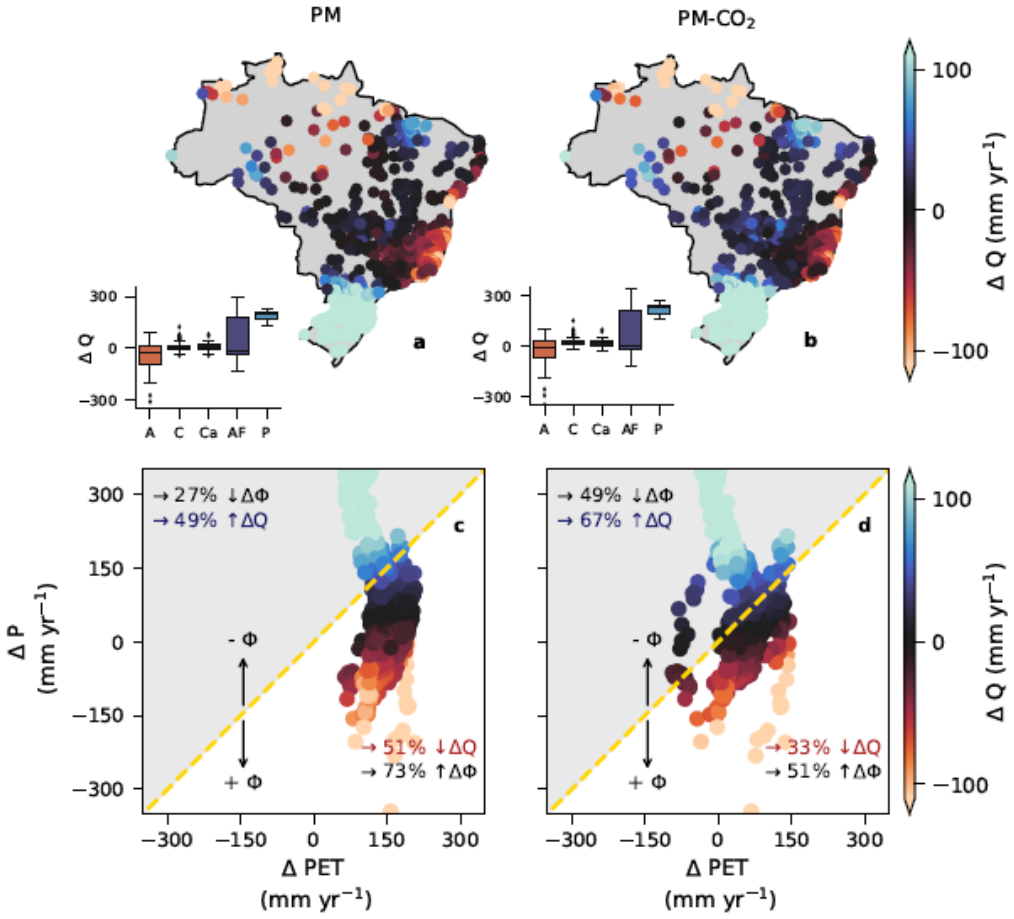

Figure 5.2. Effects of CO_2 consideration on the estimation of water availability changes. a, b, Projected changes (CMIP6 ensemble mean) in long-term mean water availability ΔQ in Brazil for the distant future (2070 – 2100) under the SSP5-8.5 scenario with PET estimated taking (or not) into account the effects of CO_2 concentration on plants' water use. PM represents the traditional Penman-Monteith equation and PM-CO_2 represents the equation proposed by Yang et al., which considers the effects of CO_2 on PET estimations. Changes per Brazilian biome are displayed in traditional boxplots (A: Amazon, C: Cerrado, Ca: Caatinga, Af: Atlantic Forest, and P: Pampa). c, d, Relationship between changes in water availability (ΔQ), precipitation (ΔP), and potential evapotranspiration (ΔPET) for the PM and PM-CO_2 approaches. A yellow, dashed line separates the catchments with positive and negative changes in the aridity index ϕ. Red (blue) numbers indicate the fraction of catchments whose water availability Q is expected to decrease (increase). Black numbers on the top (bottom) indicate the fraction of catchments whose aridity index ϕ is expected to increase (decrease).

Finally, to better understand the coupled effects of the three aforementioned limitations of the usual framework used to estimate future water availability, we computed the difference between the long-term, multi-model ensemble mean water availability estimated using our framework, referenced here as an *'alternative'* approach – which (i) takes into account the effects of CO_2 concentrations on PET estimation, (ii) uses bias-corrected simulations, and (iii) implicitly assumes an open water balance assumption by the use of the A_{eff} approach - and the '*usual*' approach, which neglects the effects of CO_2 on PET values, considers raw climate models outputs and assumes the traditional closed water balance assumption (Figure 5.3). We found differences of more than 1,000 mm.yr^{-1} for the distant future (2070–2100) long-term Q estimated between the two approaches, that surpass the uncertainties associated with climate models projections, indicating that indeed the selection of an appropriate framework plays a fundamental role on estimating future water security. The differences are more pronounced in the Caatinga, Atlantic Forest, and Pampas biomes. For the first, the '*usual'* approach seems to estimate larger water availability, as it neglects that these catchments are prone to lose water through inter-catchment water exchanges (Schwamback *et al.*, 2022). The ϕ-changes on the Caatinga does not present a clear pattern and, therefore, cannot be recognized as the cause of these underestimations. For the other two biomes, Atlantic Forest and Pampas, the opposite occurs: the *'usual'* approach tends to underestimate future water availability, mainly due to a dry bias in the projected future ϕ, caused by neglecting the influence of CO_2 concentrations in PET estimation and by the low performance of raw-climate outputs in representing rainfall events in the region (Ballarin *et al.*, 2023). We did not find any clear pattern of differences in the other two biomes, Amazon and Cerrado. Given its heterogeneous condition in terms of the A_{eff}/A_{topo} ratio and ϕ-changes, it is difficult to attribute under or overestimations to them.

In general, these findings indicate that all the three aforementioned limitations affect future water availability estimations (Figure 5.3c, d). Raw climate outputs tend to misrepresent climate variables, affecting future ϕ-projections and, consequently, future water availability estimations. 'Offline' PET formulations tend to overestimate future hydrologic drying, since they do not account for the effects of CO_2 concentrations on plants' water use. Finally, the traditional closed water balance assumption neglects inter-catchment

water exchanges, overestimating (underestimating) future water availability of 'losing' ('gaining') catchments.

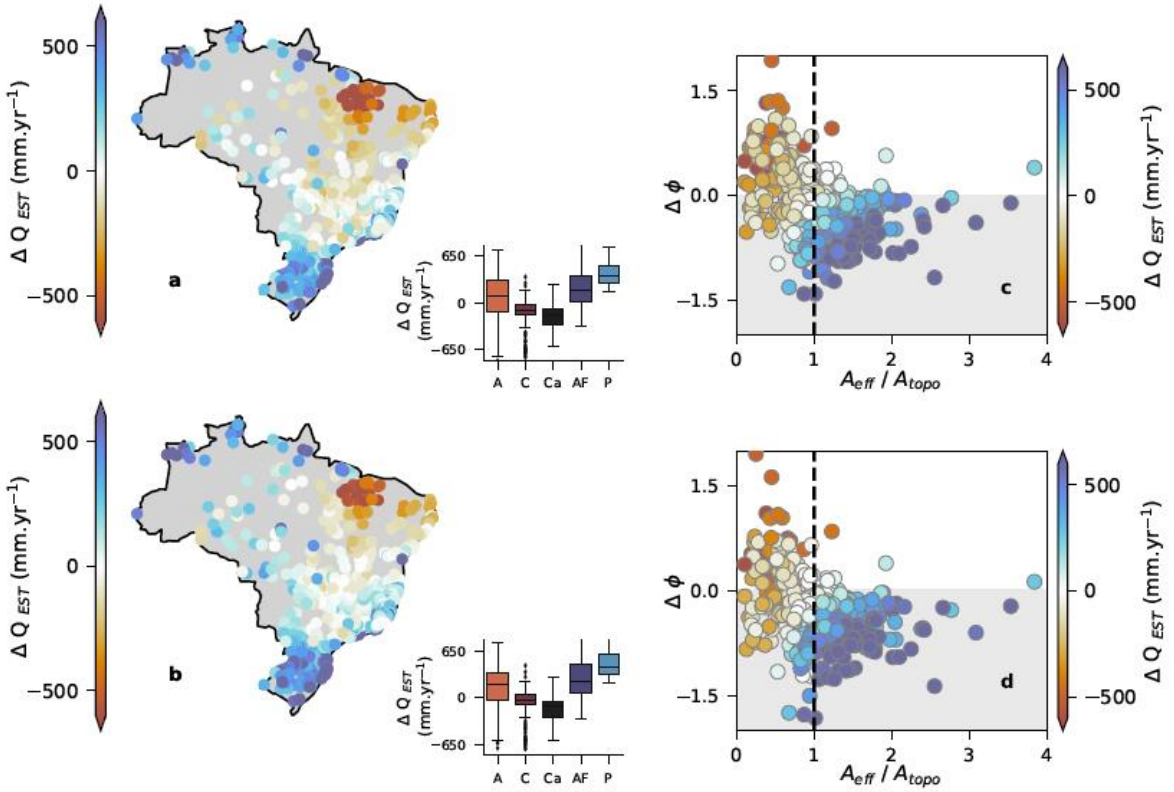

Figure 5.3. Effects of the consideration of bias-corrected data, the influence of CO_2 on PET estimation, and the open water balance assumption on the estimation of future water availability., a, b, Differences between long-term, multi-model ensemble mean distant future (2070-2100) water availability estimated using the 'alternative' and 'usual' approaches for the SSP2-4.5 and SSP5-8.5 scenarios, respectively. The former considers bias-corrected simulations, the effects of CO_2 concentrations on PET estimation using the PM-CO_2 formulation, and an open water balance assumption. The latter, on the other hand, considers raw simulations, the traditional PM formulation, and assumes a closed water balance. Differences per Brazilian biome are displayed in traditional boxplots (A: Amazon, C: Cerrado, Ca: Caatinga, Af: Atlantic Forest, and P: Pampa). c, d, Relationship between the differences in estimated water availability (ΔQ_{EST}), changes in the estimated aridity index ($\Delta\phi$), and the A_{eff}/A_{topo} ratio. A black, dashed line separates gaining ($A_{eff}/A_{topo} > 1$) and losing ($A_{eff}/A_{topo} < 1$) catchments. The light-gray background separates 'drying' ($\Delta\phi > 0$) and 'wetting' ($\Delta\phi < 0$) catchments. For instance, negative values of ΔQ_{EST} indicate that the usual approach estimate a lower water availability than those estimated by the alternative approach. The opposite is valid for positive values of ΔQ_{EST} .

5.3.2 BRAZILIAN FUTURE WATER AVAILABILITY

Given the limitations of the *usual* approach to reproduce and project future water availability, hereinafter we adopted the *alternative* framework to depict future scenarios of Brazilian water availability. We found an uneven distribution of water availability changes across the Brazilian territory (Figure 5.4). As expected, changes are projected to be more intense in the SSP5-8.5 scenario, which is the high-end of the range of future CMIP6-projections (O'Neill *et al.*, 2016), and therefore is related to more intense changes on hydroclimatic variables (Figure 5.4c, d). Despite the differences between the two future scenarios in terms of magnitude, their spatial distributions of changes are similar. For SSP2-4.5, approximately 72% (20% *std*) of the evaluated catchments may experience an increase in water availability. For the SSP5-8.5, this share slightly reduces to 67% (22% *std*). If we consider climate model uncertainties, we could observed nearly to 90% (50%) of the catchments experiencing an increased water availability. Therefore, while some models project an overall increase of water availability for almost all catchments in the country, others suggest a similar number of catchments with projected increased/decreased future water availability.

Considering the multi-model ensemble mean, water availability increases are more pronounced in southern Brazil, in the Pampas ($\Delta\bar{Q} = +219$ mm.yr^{-1}) and Atlantic Forest ($\Delta\bar{Q} = +70$ mm.yr^{-1}) biomes, where the largest increases in mean precipitation are expected to occur (Ballarin *et al.*, 2023; Fig S5.7). We did not note a clear pattern of changes in the other Brazilian biomes. Catchments located in northeastern Brazil, where most of the water security' critical conditions are found (Gesualdo *et al.*, 2021), will experience both an increase and decrease in future water availability. Specifically, *'coastal'* catchments, which show a higher vulnerability due to urbanization and increased water consumption, are prone to experience a reduction in water availability, while *'inland'* catchments will experience an increase. It is important to emphasize that this region often suffers from droughts and water shortages (Marengo; Torres; Alves, 2017) and also exhibits the lowest water availability in the country (Figure 5.1a), and therefore may be more impacted by changes in water yield. Similar results can be found for the Amazon biome: its northern part will experience the largest water reduction in the country, while its southern part will experience a rise in its water availability.

Despite using monotonic ϕ-based functional forms to estimate water availability, interestingly some catchments exhibited larger (lower) future water availability even with an increase (decrease) in its future ϕ. While approximately 51% (19% *std*) of the evaluated catchments will experience a decrease of ϕ under the SSP5-8.5 scenario, 67% (22% *std*) of them will experience an increase in water availability (note the different percentages in Figure 5.4d). This counterintuitive result can be explained by the fact that the Budyko-based functional form estimates future streamflow ratio (Q/P), and not directly Q. Thus, even with an increase in ϕ and consequently a reduction in its future streamflow ratio, some catchments exhibited a larger future water availability due to a large increase in its future P. In these cases, changes in P have a greater control on water availability changes than PET, as it (i) shows the greater influence on future ϕ values and is also (ii) accounted for in the estimation of future water availability when computing the streamflow ratio with the functional forms. Even so, PET still exerts a strong influence on water availability estimation. This can be noted in Figure 5.2, where we compared Q-estimations made using the PM and PM-CO_2 frameworks. A simple consideration of CO_2 concentrations may affect the 'drying' or 'wetting' tendency of the country.

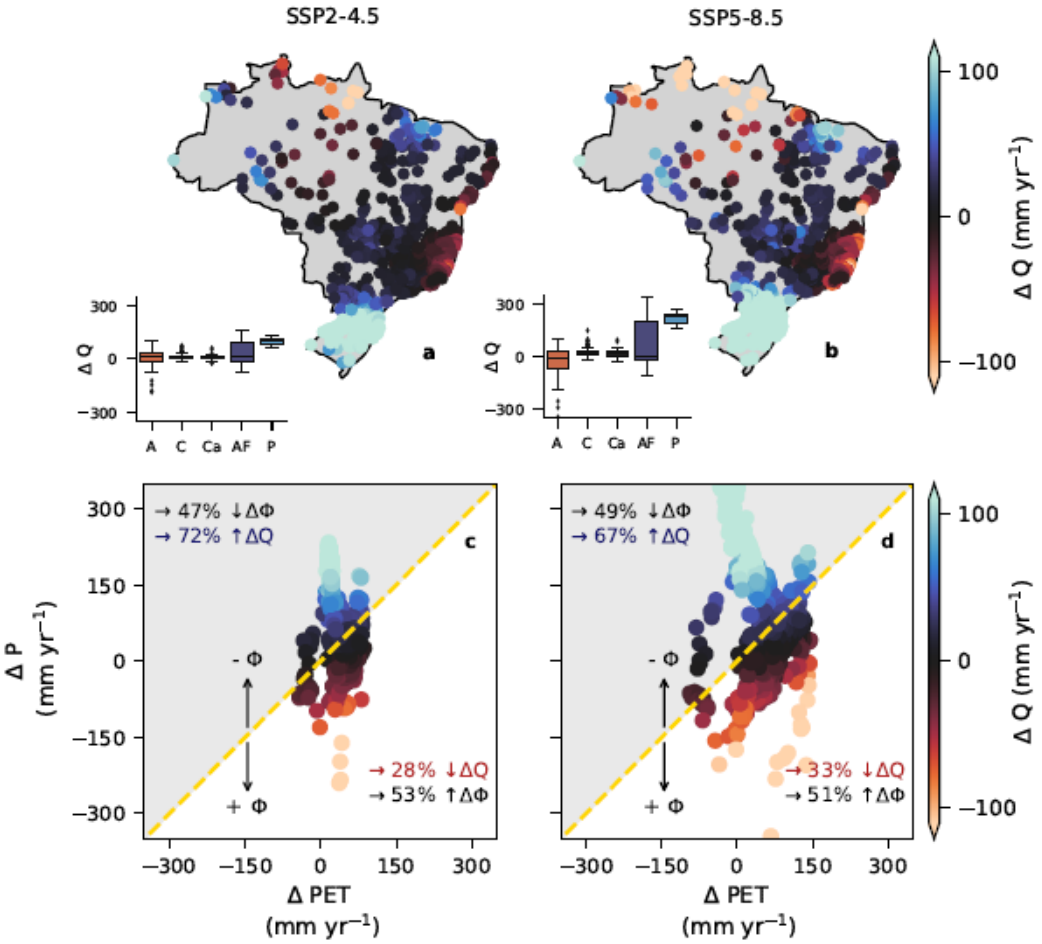

Figure 5.4. Water availability changes. a, b, Projected changes on long-term mean water availability ΔQ in Brazil for the distant future (2070 – 2100) under the SSP2-4.5 and SSP5-8.5 scenarios, respectively. Changes per Brazilian biome are displayed in traditional boxplots (A: Amazon, C: Cerrado, Ca: Caatinga, Af: Atlantic Forest, and P: Pampa). c, d, Relationship between changes in water availability (ΔQ), precipitation (ΔP), and potential evapotranspiration (ΔPET) for the SSP2-4.5 and SSP5-8.5. A yellow, dashed line separates catchments with positive and negative changes in the aridity index ϕ. Red (blue) numbers indicate the fraction of catchments whose water availability Q is expected to decrease (increase). Black numbers on the top (bottom) indicate the fraction of catchments whose aridity index ϕ is expected to increase (decrease).

5.3.3 Brazilian future water security

After including the human aspect in the water security assessment, we note that most of the evaluated catchments may worsen their water security condition in both evaluated scenarios, showing a very similar response for both SSP2-4.5 and SSP5-8.5 (Figure 5.5). Effectively and considering the multi-model ensemble mean, 81% of the catchments may

experience reduced water security over the CMIP6 high-end SSP5-8.5 scenario. The *std* of climate models projections reduced to only 5%, since water availability uncertainties were not fully translated into water security uncertainties given the lower role of it in the water security index computation. From this reduced sample of catchments that are expected to undergo a worse water security, almost 37% will experience a reduction of future water availability, which indicates that the other 63% will undergo a worse scenario due to an increase in human water use, even with an expected increase in water quantities. These percentages represent approximately 51% and 30% of all assessed catchments, respectively. In contrast, for the 19% of catchments that will face an improvement in the water security conditions, approximately 86% will experience an increase in water availability, whereas nearly 14% will get better conditions of water security even with a reduction in future water availability due to an expected decrease in human water consumption. These percentages represent nearly 16% and 3% of all evaluated catchments, respectively. These findings highlight the role of the human aspect in water security assessment. Almost 54% of the catchments will show a counterintuitive response to water security in terms of water availability. That is, 51% of the catchments will face a worse condition in terms of water security even with an increase in water availability, whereas nearly 3% of the catchments will see an improvement in water security, even with a reduction in future water availability.

To obtain a comprehensive understanding of Brazil's future water security from a spatial-scale perspective, we conducted a categorical classification of catchments based on the projected changes in both water availability and demand (Figure 5.5e, f). It should be emphasized that the complex interplay between these variables poses challenges in establishing a direct association between a specific category and a future water security condition (Figure 5.5a, b and Figure 5.5e, f). Even so, this analysis may provide valuable insights into the country's future water security. Most of the catchments located in the Cerrado (95%) and Caatinga (100%) biomes are projected to face a decreasing in water security due to an escalating water consumption, despite an anticipated overall increase in water availability. Factors contributing to this include significant expansion of croplands, with crop extents more than doubling in the past two decades (Zalles *et al.*, 2019), and increased water use, with irrigation withdrawals rising by up to 35% from 1950 to 2017 (Gesualdo *et al.*, 2021). The combined impact of changes in land cover and land use and water

demand has led to an overall reduction in water security in the Cerrado and Caatinga regions (Caballero; Ruhoff; Biggs, 2022). Moreover, both regions have witnessed severe droughts and water crises in recent years, attributed to a combination of climate change and human activities (Marengo *et al.*, 2018, 2022; Marengo; Torres; Alves, 2017; Nobre *et al.*, 2016; Otto *et al.*, 2015). These events underscore the existing vulnerability of both regions to climate variability and extremes, impacting various socioeconomic sectors within these areas. This condition is also observed in the Amazon biome: a few catchments (5%) are projected to have improved future water security. The overall condition of the biome is expected to worsen mainly due to an increase in water consumption and reduction of water availability. Despite the Amazon biome accounting for nearly 80% of Brazil's water availability and currently maintaining a healthy water security condition, the ongoing conversion of natural forests to croplands in the region, mainly in the border of the biome, combined with the projected decrease in future water availability, will pose a significant challenge for other regions of the country due to a diminished potential for water recycling (Baudena *et al.*, 2021; Leite-Filho *et al.*, 2021; O'Connor *et al.*, 2021; Staal *et al.*, 2018).

Both the Pampas and Atlantic Forest biomes, which host nearly 65% of the Brazilian population, are expected to undergo a general rise in water availability (Figure 5.4). Nevertheless, given the uneven distribution of projected changes on water consumption, it is challenging to provide a comprehensive overview of water security in these regions. The Pampas is expected to experience a better water security condition than the others evaluated biomes, with an improved future scenario for almost 40% of the catchments, despite an overall increase in projected water consumption, which is not sufficient to overcome the increase in water availability in the region. Atlantic forest will undergo a more challenging scenario, with nearly 70% of the catchments showing a worse future water security.

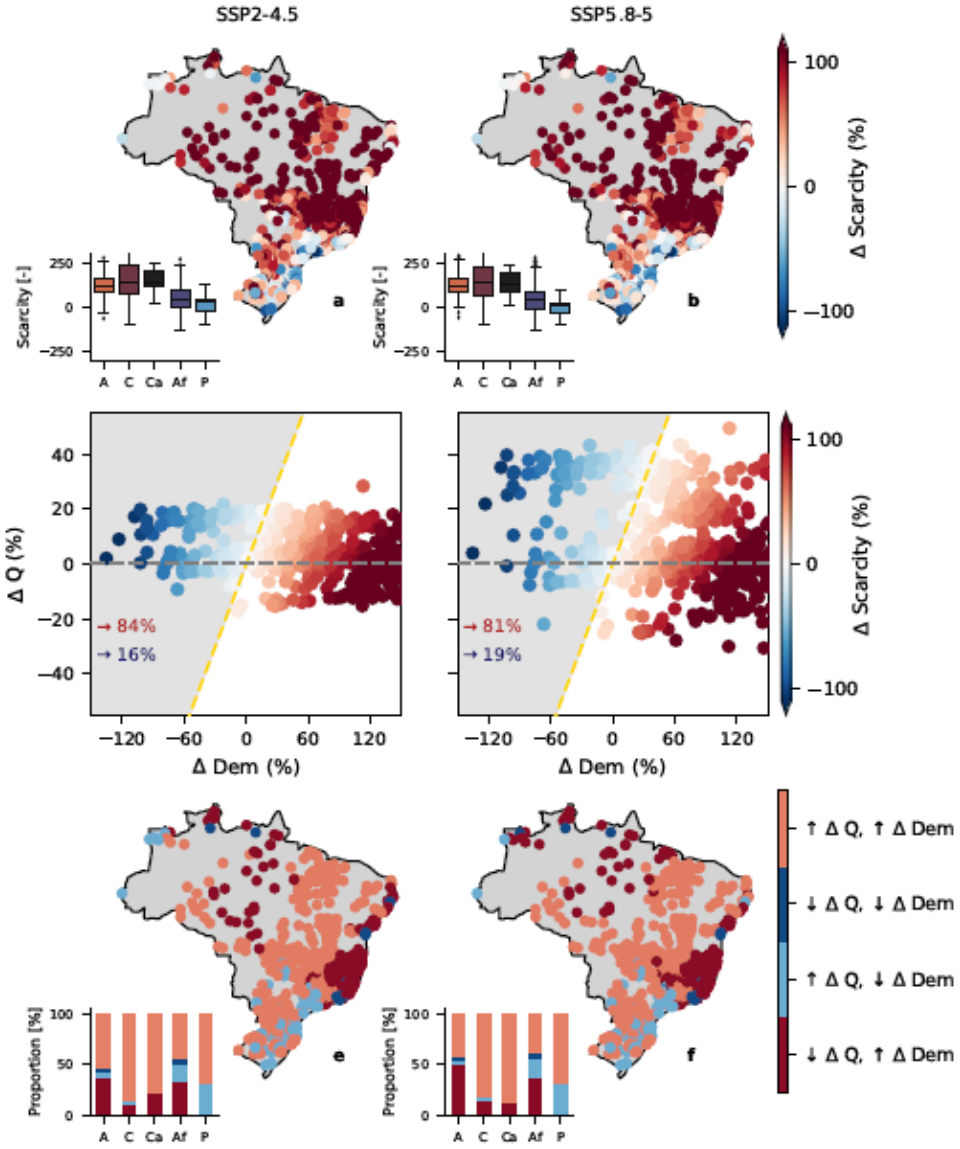

Figure 5.5. Water scarcity changes. a, b, Projected relative changes inn the long-term mean scarcity index in Brazil for the distant future (2070 – 2100) and historical period (1980 – 2010) under the SSP2-4.5 and SSP5-8.5 scenarios, respectively. Changes per Brazilian biome are displayed in traditional boxplots (A: Amazon, C: Cerrado, Ca: Caatinga, Af: Atlantic Forest, and P: Pampa). c, d, Relationship between relative changes for the distant future (2070-2100) and historical period (1980-2010) in water availability (ΔQ), water demand (ΔDem), and in the water scarcity index ($\Delta Scarcity$) for the SSP2-4.5 and SSP5-8.5. A yellow, dashed line separates catchments with positive and negative changes in the scarcity index. A gray, dashed line separates catchments with positive and negative changes in water availability. Red (blue) numbers indicate the fraction of catchments whose water scarcity is expected to get worse (better). e, f, Catchments classified in four different categorical classes according to their positive/negative changes in future water availability (ΔQ) and water demand (ΔDem). Categorical classes per biome are displayed on stretched bar plots.

Although our study presents clear evidence of a worse scenario in Brazilian future water security, it is important to emphasize that the country has one of the largest amount of freshwater resources in the world and, even with a reduction in water security, many of the evaluated catchments are projected to be far away from a water stress condition, where long-term average water availability equals long-term human water use (see Fig S5.8). Nevertheless, recent studies show that even those basins that exhibit a healthy water security condition can experience intra-annual water scarcity conditions due to the uneven distribution of water availability and water usage throughout the year (Gesualdo *et al.*, 2019; Sone *et al.*, 2022). In view of this and the expected intensification of water scarcity in a climate change context (Figure 5.5), which is also expected to inflate the occurrence of extreme drought events and water crisis in the country (Ballarin *et al.*, 2021), we recall that water security assessments remains urgently needed in the country, especially in view of its uneven distribution of water resources, which pose challenges for effective water management practices. Still, Brazil's government has not adequately aligned with climate policies, lacking investments in resilience and municipal policies for mitigating water-related climate impacts (Gesualdo *et al.*, 2021). If current environmental policies persist, we anticipate heightened water stress and increased conflicts over water uses.

5.3.4 LIMITATIONS OF THE STUDY

Here we assumed that catchments tend to follow the Budyko-based functional forms to assess future water availability. This hypothesis indirectly assumes that there will be no changes in catchments' characteristics in the future, such as changes in land cover and land use or changes in catchments' effective area, and consequently, that the calibrated functional forms will remain the same in the future. This simplification, however, may not hold for a large part of the catchments (Jaramillo *et al.*, 2022; Li; Quiring, 2022; Sterling; Ducharne; Polcher, 2013). For instance, changes in Brazilian's catchments land cover conditions due to an increase in croplands and urbanization and irrigation withdrawals will certainly worse the depicted future water scarcity scenario, since they raise both human water consumption and actual evapotranspiration, which, in turn, reduces water security (Gesualdo *et al.*, 2021; Jaramillo *et al.*, 2018; Jaramillo; Destouni, 2015; Sone *et al.*, 2022). That is, if we had taken

into account the increase of croplands and water uses, we would find an even challenging water security scenario.

Furthermore, these changes in land cover and water uses also exhibit an effect on catchments' effective area by altering hydraulic gradients between adjacent catchments which ultimately affects our future water security assessment. Finally, changes on land cover also alters PET estimation due to a change on surface resistance (r_s). This simplification might also affect both historical and future water availability estimates. New PET formulations that do not depend on such simplifications are emerging, showing an opportunity to improve further studies of future water security assessment (Kim; Garcia; Johnson, 2023). Nevertheless, it is important to highlight that even adopting this simplification in the PET estimation, the A_{eff}-corrected functional forms exhibited a very good performance in characterizing observed long-term water availability Q, being able to explain nearly 87% of its between-catchment variance (see Figure 5.1). Those values are quite similar with the ones found by Ballarin et al. (2022) when using the Priestey-Taylor PET formulation and the same functional forms, suggesting that the r_s-simplification does not exert a significant impact on our findings.

We used here a long-term perspective. This somewhat coarse temporal resolution hampers the assessment of the effects of seasonality on water availability (Zhou *et al.*, 2022). It is well-established that global warming will affect the seasonality of precipitation and potential evapotranspiration, and consequently, water-balance partitioning (de Lavenne; Andréassian, 2018; Yokoo; Sivapalan; Oki, 2008). These changes in the seasonal cycle of climate variables, coupled with changes on vegetation spatial-temporal dynamics, will certainly affect future water security and pose a significant challenge for water resources management (Liu; Lin; Cai, 2022). Furthermore, the long-term perspective is unable to capture intra-annual water insecurity situations that may arise from the heterogeneous distribution of water availability and water usage throughout the year (Sone *et al.*, 2022).

The water demand estimation used in the present study came from the National Water and Sanitation Agency (ANA), which is the official Brazilian government agency that provided information for the water resources management in the country. Despite the ANA's report provided some general information on the methodology used to estimation water demand, they do not show any values of uncertainty in their estimations. Furthermore, the

ANA's report lacks enough information to enable us to estimate suitable uncertainty values in water demand. Therefore, the uncertainty in water demand was not computed in our study. Nevertheless, we recognize the importance of addressing and quantifying uncertainties water demand in future research to improve future water security assessment.

Finally, we assessed water security from a unique 'water-quantity' viewpoint, disregarding other fundamental aspects linked to water quality and other kinds of water resources (Rockström *et al.*, 2009). Nevertheless, for a more accurate future water security assessment, it is imperative to consider them, since both water quality and quantity (i) exerts a fundamental role on water usability for humans purpose and (ii) might be affected by socio-economic developments and climate change (Liu *et al.*, 2017; van Vliet; Florke; Wada, 2017). For instance, in a global water-security assessment, van Vliet et al. (2021) suggested an increase of almost 10% in the percentage of world's population currently suffering from severe water scarcity condition when including water-quality aspects. In view of this, we recall that future studies of water security in the country should move towards integrated quality-quantity studies, considering also the interplay between this aspects from a groundwater-surface water lenses, given the importance of such connection for water conservation (Huggins *et al.*, 2023).

5.4 Conclusion

Our study reveals some important aspects for both advancing future water availability studies and for drawing a picture of Brazilian future water security to help water resources management practices. In view of the first point, here we coupled different approaches to overcome the limitations of the traditional framework to project future water availability. We showed that the use of raw climate model outputs, the consideration of a closed water balance, and disregarding future CO_2 concentrations in the estimation of PET values can significantly affect the projection of future water availability. These findings highlight the need to improve climate models to better represent observed and future hydrological and climatological processes.

Moreover, we show the importance of considering the human aspect in assessing water security. Even with an optimistic future scenario of water availability, the country is prone to experience a decrease in water security due to expected higher levels of water use. Our

findings relying on multi-model ensemble mean suggest a reduction of water security in 81% (5% *std*) of the analyzed catchments by 2100. From these catchments, 37% of these presented a reduction of future water availability, while 63% undergo a worse scenario due to an increase in human water use, highlight the importance of incorporate human-perspective in future water security assessments. Almost 54% of the catchments are projected to exhibit a counterintuitive response in terms of water availability and security: 51% of the catchments will face a worse condition in terms of water security even with an increase in water availability, whereas nearly 3% of the catchments will see an improvement in water security, even with a reduction in future water availability. We believe that the simultaneous consideration of both human and climate aspects coupled with a better representation of hydroclimatological dynamics is crucial for a better representation of water security. Even so, further studies on this topic focusing on the understanding of how changes in land cover and water uses may affect catchments' Budyko trajectories will certainly improve the assessment of water security scenarios in an uncertain future.

5.5 REFERENCES

AGHAKOUCHAK, A. *et al.* Climate Extremes and Compound Hazards in a Warming World. **Annual Review of Earth and Planetary Sciences**, [*s. l.*], v. 48, p. 519–548, 2020.

ALMAGRO, A. *et al.* CABra: a novel large-sample dataset for Brazilian catchments. **Hydrology and Earth System Sciences**, [*s. l.*], p. 1–40, 2021.

ANA. **Manual of Consumptive Water Use in Brazil**. Brasilia, Brazil: [*s. n.*], 2019.

BALLARIN, A. S. *et al.* A copula-based drought assessment framework considering global simulation models. **Journal of Hydrology: Regional Studies**, [*s. l.*], v. 38, n. October, p. 0–3, 2021.

BALLARIN, A. S. *et al.* CLIMBra - Climate Change Dataset for Brazil. **Scientific Data**, [*s. l.*], p. 1–31, 2023.

BALLARIN, A. S. *et al.* The Impact of an Open Water Balance Assumption on the Understanding of the Factors Controlling the Long-term Streamflow Components. **Water Resources Research**, [*s. l.*], v. 58, n. e2022WR032413, 2022.

BAUDENA, M. *et al.* Effects of land-use change in the Amazon on precipitation are likely underestimated. **Global Change Biology**, [*s. l.*], n. 27, p. 5580–5587, 2021.

BUDYKO, M. I. **Climate and Life**. New York: Academic Press, 1974.

CABALLERO, C. B.; RUHOFF, A.; BIGGS, T. Land use and land cover changes and their impacts on surface-atmosphere interactions in Brazil: A systematic review. **Science of the Total Environment**, [*s. l.*], v. 808, p. 152134, 2022.

CHENG, W. *et al.* Global monthly gridded atmospheric carbon dioxide concentrations under the historical and future scenarios. **Scientific Data**, [*s. l.*], v. 9, n. 1, p. 1–13, 2022.

CHRISTENSEN, J. H. *et al.* On the need for bias correction of regional climate change projections of temperature and precipitation. **Geophysical Research Letters**, [*s. l.*], v. 35, n. 20, 2008.

DAI, A. Increasing drought under global warming in observations and models. **Nature Climate Change**, [*s. l.*], v. 3, n. 1, p. 52–58, 2013.

DE LAVENNE, A.; ANDRÉASSIAN, V. Impact of climate seasonality on catchment yield: A parameterization for commonly-used water balance formulas. **Journal of Hydrology**, [*s. l.*], v. 558, p. 266–274, 2018.

DESTOUNI, G.; JARAMILLO, F.; PRIETO, C. Hydroclimatic shifts driven by human water use for food and energy production. **Nature Climate Change**, [*s. l.*], v. 3, n. 3, p. 213–217, 2013.

D'ODORICO, P. *et al.* The global value of water in agriculture. **Proceedings of the National Academy of Sciences of the United States of America**, [*s. l.*], v. 117, n. 36, p. 21985–21993, 2020.

FAN, Y. Are catchments leaky?. **WIREs Water**, [*s. l.*], v. 6, n. 6, p. 1–25, 2019.

GESUALDO, G. C. *et al.* Assessing water security in the São Paulo metropolitan region under projected climate change. **Hydrology and Earth System Sciences**, [*s. l.*], v. 23, n. 12, p. 4955–4968, 2019.

GESUALDO, G. C. *et al.* Unveiling water security in Brazil: current challenges and future perspectives. **Hydrological Sciences Journal**, [*s. l.*], v. 66, n. 5, p. 759–768, 2021.

GETIRANA, A.; LIBONATI, R.; CATALDI, M. Brazil is in water crisis — it needs a drought plan. **Nature**, [*s. l.*], v. 600, n. 7888, p. 218–220, 2021.

GORDON, B. L. *et al.* Can We Use the Water Budget to Infer Upland Catchment Behavior? The Role of Data Set Error Estimation and Interbasin Groundwater Flow. **Water Resources Research**, [*s. l.*], v. 58, n. 9, p. 1–26, 2022.

GREVE, P. *et al.* Global assessment of water challenges under uncertainty in water scarcity projections. **Nature Sustainability**, [*s. l.*], v. 1, n. 9, p. 486–494, 2018.

GREVE, P.; SENEVIRATNE, S. I. Assessment of future changes in water availability and aridity. **Geophysical Research Letters**, [*s. l.*], v. 42, n. 13, p. 5493–5499, 2015.

GUO, A. *et al.* Uncertainty analysis of water availability assessment through the Budyko framework. **Journal of Hydrology**, [*s. l.*], v. 576, n. May, p. 396–407, 2019.

HADDELAND, I. *et al.* Global water resources affected by human interventions and climate change. **Proceedings of the National Academy of Sciences of the United States of America**, [*s. l.*], v. 111, n. 9, p. 3251–3256, 2014.

HANASAKI, N. *et al.* A global water scarcity assessment under Shared Socio-economic Pathways - Part 1: Water use. **Hydrology and Earth System Sciences**, [*s. l.*], v. 17, n. 7, p. 2375–2391, 2013a.

HANASAKI, N. *et al.* A global water scarcity assessment under Shared Socio-economic Pathways - Part 2: Water availability and scarcity. **Hydrology and Earth System Sciences**, [*s. l.*], v. 17, n. 7, p. 2393–2413, 2013b.

HE, C. *et al.* Future global urban water scarcity and potential solutions. **Nature Communications**, [*s. l.*], v. 12, n. 1, p. 1–11, 2021.

HUANG, J. *et al.* Accelerated dryland expansion under climate change. **Nature Climate Change**, [*s. l.*], v. 6, n. 2, p. 166–171, 2016.

HUGGINS, X. *et al.* Groundwatersheds of protected areas reveal globally overlooked risks and opportunities. **Nature Susatainability**, [*s. l.*], v. accepted, 2023.

HUNT., J. D.; STILPEN, D.; DE FREITAS, M. A. V. A review of the causes, impacts and solutions for electricity supply crises in Brazil. **Renewable and Sustainable Energy Reviews**, [*s. l.*], v. 88, n. October 2017, p. 208–222, 2018.

JARAMILLO, F. *et al.* Dominant effect of increasing forest biomass on evapotranspiration: Interpretations of movement in Budyko space. **Hydrology and Earth System Sciences**, [*s. l.*], v. 22, n. 1, p. 567–580, 2018.

JARAMILLO, F. *et al.* Fewer Basins Will Follow Their Budyko Curves Under Global Warming and Fossil-Fueled Development. **Water Resources Research**, [*s. l.*], n. 58, p. e2021WR031825, 2022.

JARAMILLO, F.; DESTOUNI, G. Local flow regulation and irrigation raise global human water consumption and footprint. **Science**, [*s. l.*], v. 350, n. 6265, p. 1248–1251, 2015.

JAWITZ, J. W.; KLAMMLER, H.; REAVER, N. G. F. Climatic Asynchrony and Hydrologic Inefficiency Explain the Global Pattern of Water Availability. **Geophysical Research Letters**, [*s. l.*], v. 49, p. e2022GL101214, 2022.

KIM, Y.; GARCIA, M.; JOHNSON, M. S. Land-Atmosphere Coupling Constrains Increases to Potential Evaporation in a Warming Climate: Implications at Local and Global Scales. **Earth's Future**, [*s. l.*], v. 11, p. e2022EF002886, 2023.

KONAPALA, G. *et al.* Climate change will affect global water availability through compounding changes in seasonal precipitation and evaporation. **Nature Communications**, [*s. l.*], v. 11, n. 1, p. 1–10, 2020.

LE MOINE, N. *et al.* How can rainfall-runoff models handle intercatchment groundwater flows? Theoretical study based on 1040 French catchments. **Water Resources Research**, [*s. l.*], v. 43, n. 6, p. 1–11, 2007.

LEITE-FILHO, A. T. *et al.* Deforestation reduces rainfall and agricultural revenues in the Brazilian Amazon. **Nature Communications**, [*s. l.*], v. 12, n. 1, p. 1–7, 2021.

LEMAITRE-BASSET, T. *et al.* Unraveling the contribution of potential evaporation formulation to uncertainty under climate change. **Hydrology and Earth System Sciences**, [*s. l.*], v. 26, n. 8, p. 2147–2159, 2022.

LEMAITRE-BASSET, T.; OUDIN, L.; THIREL, G. Evapotranspiration in hydrological models under rising CO2: a jump into the unknown. **Climatic Change**, [*s. l.*], v. 172, n. 3–4, p. 1–19, 2022.

LI, Z.; QUIRING, S. M. Projection of Streamflow Change Using a Time-Varying Budyko Framework in the Contiguous United States. **Water Resources Research**, [*s. l.*], n. 58, p. e2022WR033016, 2022.

LIU, J. *et al.* Water scarcity assessments in the past, present, and future. **Earth's Future**, [*s. l.*], n. 5, p. 549–559, 2017.

LIU, Y. *et al.* What is the hydrologically effective area of a catchment?. **Environmental Research Letters**, [*s. l.*], v. 15, n. 10, 2020.

LIU, M.; LIN, K.; CAI, X. Climate and vegetation seasonality play comparable roles in water partitioning within the Budyko framework. **Journal of Hydrology**, [*s. l.*], v. 605, n. December 2021, p. 127373, 2022.

MARENGO, J. A. *et al.* Climatic characteristics of the 2010-2016 drought in the semiarid northeast Brazil region. **Annals of the Brazilian Academy Science**, [*s. l.*], v. 90, n. 2, p. 1973–1985, 2018.

MARENGO, J. A. *et al.* Drought in Northeast Brazil: A review of agricultural and policy adaptation options for food security. **Climate Resilience and Sustainability**, [*s. l.*], v. 1, n. 1, p. 1–20, 2022.

MARENGO, J. A.; TORRES, R. R.; ALVES, L. M. Drought in Northeast Brazil—past, present, and future. **Theoretical and Applied Climatology**, [*s. l.*], v. 129, n. 3–4, p. 1189–1200, 2017.

MCDONALD, R. I. *et al.* Water on an urban planet: Urbanization and the reach of urban water infrastructure. **Global Environmental Change**, [*s. l.*], v. 27, n. 1, p. 96–105, 2014.

MEIRA NETO, A. A. *et al.* An Aridity Index-Based Formulation of Streamflow Components. **Water Resources Research**, [*s. l.*], v. 56, n. 9, p. 1–14, 2020.

MILLY, P. C. D.; DUNNE, K. A. A Hydrologic Drying Bias in Water-Resource Impact Analyses of Anthropogenic Climate Change. **Journal of the American Water Resources Association**, [*s. l.*], v. 53, n. 4, p. 822–838, 2017.

MILLY, P. C. D.; DUNNE, K. A. Potential evapotranspiration and continental drying. **Nature Climate Change**, [*s. l.*], v. 6, n. 10, p. 946–949, 2016.

MILLY, P. C. D.; DUNNE, K. A.; VECCHIA, A. V. Global pattern of trends in streamflow and water availability in a changing climate. **Nature**, [*s. l.*], v. 438, n. 7066, p. 347–350, 2005.

MULTSCH, S. *et al.* Assessment of potential implications of agricultural irrigation policy on surface water scarcity in Brazil. **Hydrology and Earth System Sciences**, [*s. l.*], v. 24, n. 1, p. 307–324, 2020.

MYERS, N. *et al.* Biodiversity hotspots for conservation priorities. **Nature**, [*s. l.*], n. 403, p. 853–858, 2000.

NOBRE, C. A. *et al.* Some Characteristics and Impacts of the Drought and Water Crisis in Southeastern Brazil during 2014 and 2015. **Journal of Water Resource and Protection**, [*s. l.*], v. 08, n. 02, p. 252–262, 2016.

O'CONNOR, J. C. *et al.* Atmospheric moisture contribution to the growing season in the Amazon arc of deforestation. **Environmental Research Letters**, [*s. l.*], v. 16, n. 8, 2021.

O'NEILL, B. C. *et al.* The Scenario Model Intercomparison Project (ScenarioMIP) for CMIP6. **Geoscientific Model Development**, [*s. l.*], v. 9, n. 9, p. 3461–3482, 2016.

OTTO, F. E. L. *et al.* Factors other than climate change: main drivers of 2014/2015 water shortage in southeast Brazil. **Bulletin of the American Meteorological Society**, [*s. l.*], v. 96, n. 12, p. 35–40, 2015.

OUDIN, L.; MICHEL, C.; ANCTIL, F. Which potential evapotranspiration input for a lumped rainfall-runoff model? Part 1 - Can rainfall-runoff models effectively handle detailed potential evapotranspiration inputs?. **Journal of Hydrology**, [*s. l.*], v. 303, n. 1–4, p. 275–289, 2005.

PEREIRA, P. A. A. *et al.* The development of Brazilian agriculture and future challenges. **Agriculture & Food Security**, [*s. l.*], v. 1, n. April, p. 1–12, 2012.

RENNER, M.; BERNHOFER, C. Applying simple water-energy balance frameworks to predict the climate sensitivity of streamflow over the continental United States. **Hydrology and Earth System Sciences**, [*s. l.*], v. 16, n. 8, p. 2531–2546, 2012.

ROCKSTRÖM, J. *et al.* Future water availability for global food production: The potential of green water for increasing resilience to global change. **Water Resources Research**, [*s. l.*], v. 45, n. 7, p. 1–16, 2009.

RODERICK, M. L. *et al.* A general framework for understanding the response of the water cycle to global warming over land and ocean. **Hydrology and Earth System Sciences**, [*s. l.*], v. 18, n. 5, p. 1575–1589, 2014.

RODERICK, M. L.; FARQUHAR, G. D. A simple framework for relating variations in runoff to variations in climatic conditions and catchment properties. **Water Resources Research**, [*s. l.*], v. 47, n. 6, p. 1–11, 2011.

RODERICK, M. L.; GREVE, P.; FARQUHAR, G. D. On the assessment of aridity with changes in atmospheric CO2. **Water Resources Research**, [*s. l.*], v. 5, n. 51, p. 5450–5463, 2015.

RODRIGUES, D. B. B.; GUPTA, H. V.; MENDIONDO, E. M. A blue/green water-based accounting framework for assessment of water security. **Water Resources Research**, [*s. l.*], n. 50, p. 7187–7205, 2014.

SAFEEQ, M. *et al.* How realistic are water-balance closure assumptions? A demonstration from the southern sierra critical zone observatory and kings river experimental watersheds. **Hydrological Processes**, [*s. l.*], v. 35, n. 5, 2021.

SCHALLER, M. F.; FAN, Y. River basins as groundwater exporters and importers: Implications for water cycle and climate modeling. **Journal of Geophysical Research - Atmospheres**, [*s. l.*], v. 114, n. 4, 2009.

SCHWAMBACK, D. *et al.* Are Brazilian catchments gaining or losing water? The effective area of tropical catchments. **Hydrological Processes**, [*s. l.*], v. 36, n. 3, p. 1–13, 2022.

SONE, J. S. *et al.* Water Security in an Uncertain Future: Contrasting Realities from an Availability-Demand Perspective. **Water Resources Management**, [*s. l.*], 2022. Disponível em: https://link.springer.com/10.1007/s11269-022-03160-x.

STAAL, A. *et al.* Forest-rainfall cascades buffer against drought across the Amazon. **Nature Climate Change**, [*s. l.*], v. 8, n. 6, p. 539–543, 2018.

STERLING, S. M.; DUCHARNE, A.; POLCHER, J. The impact of global land-cover change on the terrestrial water cycle. **Nature Climate Change**, [*s. l.*], v. 3, n. 4, p. 385–390, 2013.

SWANN, A. L. S. *et al.* Plant responses to increasing CO2 reduce estimates of climate impacts on drought severity. **Proceedings of the National Academy of Sciences of the United States of America**, [*s. l.*], v. 113, n. 36, p. 10019–10024, 2016.

TEBALDI, C. *et al.* Climate model projections from the Scenario Model Intercomparison Project (ScenarioMIP) of CMIP6. **Earth System Dynamics**, [*s. l.*], v. 12, p. 253–293, 2021.

TEBALDI, C.; KNUTTI, R. The use of the multi-model ensemble in probabilistic climate projections. **Philosophical Transactions of the Royal Society A: Mathematical, Physical and Engineering Sciences**, [*s. l.*], v. 365, n. 1857, p. 2053–2075, 2007.

VAN VLIET, M. T. H. *et al.* Global water scarcity including surface water quality and expansions of clean water technologies. **Environmental Research Letters**, [*s. l.*], v. 16, n. 2, 2021.

VAN VLIET, M. T. H.; FLORKE, M.; WADA, Y. Quality matters for water scarcity. **Nature Geoscience**, [*s. l.*], v. 10, n. 11, p. 800–802, 2017.

VANHAM, D. *et al.* Physical water scarcity metrics for monitoring progress towards SDG target 6.4: An evaluation of indicator 6.4.2 “Level of water stress”. **Science of the Total Environment**, [*s. l.*], v. 613–614, n. September 2017, p. 218–232, 2018.

YANG, Y. *et al.* Hydrologic implications of vegetation response to elevated CO2 in climate projections. **Nature Climate Change**, [*s. l.*], v. 9, n. 1, p. 44–48, 2019.

YOKOO, Y.; SIVAPALAN, M.; OKI, T. Investigating the roles of climate seasonality and landscape characteristics on mean annual and monthly water balances. **Journal of Hydrology**, [*s. l.*], v. 357, n. 3–4, p. 255–269, 2008.

ZALLES, V. *et al.* Near doubling of Brazil's intensive row crop area since 2000. **Proceedings of the National Academy of Sciences of the United States of America**, [*s. l.*], v. 116, n. 2, p. 428–435, 2019.

ZHOU, S. *et al.* Diminishing seasonality of subtropical water availability in a warmer world dominated by soil moisture–atmosphere feedbacks. **Nature Communications**, [*s. l.*], v. 13, n. 1, p. 1–10, 2022.

CHAPTER 6

Final Remarks

6.1 General Discussion

An accurate understanding of the spatiotemporal variability of climate variables stands as one of the most pressing questions of the hydrology scientific field (Blöschl *et al.*, 2019). This aspect has garnered significant attention in recent decades and remains a subject of ongoing debate. For instance, a better understanding of climate variability is paramount for advancing the comprehension of their role on hydrological processes or better understanding the potential impacts of climate change, which was the ultimate objective of the present research (Gleick, 1989). Such advances can be used for different practical purposes, e.g., improving hydroclimatological models and their predictions that are ultimately used for water resources management and infrastructure design and planning.

The present study tried to shed light on this matter in view of the Brazilian context, focusing on enhancing our understanding of the spatiotemporal variability of climate across Brazilian catchments in a global warming context. Precisely, this research aimed to answer *How are extreme events and water availability projected to change in the future across the Brazilian catchments and how will these changes impact both Brazilian natural and social systems?*

To this end, we first developed an open access, climate change dataset for the Brazilian territory: the CLIMBra dataset. We believe the dataset can be useful not only for the hydroclimatological field, but for a broader audience. Climate change impacts goes beyond its direct effects on the water cycle and climate dynamics, showing substantial impacts to human health (Bell *et al.*, 2018; Ebi *et al.*, 2020), energy and food production (Ziervogel; Ericksen, 2010), and ecosystem functioning (Borma *et al.*, 2022; Seddon *et al.*, 2016). For instance, Ferreira *et al.*, (2023), in a commentary paper, highlighted the need for multi-disciplinary, climate change impact assessments to guide public health policies; and Cohn *et al.*, (2016) suggested that climate change effects may decline food production in the Mato Grosso state by up to 13%. In addition to the development of the dataset, we discussed in *Chapter 2* the importance of applying post-processing, bias correction techniques to the raw climate models simulations, given their low performance in representing the present conditions, which is ultimately transferred for their future simulations.

We further assessed, In *Chapter 3*, the projected changes in rainfall events of different magnitudes across Brazilian's catchments. By proposing a novel non-parametric approach, we disentangle the role of changes in rainfall frequency and intensity on driving changes of future rainfall events in the country. As we highlighted, low-to-moderate rainfall events are expected to be less frequent in the future, whereas extreme events are expected to be more intense and frequent, in accordance with the compensation hypothesis. Moreover, our results suggested that changes in frequency, rather than in intensity, rules future rainfall events in the future. Such information is paramount for informing risk assessment practices. As highlighted by recent studies, temporally compound events, such consecutive non-extreme rainfall events can trigger or aggravate floods, leading to major societal impacts (Aghakouchak *et al.*, 2020; Brunner, 2023).

The effects of climate changes in the frequency and intensity of rainfall events, coupled with the overall increase in the atmospheric water demand, is projected to heighten meteorological droughts in Brazil in the end of the century. As we showed in *Chapter 4*, most of the catchments in the country are expected to experience longer, more frequent, and intense future droughts, with high CMIP6-models agreement. Furthermore, such changes are not limited to long-term, averaged properties: an intensification of extreme severe, record-breaking droughts are also expected to occur. Despite the high spatial variability in the magnitude of changes, our results suggest that, according to the most pessimistic SSP5-8.5 scenario, at least 50% of forest, pasture, and cropland areas will experience an increase of at least 30% in droughts' severity. Moreover, according to the ANA's water used projections (ANA, 2019), most of the catchments with anticipated increases in drought events are also projected to exhibit increases in water demand, mainly dictate by the expected expansion of agricultural activities in the country. Such aspects might pose significant challenges for Brazilians' agriculture activities and ecosystems and are already been observed (e.g., Cohn *et al.*, 2016; Koh *et al.*, 2020; Libonati *et al.*, 2022).

We further confirmed these findings in *Chapter 5,* where we assessed future scenarios of water security in Brazilian catchments. The results suggested that, in general, most of the evaluated Brazilian catchments are projected to show reduced water security in the end of the century. Surprisingly, increased water consumption is expected to be the main cause of this. According to the SSP5-8.5 scenario, 51% of the evaluated catchments are expected to

undergo a worse water security scenario due to an increase in human water use, 30% will show reduced water security due to reduced water availability, and 19% will show better conditions of water security due to enhanced water availability and/or reduced water consumption. Such proportions, however, may vary depending on the method and data used. For example, as we show in *Chapter 5*, the use of different formulations of potential evapotranspiration or considerations regarding the water balance closure may result in even pessimistic scenarios of water security.

In summary, the results of the present thesis suggest that, under both evaluated CMIP6 scenarios, heavy rainfall and droughts are expected to be more common and intense by the end of the century, underscoring the imperative for adaptive strategies in water resources management and infrastructure planning in Brazil. Interdisciplinary collaboration and continued research efforts will be crucial in addressing the complex challenges highlighted here, ensuring the resilience and sustainability of Brazil's water resources.

6.2 FUTURE RESEARCH OPPORTUNITIES

During the development of the present thesis, some new ideas and research opportunities emerged. For example, we believe future research towards assessing the performance of different bias-correction methods are needed. The delta quantile method (Cannon; Sobie; Murdock, 2015) showed an excellent performance in reproducing mean and extreme properties of the observed variables, but it is known that some specific properties, such as the probability dry, are usually not well represented. Some new methods, such as the one introduced by Rajulapati and Papalexiou (2023) or machine learning based methods, can be useful to improve models simulations and, consequently, climate change risk assessments.

Besides, we believe more national-level studies towards assessing local-to-regional vulnerabilities are crucial. Here, we focused on assessing the hazard, which is a crucial information for risk assessment, but not sufficient. Understanding local vulnerabilities and how changes in the climate dynamics (rainfall and droughts) are translated to the water fluxes (i.e., floods and hydrological/agricultural droughts) are paramount for developing effective risk management strategies (Althoff; Rodrigues; Da Silva, 2021; Debortoli *et al.*, 2017; IPCC, 2022; Kreibich *et al.*, 2022). Such local-to-regional, additional studies should

incorporate not only more detailed hydroclimatic information, but also social aspects that may be relevant for the development of pratical solutions in a socio-hydrological-based design. For instance, aspects related to social vulnerabilities and exposure are paramount for a precise risk assessment Moreover, here we focused on assessing precipitation-based hazards from a univariate perspective: heavy rainfall and meteorological droughts. Other extreme events, such as heatwaves or compound heatwave and droughts, also have widespread impact and deserve more attention (Ballarin *et al.*, 2021; Libonati *et al.*, 2022b, 2022a; Nobre *et al.*, 2016).

Finally, we believe that there is a need of detection and attribution research in the country. Such studies are paramount to enhance our understanding of the role of anthropogenic activities on future climate and can be very useful for developing adaptation and mitigation strategies. Questions such as how agricultural expansion are expected to affect water security and ecosystem functioning in the country are still open and need to be tackled. Such studies might incorporate different scenarios of water use efficiency, environmental management or even political stability to design alternative pathways for water resources in the country. These aspects, however, are not trivial and should be accounted for from a more specific, local perspective, to be effective in improving the development of policies associated to risk management and water resources sustainability.

6.3 REFERENCES

AGHAKOUCHAK, A. *et al.* Climate Extremes and Compound Hazards in a Warming World. **Annual Review of Earth and Planetary Sciences**, [*s. l.*], v. 48, p. 519–548, 2020.

ALTHOFF, D.; RODRIGUES, L. N.; DA SILVA, D. D. Assessment of water availability vulnerability in the Cerrado. **Applied Water Science**, [*s. l.*], v. 11, n. 11, p. 176, 2021.

ANA. **Manual of Consumptive Water Use in Brazil**. Brasilia, Brazil: [*s. n.*], 2019.

BALLARIN, A. S. *et al.* A copula-based drought assessment framework considering global simulation models. **Journal of Hydrology: Regional Studies**, [*s. l.*], v. 38, n. October, p. 0–3, 2021.

BELL, J. E. *et al.* Changes in extreme events and the potential impacts on human health. **Journal of the Air and Waste Management Association**, [*s. l.*], v. 68, n. 4, p. 265–287, 2018.

BLÖSCHL, G. *et al.* Twenty-three unsolved problems in hydrology (UPH)–a community perspective. **Hydrological Sciences Journal**, [*s. l.*], v. 64, n. 10, p. 1141–1158, 2019.

BORMA, L. S. *et al.* Beyond Carbon: The Contributions of South American Tropical Humid and Subhumid Forests to Ecosystem Services. **Reviews of Geophysics**, [*s. l.*], v. 60, n. 4, p. e2021RG000766, 2022.

BRUNNER, M. I. Floods and droughts: a multivariate perspective. **Hydrology and Earth System Sciences**, [*s. l.*], v. 27, n. 13, p. 2479–2497, 2023.

CANNON, A. J.; SOBIE, S. R.; MURDOCK, T. Q. Bias correction of GCM precipitation by quantile mapping: How well do methods preserve changes in quantiles and extremes?. **Journal of Climate**, [*s. l.*], v. 28, n. 17, p. 6938–6959, 2015.

COHN, A. S. *et al.* Cropping frequency and area response to climate variability can exceed yield response. **Nature Climate Change**, [*s. l.*], v. 6, n. 6, p. 601–604, 2016.

DEBORTOLI, N. S. *et al.* An index of Brazil's vulnerability to expected increases in natural flash flooding and landslide disasters in the context of climate change. **Natural Hazards**, [*s. l.*], v. 86, n. 2, p. 557–582, 2017.

EBI, K. L. *et al.* Extreme Weather and Climate Change: Population Health and Health System Implications. **Annual Review of Public Health**, [*s. l.*], v. 42, p. 293–315, 2020.

FERREIRA, M. A. M. *et al.* Impact of climate change on public health in Brazil. **Public Health Challenges**, [*s. l.*], v. 2, n. 1, p. e62, 2023.

GLEICK, P. H. Climate change, hydrology, and water resources. **Reviews of Geophysics**, [*s. l.*], v. 27, n. 3, p. 329–344, 1989.

IPCC. **Climate Change 2022: Impacts, Adaptation, and Vulnerability.** Cambridge, UK and New York, NY, USA,: Cambridge University Press, 2022.

KOH, I. *et al.* Climate risks to Brazilian coffee production. **Environmental Research Letters**, [*s. l.*], v. 15, n. 10, p. 104015, 2020.

KREIBICH, H. *et al.* The challenge of unprecedented floods and droughts in risk management. **Nature**, [*s. l.*], v. 608, n. 7921, p. 80–86, 2022.

LIBONATI, R. *et al.* Assessing the role of compound drought and heatwave events on unprecedented 2020 wildfires in the Pantanal. **Environmental Research Letters**, [*s. l.*], v. 17, n. 1, p. 015005, 2022a.

LIBONATI, R. *et al.* Drought–heatwave nexus in Brazil and related impacts on health and fires: A comprehensive review. **Annals of the New York Academy of Sciences**, [*s. l.*], v. 1517, n. 1, p. 44–62, 2022b.

NOBRE, C. A. *et al.* Some Characteristics and Impacts of the Drought and Water Crisis in Southeastern Brazil during 2014 and 2015. **Journal of Water Resource and Protection**, [*s. l.*], v. 08, n. 02, p. 252–262, 2016.

RAJULAPATI, C. R.; PAPALEXIOU, S. M. Precipitation Bias Correction: A Novel Semi-parametric Quantile Mapping Method. **Earth and Space Science**, [*s. l.*], v. 10, n. 4, p. e2023EA002823, 2023.

SEDDON, A. W. R. *et al.* Sensitivity of global terrestrial ecosystems to climate variability. **Nature**, [*s. l.*], v. 531, n. 7593, p. 229–232, 2016.

ZIERVOGEL, G.; ERICKSEN, P. J. Adapting to climate change to sustain food security. **Wiley Interdisciplinary Reviews: Climate Change**, [*s. l.*], v. 1, n. 4, p. 525–540, 2010.

APPENDIX A

Supporting Information - Chapter 2

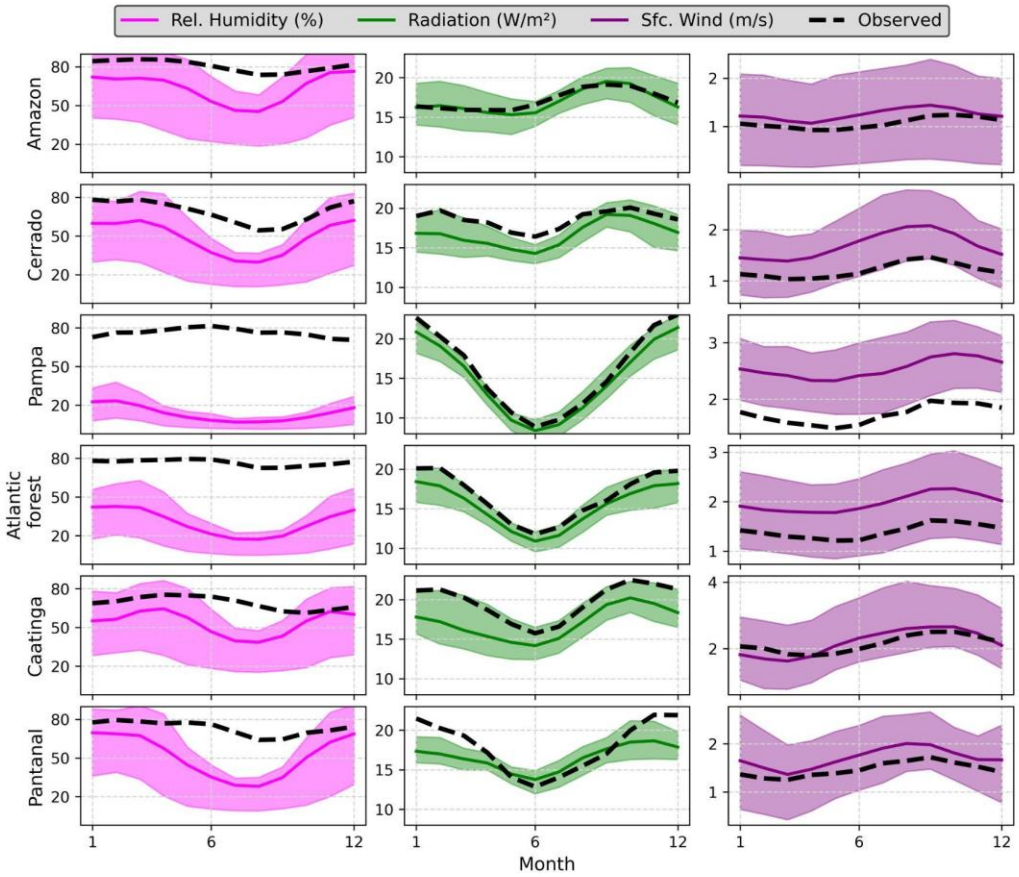

Figure S2.1. Long-term (1980-2013) monthly mean of relative humidity, solar net radiation, and near-surface wind speed, separated by Brazilian biomes. Highlighted lines represent the intra-annual cycle simulated by the raw 10 CMIP6-GCMs' *multi-model ensemble*. Dashed lines indicate the observed mean intra-annual cycle. Confidence intervals represent the maximum and minimum values simulated by the raw 10 CMIP6-GCMs.

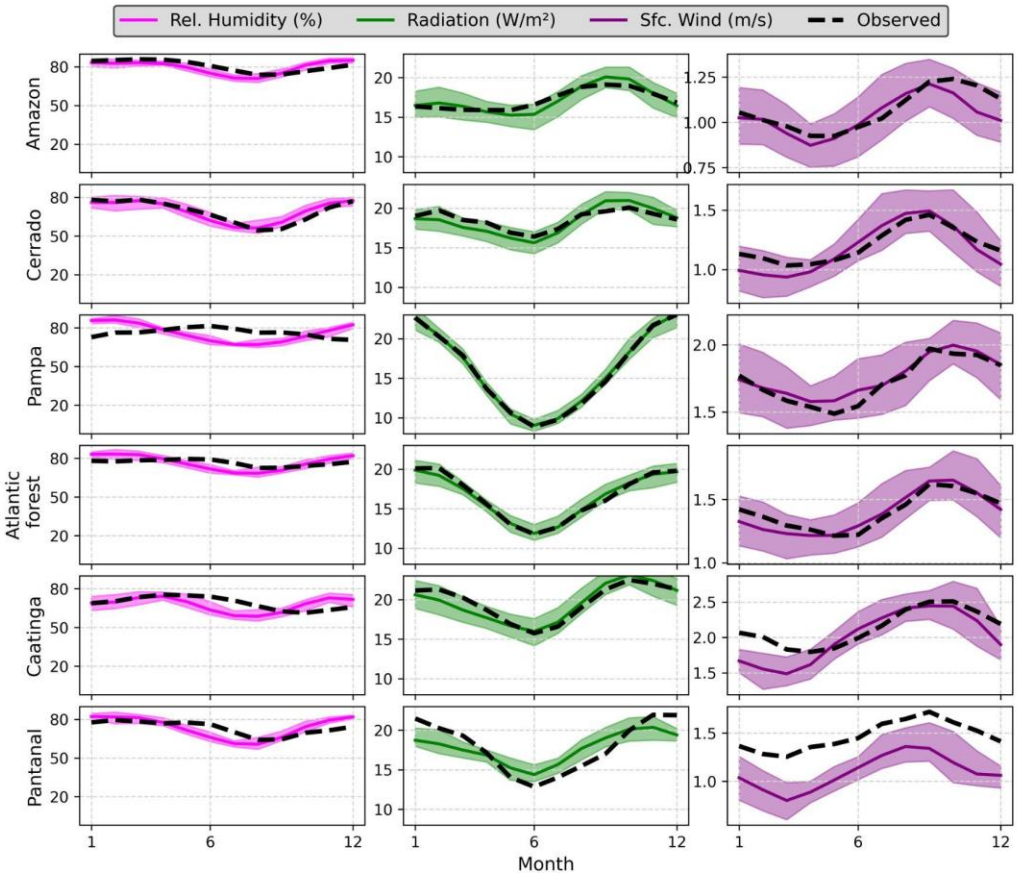

Figure S2. 2. Long-term (1980-2013) monthly mean of relative humidity, solar net radiation, and near-surface wind speed. Highlighted lines represent the intra-annual cycle simulated by the bias-corrected 10 CMIP6-GCMs' *multi-model ensemble*. Dashed lines indicate the observed mean intra-annual cycle. Confidence intervals represent the maximum and minimum values simulated by the bias-corrected 10 CMIP6-GCMs.

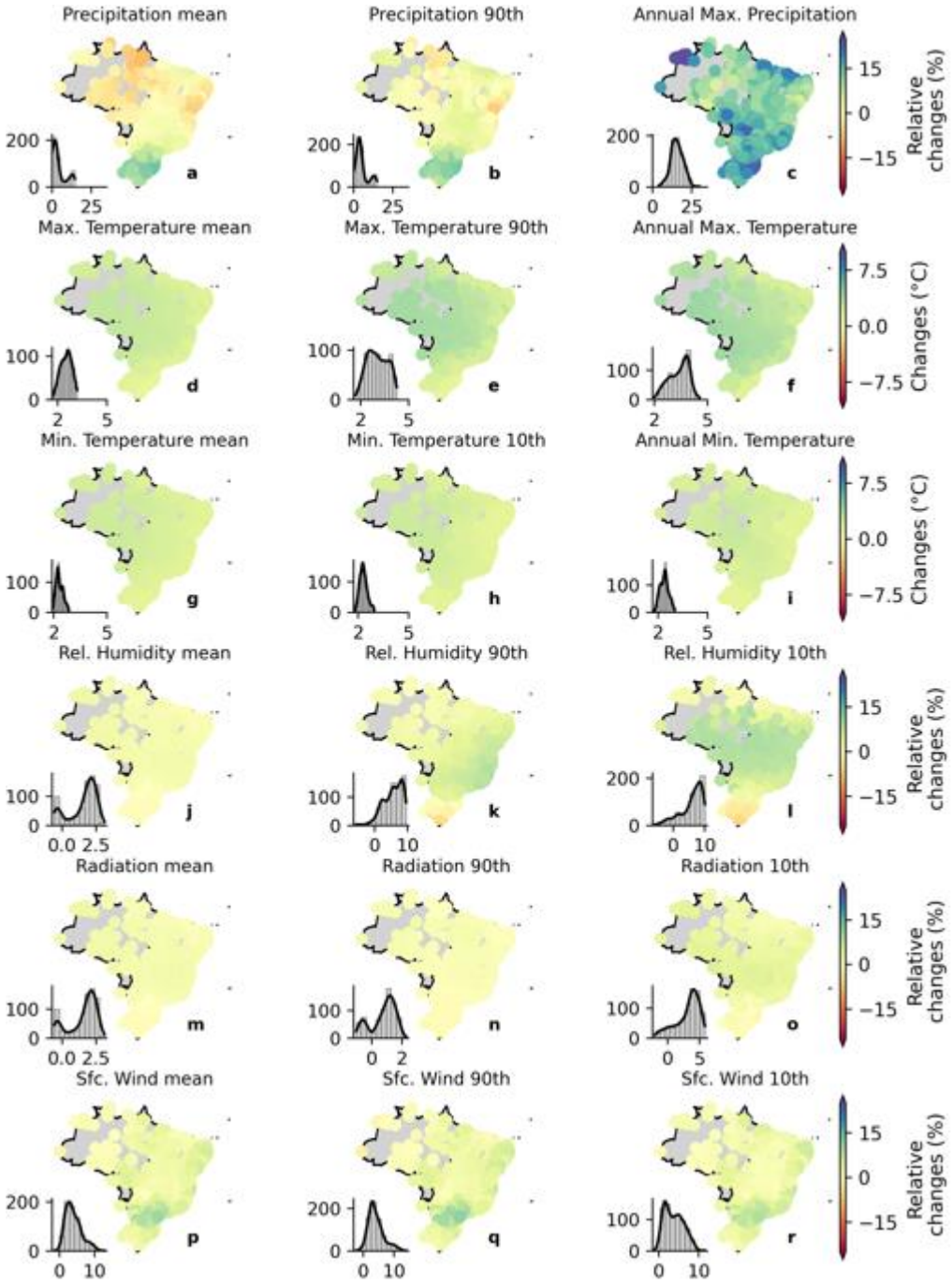

Figure S3. Relative changes in the long-term mean and extreme values of precipitation, maximum and minimum temperature, net shortwave solar radiation, relative humidity, and near-surface wind speed between the historical (1980-2013) and distant future (2070-2100; SSP2-4.5) periods (raw catchment-scale dataset). Histograms in each panel indicate the frequency of occurrence of relative changes.

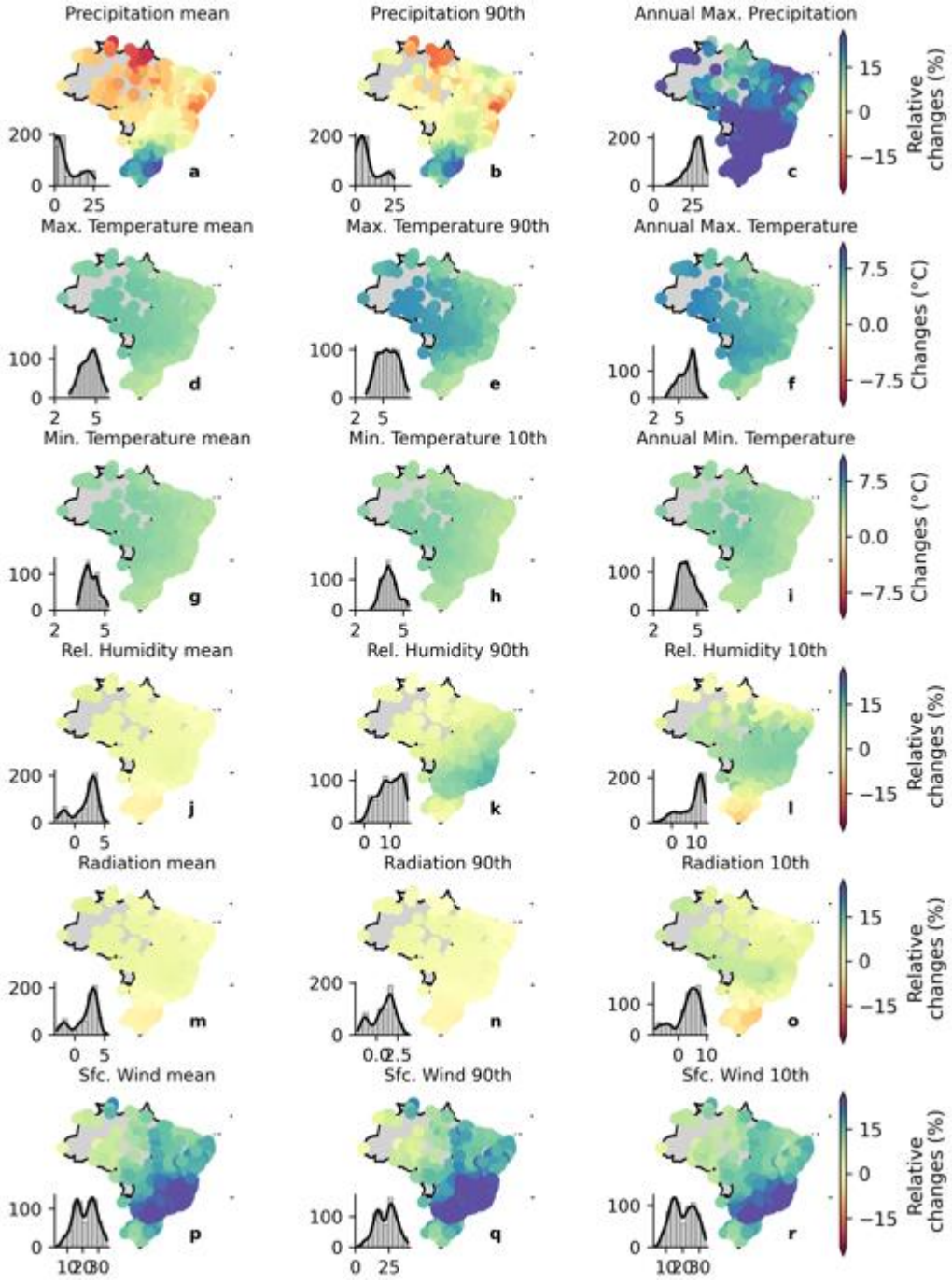

Figure S4. Relative changes in the long-term mean and extreme values of precipitation, maximum and minimum temperature, net shortwave solar radiation, relative humidity, and near-surface wind speed between the historical (1980-2013) and distant future (2070-2100; SSP5-8.5) periods (raw catchment-scale dataset). Histograms in each panel indicate the frequency of occurrence of relative changes.

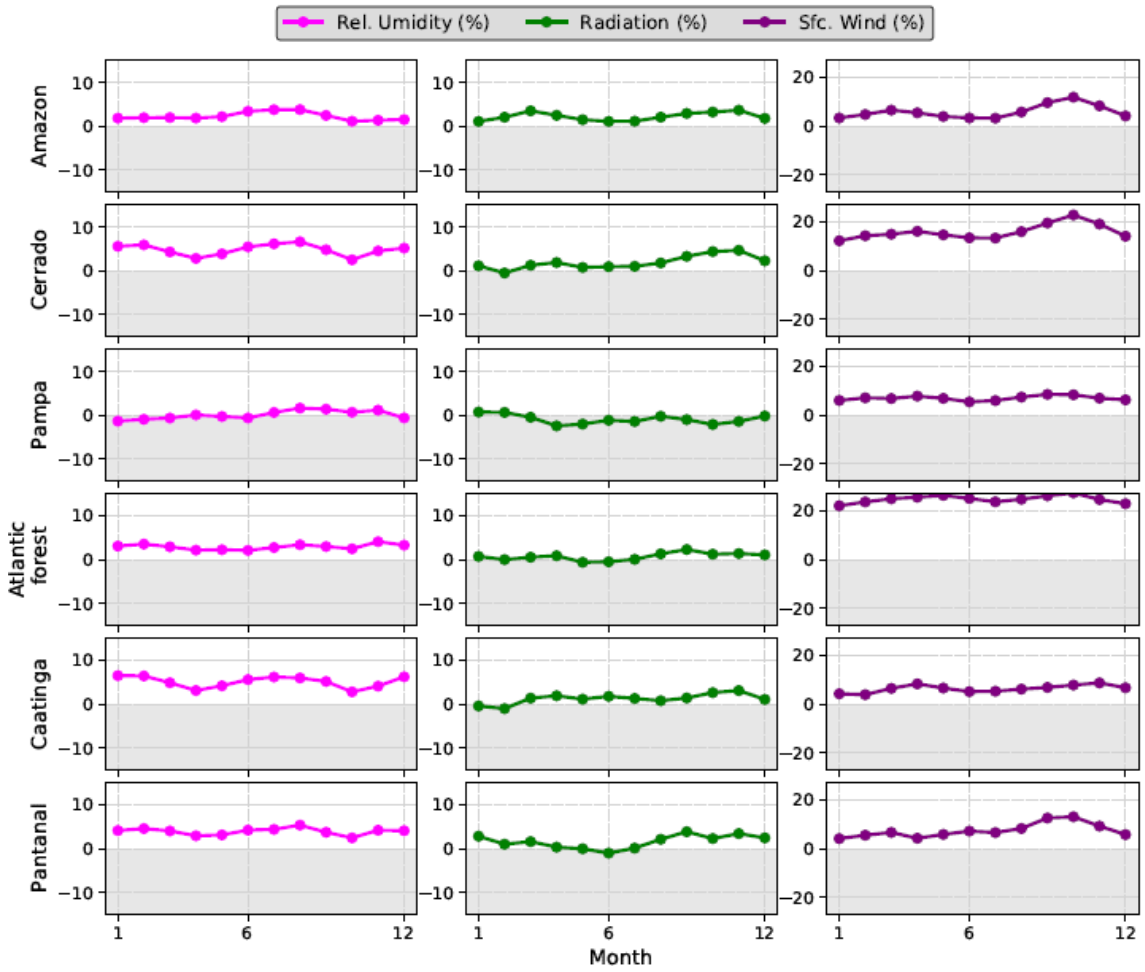

Figure S5. Relative changes between the historical (1980-2013) and distant future (2070-2100, SSP5-8.5) periods in the long-term mean intra-annual cycles relative humidity, solar net radiation, and near-surface wind speed, separated by biomes. Highlighted lines represent the changes in the intra-annual cycle simulated by the bias-corrected 10 CMIP6-GCMs' *multi-model ensemble*.

APPENDIX B

Supporting Information - Chapter 3

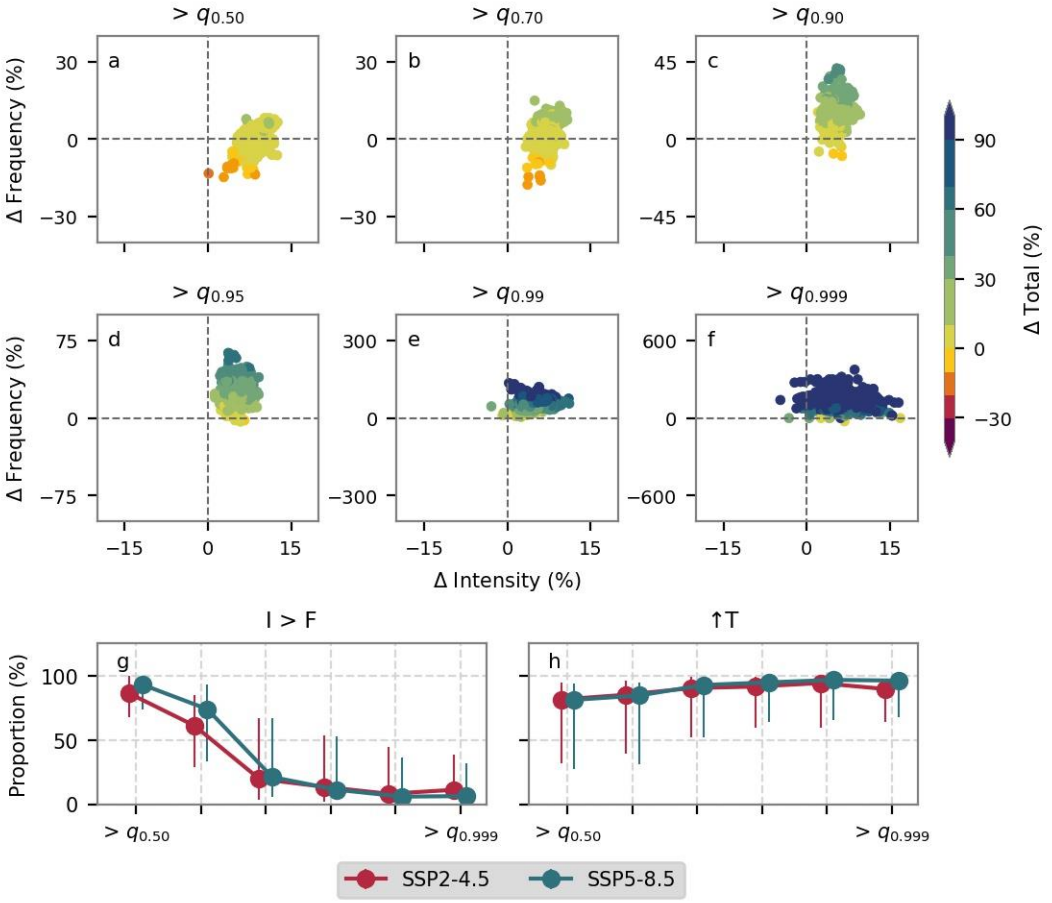

Figure S3. 1. a-f, Relative changes (CMIP6 multi-model ensemble median) between historical (1980-2010) and distant future (2070-2100; SSP2-4.5) periods in frequency, intensity and total rainfall for different quantile-thresholds obtained for the 735 catchments. Changes in frequency, intensity and total rainfall were computed for CMIP6 GCMs individually and we display the CMIP6 multi-model ensemble median of these changes. (a) $> q_{0.50}$, (b), $> q_{0.70}$, (c) $> q_{0.90}$, (d) $> q_{0.95}$, (e) $> q_{0.99}$, and (f) $> q_{0.999}$. Black, dashed lines divides the quadrants(g) Proportion of catchments were the relative change in intensity was larger than the relative changes in frequency for each quantile-thresholds intervals considering both SSP2-4.5 and SSP5-8.5 scenarios. (h) Proportions of catchments with positive relative changes in total rainfall for each quantile-thresholds intervals considering both SSP2-4.5 and SSP5-8.5 scenarios. The central points (bars) indicate the median (95% confidence intervals) proportion obtained using the 19 CMIP6 climate models.

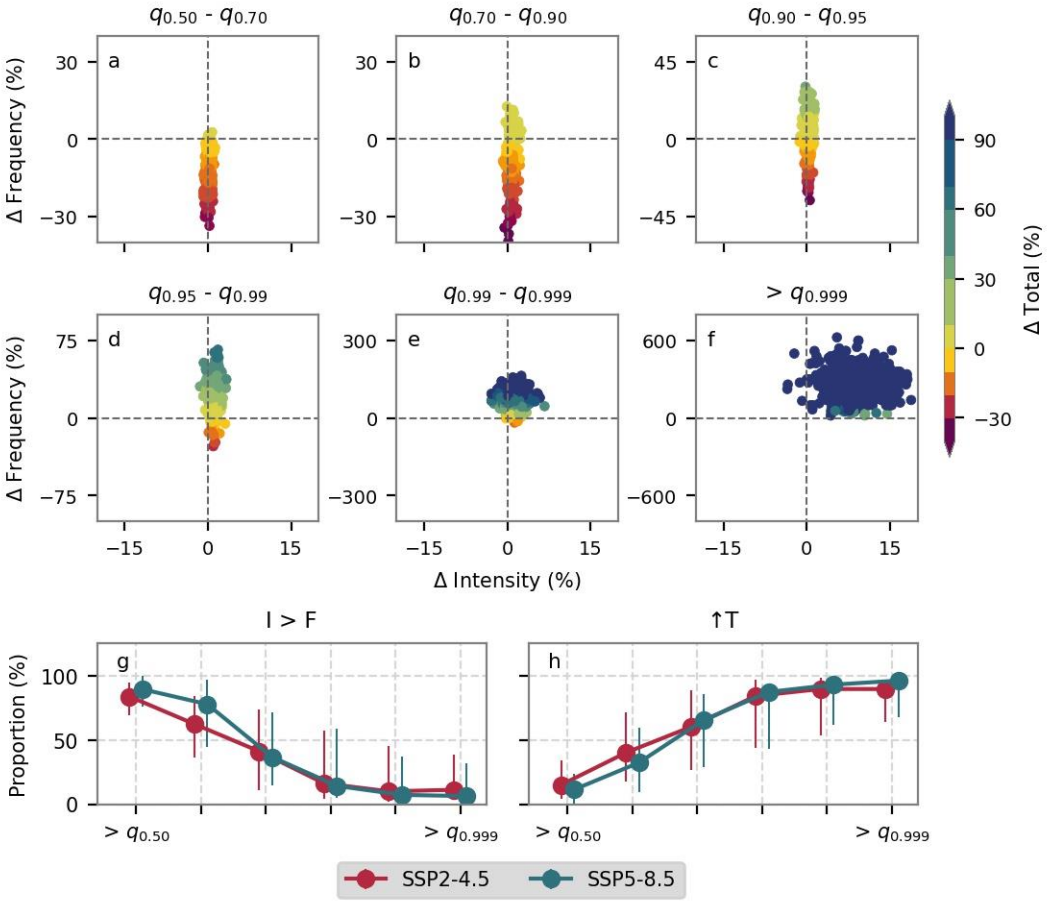

Figure S3. 2. a-f, Relative changes (CMIP6 multi-model ensemble median) between historical (1980-2010) and distant future (2070-2100; SSP5-8.5) periods in frequency, intensity and total rainfall for different quantile-intervals obtained for the 735 catchments. Changes in frequency, intensity and total rainfall were computed for CMIP6 GCMs individually and we display the CMIP6 multi-model ensemble median of these changes. (a) $q_{0.50}$ - $q_{0.70}$, (b) $q_{0.70}$ - $q_{0.90}$, (c) $q_{0.90}$ - $q_{0.95}$, (d) $q_{0.95}$ - $q_{0.99}$, (e) $q_{0.99}$ - $q_{0.999}$, and (f) $> q_{0.999}$. Black, dashed lines divides the quadrants(g) Proportion of catchments were the relative change in intensity was larger than the relative changes in frequency for each quantile-thresholds intervals considering both SSP2-4.5 and SSP5-8.5 scenarios. (h) Proportions of catchments with positive relative changes in total rainfall for each quantile-thresholds intervals considering both SSP2-4.5 and SSP5-8.5 scenarios. The central points (bars) indicate the median (95% confidence intervals) proportion obtained using the 19 CMIP6 climate models.

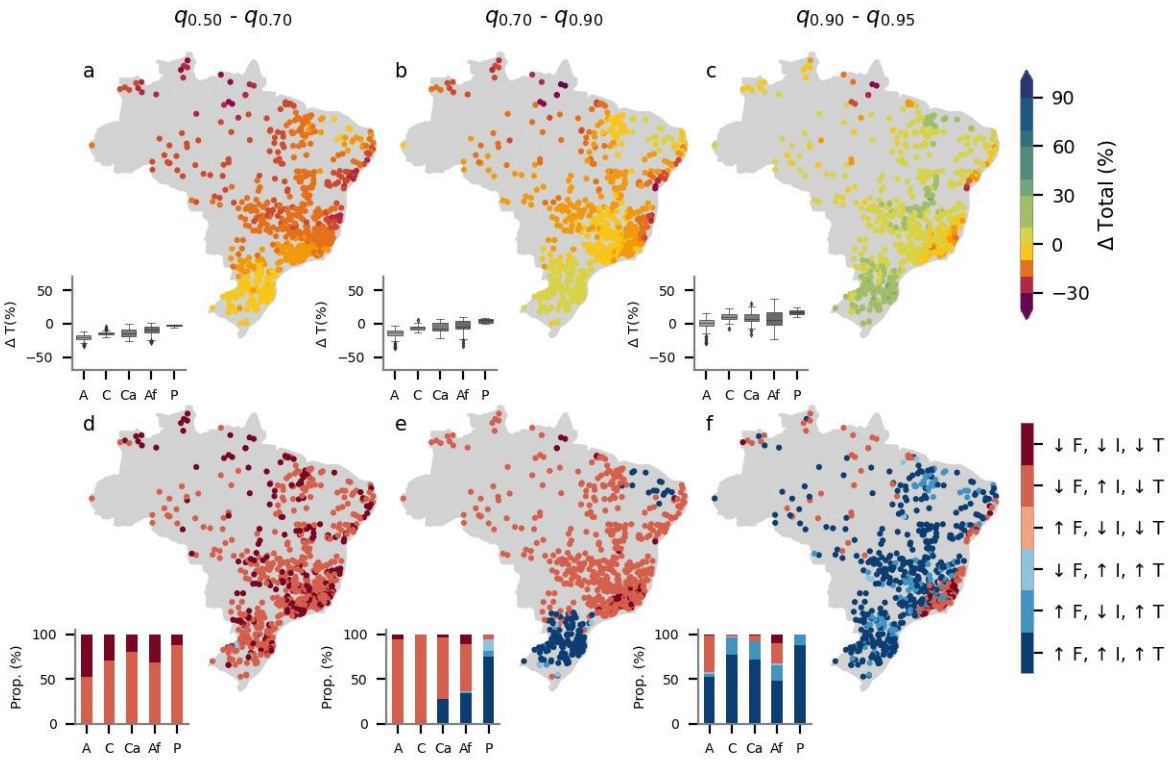

Figure S3. 3, a-c, Spatial distribution of the relative changes (CMIP6 multi-model ensemble median) between historical (1980-2010) and distant future (2070-2100; SSP5-8.5) periods in total rainfall for different quantile-intervals. (a) $q_{0.50}$ - $q_{0.70}$, (b) $q_{0.70}$ - $q_{0.90}$, (c) $q_{0.90}$ - $q_{0.95}$.. Changes in frequency, intensity and total rainfall were computed for CMIP6 GCMs individually and we display the CMIP6 multi-model ensemble median of these changes. Changes per Brazilian biome are displayed in traditional boxplots (A: Amazon, C: Cerrado, Ca: Caatinga, Af: Atlantic Forest, and P: Pampa). d-f. Catchments classified according to their condition in terms of relative changes in frequency, intensity and total rainfall for different quantile-intervals: (d) $q_{0.50}$ - $q_{0.70}$, (e) $q_{0.70}$ - $q_{0.90}$, (f) $q_{0.90}$ - $q_{0.95}$.

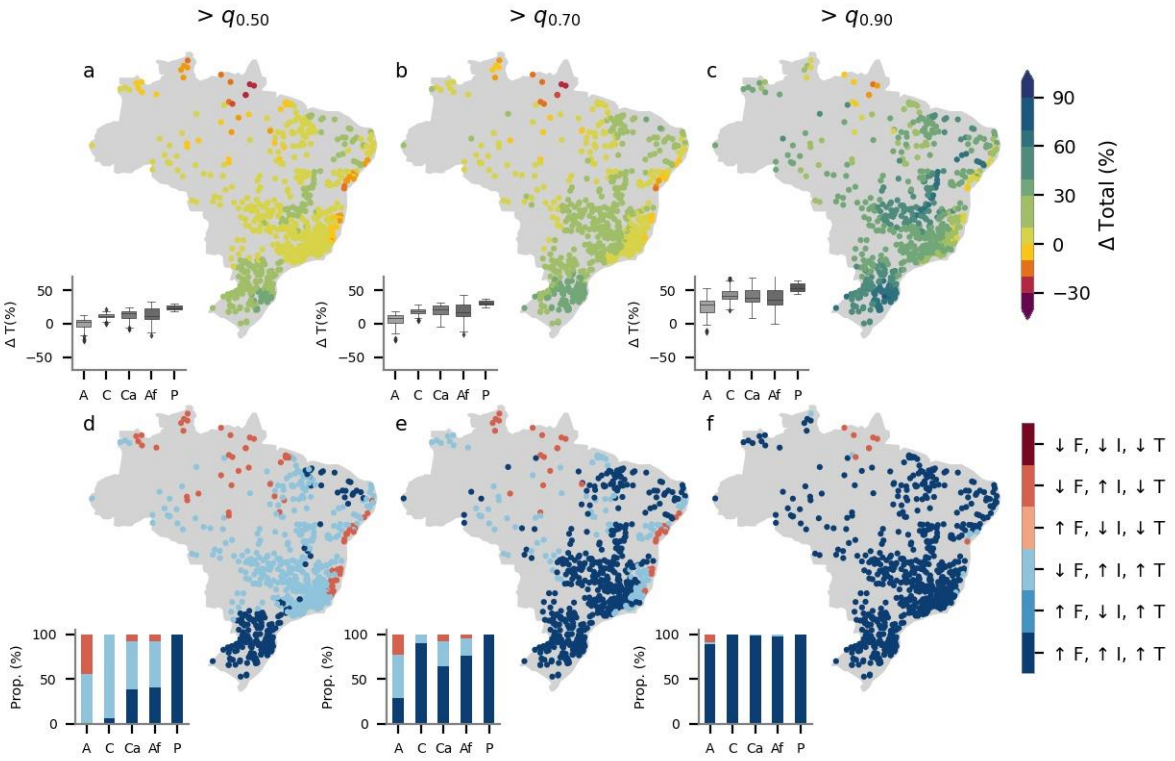

Figure S3. 4. a-c, Spatial distribution of the relative changes (CMIP6 multi-model ensemble median) between historical (1980-2010) and distant future (2070-2100; SSP5-8.5) periods in total rainfall for different quantile-thresholds. (a) > $q_{0.50}$, (b) > $q_{0.70}$, (c) > $q_{0.90}$. Changes in frequency, intensity and total rainfall were computed for CMIP6 GCMs individually and we display the CMIP6 multi-model ensemble median of these changes. Changes per Brazilian biome are displayed in traditional boxplots (A: Amazon, C: Cerrado, Ca: Caatinga, Af: Atlantic Forest, and P: Pampa). d-f. Catchments classified according to their condition in terms of relative changes in frequency, intensity and total rainfall for different quantile thresholds: (d) > $q_{0.50}$, (e) > $q_{0.70}$, (f) > $q_{0.90}$.

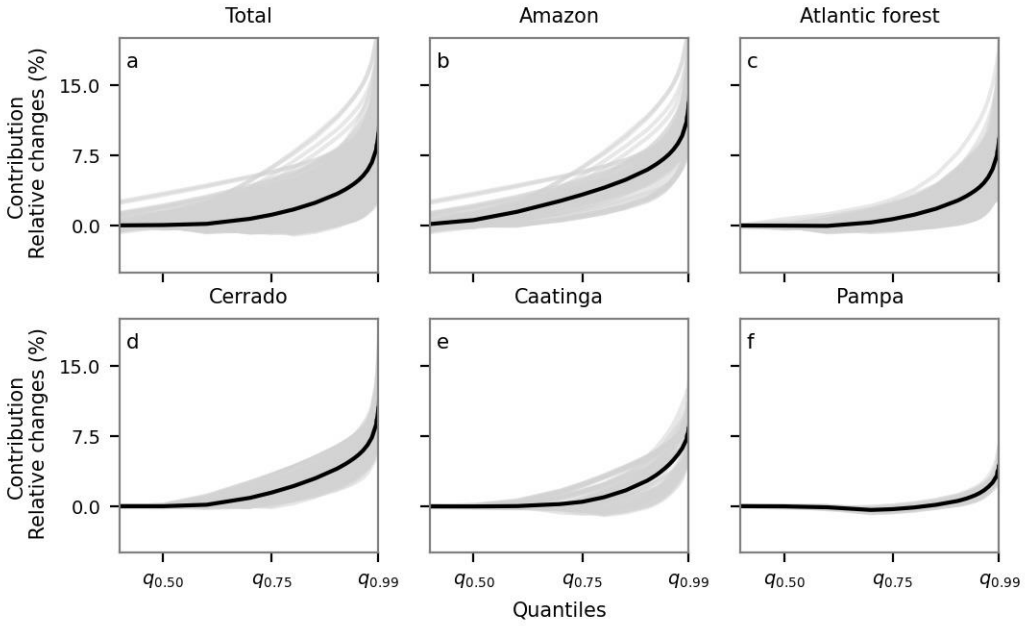

Figure S3. 5. Projected changes on the uneven distribution of rainfall events on Brazilian biomes between historical (1980-2010) and distant future (2070-2100; SSP5-8.5). Light gray lines represents the changes in rainfall contribution according to the CMIP6 multi-model ensemble median for each catchment. Black line represents the mean projected changes for each biome, considering all catchments within the biome. Rainfall contribution is computed as the fraction of rainfall surpassing a specific quantile q over the total rainfall accumulated in the period. A change of 10% on $q_{0.99}$ indicates that, in the future, rainfall events larger than the future 99-percentile are expected to contribute 10% more to the accumulated rainfall in comparison with the historical period. Since we are interested in assessing the uneven changes of the distribution of rainfall events, we didn't consider the historical period as a reference to compute the thresholds. See Pendergrass & Knutti (2018) for a detailed description.

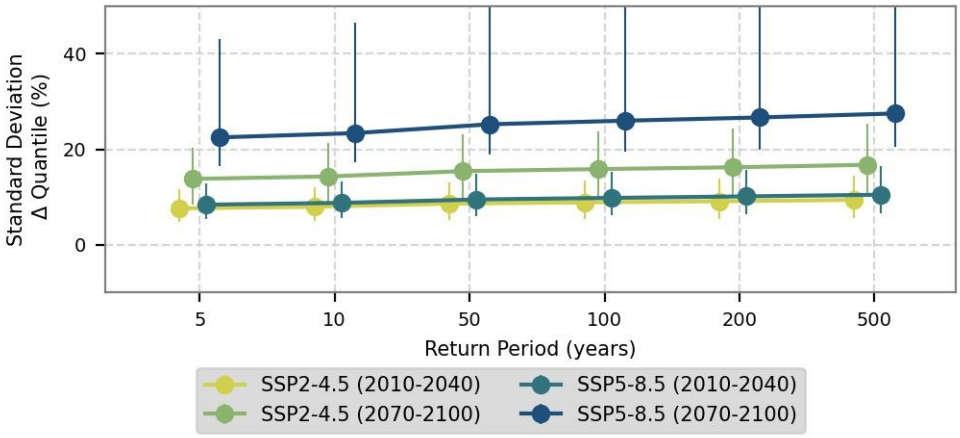

Figure S3. 6. Standard deviation of the relative changes projected by CMIP6 models using the SMEV distribution. The central points (bars) indicate the median (95% confidence intervals) standard deviation of the projected changes obtained for the 735 Brazilian catchments.

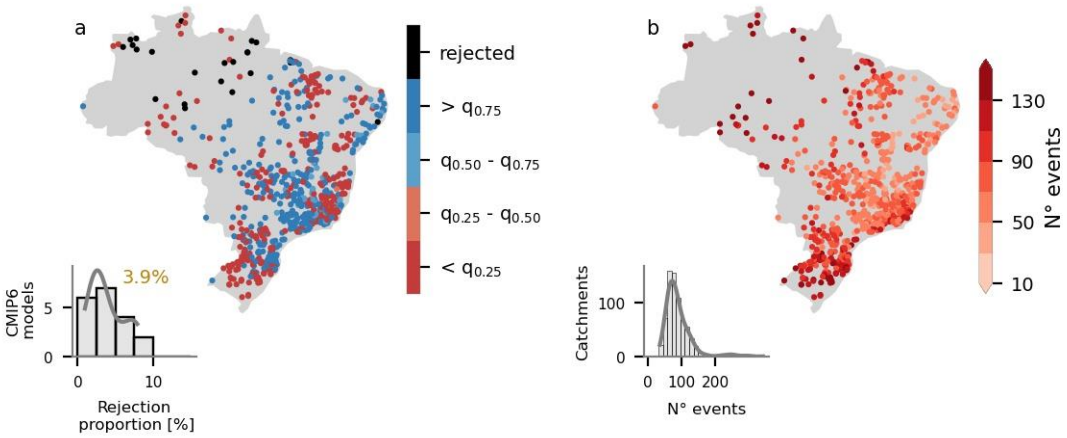

Figure S3. 7. Suitability of the Weibull distribution to represent Brazilian catchments' rainfall in the future (2070-2100; SSP5-8.5) period. a, left censoring threshold θ (quantile-based) used to define the Weibull tails. Catchments were the assumption of the Weibull tail was rejected are colored in black. The histogram exhibits the rejection proportion obtained for the 19-CMIP6 climate models simulations. Average rejection proportion is displayed in yellow. b, Average yearly number of wet-days in the tail as defined by the left-censoring threshold.

APPENDIX C

Supporting Information - Chapter 4

Text S4 - Short-term, event-based assessment

The short-term, event based analysis proceed as follows: first, we define the time frame characterizing a specific drought event. This time frame begins 6 months prior to the onset of the drought event (as we are using 6-month accumulations) and concludes simultaneously with the drought's end. Considering this drought time frame, we compute the number of wet days (N_w; $P > 1$ mm), (b) average precipitation of wet days (P_{mean}), (c) average potential evapotranspiration (PET_{mean}), and (d) the number of days when P surpasses PET (N_{wb}). We repeat this process for each drought event present in the 30-year evaluated long-term period (historical or future), and further computed the long-term averaged N_w, P_{mean}, and PET_{mean}. In sequence, we computed how these three properties are expected to change by computing the relative changes between historical and future periods (ΔN_w, ΔN_{wb}, ΔP_{mean}, and ΔPET_{mean}). Finally, we assess the relationship between the changes in drought properties and the changes in P and PET characteristics. A schematic representation of the proposed framework is displayed in Figure S. We repeat these steps for each Brazilian catchment and evaluate the results using a long-term averaged perspective.

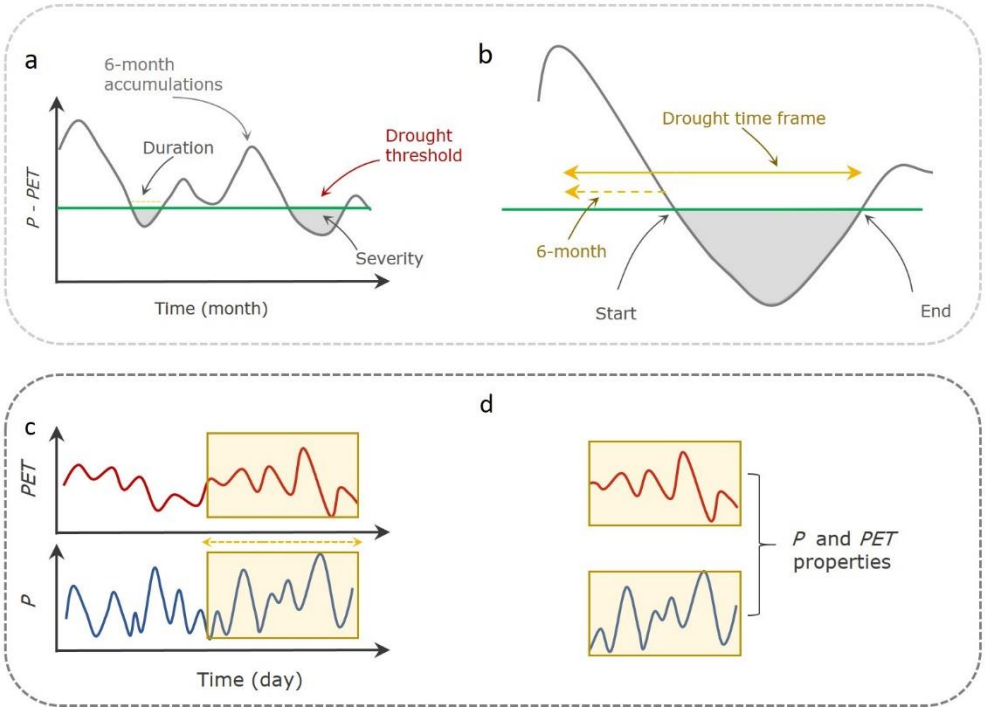

Figure S4. 1. Schematic representation of the framework proposed to assess meteorological properties using an event-based perspective. (a) 6-month P − PET accumulation time series. A green line defines the drought threshold (15-percentile). Drought events are highlighted in light gray along with their properties (intensity and duration). (b) Details of a specific drought event, indicating the start and end of it. The drought time frame is indicated in yellow, and is computed as the duration of the drought event plus 6 months. This time frame corresponds to the time window used to identify the drought event according to the Ukkola et al. (2020) framework. (c) P and PET daily time series in red and blue, respectively. Drought time frame is represented by the yellow window. (d) P and PET daily timeseries sample used to compute the meteorological properties associated to the specific drought event displayed in panel b.

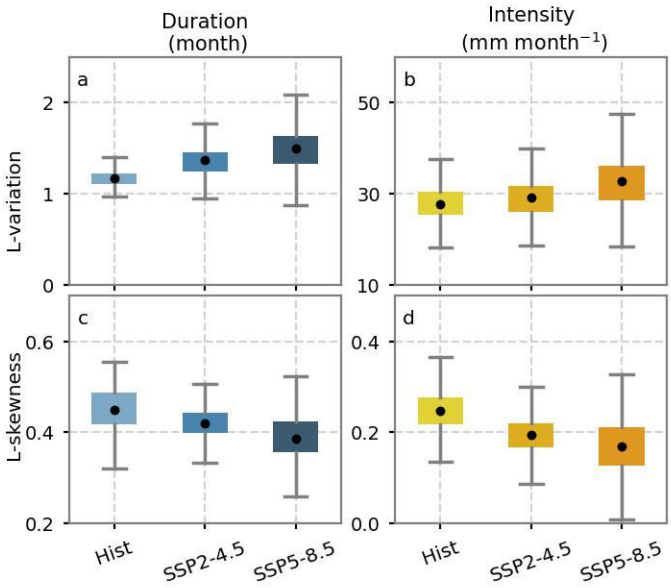

Figure S4. 2. Projected changes in 30-year, long-term L-variation and L-skewness of drought's (a, c) duration and (b, d) Intensity between historical (Hist; 1980-2010) and distant future (SSP2-4.5 and SSP5-8.5; 2070-2100) periods in Brazil. Box plots represent the CMIP6 multi-model ensemble median observed for the 735 Brazilian catchments. Only catchments with at least 10 drought events during Historical and Distant Future periods were considering for this analysis. Projected changes on drought properties are statistically significant according to the Mann Whitney U test and Monte Carlo resampling techniques (p-value < 0.05).

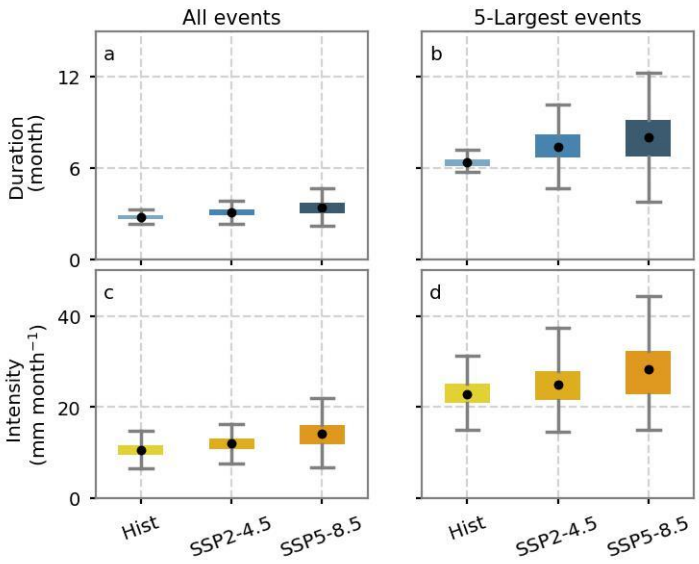

Figure S4. 3. Projected changes in 30-year, long-term averaged drought's (a, c) duration and (b, d) intensity (considering only the 5-largest values for each drought property separately) between historical (Hist; 1980-2010) and distant future (SSP2-4.5 and SSP5-8.5; 2070-2100) periods in Brazil. Box plots represent the CMIP6 multi-model ensemble median observed for the 735 Brazilian catchments. Projected changes on drought properties are statistically significant according to the Mann Whitney U test and Monte Carlo resampling techniques (p-value < 0.05).

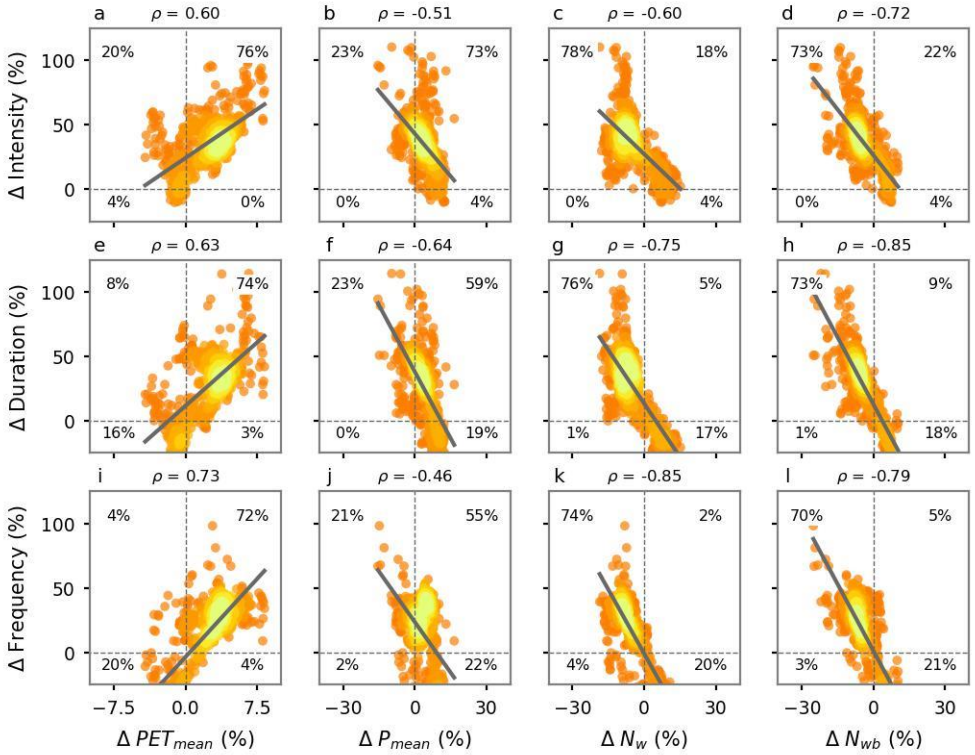

Figure S4. 4. Relationship between projected changes (SSP5-8.5; distant future) in drought properties (severity, duration, and frequency; from top to bottom) and long-term meteorological properties (PET_{mean}, P_{mean}, N_w, and N_{wb}; from left to right) for the Brazilian catchments. Pearson's correlation between projected changes is displayed on each subplot's top. Only significant correlations (p-value < 0.05) were considered. Black, dashed lines divide the quadrants. The regression line is displayed in black. The percentage of catchments (points) in each quadrant is indicated on the corners. For all plots, light colour regions indicate high density.

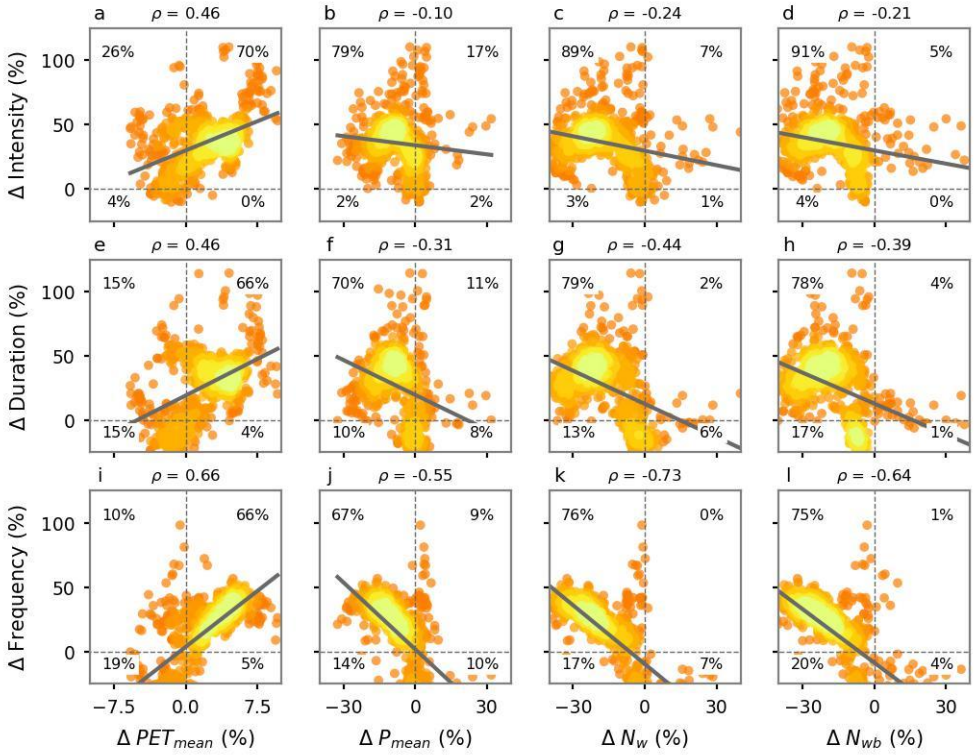

Figure S4. 5. Relationship between projected changes (SSP5-8.5; distant future) in drought properties (severity, duration, and frequency; from top to bottom) and meteorological properties (PET_{mean}, P_{mean}, N_w, and N_{wb}; from left to right) on drought-triggering periods for the Brazilian catchments. Pearson's correlation between projected changes is displayed on each subplot's top. Only significant correlations (p-value < 0.05) were considered. Black, dashed lines divide the quadrants. The regression line is displayed in black. The percentage of catchments (points) in each quadrant is indicated on the corners. For all plots, light colour regions indicate high density.

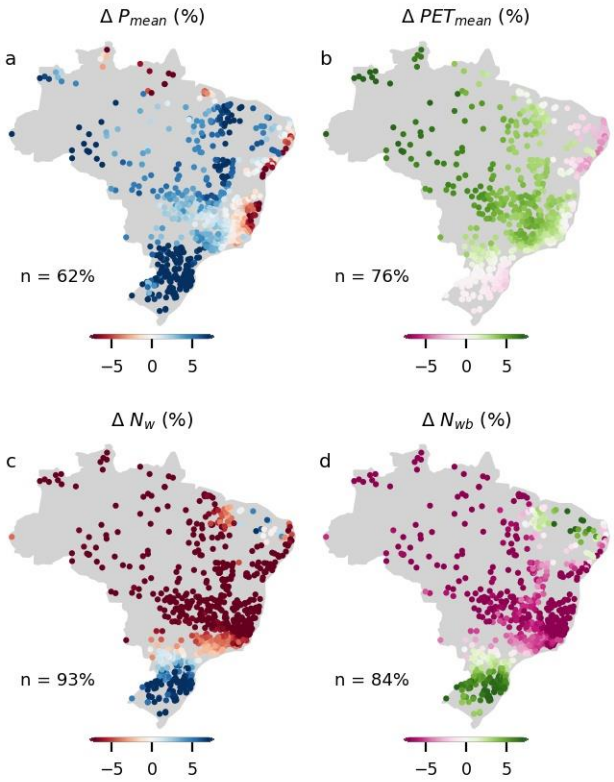

Figure S4. 6. Spatial distribution of relative changes in long-term (a) P_{mean}, (b) PET_{mean}, (c) N_w, and (d) N_{wb} for the 735 Brazilian catchments. Changes were computed considering the historical (1980-2010) and SSP5-8.5 distant future (2070-2100). n in the bottom-left corner of each map indicates the percentage of catchments with at least 70% of CMIP6 model agreement (signal of change).

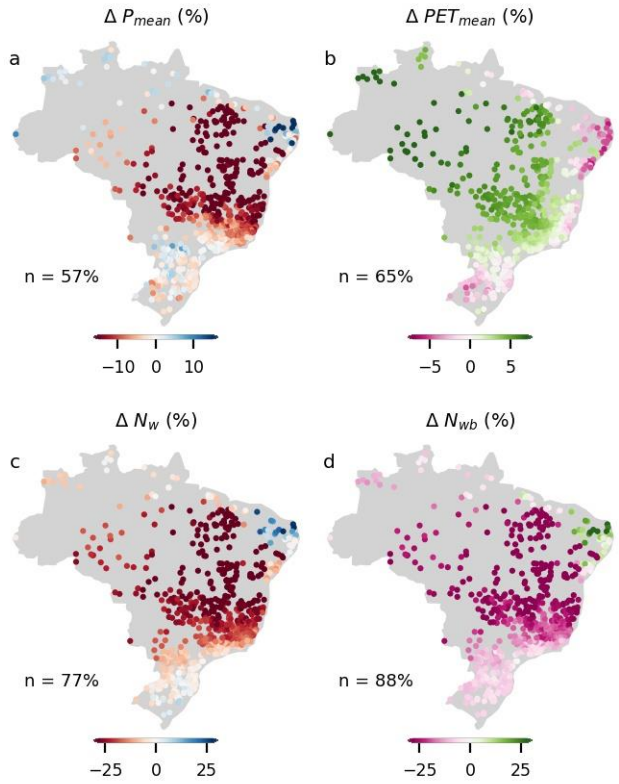

Figure S4. 7. Spatial distribution of relative changes in (a) P_{mean}, (b) PET_{mean}, (c) N_w, and (d) N_{wb} for the 735 Brazilian catchments in short-term, drought-triggering periods. Changes were computed considering the historical (1980-2010) and SSP5-8.5 distant future (2070-2100). n in the bottom-left corner of each map indicates the percentage of catchments with at least 70% of CMIP6 model agreement (signal of change).

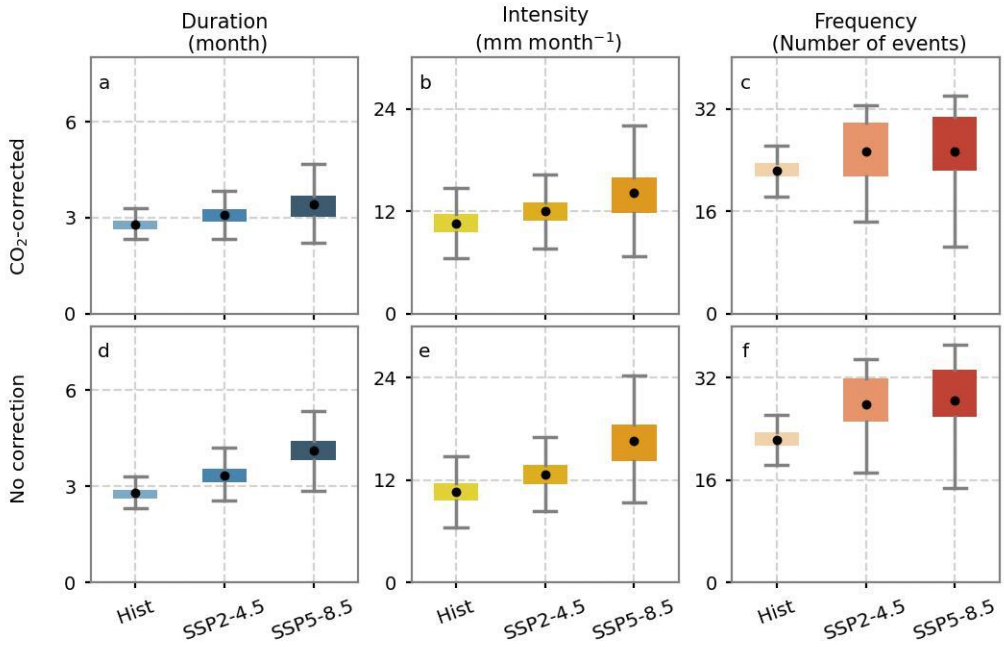

Figure S4. 8. Projected changes in 30-year, long-term averaged drought's (a, d) duration, (b, e) intensity, and (c, f) frequency between historical (Hist; 1980-2010) and distant future (SSP2-4.5 and SSP5-8.5; 2070-2100) periods in Brazil. Box plots represent the CMIP6 multi-model ensemble median observed for the 735 Brazilian catchments. Projected changes were computed using the (a-c) CO_2-corrected *PET* formulation proposed by Yang et al. (2019) and the (d-f) reference crop Penman-Monteith equation.

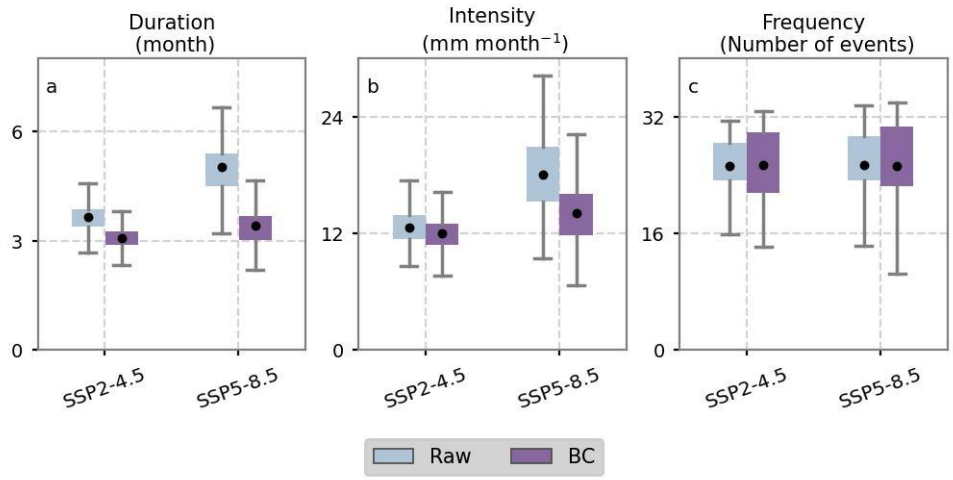

Figure S4. 9. Projected changes in 30-year, long-term averaged drought's (a) duration, (b) intensity, and (c) frequency between historical (Hist; 1980-2010) and distant future (SSP2-4.5 and SSP5-8.5; 2070-2100) periods in Brazil using CMIP6 raw and bias corrected (BC) simulations. Box plots represent the CMIP6 multi-model ensemble median observed for the 735 Brazilian catchments.

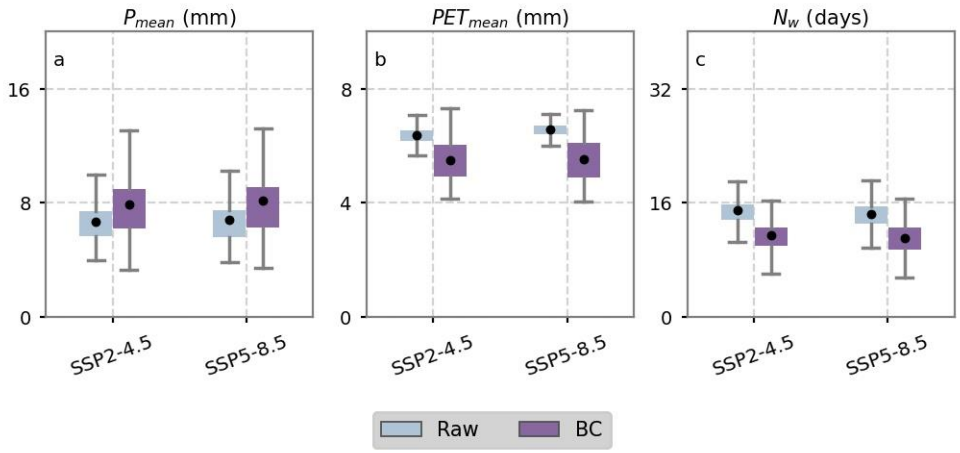

Figure S4. 10. Projected changes in 30-year, long-term averaged climate properties (a) P_{mean}, (b) PET_{mean}, and (c) N_w between historical (Hist; 1980-2010) and distant future (SSP2-4.5 and SSP5-8.5; 2070-2100) periods in Brazil using CMIP6 raw and bias corrected (BC) simulations. Box plots represent the CMIP6 multi-model ensemble median observed for the 735 Brazilian catchments.

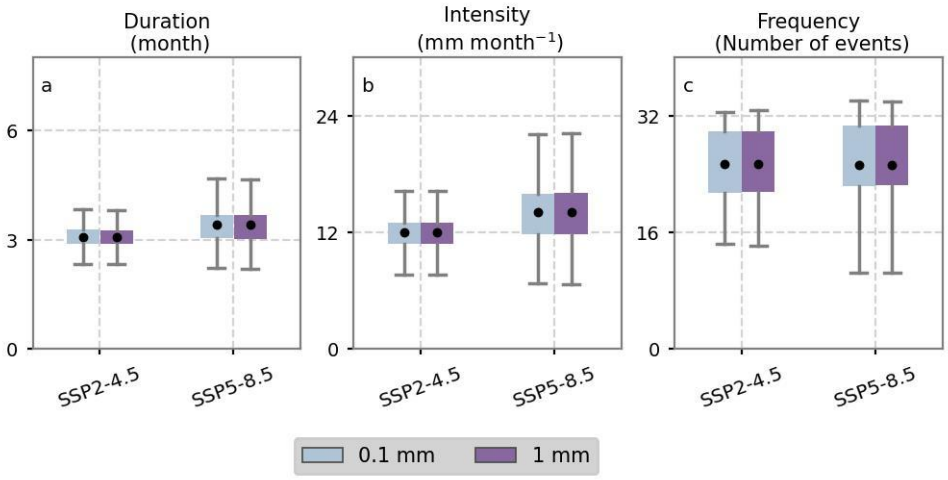

Figure S4. 11. Projected changes in 30-year, long-term averaged drought's (a) duration, (b) intensity, and (c) frequency between historical (Hist; 1980-2010) and distant future (SSP2-4.5 and SSP5-8.5; 2070-2100) periods in Brazil using 0.1 mm and 1 mm as wet thresholds. Box plots represent the CMIP6 multi-model ensemble median observed for the 735 Brazilian catchments.

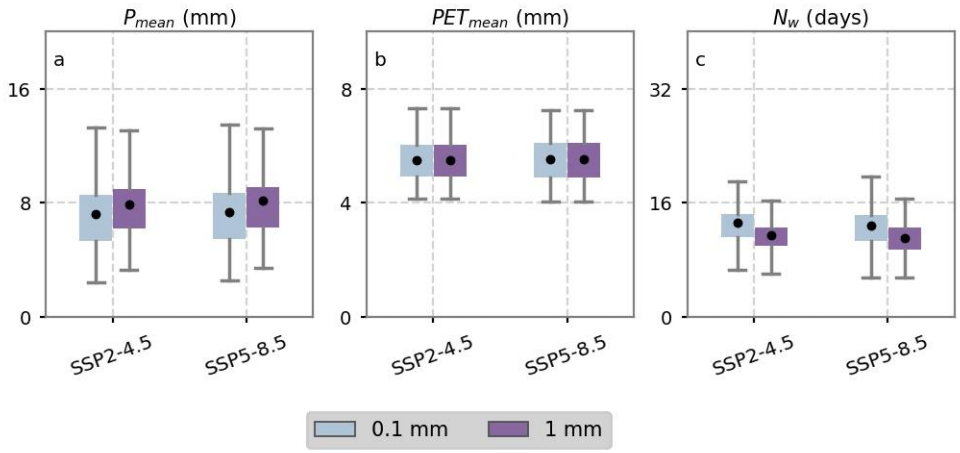

Figure S4. 12. Projected changes in 30-year, long-term averaged climate properties (a) P_{mean}, (b) PET_{mean}, and (c) N_w between historical (Hist; 1980-2010) and distant future (SSP2-4.5 and SSP5-8.5; 2070-2100) periods in Brazil using 0.1 mm and 1 mm as wet thresholds. Box plots represent the CMIP6 multi-model ensemble median observed for the 735 Brazilian catchments.

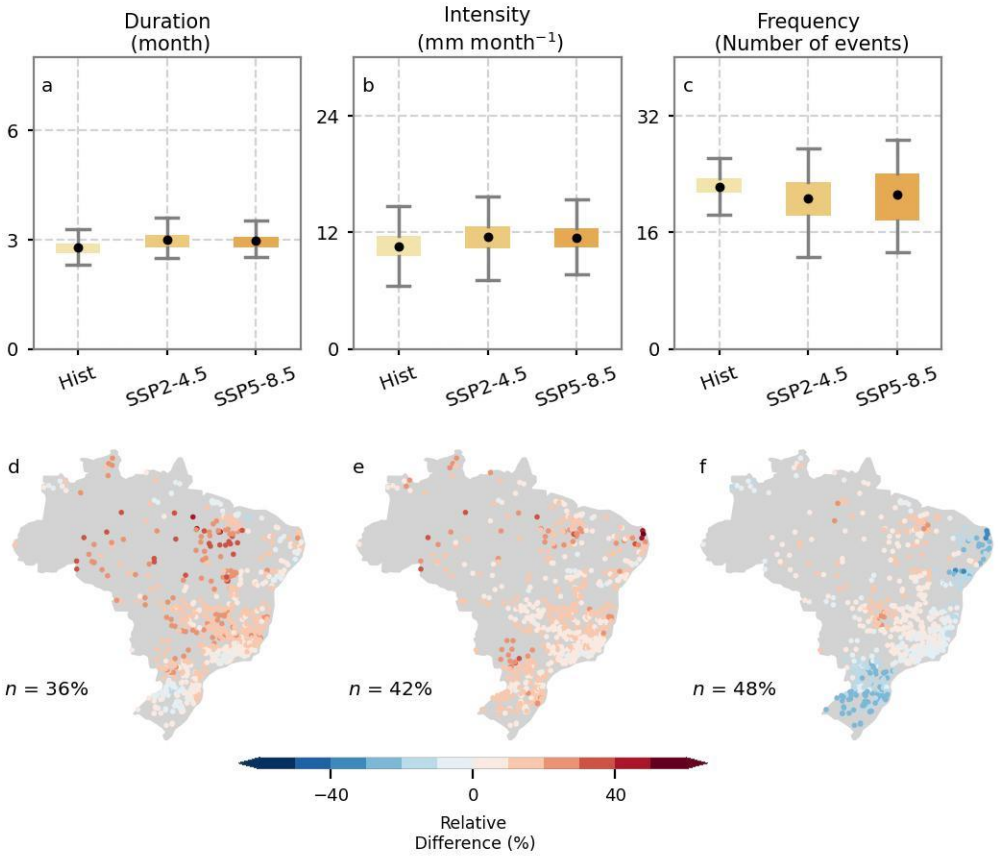

Figure S4. 13. Projected changes in 30-year, long-term averaged drought's (a, d) duration, (b, e) intensity, and (c,f) frequency between historical (Hist; 1980-2010) and immediate future (SSP2-4.5 and SSP5-8.5; 2010-2040) periods in Brazil. Box plots represent the CMIP6 multi-model ensemble median observed for the 735 Brazilian catchments. Spatial distribution of changes (d-f) was computed considering the historical and SSP5-8.5 immediate future. n in the bottom-left corner of each map indicates the percentage of catchments with at least 70% of CMIP6 model agreement (signal of change). Projected changes on drought properties for Brazil are statistically significant according to the Mann Whitney U test and Monte Carlo resampling techniques (p-value < 0.05).

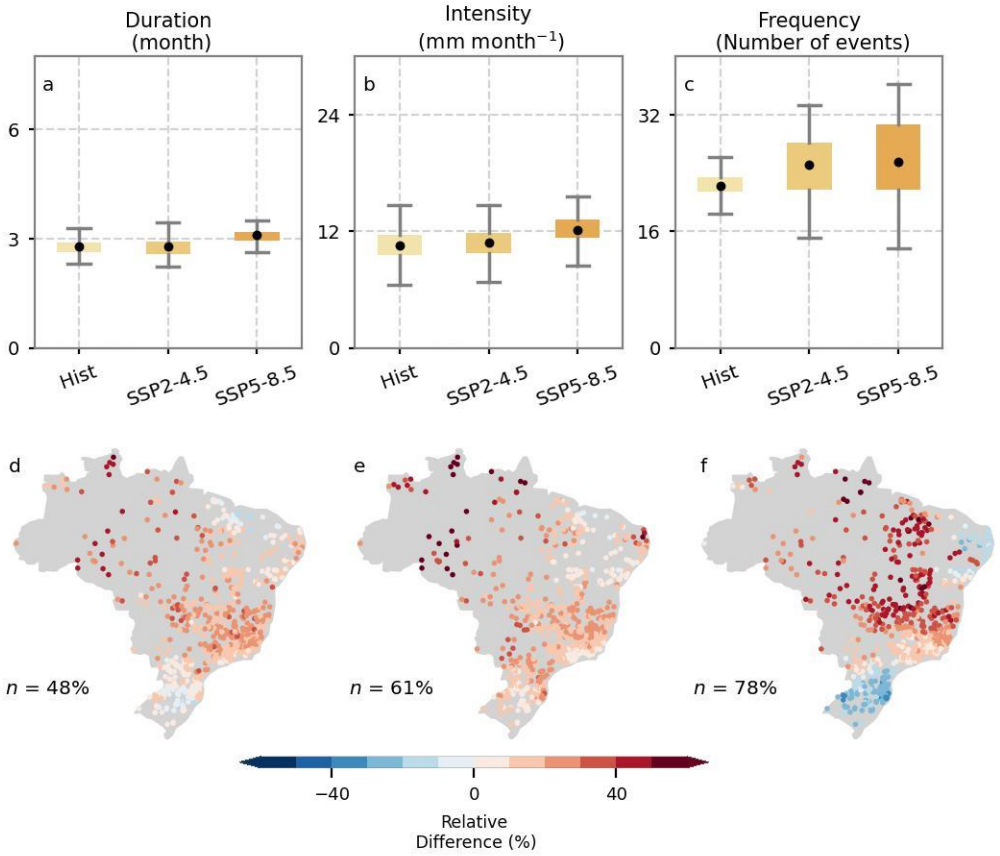

Figure S4. 14. Projected changes in 30-year, long-term averaged drought's (a, d) duration, (b, e) intensity, and (c,f) frequency between historical (Hist; 1980-2010) and intermediate future (SSP2-4.5 and SSP5-8.5; 2040-2070) periods in Brazil. Box plots represent the CMIP6 multi-model ensemble median observed for the 735 Brazilian catchments. Spatial distribution of changes (d-f) was computed considering the historical and SSP5-8.5 intermediate future. *n* in the bottom-left corner of each map indicates the percentage of catchments with at least 70% of CMIP6 model agreement (signal of change). Projected changes on drought properties for Brazil are statistically significant according to the Mann Whitney U test and Monte Carlo resampling techniques (p-value < 0.05).

APPENDIX D

Supporting Information - Chapter 5

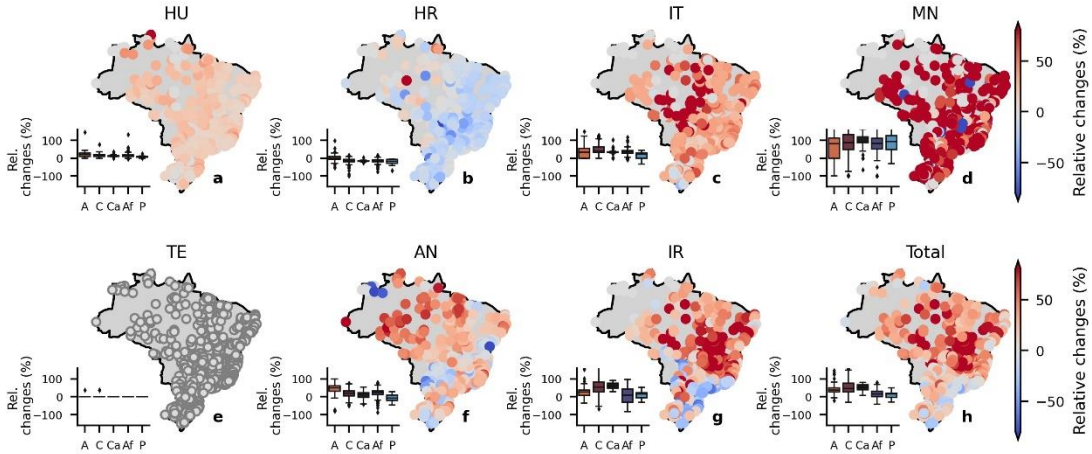

Figure S5. 1. Changes in Brazilian's water use (2020-2040). Relative changes (from 2020 to 2040) in Brazilian's water use as projected by ANA. The water uses are divided into 6 main categories: a, b, Households are subdivided into urban (HU) and rural areas (HR). c, Industry (IT). d, Mining (MN). e, Cooling water for thermal power plants (TE). f, Livestock (AN). g, Irrigation (IR). h, Total water use, computed as the sum of the 6 categories. Relative changes per Brazilian biome (A: Amazon, C: Cerrado, Ca: Caatinga, Af: Atlantic Forest, and P: Pampa) are displayed in traditional boxplots.

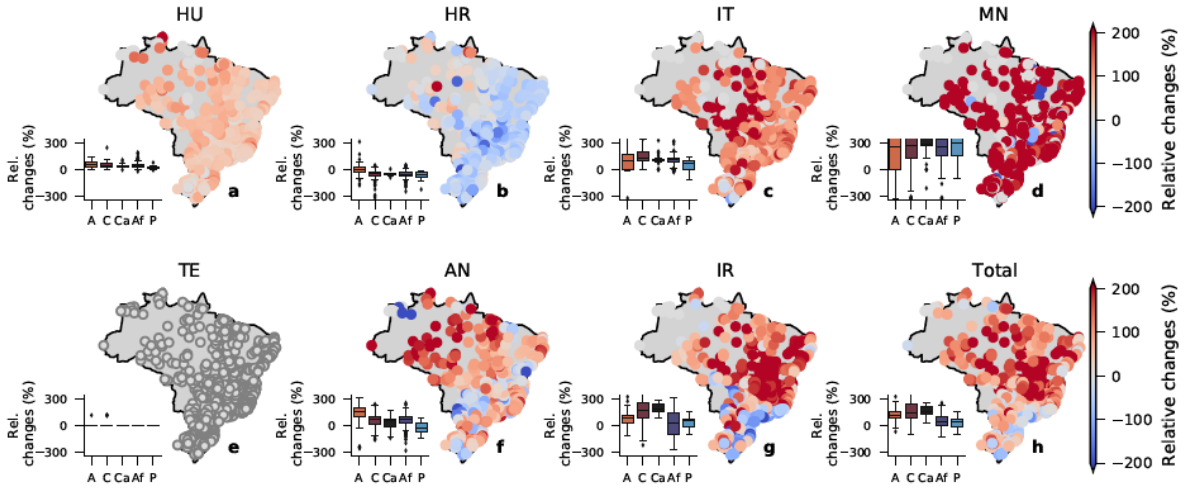

Figure S5. 2. Changes in Brazilian's water use (2020-2085). Relative changes (from 2020 to 2085) in Brazilian's water use as computed by the linear regression using ANA's projections. The water uses are divided into 6 main categories: a, b, Households are subdivided into urban (HU) and rural areas (HR). c, Industry (IT). d, Mining (MN). e, Cooling water for thermal power plants (TE). f, Livestock (AN). g, Irrigation (IR). h, Total water use, computed as the sum of the 6 categories. Relative changes per Brazilian biome (A: Amazon, C: Cerrado, Ca: Caatinga, Af: Atlantic Forest, and P: Pampa) are displayed in traditional boxplots.

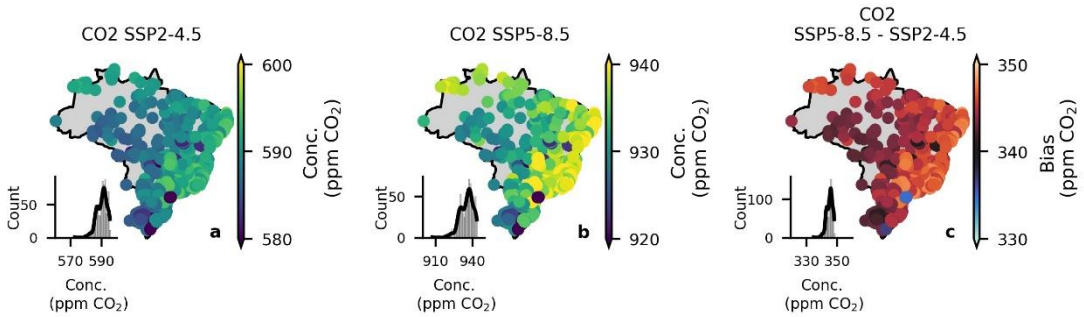

Figure S5. 3. Future CO_2 concentrations. a, long-term mean CO_2 concentration in the distant future (2070-2100) projected by the SSP2-4.5 scenario. b, same as a, but considering the SSP5-8.5 scenario. c, the difference between mean CO_2 concentrations projected by the SSP5-8.5 and SSP2-4.5 scenarios.

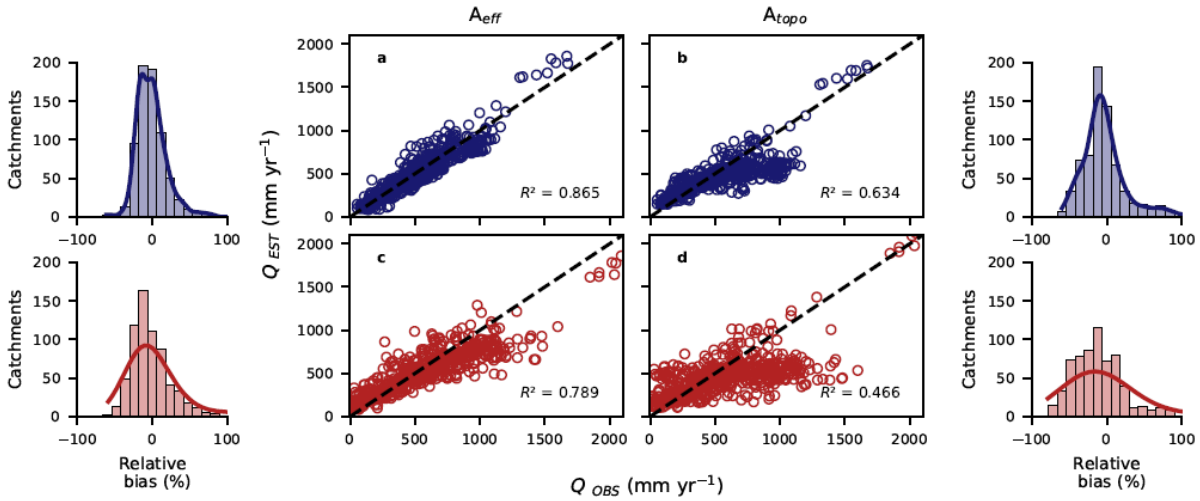

Figure S5. 4. Performance of functional forms. a. c, Details of the performance of the A_{eff}-corrected (open water balance assumption) functional forms to estimate observed water availability using bias-corrected and raw CMIP6-multimodel ensemble, respectively. b, d, Same as a and c, but using the no-correction (closed water balance assumption) functional forms. Histograms of the relative bias between estimated and observed water availability are displayed on the right (left) for the A_{eff}-corrected (no-correction) functional forms.

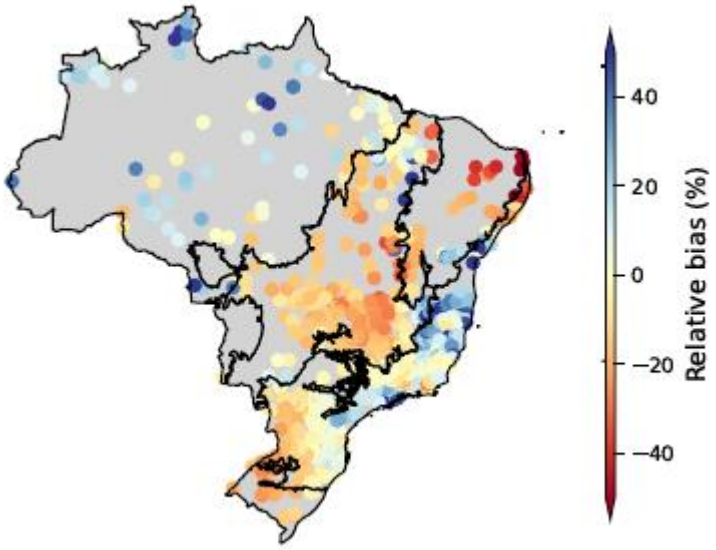

Figure S5. 5. Spatial distribution of the relative bias between observed and estimated water availability using the bias-corrected, A_{eff}-corrected functional forms.

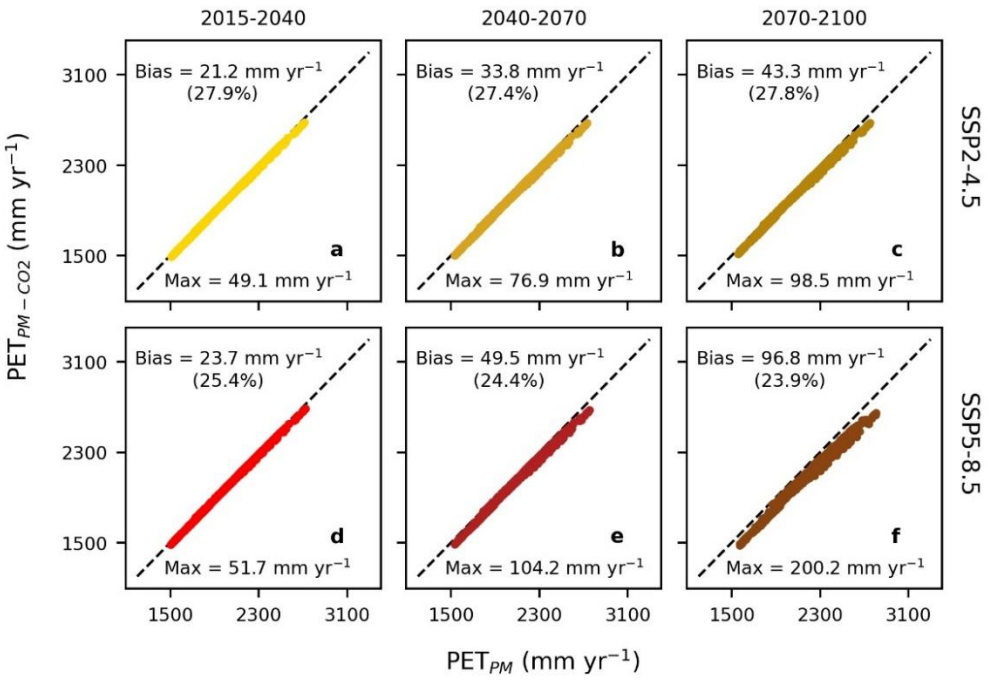

Figure S5. 6. 'Offline' PET estimations. a-c, Comparison between ensemble-mean *PET* estimated by the traditional Penman-Monteith (PM) formulation and by the modified Penman-Monteith (PM – CO2) that accounts for CO_2 concentration for the near future (2015 – 2040), intermediate future (2040 – 2070), and distant future (2070 – 2100), respectively, forced by the SSP2-4.5 scenario. d-f, same as a-c, but considering the SSP5-8.5 scenario. The mean, maximum and the standard deviation of systematic deviations (in parenthesis) are indicated in the figure.

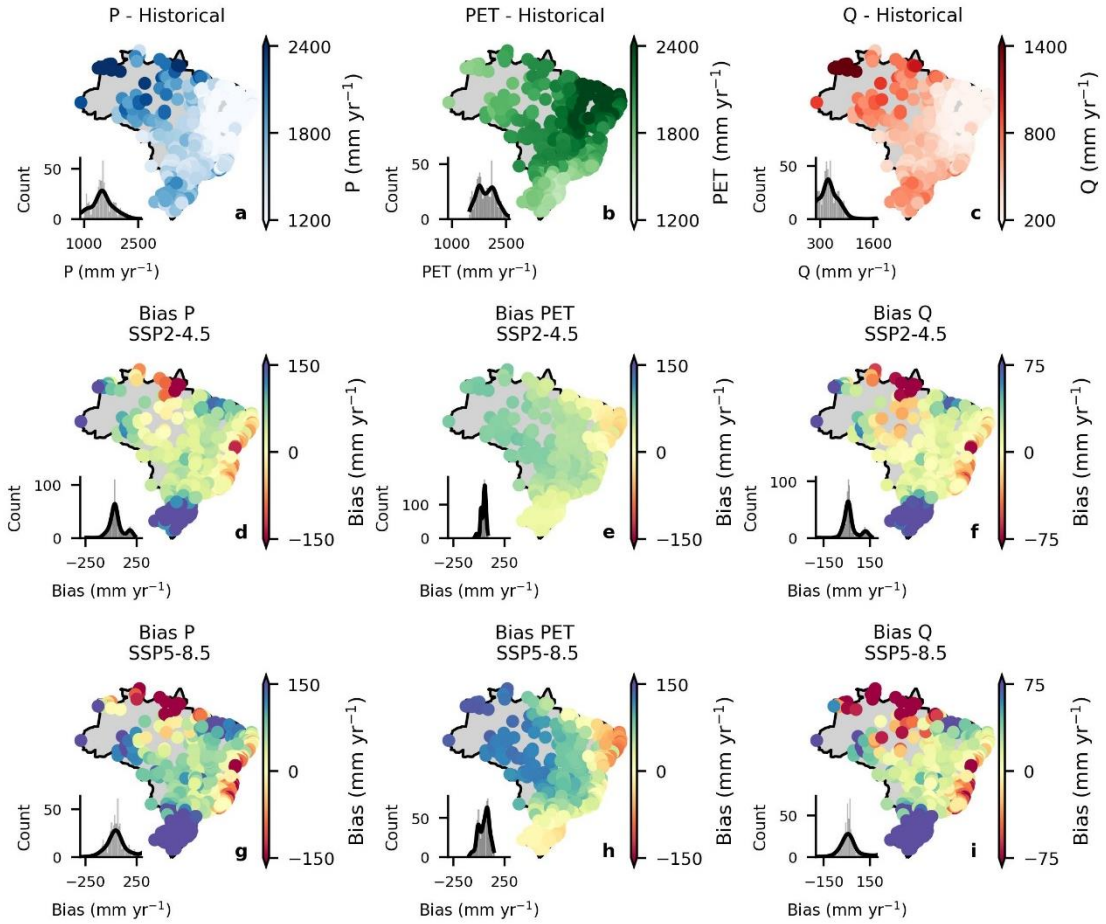

Figure S5. 7. Expected changes on future water balance components. a-c, the spatial distribution of the current long-term mean water balance components precipitation (P), potential evapotranspiration (PET), and water availability (Q). d-f, Expected changes on P, PET, and Q for the distant future (2040-2070) and SSP2-4.5. g-i, same as d-f but considering the SSP5-8.5 scenario.

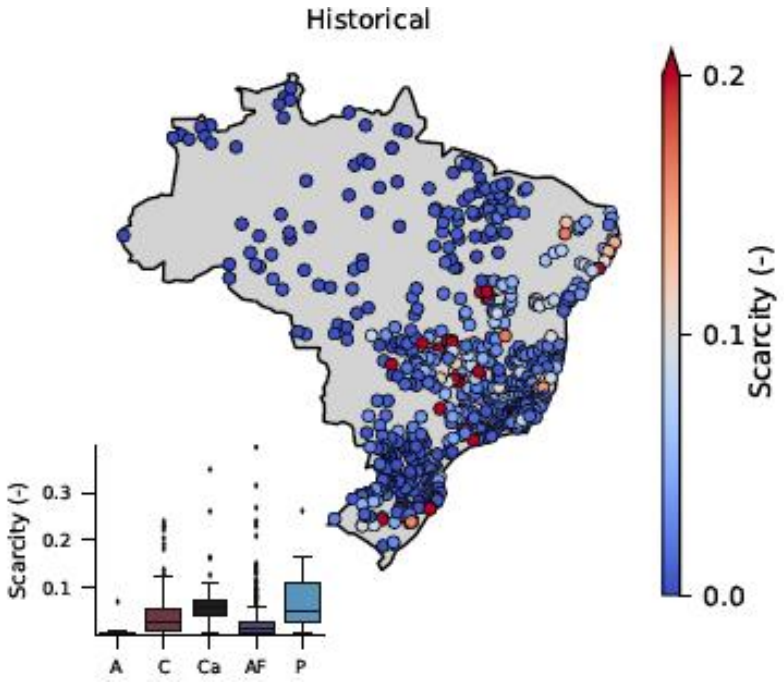

Figure S5. 8. Brazilian current water scarcity condition. Water scarcity index per Brazilian biome (A: Amazon, C: Cerrado, Ca: Caatinga, Af: Atlantic Forest, and P: Pampa) are displayed in traditional boxplots.


EESC • USP